Alternative Splicing Regulation of Human Telomerase Reverse Transcriptase (TERT): Cancer Therapeutic Implications, Discovery of Novel TERT Isoforms, and Impact of Exercise and Aging

by

Jeongjin Kim

A dissertation submitted in partial fulfillment
of the requirements for the degree of
Doctor of Philosophy
(Movement Science)
in the University of Michigan
2023

Doctoral Committee:

Assistant Professor Andrew T. Ludlow, Chair
Professor Greg Cartee
Associate Professor Jacob M. Haus
Professor Mats Ljungman

Jeongjin Kim

snujjk@umich.edu

ORCID iD: 0000-0002-6959-8544

Dedication

To my beloved father, Dr. Jae Man Kim, whom I long to see. He was my mentor and hero, and I always wanted to be like him. Despite his dreams of becoming a farmer, he selflessly gave up his dreams to support our family, enabling me to grow up wonderfully. I hope that my father looks down on me proudly from heaven.

Acknowledgements

I would like to acknowledge Dr. Andrew T. Ludlow. It was very fortunate that I became his first student. He has consistently provided great research advice, guiding me to become a better scientist every day. Not only in my academic life, but he also took care of my life outside of the university. When I got to the United States, he helped me settle down here and truly understood my tough situations as an international student. When I became a father of twin sons, he simply provided all the necessary items for me to raise my children and alleviate pressure from my financial situations. Moreover, he deeply understood my roles as a father and a researcher and always tried to help me overcome any problems I encountered. He also assisted with my immigration process, leading to my recent attainment of permanent residency. I genuinely appreciate his support, and I would not have gone through everything if I had not met him. Thank you so much Andy!

I want to acknowledge all the lab members, both past and present. Thanks to the work of previous lab members, I was able to publish multiple papers during my Ph.D. program and begin conducting my independent research with a solid foundation. I'd like to extend special thanks to Alex Ahn, Andy's second Ph.D. student, who not only supported my research but also shared enjoyable moments outside the lab. His meticulous experimental skills were invaluable to my work, and I have every confidence in his continued success in the lab. Thank you, Alex. I also want to express my gratitude

to James Shadiow, now Dr. Shadiow, for being a great friend and sharing many enjoyable moments with me. I must also give special thanks to the KBs (Korean Boys), Seongeun Kwak and Cheehoon (Chris) Ahn, for being my pillars of emotional support throughout my Ph.D. journey. Having our offices close to each other allowed us to share not only discussions on research but also our life experiences and amusing anecdotes, making the journey more enjoyable.

I want to acknowledge my dissertation committee, Dr. Greg Cartee, Dr. Jacob M. Haus, and Dr. Mats Ljungman, for their participation in my doctoral training. Their valuable feedback during the dissertation proposal played a crucial role in shaping the direction of my research. Additionally, when I needed reference letters during my job interview process, I reached out to Dr. Cartee and Dr. Haus. Despite their busy schedules, they kindly provided the supporting letters that allowed me to pursue my next career step. I met Dr. Ljungman during my lab rotation, and I received significant assistance from his lab members, allowing me to establish a working bioinformatics pipeline essential for my dissertation research. I also appreciate his personal time in meeting with me to provide career advice.

I would like to acknowledge the funding I received from the School of Kinesiology and Rackham Graduate School, as well as support from various sources, including Andy's successful acquisition of large-scale grants.

I want to acknowledge my wife and love, Jieun Jang, whom I first met in 2016 and married in 2018. She is also a graduate of Seoul National University College of Nursing and was working as a nurse at ASAN Medical Center, one of the best hospitals in South Korea when we first met. She made the selfless decision to quit her job and

accompany me to the United States to support my dreams. We have shared countless moments together, both happy and challenging. Despite the difficulties she faced, taking care of our twin sons without family nearby due to our distance from South Korea, she graciously understood the demands of my Ph.D. journey and provided unlimited support. I want to express my love and gratitude to Jieun, and I love you dearly. To Hayul Kim and Hamin Kim, my sons, I'm not sure if you'll read this in the future, but know that I love you both immensely, and you have reshaped my life's purpose. Since your birth in 2020, my life revolves around you two, and my love for you is boundless and everlasting.

Last but not least, I would like to acknowledge my mother, Hyunmi Park. When I was young, her role as a dedicated homemaker, caring for me and my younger sisters, was instrumental in shaping us into responsible and well-rounded individuals. I can't even begin to imagine the sacrifices she made and the challenges she faced while raising us, especially considering she was also caring for both my grandparents at home, including my grandmother, who suffered from Alzheimer's disease. Despite the situation, she always showered us with boundless love and created countless happy memories. When I lost my father, which was an incredibly difficult time for our family, we have all been struggling, but I know that she is the one who had the most difficult time. Mom, thank you for trying to overcome this situation and trying to stand independently. I appreciate your strength and for staying healthy so that I can talk to you, and my sons can have a good time with their grandma. I can't express enough how grateful I am for your unwavering love and dedication. Though I may not say 'I love you' often, please

know that I deeply appreciate everything you did in raising my sister and me, and that I love you dearly.

Table of Contents

List of Figures

List of Tables

List of Appendices

Abstract

Aging is associated with an elevated cancer risk due to the cumulative genetic mutations, cellular damage, and loss of immune cell function. Telomeres, the protective caps at the ends of linear chromosomes, naturally shorten with age, making them a key biomarker of the aging process. Higher levels of physical activity and exercise compared to a sedentary lifestyle are consistently linked to enhanced telomere maintenance in immune cells. Longer telomeres in immune cells may lead to greater anti-tumor immunosurveillance which may underpin the reduced risk of cancers observed in more active individuals. Telomeres are maintained by telomerase, the enzyme that can synthesize telomere repeats. Telomerase is predominantly repressed in somatic cells and is re-activated by cancer cells to ensure their immortality. Conversely, overexpression of telomerase extends lifespan of animals and exercise is associated with higher levels of telomerase activity in immune cells and other tissues. Telomerase activity is regulated by the mRNA and protein expression of TERT, which is the rate-limiting component of telomerase. A key mechanism of TERT mRNA and protein expression regulation is alternative RNA splicing (AS). However, we do not currently know the transfactors that dictate splicing choice, the impact of exercise on thymus TERT AS, the full catalogue of TERT AS isoforms, or the function of most TERT AS isoforms. Understanding the regulation of TERT and telomerase has implications for both aging and cancer therapies, as upregulation of telomerase activity can slow down telomere shortening, potentially

mitigating the aging process, while inhibiting telomerase can offer a strategy to impede cancer growth. Thus, the major objectives of my dissertation were to elucidate new transfactors important to cancer cell TERT AS regulation, examine how exercise impacts TERT AS regulation in the thymus, and determine the catalogue of TERT AS isoforms and their functions. The central premise was that TERT AS exhibits distinct regulation depending on the physiological context, and a more complete understanding of telomerase regulation will result in novel therapies for cancer and aging. We tested this central premise in four separate but related projects as part of my dissertation work. In the first study, we found that a splicing factor, SF3B4, regulated TERT AS in lung cancer cells, and when SF3B4 was reduced, it inhibited telomerase activity and cancer cell growth, indicating a potential novel cancer therapeutic target. In the second study, we identified lung cancer-specific TERT AS regulatory factors (U2AF2 and SRSF2). In the third study, we observed that aging reduced thymus TERT expression and three weeks of voluntary wheel running impacted the AS of TERT in transgenic mice expressing human TERT. In the fourth study, we discovered a novel TERT isoform, Delta 2-4, and determined that it does not function in telomere biology but rather protects lung cancer cells from apoptosis. Collectively, these studies advance our understanding of telomerase regulation, thereby offering potential implications for cancer and aging therapies, and also establishes a fundamental basis for future studies, ultimately leading towards a more complete understanding of telomerase regulation.

Chapter 1 – Introduction

Primary aging is the inevitable decline in physiological resiliency that results in increased risk of diseases, morbidity, and mortality. Over the past few years, the driving pathways of primary aging have been identified, called the hallmarks of aging [1]. Experts have identified 12 hallmarks in three categories: 1) primary (genomic instability, telomere attrition, epigenetic alternations, loss of proteostasis, disabled macroautophagy); 2) antagonistic (deregulated nutrient-sensing, mitochondrial dysfunction, cellular senescence); and 3) integrative (stem cell exhaustion, altered intercellular communication, chronic inflammation, dysbiosis). Secondary aging is the acceleration of aging caused by diseases and environmental factors (including lifestyle factors of physical activity and diet). Many of the primary aging factors listed above are impacted by sedentary living and poor lifestyle habits resulting in accelerated aging phenotypes. Conversely, exercise has been shown to directly impact several of the primary aging pathways including telomere attrition, genomic stability, mitochondria, and cellular senescence, resulting in reduced disease risk and enhanced healthy life expectancy but not maximal lifespan. Further, these primary aging pathways are also linked to an increased risk of cancer development as advanced age is the greatest risk factor for cancer development. Interestingly, there is substantial overlap between the hallmarks of aging and the hallmarks of cancer [2]. Particularly important to this thesis is the overlap of telomere biology, mitochondria, cellular senescence, and genomic stability. The Ludlow

laboratory currently focuses on lung cancer for the following reasons: 1) it is highly age related [3-5]; 2) telomere biology has been indicated in the diagnosis, prognosis, and development of lung cancer [6-8]; and 3) we have made substantial progress in understanding telomere biology in lung cancer cell lines.

Lung cancer is a leading cause of cancer-related deaths accounting for more than 1.8 million deaths per year, with poor survival rates, and limited treatment options necessitating the development of new treatments [9]. Cancer cells are immortalized cells that must achieve telomere maintenance to proliferate unlimitedly [10]. Telomeres are regions of repeated DNA sequences at the end of linear chromosomes [11]. Since DNA polymerase cannot fully replicate the lagging strand of DNA, telomere length shortens 50-150 base pairs with each cell division [12]. When telomere length becomes critically short (less than 5 kilobases), at the critical telomere length shelterin proteins can no longer prevent telomere ends from being recognized as DNA double-strand breaks, a DNA damage response will be induced, finally resulting in cessation of cell division [10]. Thus, a telomere maintenance mechanism is necessity for unlimited cell division. To achieve this, more than 85% of cancer cells rely on reactivation of telomerase, which can maintain or elongate telomere length by *de novo* telomere synthesis [13]. Due to the reliance on telomerase in majority of cancer cells, telomerase inhibition has emerged as a potential cancer therapy, as inhibiting telomerase can induce cancer cell death [14]. However, current direct telomerase inhibitors have been proven toxic and ineffective, highlighting the need for alternative approaches. In addition to cancer, telomerase regulation takes critical roles in aging, which is a different side of emerging problems in our current society. In fact, aging is the number one risk factor for many chronic diseases and cancer [15].

The ability to repair damaged cells and control cell division is reduced during aging underlying many age-related diseases [16]. An important aspect controlling the regenerative capacity of cells is telomere length and telomerase enzyme activity. Telomerase is active during fetal development, suppressed in most somatic tissues, and reactivated in the majority of cancers [10]. Regarding physiological stress in telomere biology, aging is a recognized main contributor to decreased production of naïve T cells and thymic involution [17], leading to compromised immunosurveillance against tumors [18]. Interestingly, exercise has been linked to the upregulation of telomerase activity in immune cells (e.g., PBMC), and individuals who maintain an active lifestyle have been found to exhibit longer telomeres [19] and have reduced risk of development of certain cancers [20-22]. Further, thymic output (greater numbers of mature T cells) is greater in master's athletes compared to healthy age-matched controls [23]. Exercise is clearly a potent stimulus to the immune system that may combat aspects of the aging process, however, the underlying mechanisms governing telomerase regulation in the immune system during aging and with or without exercise remain elusive. The regulation of telomerase with aging is critical because activation of telomerase in a physiological context (i.e., in response to regenerative stress and to repair damage following injury or intense/damaging exercise) is critical to maintain tissue homeostasis but telomerase must also be suppressed to prevent cancerous growth [24]. Thus, complete understanding of telomerase regulation is required to develop novel therapies for cancer or aging. When it comes to telomerase regulation, the long-held paradigm in the field was that transcriptional regulation of the telomerase reverse transcriptase gene (TERT) controlled telomerase activity in most cell types. However, recent evidence indicates that post-

transcriptional mechanisms such as alternative splicing are equally important to the repression or activation of telomerase coding *TERT* mRNAs [25]. Data from our laboratory indicate that alternative splicing (AS) regulation of human *TERT* (*hTERT*) can be manipulated to shift splicing from active to inactive telomerase coding *TERT*, so that telomerase activity can be inhibited [26, 27]. However, the effect of such manipulations on telomerase expressing non-cancerous cells, such as stem cells, hasn't been tested. In addition, focus of the studies was limited on expression of few major TERT isoforms, although many TERT isoforms have been discovered. In fact, the alternative splicing of *hTERT* results in 21 known mRNA variants [28], most of which do not have known functions, nor do we understand how their expression and alternative splicing are regulated. The methods and cell types utilized to date to determine the identity and function mRNA variants of *hTERT* have mainly been from cancer cells leaving the possibility for cell-type specific isoforms that have not yet been identified. Regarding telomerase regulation in a physiological context, we recently demonstrated increased *hTERT* expression and altered alternative splicing of exons 7-8 in response to a bout of treadmill running in mouse skeletal muscle and cardiac muscle (left ventricle) [29]. However, the *hTERT* expression in other tissues, such as thymus or the impact of aging on *hTERT* expression are currently unknown. To begin to answer these questions we propose four aims to make significant advances in understanding alternative splicing regulation of *hTERT* in different contexts, cancer and aging, with therapeutic implications.

Aim 1. To inhibit telomerase by targeting *TERT* AS in lung cancer cells. We hypothesized that telomerase could be inhibited by manipulation of *TERT* alternative splicing. Our approach was to analyze public cancer databases and our loss of function

screen to identify a candidate splicing factor. We identified SF3B4, a splicing factor with high expression in cancer and was related to *TERT* AS. To test our hypothesis that SF3B4 was mechanistically related to TERT AS in lung cancer, we performed loss of function studies and measured *TERT* AS, telomerase activity, telomere length, and clonogenicity in non-small cell lung cancer cells. Interaction between SF3B4 and *TERT* sequences was determined by RNA-protein pull down analysis.

*This research has been published in the journal Molecular Cancer Research, with Jeongjin Kim as a co-first author [30]. Jeongjin Kim carried out Terminal Restriction Fragment (TRF) analysis of Calu-6 DR8 deletion mutants, generation of an R script to process The Cancer Genome Atlas (TCGA) data, Immunoblot to compare primary human bronchial epithelial cell (HBEC) versus non-small cell lung cancer cells, SF3B4 knockdown with siRNA and rescue with siRNA resistant SF3B4 overexpression, siRNA titration experiment, ddPCR measurement of *TERT* mRNA variants to determine splicing ratio, ddTRAP to measure telomerase activity, clonogenic assay, measurement of telomere biology (telomerase activity, alternative splicing of *TERT*, growth rate, and telomere length changes) in shRNA treated Calu-6 cells, RNA pull down assay, measurement of cancer associated splicing events in Calu-6 following knockdown of SF3B4, and viability assays with siRNA/shRNA knockdown of SF3B4 and rescue condition.

Aim 2. To define cancer cell specific *TERT* AS regulation. We hypothesize that cancer cell specific telomerase inhibition can be achieved by defining the differences in *TERT* AS regulation between cancer cells and normal telomerase expressing cells. *TERT* AS regulators will be determined in induced pluripotent stem cells (iPSCs), neural progenitor

cells (NPCs), and cancer cells (Calu-6 cells). Cell type specific *TERT* AS regulator candidates will be tested with siRNA knockdown.

*This research has been published in PLoS ONE with Jeongjin Kim as a co- first author [31]. Jeongjin Kim carried out most of experiments and analyses except iPSC differentiation into NPC, measurements of *TERT* mRNA variants, telomerase activity, and telomere length in iPSC differentiation, and measurements of *TERT* mRNA variants and telomerase activity in Calu-6 cells from different cell densities.

Aim 3. To determine the impact of exercise and aging on the expression profile of *hTERT* mRNA variants. We hypothesize that expression of *hTERT* and ratio of FL *hTERT* to minus beta *hTERT* in thymus would decrease with aging and exercise would counteract the age-driven decrease. Our approach was to measure the expression level and splicing ratio of *hTERT* mRNA variants by exons 7-8 inclusion and exclusion assays. We collected thymus tissues from transgenic mice expressing *hTERT* of different ages (young, 6 months; middle-aged, 12 months; old, 18-22 months) with or without access to a running wheel (i.e., exercise compared to sedentary). Next, we tested our hypothesis by collecting thymus tissues from middle-aged (16 months) transgenic mice at Pre-, Immediately post-, or 1-hour post treadmill exercise. We measured the expression level of the *hTERT* mRNA variants in thymus tissue.

Aim 4. To discover novel TERT isoforms and functions. We hypothesized that novel TERT isoforms existed beyond the 21 previously observed isoforms, and that the novel isoforms will have distinct functions from the full-length TERT protein. We compared *TERT* full-length mRNA variant expression of induced pluripotent stem cells (iPSCs) to lung cancer cells and identified a novel potential protein coding *TERT* mRNA variant,

Delta 2-4 (skips exons 2-4). We validated the mRNA expression of the *TERT* mRNA variant in a panel of human cell lines and human tissues with RT-PCR in human cell lines. We determined the role of the novel TERT isoforms in telomere biology by gain and loss of function studies.

The primary objective of my dissertation was to attain a more comprehensive understanding of telomerase regulation through the four distinct studies, each offering a unique perspective (Figure 1.1). Completing this is critically important because cancer is a leading cause of death in our aging society that urgently needs novel therapeutic approaches for cancer while preserving physical function and quality of life with aging.

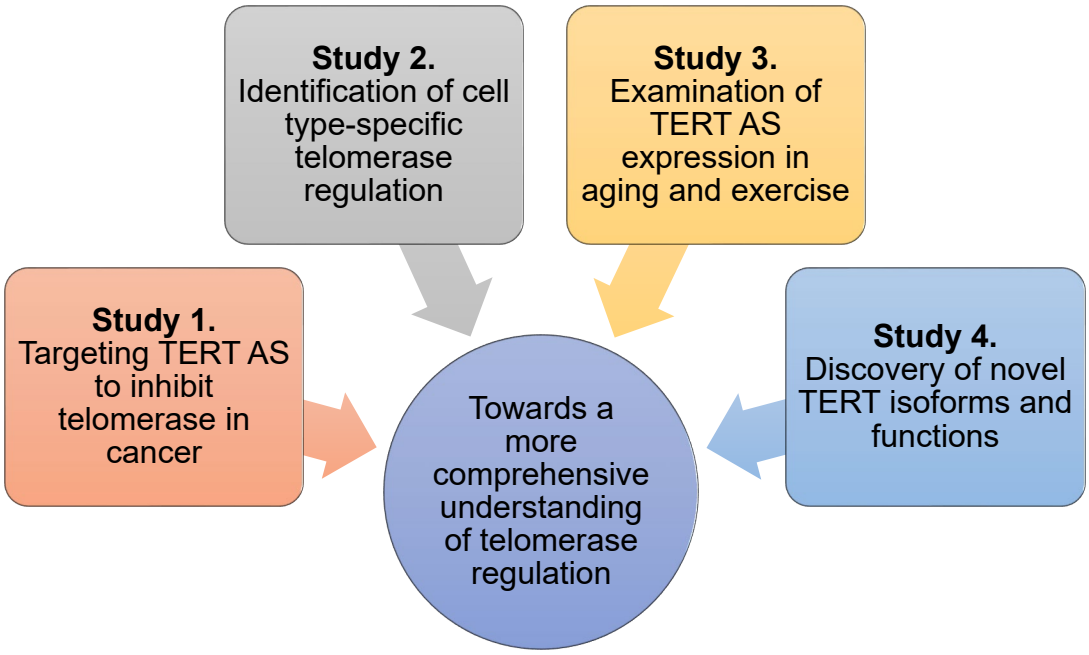

Figure 1.1. Overview of dissertation: converging paths towards a more comprehensive understanding of telomerase regulation.

Chapter 2 – Literature Review

2.1. Telomeres

Seminal ideas by Thomas Hunt Morgan, who hypothesized that genes were arranged on a chromosome like beads on a string, implying a beginning and an end [32]. Then, Hermann Muller (based on findings of Barbara McClintock [33]) observed that x-ray induced DNA breaks behaved differently compared to the ‘free’ or natural ends of linear chromosomes [34]. This led to the naming of the ends of linear chromosomes as ‘telomeres’ from the Greek words for ‘end’ (telos) and ‘part’ (meros) (reviewed by Shay and Wright 2019) [35].

2.1.1. Telomere structure and functions

Telomeres represent a unique challenge for cells in that they could be recognized as double stranded DNA breaks and thus trigger a DNA damage response which would halt cell growth and division. Cells have solved this “end protection problem” by utilizing a repeat sequence (5’-TTAGGG$_n$-3’) that is bound by a specialized protein complex called shelterin that binds to and protects the chromosome end thereby preventing spurious recognition of the ends as broken DNA (Figure 2.1). As a result, telomeres and shelterin protect genome from nucleolytic degradation, unnecessary recombination, repair and interchromosomal fusion [36]. As shown in Figure 2.1, shelterin complex

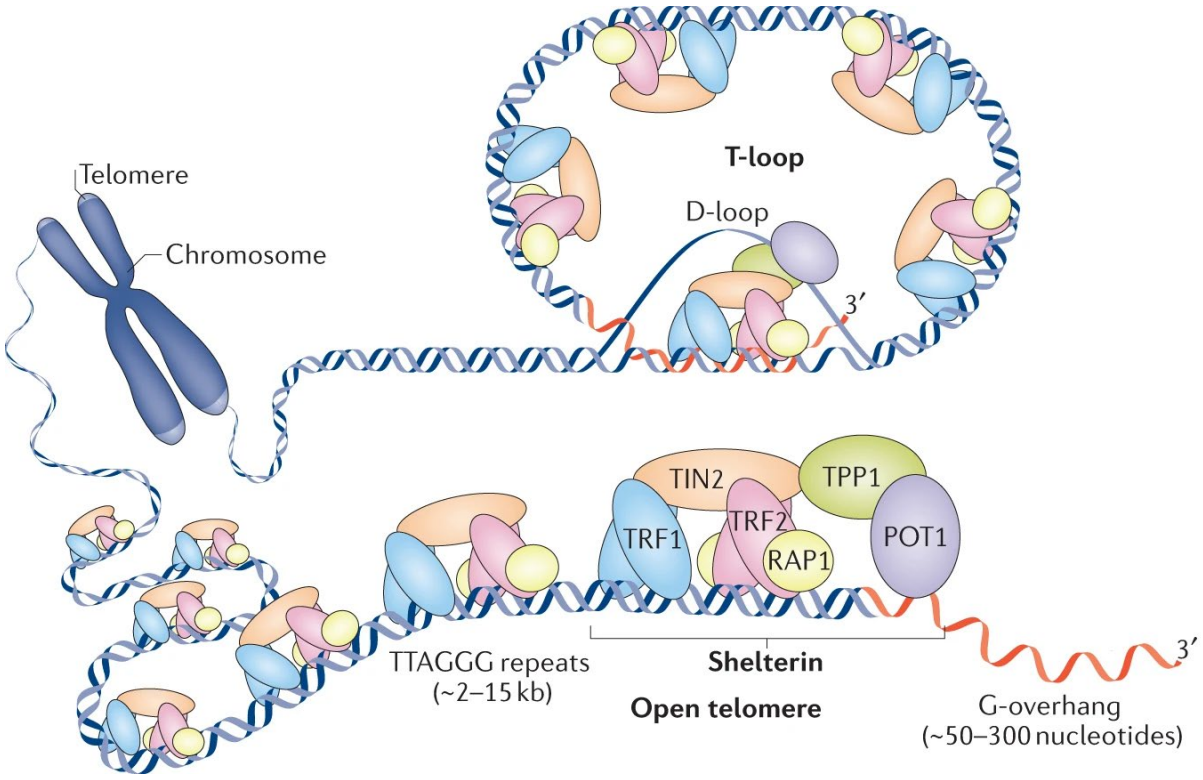

Figure 2.1. Telomere structure and shelterin complex (adapted from Lim and Cech, 2021). Telomeric DNA consists of both double-stranded DNA and single-stranded DNA (G-overhang). 5'-TTAGGG is the DNA telomere repeat sequence in cells of vertebrates including humans and mice. Due to having both double and single stranded DNA, strand invasion occurs to form a displacement loop (D-loop) and a telomere loop (T-loop). Shelterin complex comprises six proteins (RAP1, TRF2, TRF2, TIN2, TPP1 and POT1) that binds and protects telomeres at the ends of chromosomes.

comprises six proteins: RAP1, telomeric repeat-binding factor 1 (TRF1), TRF2, TERF1-interacting nuclear factor 2 (TIN2), protection of telomeres protein 1 (POT1) and ACD Shelterin Complex Subunit And Telomerase Recruitment Factor (ACD also commonly referred to as TPP1) [37]. In addition to end-protection function by binding telomere, shelterin also provides a sensing mechanism of telomere length. TRF1 and TRF2 are homodimers binding telomeric double strand DNA, while the POT1-TPP1 heterodimer

binds and caps the telomeric 3' tail. TIN2 connects TRF1 and TRF2 dimers with POT1-TPP1 to form the shelterin complex. RAP1 is an accessory subunit of TRF2 contributing to telomere protection [37]. Telomeres perform a second critical function and in doing so solve a second critical problem, which is called the "end replication problem". Olovnikov [38] and Watson [39] first pointed out the implications of this "end replication problem". Lacking a means to replicate chromosome ends, chromosomes would shorten with each cell doubling, eventually reaching a critical point leading to cell senescence or death. Preparing for cell division, chromosomes are replicated but the ends of linear chromosome cannot be replicated completely during lagging strand DNA synthesis. This is due to the placement of the final Okazaki fragment which leads to the loss of a small piece of DNA with each cell division [40]. If coding information was found near the near the ends of chromosomes, cell division would result in the loss of important genetic information. Since telomeres are non-coding DNA, losing a small piece of telomeres is not immediately consequential to the function of a cell. Therefore, telomeres solve the end replication problem and protect the genetic/DNA coding information in cells from loss during DNA replication and cell division. A final important function of telomeres is in the regulation of gene expression. In human cells telomeres help form the 3-dimensional architecture of DNA in the nuclei. Telomeres form intrachromosomal looping structures that contact distal enhancers and repressors of gene expression up to 10 megabases away from the telomere [41]. Therefore, telomere shortening or changes in telomere length can have profound effects on gene expression regulation and thus the physiology and phenotypes of cells by impacting gene

expression. This has been called **t**elomere **p**osition **e**ffects **o**ver **l**ong **d**istances or TPE-OLD [41].

2.1.2. Telomere shortening in cell replication – The Hayflick limit

In a replicating cell, chromosomes need to be replicated and segregated into two daughter cells. When chromosome replication occurs, telomeres shorten by 50-200 bases due to incomplete synthesis of lagging strand [42]. As a result, telomere length has been considered to be a 'molecular clock' for cells that are actively replicating such as skin cells and cells found within gastrointestinal tract and bone marrow. When a single or small group of telomeres in a cell reach a 'critically shortened length', the T-loop structure is disrupted, and the short telomeres become dysfunctional/exposed to cellular mechanisms of damage detection and repair. This induces a DNA damage response that triggers replicative senescence. In fact, replicative senescent cells can be experimentally determined by observing co-localization of DNA damage response proteins (53BP1, gammaH2AX, Rad17, ATM, and Mre11) with telomeres which is called telomere-associated DNA damage response foci (TAFs) or telomere-induced DNA damage foci (TIFs) [43, 44]. Replicative senescence is defined as an irreversible cellular state where cells can no longer replicate but cells are metabolically active and continue to secrete factors that contribute to aging that is called the senescence-associated secretory phenotype (SASP) [45]. When telomeres are functional on the other hand, they form a lariat-like structure called a T-loop by 3' single strand DNA being attached to the part of opened telomeric double strand DNA forming D-loop [46] (Figure 2.1). Telomere repeat binding factor 2 (TERF2/TRF2; Figure 2.1) is critical in the formation of

the T-loop structure, and when telomeres lack TRF2 chromosome end-to-end fusions occur and cause replicative senescence. As telomeres become dysfunctional, the replicative capacity of the cells in a tissue becomes compromised. This phase of senescence is called the senescence stage 1 (M1) and signals the end of a cells replicative capacity also termed the “Hayflick limit”. However, cells can escape senescence (M1) by inactivation of pRB/p16 or p53 [10, 47]. For example, SV40 large T-antigen can inactivate p53 and pRB leading to abrogation of apoptotic mechanisms, resulting in escape of M1 stage and continued proliferation of cells with short and potentially dysfunctional telomeres [48]. As cells replicate past M1 telomeres continue to shorten. Eventually telomeres are completely eroded, and cells enter a second senescence stage called “crisis” or senescence state 2 (M2). During crisis, cells have very short telomeres, their chromosome ends fuse, and they exhibit genomic instability (breakage-fusion-breakage cycles during cell replication of fused telomeres), whereby cells undergo cell death by apoptosis [47, 49]. However, rare clones can escape crisis and achieve immortalization with very low frequency of 3×10^{-7} only when the clones can maintain their telomeres either by activation of telomerase or alternative lengthening of telomere (ALT) [50]. This senescence process is shown in Figure 2.2.

2.1.3. Telomere maintanance mechanisms – telomerase and ALT

Telomerase is a ribonucleoprotein enzyme that can de novo synthesize 5’-TTAGGG repeats using a reverse transcriptase enzyme activity in S phase to maintain or elongate telomeres. Telomerase is preferentially recruited to the shortest telomeres, as telomere length does not shorten equally across all chromosome ends but follows a

Gaussian distribution. Telomerase consists of an RNA template component (telomerase RNA, TERC) and a catalytic subunit telomerase reverse transcriptase (TERT) along with several accessory proteins including the RNA binding Dyskerin complex that are critical for its enzymatic activity [51] (Figure 2.3). Telomerase is not active in all cells at all times and its activity is tightly regulated and depends on many factors such as developmental stage and cell type. For example, during fetal development active telomerase maintains telomere length while telomerase activity is silenced in most somatic tissues. In certain types of cells such as germline cells, telomeres are maintained unless dysregulated by genetic mutation. However, regardless of the telomerase activity, telomere length still decreases over time in replicating cells such as adult stem cells as shown in Figure 2.2. In addition to the telomerase mediated telomere elongation, certain types of cells can maintain telomere length by ALT. ALT is a telomerase independent telomere maintenance mechanism that utilizes a homologous recombination (HR)-mediated process to maintain/elongate telomeres. Typically, cells relying on ALT possess longer average telomere length that is also very heterogeneous compared to cells relying on telomerase to maintain telomeres.

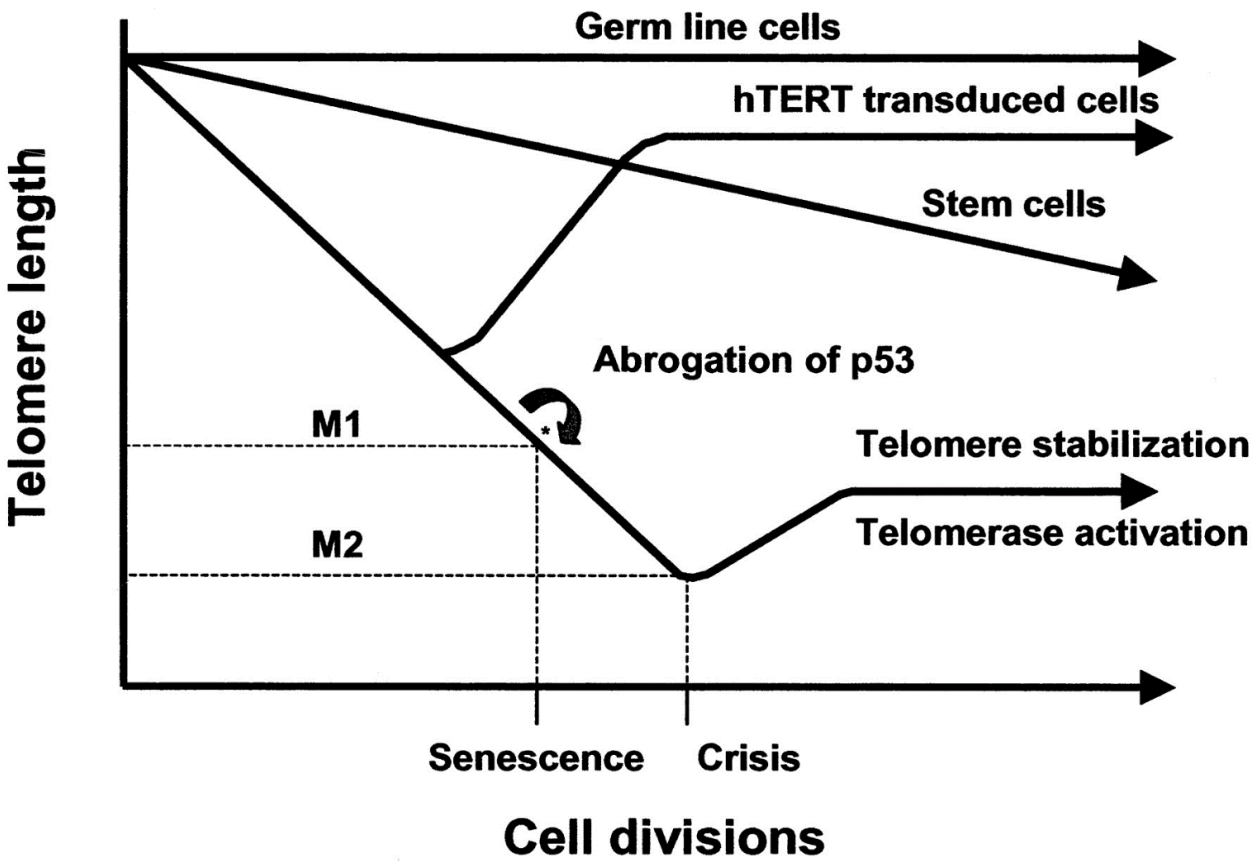

Figure 2.2. Two-step hypothesis of cellular senescence and immortalization (adapted from Cong et al., 2002).

While Germ line cells can maintain the telomere length (Y axis), telomeres of other cells shorten as cells divide (X axis). Stem cells expressing active telomerase have slower telomere attrition rate compare to other cells without telomerase activity. When human telomerase reverse transcriptase (hTERT) is transduced in the telomerase negative cells, telomerase activity is elevated and telomere length can be elongated and maintained. Cells with critically short telomeres enters first senescence stage (M1) and abrogation of p53 can bypass this stage eventually leading to second crisis stage (M2). Rare cells can escape crisis and achieve immortalization only when the clones can maintain their telomeres either by activation of telomerase or alternative lengthening of telomere (ALT).

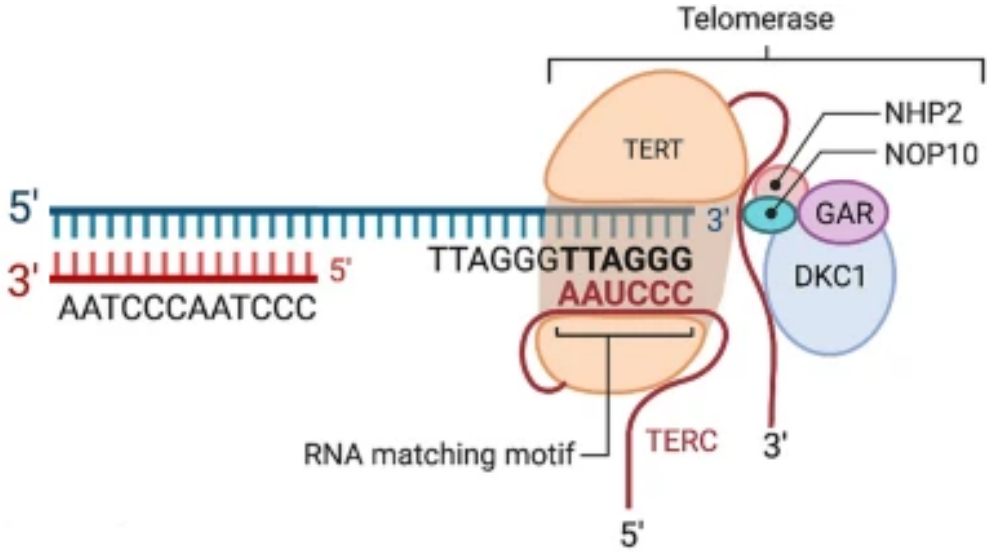

Figure 2.3. Telomerase consisting of TERT, TERC and Dyskerin complex (adapted from Muoio et al., 2022).

Telomerase is a ribonucleoprotein complex that consists of **te**lomerase **r**everse **t**ranscriptase (TERT), **te**lomerase **R**NA **c**omponent (TERC, also called TR) and Dyskerin complex (DKC1, GAR, NOP10 and NHP2). Telomerase uses RNA matching motif of TERC to bind to single-stranded telomeric DNA and synthesizes telomeres.

2.2. Aging

While chronological aging is determined by the time which an organism has been alive, biological aging, also referred to as physiological aging is determined by changes in a multitude of physiological systems and cells that culminate in phenotypes commonly associated with older individuals in a species. By definition, aging is an age-dependent (chronological) or age-progressive decline in intrinsic physiological function, leading to an increase in age-specific mortality rate (i.e., a decrease in survival rate) and a decrease in age-specific reproductive rate. While chronological aging is

straightforward to quantify (passage of time in years or other measure of time) biological aging is much more difficult to quantify. To attempt to organize the numerous proposed biomarkers of aging, researchers in the field have consolidated the biomarkers into broad “hallmarks” of the aging process. There are nine hallmarks of aging: telomere attrition, cellular senescence, stem cell exhaustion, genomic instability, epigenetic alterations, loss of proteostasis, deregulated nutrient-sensing, mitochondrial dysfunction, and altered intercellular communication [52].

2.2.1. Primary aging and secondary aging

Aging consists of two aspects: primary aging and secondary aging. Primary aging is inevitable and unavoidable changes that are primarily determined by genetics. Primary aging causes deterioration in cellular structure and biological functions independent of environmental factors or disease in healthy individuals [53]. On the other hand, secondary aging refers to additional age-related decline in structural and functional changes caused by environmental factors or diseases [53]. The consequence of slowing primary aging is an extended maximal lifespan, and one example of an intervention is caloric restriction, as observed in rodent models. Whereas the consequence of slower secondary aging is an increased median lifespan, and one example of an intervention capable of increasing median life span is exercise training [54]. Although interventions that can reverse or slow primary aging are in their beginning phases of experimental testing [55, 56], it is well established by many decades of evidence based recommendations that secondary aging can be slowed down with

individual’s efforts, such as endurance and resistance exercise training to keep functional capacity and prevent disease [57].

2.2.2. Telomeres and telomerase in aging

Among the hallmarks of aging, telomere attrition or telomere shortening has been widely associated with many age-related phenotypes and with other biomarkers of biological aging. The fact that short telomeres can induce cellular senescence and stem cell exhaustion, is associated with major diseases of aging (cardiovascular disease and cancer), and short telomeres are related to increased risk of mortality in the oldest of old, make it a keystone in understanding the biology of aging. Genetic knockout of telomerase in mice results in telomere shortening leading to shortened life span, a reduced capacity to respond to stresses such as wound healing and hematopoietic ablation, and an increased incidence of spontaneous malignancies [58]. While mice with hyper-long telomere showed less metabolic aging and longer lifespans [59] and telomerase activators, such as TA-65, elongated short telomeres leading to increment of health span of human adult and old mice without increasing cancer incidence [60]. These seminal findings make telomeres a cornerstone in understanding geroscience and progressing towards interventions to reduce the burdens of biological aging. Moreover, genetic diseases of short telomeres resulting in early death due to bone marrow and lung failure underscore the importance of telomere length regulation in aging and physiology. Telomere length also directly controls the expression of inflammation inducing factors via the TPE-OLD mechanism mentioned earlier. For example, ISG15, that enhances secretion of pro-inflammatory cytokines such as

CXCL1, CXCL5, IL-1 and IL-6 [61], is upregulated with telomere shortening and contributes to the chronic inflammatory state associated with human aging [62]. In addition, evidence has shown that cellular senescence (including telomere induced or replicative senescence) is accompanied by a striking increase in the secretion of 40-80 factors/proteins participating in intercellular signaling that has been termed senescence-associated secretory phenotype (SASP). In sum, short telomeres cause and are associated with many age-related phenotypes and the shortening of telomeres occurs in all cells regardless of DNA and cellular replication which make understanding telomere maintenance mechanisms fundamental in all human cells.

2.2.3. Telomeres, telomerase, and aging in different types of tissues

Healthy human cells can be largely divided into two groups based upon their ability to divide and replicate. Cells that can replicate include labile cells and stable cells. Labile cells (i.e. skin stem cells, hematopoietic stem cells and gastrointestinal stem cells) are somatic cells that actively divide to replace physiological loss of cells. Stable cells spend most of the time in the quiescent G0 phase of the cell cycle and replicate only when needed (i.e. quiescent stem cells that are activated when wound healing is needed). Satellite cells in muscle tissues and parenchymal cells of the liver, kidney, and pancreas are examples of stable cells. For both labile and stable replicating cells, telomere length shortens with aging as cell division accompanies loss of telomeric repeats and older organisms have undergone more cell divisions. In contrast, permanent cells or post-mitotic cells are cell types that do not replicate. Especially in long-lived mammals like humans, cells that do not divide and can live for decades are

called long-lived post-mitotic cells (LLPMCs). Muscle fibers in skeletal muscles and neuronal cells in the brain are examples of LLPMCs. Telomere shortening in post-mitotic cells with aging has been controversial. Despite initial studies showing a lack of telomere shortening in post-mitotic cells, emerging evidence now strongly supports that telomeres indeed shorten with aging. For example, a cross-sectional analysis of post-mortem tissues of 87 adults across the age span (19- 77 years) showed that telomeres shortened at an equivalent rate in leukocytes, skeletal muscles, skin and subcutaneous fat [63]. Recent evidence from a larger cross-sectional study that measured telomere length in more than 25 tissue types from 952 human donors (6,391 unique tissue samples) supports the hypothesis that telomere length is negatively correlated with age in most tissues including post mitotic tissues such as brain tissue [64]. The most well-described reason for telomere shortening regardless of cell division is oxidative damage in cells (reviewed by Barnes et al. 2019) [65]. Post-mitotic cells mostly rely on their intracellular capacities for repair and renewal such as autophagy, mitophagy, antioxidant enzymes and DNA repair machinery. Due to age-dependent dysfunctional mitochondria and the decrease in efficiency of the cellular repair mechanisms of oxidative damage, production of reactive oxygen species (ROS) and resulting oxidative damage (stress) increases with aging. Since telomeres (5'-TTAGGG) have a large portion of guanine nucleotides and the guanine base is the most sensitive base to oxidative damage inducing 8-oxoguanine (8-oxoG), telomere shortening, and telomere DNA damage can occur via 8-oxoG related mechanisms. When the guanine rich telomeres are damaged it must be repaired however this mechanism of repair can cause further problems. The DNA repair enzyme OGG1 DNA glycosylase can introduce DNA single strand nicks and

when multiple DNA single strand nicks occur on both leading strand and lagging strand at the same time, this can lead to a double strand break (DSB) leading to shortening of telomeres. In addition, a DNA single strand nick can be excised by a single-strand nuclease leading to shortening of telomeres. This telomeric DSB (tDSB) can induce not only shortening of telomere, but also permanent DNA damage response regardless to the length of telomere in post mitotic cells. When tDSB occurs in proliferating human cells undergoing S-phase, it can be repaired by homologous recombination (HR) [66]. However, since post mitotic cells do not undergo S-phase, thus tDSB is not repaired by the HR mechanism in the post mitotic cells. In fact, recent evidence showed that post-mitotic cardiomyocytes became senescent with increased persistent TAFs/TIFs (i.e., indicator of telomere damage) in response to aging and ROS independent to telomere length[67]. The persistent telomeric DNA damage response is caused by inefficient repair capacity that is fueled by shelterin protein TRF2, as TRF2 actively inhibits the DNA damage response factors from recognizing the telomere end as a DNA break[68]. In addition to tDSB by 8-oxoG, 8-oxoG formation can lead to telomere shortening by another mechanism. Since TRF2 protects telomere from an enzyme called resolvase that excises the telomere T-loop and 8-oxoG formation induces loss of shelterin protein TRF2 binding on telomere, loss of TRF2 binding leads to telomere shortening. Lastly, a recent study showed that telomeric 8-oxoG itself can induce premature replicative senescence even in the absence of telomere shortening by activating ATM and ATR signaling (ATM and ATR kinases orchestrate DNA damage response) and enriching for markers of telomere dysfunction in replicating cells [69]. This study utilized a very specific chemoptogenetic method to induce telomere specific DNA damage, providing

even more strength to the idea that telomere integrity and length are important phenotypes that are causally related to physiological aging. In summary, telomere length shortens, and telomere induced DNA damage increases with aging across most tissues in humans and this drives cellular senescence in both replicating and non-replicating cells types leading to age-related phenotypes.

2.3. Cancer

2.3.1. Telomeres and telomerase in cancer

Cancer occurs when cell proliferation is dysregulated. Uncontrolled cell division and metastasis of cancer cells to vital organs eventually leads to multiorgan failure and death. When the cell cycle becomes dysregulated and the cells start to divide out of control, telomere shortening can act as a potent tumor suppressor by inducing telomere related replicative senescence if no telomere maintenance mechanism is activated, crisis and apoptosis can occur (Figure 2.2). Since most somatic cells do not possess a telomere maintenance mechanism, repeated cell divisions will make telomeres critically short and deprotected. This will trigger a DNA damage response (DDR) that results in cell cycle arrest or apoptosis. Due to this mechanism telomere shortening can be a tumor suppressing mechanism. Besides telomere length acting as a tumor suppressive mechanism, cells have evolved a system of proteins and cell cycle check points that ensure cell replication occurs correctly without detrimental mutations. The proteins that act to keep mutant cells from proliferating are called tumor suppressor genes or proteins. One critical tumor suppressor gene is TP53 gene which mediates cell cycle arrest and apoptosis responses in damaged cells. However, when mutations disrupt

tumor suppressor genes, such as a mutation in the TP53 gene, the mutant cells can bypass cell cycle arrest or apoptosis and reach the crisis stage (M2) with chromosome instability that possibly induces more cancerous mutations on DNA. For the mutant cells at the crisis stage (M2) to keep dividing without cellular death, the cells must achieve telomere maintenance to become cancer cells. Cancer cells achieve telomere maintenance by telomerase reactivation or alternative lengthening of telomere (ALT).

2.3.2. Cancer and aging

Cancer risk increases with aging. Since aging is also related to short telomeres, the association of short telomeres and cancer has been explored. In fact, short telomeres have been observed in most precancerous lesions and result in a higher chance of cancer progression. Also, studies revealed a higher prevalence of cancers in the short telomere syndromes compared to general population [70]. However interestingly, evidence has shown that higher cancer risk was also found with longer telomeres from observations of families with cancer predisposition as well as population studies. This phenomenon is called the “telomere length paradox” because both short and long telomeres are associated with a higher chance of cancer progression (Reviewed by Aviv et al. 2017) [71]. In fact, both short and long telomeres can be associated with higher cancer risk depending on the circumstances. When a cell has long telomeres, it means that longer telomeres allow for more cell divisions, more replicative and damage induced errors (i.e., mutations to somatic cell DNA) and thus a higher mutation burden compared to shorter telomere cells which would replicative senesce before accumulating detrimental mutations. An example is the association of

longer telomeres in germline cells with a wide variety of cancers including melanoma and glioma caused by common polymorphism near *TERT* gene (i.e., *TERT* promoter mutations) which leads to a higher amount of active telomerase. In addition to human study, mouse models have also been utilized to understand the association of telomere length with cancer progression. Mice have longer telomeres than humans, and mouse telomerase is active in most mouse somatic cells in contrast to human telomerase which is inactivated in human somatic cells. By using a genetically modified mouse model (TR knockout, lacks telomerase enzyme activity, has shorter telomeres compared to wild type littermates), it has been revealed that mice with short telomeres having fewer cancer incidents compared to wild type littermates [72]. The idea of underlying mechanism is that short telomeres and lack of telomerase activity (mouse cells are now more like human cells) prevent or block continued cell replication and thus promote senescence and apoptosis and in effect prevent cancerous progression. However, when TP53 gene is deleted in telomerase deficient mice that have short telomere, the mice developed more tumors, and these neoplasms showed hallmarks of genomic instability, including signatures of chromosome end-to-end fusions and breakage–fusion–bridge cycles [73]. This means that short telomeres can actually accelerate cancer progression due to chromosome instability if cell cycle arrest mechanism at M1 senescence is impaired by mutation in tumor suppressor genes. As a result, both short telomere and long telomeres are associated with higher chance of cancer progression. This makes understanding telomerase regulation extremely important as too little and too much telomerase could set up cells for cancerous progression. Thus a “goldilocks”

phenomenon has been used to describe the amount of telomerase and telomere length that might be ideal for healthy outcomes as one ages.

2.4. Genetic diseases

2.4.1. Telomeres and telomerase in genetic diseases

Loss of telomerase activity during fetal development due to mutations in several important telomerase regulatory genes results in inheritance of short telomeres. Since many different genes (15 genes identified to date [70]) result in inheritance of short telomeres, the field calls these diseases the “short telomere syndromes” and there is a spectrum of phenotypes associated with different mutations. Short telomere syndromes show mostly autosomal dominant inheritance, meaning mutation on one of chromosomes from one of parents is sufficient to cause the syndrome (e.g., haploinsufficient). Mutations causing short telomere syndrome have been found in most of genes forming the telomerase complex such as TERT, TR, Dyskerin, NAF1, NHP2, NOP10, and shelterin complex protein TIN2 (encoded by *TINF2*), TPP1, and other genes for telomerase assembly, telomere helicase, TR 3’ end maturation and TR deadenylation. Since short telomeres induce cellular replicative senescence, patients with short telomere syndrome have a larger portion of senescent cells compared to healthy people. The reduction of replicative capacity is deleterious for tissues that require higher turnover rate such as skin and bone marrow and this can lead to the phenotypes characteristic of these diseases. For example, dyskeratosis congenita (DC) that is caused by germline mutations in telomere biology genes and characterized by very short telomeres and cancer-prone inherited bone marrow failure syndrome [74]. On

the other hand, short telomeres in cells that occasionally divide also cause diseases. For example, observation derived from the human genetic studies shows that lung is vulnerable to the short telomere syndromes leading to pulmonary fibrosis despite its slow turnover (few times each year). In fact, patients with DC show premature mortality and the main causes of mortality are bone marrow failure/immunodeficiency (60–70%), pulmonary complications (10–15%) and malignancy (10%) [75]. The timing when telomere shortening emerges also matters in short telomere syndromes as children and young adults develop disease in high-turnover tissues such as the bone marrow while adults generally develop disease in slow-turn over tissues such as lung and liver [70]. With strong cause and effect relationships to aging, cancer and genetic disease, understanding how telomere length is regulated mainly through telomerase regulation is critical to making biomedical advances in this field (i.e., if one wants to manipulate telomerase to elongate or shorten telomeres therapeutically).

2.5. Telomerase regulation

The expression pattern of telomerase is that during early fetal development, telomerase is active, but upon tissue specialization (between 12-20 weeks of development) tissues turn off telomerase. The shutting off of telomerase is thought to be controlled through transcriptional mechanism but recent evidence below indicates that alternative splicing is also involved. The shutting off of telomerase allows for somatic cell telomere shortening to provide a replication clock and to aid in tumor suppression as discussed above. However, in cancer cells telomerase is turned back on through a variety of mechanisms discussed in detail below. The expression pattern (cancer

specificity) and the idea that most somatic cells do not require telomerase activity to survive lead to many attempts to inhibit telomerase as a nearly universal cancer therapy. However direct targeting of telomerase enzyme activity has failed for the following reasons: 1) the long lag phase is required for cancer cells to have critically short telomere after telomerase inhibition and 2) only a few hTERT molecules are required for cancer cells to survive but complete inhibition of TERT expression is hard to be achieved [76]. In contrast to inhibition of telomerase, several groups have attempted to activate telomerase therapeutically in regenerative and aging medicine such as TA-65 from Telomerase Activation Sciences (TA Sciences). However, this has failed because of non-significant telomere lengthening effects from using drugs due to lacking understanding of underpinning mechanisms for telomerase activation [77]. To test the promise of telomerase more fully as a therapeutic target a deeper understanding of its regulation is required to develop new and novel therapeutic approaches for both regenerative/aging medicine and cancer.

2.5.1. Transcriptional regulation of *TERT*

Telomerase is a low abundant ribonucleoprotein enzyme consisting of two core subunits: a protein subunit telomerase reverse transcriptase (TERT) and telomerase RNA component (TR). The number of telomerase holoenzymes was estimated as only ~35 ([78]) or ~250 ([79]) per cell and for comparison purposes another ribonucleoprotein complex U1 is estimated as 1 x 10^6 [80]. In humans, the mRNA expression of the catalytic subunit TERT has been considered as a major telomerase activity limiting

component because overexpression of TERT but not TR can increase telomerase activity in human cells. In addition, the estimated number of TERT protein was ~400 per cell which was lower than the number of estimated hTR that was ~1000 per cell [79]. This also points out a disconnect between TERT molecules and the number of assembled telomerases which points to the potential for off telomere TERT functions (i.e., non-canonical TERT functions). Because most cancer types rely on reactivation of telomerase to maintain telomere length to keep dividing, telomerase activity regulatory mechanisms have been studied mostly in cancer cells. Since TERT expression is the major telomerase activity limiting factor, telomerase studies in cancer have focused on *TERT* gene expression regulation that is largely divided into transcriptional regulation and post-transcriptional regulation. Transcriptional regulation refers to how the number of pre-messenger and messenger RNAs that are produced in a specific cell type are regulated. Commonly studied mechanisms related to transcriptional regulation are promoter binding transcription factors, chromosomal rearrangements, and epigenetic modifications. *TERT* core promoter consists of 260 basepairs containing GC boxes that bind the zinc finger transcription factor SP1 that upregulates *TERT* transcription and E-boxes that bind both transcriptional enhancers and repressors [81]. In addition to SP1, c-MYC and HIF-1α (HIF: Hypoxia Induced Factor) are also transcription factors that are known to be bound to *TERT* promoter and upregulate transcription of *TERT*. Interestingly, these transcription factors are also regulated by exercise. For instance, HIF-1α is known to mediate adaptive responses to oxidative stress by nuclear translocation and regulation of gene expression [82]. Also, c-MYC and STAT3 are known to be upregulated by exercise [83, 84]. SP1 has been also found to be enriched

in the promoter regions of exercise-responsive genes [85] and these support the activation of *TERT* transcription induced by exercise. When *TERT* promoter is mutated, it can lead to reactivation of telomerase in cancer by increment of *TERT* transcription. For example, recurrent somatic mutation in the *TERT* promoter is found in cancer of central nervous system (43%), bladder (59%), thyroid (follicular cell derived, 10%) and skin (melanoma, 29%) [86] whereas promoter mutation is less frequently found in cancer of lung, stomach, ovary, uterus, kidney and prostate (Kidney [86]; others [87]). The two most common *TERT* promoter mutation found in cancer are C>T transitions at transcription start site also referred as C228T and C250T mutation. This mutation induces an 11-base pair nucleotide fragment that provides a new consensus binding site for E-twenty-six (ETS) transcription factors [88]. *TERT* promoter mutation can be cooperated with mutations on other genes such as BRAF, FGFR3 and IDH. For example, mutation on BRAF results in activation of mitogen-activated protein kinase (MAPK) and/or phosphatidylinositol 3-kinase-serine threonine protein kinase (PI3K-AKT) pathway leading to upregulation of ETS system that eventually accelerates *TERT* expression [89]. However, when one considers the overall number of tumors with *TERT* promoter mutations compared to those without (lung, breast, prostate, colon and pancreas have very small incidence of activating *TERT* promoter mutations) the overall mechanisms of *TERT* activation in cancer cells are still poorly understood. Next, chromosomal rearrangement refers to a type of mutation that results in alteration of chromosome structure. This involves amplification of the *TERT* gene and rearrangement of cis-elements enhancers. In fact, increased *TERT* gene copy number (amplification) was observed in certain types of tumor cell lines and primary tumors

including lung tumors, cervical tumors, breast carcinomas and neuroblastomas [90]. From systematic analysis, 65% of *TERT* promotor structural variants were predicted to be related to repositioning of enhancer elements that activate *TERT* transcription [91]. However, no experimental evidence to date indicates that these rearrangement lead to increased *TERT* mRNA expression or telomerase activity. Lastly, epigenetic modification includes DNA methylation and histone modification. Regarding DNA methylation, two regions near *TERT* gene have been identified: core (proximal) promoter region near *TERT* promoter and ***T****ERT* **h**ypermethlyated **o**ncological **r**egion (THOR) that is located distal to the transcription start site of *TERT* composed of 52 CpG islands [92]. In contrast to common premise that DNA methylation represses gene expression, hypermethylation on these regions have been observed and correlated with increased TERT expression in patients with pediatric brain tumors [93], pancreatic cancer [94] and medullary thyroid carcinoma [95]. When it comes to histone modification, histone acetylation and deacetylation was shown to be a common underlying feature to regulate TERT expression in human cells [96, 97]. Also, *TERT* gene was found to be a direct target of the histone methyltransferase SMYD3 [98]. Lastly, chromatin remodeling has been known to modulate telomerase expression in human cancer cells[99]. Although the production of *TERT* pre-mRNA level can be regulated by the described transcriptional regulation, it does not result in the production of telomerase active TERT without being properly spliced, exported to the nucleus, translated, the TERT protein returned to the nucleus and complexed with the telomerase RNA component and other accessory proteins of the telomerase holoenzyme. The most proximal level of regulation of *TERT*

gene expression following transcription is the splicing of the pre-mRNA to messenger RNA (mRNA).

2.5.2. Alternative splicing regulation of *TERT*

Splicing of genes occurs on newly transcribed pre-RNAs of genes. When a gene is transcribed into a pre-mRNA the exons or coding sequences are separated by non-coding sequences called introns and the transcripts must be processed (spliced) to generate a protein coding unit. To form a mature messenger RNA (mRNA) the introns must be removed or spliced out and the exons joined together in a process called splicing. The central components of splicing in pre-mRNAs are the splice sites, which include the 5' and 3' splice sites and the branch point sequence. These sites collectively mark the boundaries between exons and introns and guide the removal of introns and ligation of exons governed by the splicing machinery, including the spliceosome complex. The spliceosome is a megadalton enzyme complex that is very dynamic and is an energetically dependent to undergo intron excision and exon ligation. The spliceosome consists of a family of small nuclear RNA proteins, splice factors, and RNA binding proteins that dictate splicing choice (i.e., inclusion or exclusion of certain exons and introns). Splicing can be categorized as either constitutive, where all exons are joined in a fixed order, or alternative, a process that produces diverse mature mRNAs from a single pre-mRNA. In a sense, alternative splicing is a mechanism that can achieve tight regulation of functional isoform levels in cells and can generate proteome diversity, both within cells, in response to external cues (heat, hypoxia, nutrients, etc.) and between tissues (generation of tissue specific isoforms). Alternative splicing events

are further categorized into alternative 5’ splice site (i.e., alternative 5' splice sites are selected), alternative 3’ splice site (i.e., alternative 3' splice sites are selected), cassette exon (i.e., one or more exons are either included or excluded in the mature mRNA), mutually exclusive exons (i.e., exons that are mutually exclusive), and retained intron (i.e., intron is not fully excised and remains part of the mature mRNA) (Figure 2.4; [100]). Once all the exons are joined together, the mature mRNA can be exported from the nucleus and translated into protein in the cytosolic ribosomes. The regulation of splicing primarily involves two main components: *cis*-acting elements (*cis*-elements) and *trans*-acting factors (transfactors). *Cis*-element is an RNA sequence that is located in either exons or introns of pre-mRNAs and recruit transfactors to regulate splicing. Transfactor is a type of regulatory protein or molecule that plays a role in the control of splicing decisions. These transfactors interact with the *cis*-elements within the pre-mRNA to influence splice site selection and the inclusion or exclusion of specific exons. Specifically, transfactors can include various types of RNA-binding proteins and other molecules that bind to specific *cis*-elements, such as exonic splicing enhancers (ESEs) and exonic splicing silencers (ESSs), as well as intronic splicing enhancers (ISEs) and intronic splicing silencers (ISSs). By binding to these *cis*-elements, transfactors can either promote or inhibit the splicing of adjacent exons, thereby regulating alternative splicing patterns and ultimately determining the composition of the mature mRNA [100].

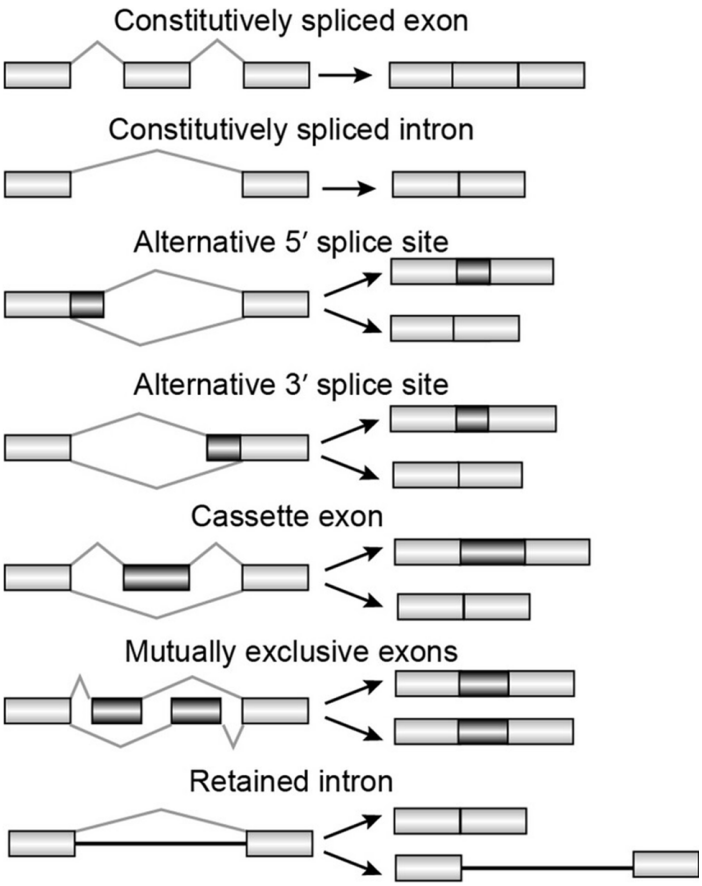

Figure 2.4. A Schematic of constitutive and alternative splicing (adapted from Dvinge, 2018). During constitutive splicing, introns are removed, and all exons are put together in an order. Alternative splicing is divided into categories: Alternative 5' splice site, Alternative 3' splice site, Cassette exon, Mutually exclusive exons, and Retained intron.

Both constitutive and alternative splicing can occur co-transcriptionally or post-transcriptionally. What dictates whether an intron is spliced out co-or post transcriptionally is currently unknown but could be due to a variety of mechanisms including DNA methylation, chromatin marks, RNA polymerase II pausing, RNA polymerase II speed, promoter elements, intron length, splice site strength, RNA secondary structure, and transcriptional rate [101]. No specific data exists to date on

whether *TERT* is co- or post-transcriptionally spliced. However, our pilot data based on BruChase-Seq using bromouridine (Bru) showed that *TERT* RNA still contains introns 2,4,11 and 14 after 6 hours of transcription, and this indicates that *TERT* is post-transcriptionally spliced. From recent work, it is suggested that the majority of the *TERT* RNA is sequestered in the nucleus preventing its translation into protein as a novel regulatory mechanism. Specifically, it has been shown that when *TERT* mRNA/pre-mRNAs retain intron 11 (11th intron) the RNAs are sequestered in nucleus and only exported out to cytoplasm at mitotic phase once intron 11 is spliced out [102]. This mechanism provides an elegant model for the regulation of full-length *TERT* splicing and control of telomerase activity, but it does not explain why cells would alternatively splice *TERT* to so many additional isoforms besides intron 11 retention.

When it comes to genes and their RNA isoforms, the full-length isoform of a gene is commonly the longest protein coding form and most abundant transcript, but this is not always the case as some genes have other isoforms (transcripts) that are more abundant. When splicing occurs in this process, the exons are not always joined together in the same order and this process is called alternative RNA splicing (AS). Specifically, AS can produce different isoforms from a single gene by removing/putting introns/exons in different ways that are catalyzed by the spliceosome and many RNA binding proteins. For example, some exons can be removed to form a mRNA (exon skipping) or some introns can be remained in a mRNA (intron retention). As a result, AS can expand the protein coding capacity of the genome as one gene can form several proteins with similar or even opposing (dominant-negative) functions. AS can also help regulate the amount of full-length mRNAs by coupling AS to non-sense mediated decay

(AS-NMD). The most common AS events are exon skipping, intron retentions, alternative 5' and 3' splicing sites, and mutually exclusive exons. AS generates proteome diversity as nearly 95% of human genes undergo alternative splicing [103]. Since AS functions to control the abundance of protein coding isoforms and to regulate the function of resulting isoforms, it plays a very important role in phenotypes and tissue specific isoform expression and the *TERT* gene is an examples of this type of regulation. During fetal development, high telomerase activity is suppressed as development and tissue specification (i.e., differentiation) proceeds. As a result, most somatic cells lack telomerase activity. Underlying mechanisms are supported by a seminal study carried out by Ulaner et al. [104] showing that telomerase activity during the development is regulated by both transcriptional and post transcriptional gene regulatory mechanisms. During development of human heart, *TERT* transcription became undetectable around 11-13 weeks (transcriptional regulation), whereas alternative splicing extinguished telomerase activity but that *TERT* transcripts were still produced around 17 weeks in fetal kidney development (post transcriptional regulation)[104]. These human fetal tissue development data indicate that *TERT* AS splicing is a regulated and non-random process to control telomerase activity in cells and tissues. Regarding telomerase activity, AS of *TERT* pre-mRNA impacts the amount of telomerase active TERT. *TERT* is a 16 exon 15 intron gene and only full-length *TERT* or *TERT* with all 16 exons in sequence can go on to generate TERT proteins that can form active telomerase (Figure 2.5) [25].

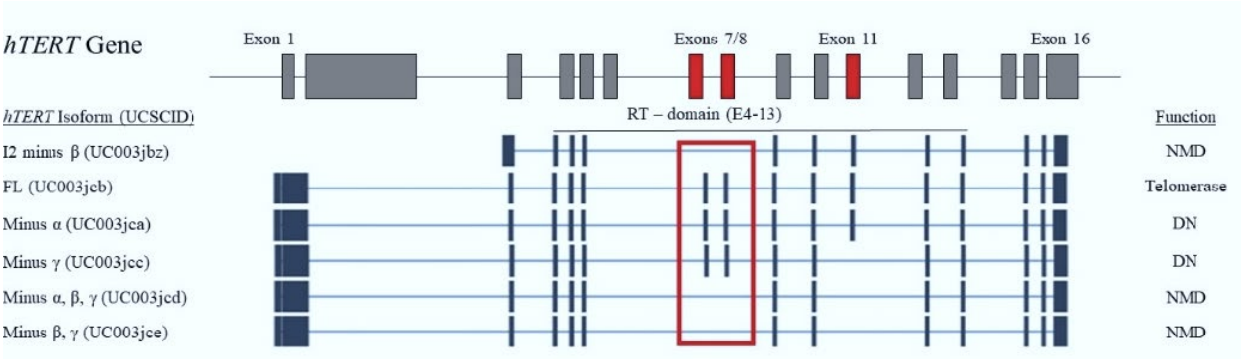

Figure 2.5. A cartoon of *hTERT* gene and alternatively spliced isoforms (adapted from Slusher et al., 2020).

Human TERT (hTERT) gene consists of 16 exons with 15 introns and alternative splicing produces different isoforms. Only full-length (FL) TERT (UCSCID:UC003jcb) can synthesize telomere repeats and other isoforms with skipped exons cannot. Reverse transcriptase (RT) domain includes exon 4 to 13. The most dominant AS event is skipping of exons 7 and 8 which is indicated by red colored box. Some isoforms are degraded by nonsense mediated decay (NMD), or inhibit active telomerase by competing for telomerase RNA component (TR or TERC) and acting as a dominant negative (DN) telomerase. Alpha refers to 36 nucleotides at the 5' end of exon 6, beta refers to exons 7 and 8, and gamma refers to exon 11.

AS of *TERT* is known to produce up to 21 different AS isoforms, some with known functions and others with unknown functions. TERT has several critical protein domains where AS could impact the ability of *TERT* transcripts to form telomerase (TEN (telomerase N-terminus domain), TRBD (Telomerase RNA binding domain), RT (reverse transcriptase domain) and CT (C-terminus domain) shown in Figure 2.6) [28]. For instance, the initial cloning of *TERT* revealed several truncated mRNAs with splicing of the reverse transcriptase (RT) domain of TERT. The RT domain of TERT consists of exons 4-13 and known TERT isoforms with AS events in this domain have shown to

impair telomerase activity. For example, minus alpha (-α or Δα) *TERT* mRNA variant that lacks the first 36 nucleotides of exon 6 is translated to an inactive telomerase and inhibits telomerase by competition with FL TERT for TR molecules and thus resulting in telomere shortening when expressed for sufficient duration in cultured cells [105, 106]. In addition, it was suggested that minus gamma (-γ or Δγ) that lacks exon 11 may have dominant negative effects (reducing telomerase activity) [107]. On the contrary to minus alpha and gamma TERT isoform that are still in-frame after exon skipping (See asterisk in Figure 2.6), some alternative splicing events can induce frame shifting and premature stop codons resulting in lack of telomerase activity. For instance, the most abundant *TERT* exon skipping event occurs at exons 7-8 forming a frameshifted and truncated TERT isoform called minus beta (-β or Δβ) which is either degraded by AS-NMD or a small amount is translated and acts as a dominant-negative telomerase. In fact, Ulaner et al. [104] showed that during fetal kidney development exons 7-8 are skipped from week 17-18 along with the loss of telomerase activity. Another example of frame shifted TERT isoform is shown by Penev et al. [108] that exon 2 is skipped that induces two tandem premature stop codons in exon 3 during stem cell differentiation as a developmental switch to aid in repressing telomerase activity in differentiated somatic cells (Δ2 in Figure 2.6). Why there is such extensive alternative splicing of a low abundant gene like *TERT* is an open question.

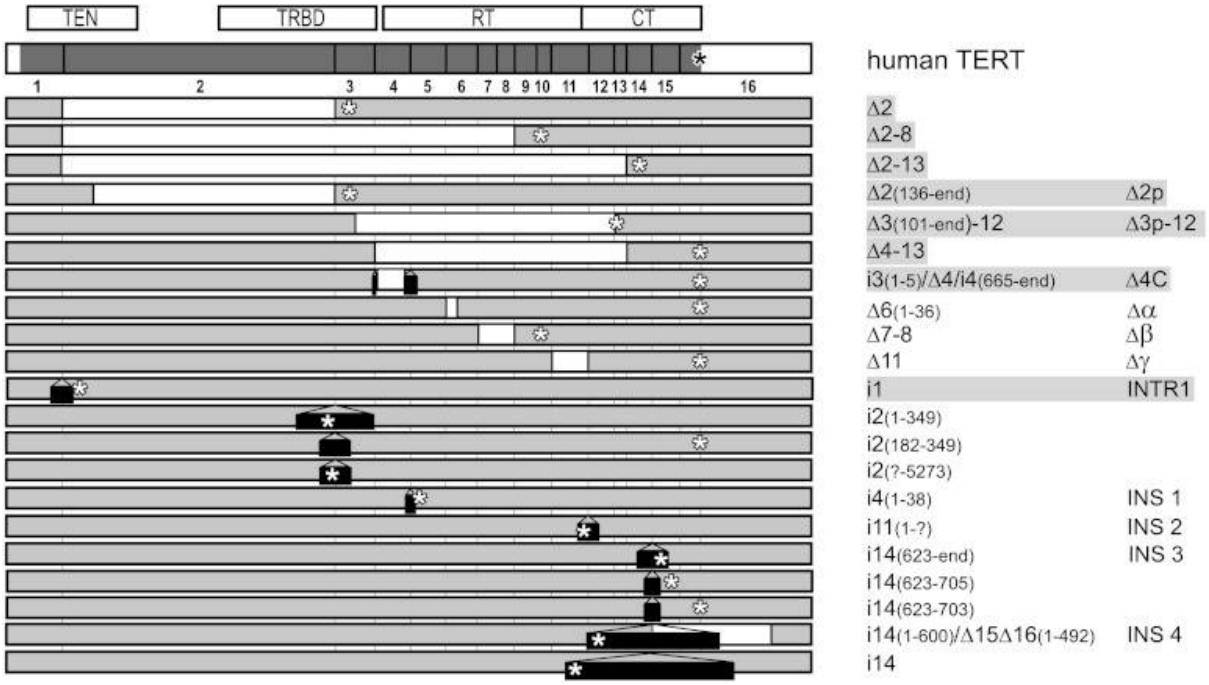

Figure 2.6. 21 TERT AS isoforms. (Asterisks indicate stop codon; Hrdličková et al., 2012).

hTERT gene has critical protein domains including **T**elomerase **E**ssential **N**-terminal domain (TEN), **T**elomerase **R**NA **B**inding **D**omain (TRBD), **R**everse **T**ranscriptase domain (RT), and **C**-**T**erminal **E**xtension (CTE). AS events (exon skipping and intron retention) result in different isoforms and 21 TERT isoforms are depicted in the figure. AS events also induce frame shifting and premature stop codon which is marked as asterisk.

2.5.3. Alternative splicing of *TERT* in aging

Limited evidence has explored how aging could impact the expression and AS of *TERT*. In general, it is thought that TERT expression is decreased with age [109] and that this is likely a cancer protective mechanism. However recent evidence from an in vitro aging model indicated that [110], *TERT* transcript levels increased with advancing passages (a proxy for aging) but none of the transcripts contained the RT domain of

TERT and did not form telomerase active TERTs. No studies to date have performed an analysis of in vitro aged cells or cells/tissue from aged organisms to characterize the TERT AS isoforms that are expressed. This leaves a gap in our knowledge about how telomerase activity is repressed in near senescent cells and tissues. This question would be important to answer considering that if a pre-senescent cell were to splice *TERT* to FL it could progress to an immortal cancer cell.

2.5.4. Alternative function of full-length TERT

Since the canonical function of TERT is to form telomerase and synthesize telomere repeats, other functions of TERT proteins are considered as “alternative functions” or “non-canonical functions” of TERT. The alternative roles of full-length TERT protein that have been identified to date are involved in the modulation of mitochondrial function, to enhance cell proliferation and to participate in key signaling pathways such as Wnt/beta-catenin pathway. Specifically, 10-20% of full-length TERT protein has been shown to be localized to mitochondria and its nuclear export is induced by oxidative stress followed by phosphorylation of tyrosine 707 of TERT by Src kinase family [111]. It has been also found that mitochondrial full-length TERT binds to and protects mitochondrial DNA, which might help to maintain proper electron transport chain function. Also, mitochondrial TERT inhibits endogenous ROS production [112] and apoptosis[113]. Another supporting evidence is that overexpression of Tert in mouse using adeno-associated virus (AAV)-mediated gene therapy and in human iPSC derived

cardiomyocyte altered mitochondrial morphology and dynamics to protect heart/cardiomyocytes from ROS generated by doxorubicin treatment [114].

2.5.5. Alternative function of TERT alternative splicing isoforms

Besides the non-canonical functions of full-length TERT protein, a few of the AS isoforms of TERT have been shown to be functional outside of telomere biology. Among the 16 exons of *TERT*, exons 4-13 are translated into the reverse transcriptase (RT) domain. The TERT isoforms that have manipulated RT domain such as the β-deletion isoform (Δβ or - β) lacking exons 7 and 8, the α-deletion isoform (Δα or -α) lacking the first 36 nucleotides of exon 6, and Δ4-13 isoform lacking exons 4 to 13 have been studied for alternative splicing and alternative functions of TERT. In a study by Dean Betts group, inhibition of Δα or Δβ isoforms in human embryonic stem cells (hESC) promoted spontaneous hESC differentiation and showed that TERT isoform switching is associated with stem cell's pluripotency and differentiation [115]. In a study by the Blackburn group, when a cDNA for the β-deletion isoform was overexpressed in HeLa cells β-deletion protein was detected despite the cDNA containing a premature stop codon and it is expected to undergo nonsense mediated decay. The expressed β-deletion protein was localized to nucleus and mitochondria and protected breast cancer cells from cisplatin-induced apoptosis assumedly by inhibited endogenous telomerase activity [116].

Another isoform of TERT, Δ4-13 has been studied for alternative functions TERT isoforms. This isoform was chosen for study because it was expressed in telomerase negative cells and tissues and was in the original open reading frame, making it likely to

form a truncated TERT protein. Hrdlickova et al., found that the Δ4-13 isoform was detected in both telomerase positive and negative human cells and overexpression of the Δ4-13 isoform induced elevated proliferation rates in several cell types by stimulation of Wnt signaling pathway [28]. They used a TERT antibody targeting the c-terminus of TERT and confirmed protein expression after overexpression of the isoform in Saos2 and U2OS, that are two cancer cell lines without telomerase activity. They also observed reduction of proliferation by transfection of delta 4-13 targeting siRNAs in U2OS. These data indicate that AS of *TERT* plays several functional roles: 1) to regulate the amount of FL TERT to regulate telomerase activity; 2) to generate dominant-negative proteins to regulate telomerase and telomere length; and 3) to generate proteins with functions outside of telomere biology.

2.5.6. Mouse model to study telomerase regulation

Mouse models have been used to study telomerase regulation and to compensate for limited accessibility of human tissues and cells. In contrast to human somatic tissues that express undetectable or low levels of telomerase and TERT, *Mus musculus*, mice used in research laboratories have wide range of somatic tissues expressing robust levels of telomerase activity and TERT [117]. Mouse cells have longer telomeres than human cells and telomere attrition is not a major cause of cellular senescence [118]. Also, mouse cells are more prone to transform to cancer than human cells at least in part due to longer telomeres and constitutive TERT expression and telomerase activity [119, 120]. To understand the underlying mechanisms of species-

specific telomerase regulation, a hTERT-BAC (Bacterial Artificial Chromosome) mouse model which expresses the complete human *TERT* gene in mouse cells was generated [121]. The BAC clone contains the ~ 54-kb *hTERT* gene including an 11-kb upstream region, all of the exons and introns, and 1.2-kb downstream region. By measuring the expression level of mouse *Tert* (*mTert*) and *hTERT*, it was confirmed that expression of *hTERT* in the transgenic mouse is repressed and mimics *hTERT* expression patterns in human cells. They also compared the promoter sequences of two species to find regulatory *cis*-element differences. They found non-conserved GC-box in the human proximal promoter of *TERT* that were absent in the mouse *Tert* proximal promoter. Specifically, they then induced mutations on the *hTERT* promoter and *mTert* promoter including GC-boxes (putative Sp1 sites), putative E2F-binding sites, canonical and noncanonical E-boxes, putative Ets-binding sites, and putative binding sites for a zinc-finger repressor CTCF and identify the non-conserved GC-box located at –31 to –24 in the *hTERT* promoter as the human-specific repressive element. They concluded that the *cis*-elements on the human promoter were repressors of *TERT* transcription that were lacking from the mouse promoter leading to higher *mTert* mRNA expression and thus telomerase activity in the mouse somatic cells [121]. One drawback of the transgenic mouse model is that telomerase activity was unable to be explored because hTERT cannot be assembled into mouse telomerase due to its incompatibility with other mouse telomerase components such as mouse TR. Nonetheless, the hTERT-BAC construct includes all exons and intron sequences and this makes the mouse model applicable to study regulation of *TERT* such as alternative splicing. Additional studies have utilized transgenic models expressing *mTert* in human cells or chimeric

mTert/hTERT (interchange of hTERT promoter with *mTert* promoter, and human introns 2 and 6 added into the mouse *Tert* genomic locus) in both human cells and mouse cells [122, 123] and shown the importance of genomic context, not only the promoter, in regulating TERT expression. However, alternative splicing regulation of *TERT* was not studied in the transgenic mouse model until our recent publication.

2.6. Telomeres and telomerase in exercise

This section (2.6) is adopted from a non-final version of an article published in final form in Exercise and Sport Sciences Reviews, with Jeongjin Kim as the first author [19].

2.6.1. Telomeres in exercise

Two seminal studies pointed out that moderately active adults across the age-span tended to have longer telomeres [124, 125]. Cherkas et al. 2008 measured leukocyte telomere length and collected self-reported physical activity levels in a large cohort of individuals, including twins. These data indicated a positive linear relation between telomere length and physical activity level [125]. Similarly, Ludlow et al. 2008 reported a positive linear relation between peripheral blood mononuclear cells (PBMC) telomere length and exercise energy expenditure up to moderate levels of physical activity [124]. However, a subgroup of self-identified as “Master’s Athletes” that performed greater than 8 hours per week of exercise had shorter telomeres compared to age-matched moderately active participants [124]. This observation led to the

conclusion that the relation between exercise and immune cell telomere length could have an “inverted U” shape, meaning there appears to be a “Goldilocks level” of physical activity/exercise that results in telomere maintenance; too much and too little exercise result in accelerated telomere shortening. Several other reports have replicated this “inverted U” finding [126], while others have observed a linear relationship between exercise amount [127, 128], while other reports have not observed a relation [129, 130]. These inconsistent results point to the need for more carefully controlled studies and the need for standardized reporting of exercise variables and telomere length measurements. A potential explanation for these discrepant results could be recall bias of physical activity, degraded DNA samples, and other physiological or psychological variables that were not statistically controlled for such as psychological stress or cortisol levels [131].

Beyond survey-based physical activity research presented above, the gold-standard measure of physical fitness, maximal oxygen consumption (VO_{2max}) has been associated with telomere length in several studies. For instance, measuring telomere length between athletes and non-athletes finds a positive association between VO_{2max} and telomere length. Endurance trained athletes who have a greater VO_{2max} have been observed to have longer telomeres compared to age-matched controls in a variety of human tissues (skeletal muscle [132] and leukocytes [133, 134]). Implementing an endurance exercise training program has also been observed to increase VO_{2max} and maintain telomere length as well in a variety of human tissues (leukocytes [135, 136] and skeletal muscle [137]). On the other hand, two other studies have found no association between VO_{2max} and leukocytes telomere length [138, 139]. Several factors

could have led to these mixed findings such as the training age (how many years of training), biological age of the subjects, the intensity of the training (elite performance versus health and fitness), the tissue type analyzed (i.e., immune cells versus skeletal muscle), and telomere length measurement techniques employed (PCR, southern blot, fluorescence in situ hybridization). Nonetheless, several meta-analyses of telomere length and exercise related variables have recently been published [129, 130, 140, 141], highlighting that there appears to be a moderately strong relationship between exercise and telomere length. Considering that one or a few very short telomeres lead to cellular senescence, new methods that measure the quantity of shortest telomeres could produce additional insights. In summary, current literature supports that exercise most likely attenuates age-related telomere shortening, but the exact dose of exercise and impacted tissues need further elucidation and research. Additionally, more functional outcomes such as cellular senescence markers (beta-galactosidase, p53, p21 and p16 expression, TAFs/TIFs) [142], indicators of DNA damage, expression of DNA repair proteins/enzymes, and their associations with telomere length and exercise should be documented.

Following up on the epidemiological/cross-sectional study in humans [124], Ludlow et al. evaluated the impact of long-term exercise (44 weeks) on telomere dynamics in a wild-derived short telomere mouse model (CAST/EiJ) over the course of one year [143]. Telomere length was measured in skeletal muscle (gastrocnemius), cardiac muscle (ventricles), and liver from three groups of mice; sedentary young (8 weeks of age), sedentary older (52 weeks of age) and older active mice (52 weeks of age with access to running wheel). Liver, heart, and skeletal muscle were examined for

telomere length. In both liver and cardiac muscle, it was observed that one-year-old sedentary mice had the shortest telomere length and that the one-year-old exercised mice were not different from the sedentary young animals. In contrast in skeletal muscle, the young animals and the sedentary one-year old animals had similar telomere lengths, while the one-year-old exercise group exhibited significant telomere shortening, indicating a tissue-specific response to the exercise stimulus. Similar to these observations, Collins et al. 2003 observed overtrained athletes had shorter skeletal muscle telomeres compared to age-and-training matched healthy athletes [144]. In a follow up study by the same group in healthy athletes, training volume and years spent training were also associated with shorter skeletal muscle telomeres [145]. These authors speculated that the shorter telomeres in the more active individuals could be due to the addition of muscle fiber nuclei with shorter telomeres following satellite cell replication to repair exercise-induced muscle fiber injuries [146]. Alternatively, rather than satellite cell replication, which is unlikely to occur in response to voluntary wheel running [147] or typical endurance running training in humans, exercise-induced oxidative stress could have impacted telomere length and telomere dynamics in the skeletal muscles. Ludlow et al. followed this rationale because the nucleotide guanine (G), which telomeres are rich in (TTAGGG), is very sensitive to oxidative damage forming 8-oxoguanine (8-oxoG). Oxidized guanine has been shown to accumulate in telomeric regions, is associated with induction of cellular senescence phenotypes, and increases in aging humans [69, 148]. When a common oxidizing agent (hydrogen peroxide) was treated isolated flexor digitorum brevis muscle fibers with for five days and subsequently analyzed telomere length, oxidant-induced telomere shortening was

observed in muscle fibers from both mouse strains, and it was partially rescued by the antioxidant N-acetyl-cysteine [149]. These data indicate that telomere damage-induced shortening could occur by exercise-induced oxidative stress rather than a cell replicative mechanism for telomere shortening in post-mitotic muscle fibers. It is important to highlight several recent lines of evidence that indicate the importance of telomeres in senescence of long-lived post-mitotic cells such as skeletal muscle [150] and cardiac muscle [151].

2.6.2. Telomerase activity regulation in exercise

Measuring telomerase activity can provide interesting insights about exercise and mechanistic insights into how exercise may delay or prevent telomere shortening. Many of the initial telomere biology and exercise reports focused mainly on telomere length and did not measure telomerase activity, most likely since measuring telomerase activity is challenging due to its low abundance in adult somatic cells and problematic PCR-based techniques. However, certain adult cell types, such as immune cells (i.e., T cells) can express *TERT* and telomerase when physiologically perturbed [152]. There is also strong evidence that exercise is a potent immune perturbation resulting in immune cell proliferation [153]. In fact, previous studies have indicated increased telomerase activity in immune cells following exercise interventions. In 2009, Werner et al. showed that older athletes had higher levels of PBMC telomerase activity compared to both young and aged sedentary controls, while similar telomerase activity to younger athletes [154]. More recently, Werner et. al., 2019 showed that both acute aerobic exercise and aerobic exercise training increased telomerase activity in immune cells of study participants

[136]. However, whether the telomerase activity is upregulated transiently after exercise or basal telomerase activity becomes chronically higher in trained individuals even in resting state remains still unclear because the studies referenced above either were specifically designed to measure the acute effects of exercise or did not report the conditions under which the cell samples were collected. Meaning it is unknown if the participants could have exercised within a short period of time prior to the sample collections. Similarly in humans, Hagman et al. first illustrated that regular exercise training (soccer) significantly increased telomerase activity in mononuclear cells of young athletes compared to the age-matched sedentary cohort [155]. When telomerase activity was measured by Ludlow et al. in PBMCs from older adults with a wide variety of physical activity levels, it was similar between sedentary and more physically active older individuals [124], in contrast to the above data. A recent meta-analysis and systematic review was performed on this topic by Denham and Sellami and indicated that both acute exercise and long-term exercise training increase telomerase activity in various tissues of mammals [156]. However, having constantly increased levels of telomerase activity in cells may not be beneficial. For instance, if a cell has a checkpoint mutation or other precancerous lesion having unregulated telomerase activity could promote cancerous formation. Telomerase activity needs to be tightly regulated in an on-off fashion to restrain uncontrolled proliferation. This type of telomerase regulation is observed in antigen-stimulated immune cells [152], thus it is important to understand if telomerase regulation (i.e., ability to turn telomerase on and off again) is improved with exercise or not, not just whether telomerase activity is higher or lower.

2.6.3. TERT expression by acute aerobic exercise and aerobic exercise training

Changes in *TERT* mRNA levels following exercise have been documented by several groups. Ludlow et al. previously documented that 44 weeks of exercise training in mice (CAST/EiJ mice) induced an increase of mouse telomerase reverse transcriptase (*mTert)* mRNA levels in skeletal muscles when compared to sedentary animals [143]. In a subsequent study, the same group found that an acute bout of treadmill exercise (~60 - 70% of maximal speed) elicited an increase in *mTert* mRNA levels, concurrent with an increase of telomerase enzyme activity in the hearts of female C57BL/6 mice [157]. Studies by Werner et al. similarly indicated that three weeks of voluntary wheel running was sufficient to increase protein levels of mouse TERT in rodent mononuclear cells, aortic endothelial cells, aortas, and cardiac tissue [154, 158]. Werner's team further showed that endothelial nitric oxide synthase and insulin-like growth factor-1 signaling were important for the exercise induction of mouse TERT protein expression and telomerase activity. Since these studies, several groups have utilized human peripheral blood mononuclear cells (PBMCs) and determined that an acute bout of aerobic exercise increased human *TERT* mRNA expression [159, 160].

2.6.4. Exercise effects on TERT alternative splicing isoforms

The post-transcriptional regulation of *mTert* is different than *hTERT*. Sayed et al. recently utilized long-read RNA sequencing of targeted amplicons (PCR-targeted *TERT* amplification) to compare the AS isoforms of *TERT* in human cancer cells (HeLa) against mouse immortal cells (NIH 3T3) [27]. The findings of targeted long-read sequencing analysis revealed, for the first time, that the majority (>85%) of *mTert*

transcripts were spliced to the telomerase activity-coding FL *mTert*, while most *hTERT* transcripts were AS to non-telomerase-coding *hTERTs* (>60%). These differences in mouse and human *TERT* regulation force researchers to carefully interpret their results from exercise interventions on *TERT* and telomerase when investigating both cells/tissues for either humans or rodents.

To study *hTERT* expression, AS, and regulation in tissues difficult to obtain from humans, a transgenic mouse model can be used as the mouse model expresses the human *TERT* gene (*hTERT*) including the 5' and 3' regulatory sequences, exons and introns [121]. This mouse model, commonly referred to as the hTERT bacterial artificial chromosome (hTERT-BAC) mouse, served as an in vivo model to study the gene expression regulation of *hTERT* in tissues following environmental exposures. Importantly, this mouse model recapitulated the expression pattern of *hTERT* as observed in human tissues (i.e., repression of *hTERT* in somatic cells besides the testis and thymus) [29, 121]. Also, the splicing patterns of *hTERT* were preserved indicating that the mouse splicing machinery recognized the human gene-splicing elements like the human splicing machinery does. However, several limitations should be mentioned with this mouse model. First, *hTERT* proteins cannot form active telomerase complexes with mouse telomerase RNA [161], thus no telomerase activity changes will be formed by changes in *hTERT* expression in the mouse tissues/cells. Second, telomere length regulation still occurs by endogenous mouse *Tert* (*mTert*) and mouse telomerase, limiting our ability to measure telomere length changes by interventions.

Recently, Slusher et al. utilized the hTERT-BAC mouse model and performed an aerobic (treadmill running) exercise to begin understanding how exercise impacts AS of

hTERT mRNAs [29]. The mice ran on a treadmill for 30 minutes at 60% maximum speed and tissues were collected immediately following, 1-, 24-, 48-, and 72-hours following the exercise bout (i.e., in recovery) and compared to control animals that were exposed to a motionless treadmill for 30-minutes and tissues immediately harvested. FL *hTERT* (exons 7/8 included) and minus beta *TERT* (skipping of exons 7/8 indicated by 6/9 junction primers) were measured by RT-PCR in skeletal muscle, cardiac muscle, and the brain. In comparison to the no exercise condition, an overall increase in *hTERT* mRNA was observed at 1-hour post-exercise in the skeletal muscle samples. Splicing ratios were also altered in the skeletal muscle with a significant increase in FL during recovery (72-hours). In contrast, the cardiac muscle (left ventricle), had a different AS pattern but a similar increase in *hTERT* transcripts. The percentage of FL *hTERT* coding transcripts in comparison to total *hTERT* decreased in recovery from exercise (1-, 24-, and 48-hours). Minimal changes were observed in the brain, but this does not rule out that specific regions of the brain may be better targets for future analysis (i.e., hippocampus, nucleus acumbens, or caudate). These tissue-specific responses led to the hypothesis that hTERT and its isoforms likely play specific roles in certain tissues and contexts. While further research will be needed to elucidate the functions of these TERT isoforms in cardiac versus skeletal muscle, these data support the hypothesis that TERT and telomerase are a part of the exercise induced adaptations.

2.6.5. Impact of exercise on shelterin

Another area of exercise and telomere biology that has been investigated is how shelterin components are impacted by exercise. Werner et al. 2008 first documented

that exercise (voluntary wheel running for three weeks) impacted *Terf1* (TRF1) and *Terf2* (TRF2) shelterin mRNA and protein expression in cardiac tissues [158]. Ludlow et al. followed this up with tissues collected from one-year-old mice, which underwent 48 hours of exercise washout following 44 weeks of voluntary wheel running [143]. In this research study, expression of shelterin components was analyzed at the mRNA and protein levels (for *Terf1* (TRF1) and *Terf2* (TRF2)) in skeletal muscles, liver, and cardiac muscle (left ventricle). In the liver tissue, a few changes in the expression of shelterin components was observed indicating that neither age nor exercise had a striking impact on this tissue. In cardiac muscle, however, shelterin changes were more pronounced, while age overall resulted in reduced shelterin expression that was attenuated in exercised animals. This indicates that exercise (voluntary wheel running) results in favorable remodeling of telomere biology, likely resulting in part of the exercise-induced cardioprotective phenotype. In the skeletal muscle, muscle-specific effects were observed between the extensor digitorum longus (EDL) and plantaris muscle for expression of *Terf1* (TRF1) and *Terf2* (TRF2). The plantaris muscle from older sedentary animals had increased expression of TRF1 compared to the older exercised animals and young animals, while minimal changes in TRF1 levels were observed in the EDL. Interestingly, overexpression of TRF1 in dividing cells results in progressive telomere shortening [162]. Therefore, exercise may help maintain telomeres by attenuating an age-related increase in TRF1 protein.

To study the initial signaling mechanisms that could be driving the adaptive process associated with changes in telomere biology induced by exercise, Ludlow et al. utilized an acute exercise model in mice, specifically a bout of treadmill running followed by

analysis of tissues in recovery from exercise to explore how these two variables impacted expression of shelterin components [157]. Ludlow et al. investigated shelterin expression in three groups of mice; a sedentary control group, and two groups that underwent an intensity controlled (60% of maximal running speed on the treadmill) 30-minute bout of exercise and had tissues collected either immediately following exercise or 1-hour post exercise [157]. *Terf1* mRNA levels were significantly reduced immediately following exercise in the plantaris muscle, recapitulating training-induced effects. In addition, increased p38 MAPK activation (phosphorylation) was correlated with changes in *Terf1* mRNA levels. When C2C12 mouse myotubes were treated with calcium ionophore, it resulted in increased p38MAPK phosphorylation and reduced levels of *Terf1* mRNAs, recapitulating exercise phenotypes. These results support that the increased intracellular calcium-associated with muscle contractions during exercise results in increased activation (phosphorylation) of p38 MAPK and reduced mRNA levels of *Terf1* in rodent skeletal muscle. In the hearts of these same mice, Ludlow et al. measured shelterin protein levels and mRNA levels of DNA repair and response genes (*Chk2* and *Ku80/Xrcc5*) [157]. In contrast to skeletal muscle, increased TRF1 and TRF2 protein and mRNA levels, greater expression of DNA-repair and -response genes (*Chk2* and *Ku80/Xrcc5*) and greater protein content of phosphorylated p38 MAPK were observed at immediately post-exercise compared with both controls and 1-hour post-exercise animals [157]. These data provide insights into how physiological stressors remodel the heart tissue and how an early adaptive response mediated by exercise may be maintaining telomere length and/or stabilize the heart genome through the upregulation of telomere-protective genes.

Chapter 3 – Intronic Cis-Element DR8 in hTERT Is Bound by Splicing Factor SF3B4 and Regulates hTERT Splicing in Non-Small Cell Lung Cancer

Slusher, A. L., **Kim, J. J.**, Ribick, M., Pollens-Voigt, J., Bankhead III, A., Palmbos, P. L., & Ludlow, A. T. (2022). Intronic Cis-Element DR8 in hTERT Is Bound by Splicing Factor SF3B4 and Regulates hTERT Splicing in Non–Small Cell Lung Cancer. *Molecular Cancer Research*, *20*(10), 1574-1588.

3.1. Abstract

Splicing of the *hTERT* gene to produce the full length (FL) transcript is necessary for telomerase enzyme activity and telomere-dependent cellular immortality in the majority of human tumors, including non-small cell lung cancer (NSCLC) cells. However, the molecular machinery to splice *hTERT* to the FL isoform remains mostly unknown. Previously we reported that an intron 8 *cis*-element termed ‘direct repeat 8’ (DR8) promotes FL *hTERT* splicing, telomerase and telomere length maintenance when bound by NOVA1 and PTBP1 in NSCLC cells. However, some NSCLC cells and patient tumor samples lack NOVA1 expression. This leaves a gap in knowledge about the splicing factors and *cis*-elements that promote telomerase in the NOVA1 negative context. We report that DR8 indeed regulates FL *hTERT* splicing in the NOVA1 negative and positive lung cancer contexts. We identified splicing factor 3b subunit 4 (SF3B4) as an RNA *trans*-factor whose expression is increased in lung adenocarcinoma (LUAD) tumors

compared to adjacent normal tissue and predicts poor LUAD patient survival. In contrast to normal lung epithelial cells, which continued to grow with partial reductions of SF3B4 protein, SF3B4 knockdown reduced *hTERT* splicing, telomerase activity, telomere length, and cell growth in lung cancer cells. SF3B4 was also demonstrated to bind the DR8 region of *hTERT* pre-mRNA in both NOVA1 negative and positive NSCLC cells. These findings provide evidence that DR8 is a critical binding hub for *trans*-factors to regulate FL *hTERT* splicing in NSCLC cells. These studies help define mechanisms of gene regulation important to the generation of telomerase activity during carcinogenesis.

3.2. Introduction

Telomeres (5'-TTAGGG$_n$) cap the ends of linear chromosomes [11] and shorten by 50-200-nucleotides with each cell division [12, 163, 164]. This "end replication problem" is partially compensated by the telomerase enzyme [165]. Telomerase activity is repressed during human development and in adult somatic cells [13, 166], which leads to progressive telomere shortening. Telomere shortening and replicative senescence serve as key barriers to prevent somatic cell progression to malignant cancer cells [167-169].

A telomere maintenance strategy must be adapted for cancer cells to become immortal. The majority of human cancers (~85%) including lung cancers, reactivate the telomerase enzyme to maintain short telomeres in cancer cells [13, 170, 171]. Telomerase is a near universal target for cancer therapeutic strategies. Despite intense efforts to develop telomerase inhibitors, such therapies are not currently available. The telomerase enzyme consists of the telomerase RNA template (*hTERC*), the protein catalytic subunit telomerase reverse transcriptase (*hTERT*), and numerous accessory proteins [78, 172, 173]. Quantitative analysis demonstrates that telomerase-positive cells express between 11,000 and 112,000 *hTERC* RNA molecules and between 1 and 30 *hTERT* mRNA molecules per cell [174, 175]. Although both *hTERC* and *hTERT* mRNA levels increase in cancer cells [174], *hTERT* is commonly identified as the rate-limiting component of active telomerase in cancer cells [176]. These findings highlight the importance of *hTERT* as a potential target to attenuate cancer progression and survival.

The majority of research on *hTERT* expression in cancer cells has focused on transcriptional regulation [93, 177, 178]. However, our laboratory and others have shown that additional RNA-processing mechanisms, such as alternative RNA splicing, provide another level of regulatory control contributing to *hTERT* expression and telomerase reactivation [26, 27, 102, 108, 179]. The *hTERT* gene contains 16 exons that must all be present in sequence to produce the full length (FL), catalytically active transcript necessary to generate telomerase activity [179]. The FL isoform represents the minority of the transcriptional output of *hTERT* [174] as the majority of *hTERT* transcripts are alternatively spliced. The major alternative splicing variant (ASV) is the minus β isoform which skips exons 7 and 8 of the reverse transcriptase (RT)-domain. While alternative RNA splicing is tightly regulated during embryonic development and in adult somatic cells, cancer is associated with aberrant splicing [180]. Underscoring the importance of understanding *hTERT* alternative splicing regulation is the recent data that alternatively spliced isoforms of *hTERT* exist in normal cells and help repress the production of the FL isoform by shunting transcripts to be degraded or towards low abundant isoforms lacking telomerase activity [28, 108]. Thus, stem cells and normal cells appear to have regulated *hTERT* expression and alternative RNA splicing (AS) while *hTERT* expression and AS is dysregulated in cancer. Therefore, understanding the regulation and dysregulation of *hTERT* may reveal new telomerase inhibitor development opportunities.

The *hTERT* gene contains an intronic *cis*-element located within intron 8 termed direct repeat 8 (DR8) that is essential for the regulation of *hTERT* FL splicing [27, 181]. Our group recently discovered that the RNA-binding protein NOVA1 binds to DR8 and

recruits the polypyrimidine-tract binding protein 1 (PTBP1) to DR8 to promote FL *hTERT* splicing, telomerase enzyme activity, telomere length maintenance, and sustain the growth and survival of non-small cell lung cancer (NSCLC) [26, 27]. In the present study, we utilize TCGA lung adenocarcinoma (LUAD) patient data to show that *hTERT* is expressed in both matched tumor adjacent normal tissue and in tumor samples. Our data indicate that tumor adjacent normal samples lack FL *hTERT* expression, but that FL *hTERT* is expressed at significantly higher levels in the tumor samples. These data highlight the importance of splicing regulation changes in addition to transcriptional mechanisms that result in FL *hTERT* specifically in cancer cells. In addition, we demonstrate that CRISPR-mediated DR8 deletion *in vitro* reduces FL *hTERT* splicing, attenuates telomerase activity, shortens telomere length, and attenuates cell growth in Calu6 (a NOVA1 negative NSCLC cell line). Finally, we identified splicing factor 3b subunit 4 (SF3B4) as an RNA binding protein upregulated in NSCLC patient tumor samples in the TCGA LUAD cohort, and that increased SF3B4 expression is associated with poor survival outcomes compared to lower expressing tumor samples. We demonstrate that SF3B4 also binds to the DR8 region of *hTERT* pre-mRNA in H1299 and Calu6 NSCLC cells, and that SF3B4 knockdown reduces FL *hTERT* splicing and telomerase enzyme activity in a NOVA1 independent fashion.

3.3. Materials and Methods

3.3.1. Plasmids

As previously performed [26], we deleted hTERT DR8 by using guide RNAs flanking DR8 (pre-DR8 guide—5′-ATCTGCTTGCGTTGACTCGC-3′ and post DR8: 5′-TTATTTTCGGGAAGCGCTAT-3′) and cloned these guides into PX458 [182], which were a gift from Feng Zhang (Addgene plasmid # 48138; http://n2t.net/addgene:48138; RRID:Addgene_48138). To express hTERT (pBABE lox-hTERT-lox – puro, RRID:Addgene_111380), retrovirus was made by co-transfecting 5 μg of proviral hTERT plasmid and 2 μg of packaging plasmids pMD2.G and pCMV-VSV-G (RRID:Addgene_8454) using Lipofectamine 3000 (Invitrogen, Carlsbad, CA) into 293T cells (RRID:CVCL_0063). For the rescue experiment, siRNA resistant (resistant to all three siRNAs used in this study, cDNA was codon optimized) SF3B4 plasmid with Flag tag on C-terminus was designed and generated by GeneArt Gene Synthesis (Invitrogen) based on the SF3B4 mRNA sequence (NM_005805.5) and inserted into pcDNA3.1+ mammalian expression vector. To generate an empty control vector for our experiments, SF3B4 was excised with restriction enzymes (BamHI and XhoI) and standard procedures were used to ligate and clone the resulting empty (lacking the SF3B4 ORF) pcDNA 3.1+ FLAG plasmid.

3.3.2. Cell Culture and Cell Lines

NSCLC cell lines (A549 (RRID:CVCL_0023), Calu6 (RRID:CVCL_0236), Calu6 with stable hTERT expression (derived in laboratory) and NCI-H1299 (RRID:CVCL_0060)) were maintained in culture at 37°C in 5% CO_2 in 4:1

DMEM:Medium 199 supplemented with 10% cosmic calf serum (HyClone, Logan, UT). All unmodified cell lines were obtained from American Type Culture Collection (ATCC, Manassas, VA). Human bronchial epithelial (HBEC, primary ATCC - PCS-300-010) and HBEC3-KT cells (ATCC - CRL-4051, RRID:CVCL_X491) were maintained in bronchial epithelial growth media (ATCC - PCS-300-030) supplemented with a bronchial epithelial cell growth kit (ATCC - PCS-300-040) on collagen coated plates (porcine gelatin, Sigma). Cell line identity was verified by the vendor (ATCC).

3.3.3. Animals

Crl:NU(NCr)-Foxn1^{nu} athymic nude mice (~4-6 weeks old, RRID:RGD_5508395) were purchased from Charles River (Wilmington, MA). All animal experiments were approved by the University of Michigan Institutional Animal Care and Use Committee (IACUC) and conducted as per the institutional guidelines.

3.3.4. Xenograft

Single cell clones from the H1299 NSCLC cell line with either YCAY to YAAY mutations or full deletion of the DR8 region within intron 8 of the *hTERT* gene using CRISPR/Cas9 were utilized [26]. Cells were cultured and a total of $1.0 \cdot 10^6$ cells in 100 µL of 1x PBS were injected subcutaneously into both hind flanks of athymic NRC nu/nu mice (2 injections per mouse). Body mass and tumor volumes were monitored by digital scale and caliper, respectively, twice weekly. Tumor volume was calculated according to the following formula: volume = (width^2 x length)/2. Three types of control clones were

used: Control clone 1 = H1299 parental cells; control clone 2 = Single cell sorted clone; control clone 3 = Cas9-no guide vector transfected and sorted wild-type clone.

3.3.5. RT-Droplet Digital PCR

RNA was extracted using RNeasy® Plus Mini Kit (Qiagen, Hilden, Germany) then cDNA synthesized using SuperScript IV First-Strand cDNA Synthesis System (Invitrogen,). All cDNAs were diluted to 1:4 using nuclease-free water and stored at −20 °C until analysis of *hTERT* and SF3B4 expression levels (Supplemental Table 3.1) by droplet digital PCR (ddPCR; Bio-Rad, Hercules, CA). For *hTERT* alternative splice variant analyses, diluted cDNAs were used within 48 hours of production in ddPCR reactions. Total *hTERT* gene expression levels were determined by summing the absolute quantification of the exon 7-8 containing transcripts plus exon 7-8 skipping transcripts (determined by exon 6-9 junction RT-ddPCR). Full length and alternatively spliced *hTERT* percentages were determined according to the following formulas: Percent Potential FL = Exon 7-8 containing transcript / Total transcript; Percent alternatively spliced = 100 – Percent Potential FL. Absolute values of *hTERT* transcripts containing exons 7/8 or exons 6/9 (minus β) as determined by ddPCR are shown in supplemental figures.

3.3.6. Droplet Digital TRAP Assay for Telomerase Activity

Quantification of telomerase enzyme activity was determined by the droplet digital TRAP assay [183, 184]. In brief, a $1.0 \cdot 10^6$ cell pellet was lysed in NP-40 lysis buffer, diluted to a final concentration of $1.25 \cdot 10^3$ cells/μL, and 1 μL added to an extension reaction (50 cell equivalents per μL) for 60 min followed by a 5 min heat inactivation of

telomerase at 95°C. An aliquot (2 μL) of extension products containing an equivalent of 100 cells was amplified in a droplet digital PCR for 40 cycles. Droplet fluorescence intensity and number were read and counted on the QX200 Droplet Reader (Bio-Rad). Data were calculated to represent telomerase extension products per cell equivalent.

3.3.7. Terminal Restriction Fragment Assay for Telomere Length Analysis

The average length of telomeres (terminal restriction fragment lengths) was measured as previously described [185] with the following modifications: A DIG-labeled DNA molecular weight marker II ladder was loaded on either side of the samples (Millipore Sigma, St. Louis, MO). DNA was transferred to Hybond-N+ membranes (GE Healthcare, Piscataway, NJ) using overnight transfers. The membrane was briefly air-dried and DNA was fixed by UV-crosslinking. Membranes were then probed for telomeres using a digoxigenin (DIG)-labeled telomere probe, detected with a horseradish peroxidase-linked anti-DIG antibody (Cat no. 11093274910; Roche, Basel, Switzerland, RRID:AB_2734716), exposed with CDP-star (Cat no. 11759051001; Roche), and imaged (Chemidoc XRS + Molecular Imager, Bio-Rad).

3.3.8. Genome-Editing and Engineering (CRISPR/Cas9)

H1299 DR8 mutant and DR8 deletion cell lines were previously generated and described [26]. Two guide RNAs were designed to delete *hTERT* DR8 (pre-DR8 guide: 5'-ATCTGCTTGCGTTGACTCGC-3'; post-DR8 guide: 5'-TTATTTTCGGGAAGCGCTAT-3'). Guide RNAs were cloned into PX458 (Plasmid #48138: pSpCas9[BB]-2A-GFP; Addgene, Watertown, MA). Cells were simultaneously transfected with two guide RNAs

using Lipofectamine 3000 (ThermoFisher Scientific, Waltham, MA) and flow sorted into individual wells of a 96-well plate 48 hours post transfection for the top 5% green fluorescent protein (GFP)-positive cells. Wells with growing single cell clones were scaled up stepwise to a six-well plate then a 10 cm dish upon reaching confluence. Finally, cells were collected for DNA extraction and genotype analysis of CRISPR mutation validation using PCR with primers designed to identify the presence or deletion of the 480-bp sequence containing DR8 of *hTERT* (Supplemental Table 3.1). Sanger sequencing was also utilized to verify that recombination occurred between two *hTERT* alleles and not a different sequence within the genome.

3.3.9. Transient siRNA and Rescue Experiments

Cell lines were plated at a density of $2.5 \cdot 10^5$ cells (Calu6 TERT OE), $3.0 \cdot 10^5$ cells (Calu6), or $4.0 \cdot 10^5$ cells (A549, H1299, HBEC-3KT, and primary HBEC) per well in a 6-well plate for 24 hours. Cells were then transfected for 48 (A549) or 72 hours (Calu6, H1299, Calu6 TERT OE, HBEC-3KT, and primary HBEC) with 10 nM of either non-silencing controls (sc-37007) or a pool of three siRNAs targeting SF3B4 (sc-38313; sense RNA sequences – 1) 5'-CUGAGAUUGAUGAGAAGUU-3', 2) 5'-CAGGCAACUCCAAAGGUUA-3', 3) 5'-GUCCUAUCACCGUAUCUUA-3'; Santa Cruz Biotechnology, Dallas, TX) prepared with Opti-MEM (Gibco, Carlsbad, CA) and RNAimax (Invitrogen). For rescue experiments, siRNAs were transfected for 24 hours using RNAi max and then plasmids (either siRNA resistant plasmid or empty control vector) were transfected with lipofectamine 3000 (ThermoFisher Scientific, Waltham,

MA) and incubated for 48 hours. Finally, cells were washed, trypsinized, counted, and pelleted for RNA extraction, western blot analysis, and telomerase activity.

3.3.10. Alamar Blue Assay

Cells were plated for the siRNA/rescue experiment, and prior to cell collection, cells were incubated with Alamar blue reagent (1x) for two hours. Media was collected, plated into 96 well plate, and read on a plate reader (Molecular Devices SpectraMax iD3) at 545 nM excitation and 590 nM emission.

3.3.11. Western Blot Analysis

Total protein lysates were extracted from tissue culture cells using Laemmli buffer (Bio-Rad) and boiled for 10 mins at 95°C. Prepared lysates were resolved by SDS-polyacrylamide gel electrophoresis, transferred to polyvinylidene fluoride membranes, and detected with a rabbit polyclonal antibody for SF3B4 (Cat. No. ab157117; Abcam, Cambridge, UK) diluted 1:1000 in 5% non-fat dry milk. Protein loading was determined with stain free total protein blots (Stain free gels, Bio-Rad) or with a mouse monoclonal antibody for β-Actin (Cat. No. 3700; Cell Signaling Technology, RRID:AB_2242334) diluted 1:20000 in 5% BSA (Cat. No. BP1600-100; Fisher Scientific).

3.3.12. Colony Formation Assay

Cell were treated as described above for either siRNA transfections or rescue experiments. After 24 hours of siRNA and/or plasmid treatments, cells were trypsinized, counted, and plated in triplicate at three different densities (500, 1000 and 200 cells per

well in a 6 well plate) for each condition. Media was changed every four days, and once visible clones were present, they were fixed and stained with Crystal violet. Plates were imaged and the number of colonies were counted by ColonyCountJ [186].

3.3.13. Stable Cell Line Generation

Stable cell lines with shorthair pin RNAs (shRNA; pGIPZ (RRID:Addgene_121488), Horizon Discovery) were generated for Calu6 and HBEC-3KT cells. Lentivirus was generated for non-silencing scramble control and three shRNAs targeting SF3B4 (shRNA 1 – 5’-GCCCTCTCCCTCAGTAAAT; shRNA2 – 5’-ACAGGCAACTCCAAAGGTT; shRNA3 – 5’-CTGACTATGCCATTAAGAT). Lentivirus was generated by transfecting 293T cells (RRID:CVCL_0063) with shRNA plasmid, and helper plasmids (psPAX, pMD). Viral supernatants were collected, and target cells (HBEC-3KTs and Calu6) were infected. Following infection, cells were treated with puromycin and populations of stably selected cells were cultured and analyzed in subsequent experiments. All selected cells were GFP positive, and shRNA induced knockdown was confirmed by western blot analysis.

3.3.14. *In vitro* Transcription and RNA Pulldown with Desthiobiotinylated 3’-end Labeled RNA Baits

Complementary single stranded oligonucleotides (24-nt) containing a T7 promoter sequence at the 5' end were designed to include the predicted (GTGTGA/GUGUGA; DNA/RNA) or mutated (TTTTTT/UUUUUU; DNA/RNA) SF3B4 binding motif located within the DR8 region of *hTERT* gene. Complementary oligos

were dissolved in annealing buffer (10 mM Tris ph 7.5 – 8.0; 50 mM NaCl; 1 mM EDTA; Sigma-Aldrich, St. Louis, MO, USA), heat annealed at 95ºC for 5 minutes, cooled to room temperature slowly, and then *in vitro* transcribed (MEGAshortscript T7 Transcription Kit, Invitrogen; Carlsbad, CA, USA). A 45 min DNase step was performed prior to RNA purification with an RNA affinity column (RNeasy minelute, Qiagen). RNA was 3' end labeled with desthiobiotin and ethanol precipitated (Pierce RNA 3' end desthiobiotinylation Kit, Invitrogen). Cell lysates were prepared according to manufacturer's instructions (Pierce Magnetic RNA-protein Pulldown Kit; Thermo Scientific), precleared with empty streptavidin beads for 60 minutes at 4ºC with continuous rotation, and then exposed to RNA containing beads overnight at 4ºC with continuous rotation. Following two washes, RNA-interacting proteins were eluted from the beads with a biotin containing elution buffer (30 μL) for 30 minutes at 37°C on a shaker, boiled at 95°C for 10 minutes in 2x Laemmli buffer containing β-mercaptoethanol, and stored at -20°C until RNA-protein complexes were immunoblotted as described above to determine the interaction of SF3B4 to DR8.

3.3.15. Bioinformatics and Statistical Analyses

TCGA LUAD RNA-Sequencing paired-end read data was downloaded from the GDC data portal after obtaining dbGaP NIH controlled-access. The data/analyses presented in the current publication are based on the use of study data downloaded from the dbGaP web site, under phs000178.v10.p8 (phs000001.v1.p1/https://www.ncbi.nlm.nih.gov/projects/gap/cgi-bin/study.cgi?study_id=phs000001.v3.p1). Patient clinical metadata was sourced from

the GDAC Firehose [187]. Unique tumor samples were selected per patient by ordering patient barcodes alphanumerically and selecting the first. Reads were mapped and quantified to GRCh38 using Salmon (RRID:SCR_017036) v0.11.3 with sequence, GC, and position bias correction parameters turned on [188]. Refgene gene and transcript annotations were sourced from the UCSC genome browser (RRID:SCR_005780) 6/5/2017 [189]. Transcripts per kilobase million (TPM) values were upper quartile normalized across LUAD patients.

Statistical data analysis and visualizations were generated using the R statistical programming language [190]. Cox regression and log-rank tests were used to quantify the association of gene or isoform expression with patient survival [191]. Cox proportional hazards regression was performed using gene/isoform expression as a continuous variable. To construct Kaplan Meier (KM) plots, patient cohorts were stratified into high and low gene/isoform expression groups by evaluating five thresholds: 10th, 25th, 50th, 75th, and 90th percentile of patient cohort expression. A log-rank test was used to quantify the significance of differences between patient groups. Unless otherwise noted, Student's *t*-tests were used to determine statistically significant differences between group means. Statistical significance being defined as a p-value ≤ 0.05.

3.4. Results

3.4.1. FL *hTERT* Splicing is Associated with Decreased Lung Cancer Patient Survival

The complete *hTERT* gene consists of 16 exons and 15 introns. All 16 exons must be present in full to produce the catalytically active telomerase enzyme (Figure 3.1A). Exons 7 and 8, highlighted in red, represent a key splicing event that results in the production of the catalytically active FL *hTERT* transcript (exon 7-8 containing) or the catalytically inactive minus β ASV (exon 7-8 skipping). In contrast to DR8, the direct repeat 6 (DR6) and variable number tandem repeat 6.1 (VNTR6.1) sequences within intron 6 of *hTERT* pre-mRNA are integral in regulating the major *hTERT* alternative splicing isoform minus Beta (Figure 3.1A) [181].

To determine the frequency and distribution of common *hTERT* splice variants within NSCLC (Figures 3.1B and C), we utilized publicly available RNA-sequencing data from the TCGA splice variant database (TSVdb) for both LUAD and lung squamous cell carcinoma (LUSC) patient samples [192]. The percentage of FL *hTERT* transcripts are ~24% for LUAD and ~21% for LUSC, whereas minus β containing ASVs comprise ~70% and ~64% of transcripts for LUAD and LUSC, respectively (Figure 3.1C). The remaining (≤ ~10-15%) *hTERT* ASVs are specific to the minus α (a 36-nt deletion at the 5' end of exon 6 resulting from a cryptic splice site) and minus γ (exon 11 skipping) variants within the RT-domain that may act as dominant-negative telomerase inhibitors but are expressed at extremely low levels in lung cancers (Figures 3.1 B and C) [105-107]. These data confirm that the FL *hTERT* isoform is a minor isoform compared to alternatively spliced isoforms of *hTERT.*

To examine *hTERT* expression and alternative RNA splicing in NSCLC patients (n = 503), TCGA LUAD patient data was utilized to determine if *hTERT* is expressed in tumor adjacent (normal) samples (Figure 3.1D). The expression of *hTERT* at the gene level and FL *hTERT* transcript level (uc003jcb, NM_198253) were compared in matched patient samples (normal and tumor [n = 12]). As expected, both tumor adjacent normal and tumor samples expressed *hTERT,* and expression was significantly greater in tumor compared to tumor adjacent normal samples ($p = 0.005$; Figure 3.1D). Additionally, FL *hTERT* (uc003jcb, NM_198253) expression was expressed exclusively in the tumor samples ($p < 0.001$; Figure 3.1E). The relationship between *hTERT* gene expression (total) and expression of FL *hTERT* with LUAD patient survival was also explored, and modest associations were observed for FL *hTERT* and overall survival at several thresholds (Supplemental Figures 3.1A-J). These data indicate that increases in transcription and changes in post-transcriptional regulation of *hTERT* leads to telomerase enzyme activity in lung cancer and support the observations that elevated FL *hTERT* expression and telomerase enzyme activity in lung cancers are associated with significant reductions in patient survival outcomes following surgery [7, 193].

3.4.2. DR8 *Cis*-Element Mutation or Deletion Prevents NSCLC Growth in a Xenograft Model

Our laboratory recently utilized CRISPR/Cas9 to delete a 480-nt fragment or mutate a cluster of seven NOVA1 YCAY binding sites (YCAY to YAAY mutations) within the DR8 region of *hTERT* in the H1299 NSCLC cell line (Figure 3.1F) [26]. Compared to H1299 control clones (H1299 parental, single cell sorted, and Cas9-no guide vector

transfected and sorted wild-type clones), DR8 deletion clones exhibited reduced FL *hTERT* expression, a significant reduction in telomerase activity (Supplemental Figures 3.1K and L), and progressive telomere shortening *in vitro* [26].

We previously observed that several of these clones died in culture while others survived, including one of the deletion lines and one of the mutation lines used in this study, despite progressive telomere shortening [26]. While it would be an expected result that an *hTERT* knockout line would not form tumors *in vivo*, these lines were not *hTERT* null but rather *hTERT* low. Therefore, xenografts were performed to determine if the pressures of an *in vivo* environment could drive the DR8 manipulated and low telomerase cells into crisis. Wild-type control H1299 cell lines containing DR8 (n = 3 cell lines [1. parental/population control, 2. single cell sorted and expanded as in the CRISPR clones, and 3. Cas9-no guide transfected and sorted]), H1299 clones with DR8 YCAY to YAAY mutations (n = 3 independent cell lines), and H1299 clones with complete DR8 deletions (n = 2 independent cell lines) were injected into both hind flanks of female athymic nude mice (3 mice per clone; 2 injections per mouse) [26]. Body weight was not different in any of the groups (Supplemental Figure 3.1M). However, tumor growth rates were significantly attenuated in the H1299 DR8 mutation clones and completely absent in H1299 DR8 deletion clones compared to mice injected with H1299 control clones (Figure 3.1G). These results suggest that the presence of the intronic *cis*-element DR8 confers a tumor growth and survival advantage *in vivo* that likely results from the ability of the H1299 control clones with wild-type *hTERT* DR8 being able to maintain telomeres while clones with DR8 mutations or deletion lack a stable and robust telomere maintenance system.

3.4.3. DR8 Deletion Alters *hTERT* Splicing in NOVA1 Negative Cells

Previously we observed that DR8 was important in H1299 cells which express PTBP1 and NOVA1 [26, 27]. While the majority of NSCLC cell lines express NOVA1, we sought to determine if NOVA1 was expressed in tumor patient samples. NOVA1 expression was analyzed by TCGA RNA seq. data (downloaded from Protein Atlas) and observed that 11% (55 of 500 tumors) had RNA seq. fragments per kilobase of transcript per million (FPKM) values greater than 1 FPKM for NOVA1 mRNA. The vast majority of the LUAD patient tumors had FPKM values less than 1 (89%, 445 of 500) with 19.4% having undetectable levels of NOVA1 mRNA, indicating that NOVA1 is not typically expressed in LUAD patient samples. This finding makes it important to understand telomerase regulation in the NOVA1 negative context. Thus, we aimed to determine whether or not DR8 was important in NSCLC cell lines lacking NOVA1 expression, such as Calu6 cells which may be more similar to the vast majority of lung cancer patient tumors [26]. A 480-nt fragment containing the DR8 region of *hTERT* was deleted using two CRISPR guide RNAs in Calu6. Four Calu6 clones had on-target deletion of the DR8 (Table 3.1; Supplemental Figures 3.2A and B). Cellular growth rates were attenuated in each DR8 deletion clone (Supplemental Figure 3.2C), with the Del. 1 and Del. 4 clones failing to grow beyond ~30 and 35 population doublings, respectively. DR8 deletion clones also exhibited significantly lower exon 7-8 containing *hTERT* transcript levels compared to population controls (Supplemental Figure 3.2D), and this promotion of exon 7-8 skipping resulted in an *hTERT* splicing shift from FL towards the minus β ASV and a significant reduction in telomerase enzyme activity compared to

Calu6 population controls (Figures 3.1H and I; Supplemental Figure 3.2E and F). Similarly, the Del. 2 clone exhibited very modest shortening of telomeres (Figure 3.1J). Over a period of 17 population doublings (PD; 51 PDs vs 68 PDs), telomeres shortened about 0.5kb (from ~2.0 kb to ~1.5 kb) at a rate of 29.4 bp per division, which is increased compared to wild-type (WT) cells that maintained telomere length. Therefore, the remaining amount of telomerase in this clone was not sufficient to fully maintain telomeres. Of note, despite reducing *hTERT* gene expression, FL splicing, and telomerase enzyme activity, telomere length appeared to be maintained in the Del. 3 clone (Supplemental Figure 3.2G). It is possible that Del. 3 represents a rare clone in which the reduced FL *hTERT* mRNA, and small amount of telomerase enzyme activity remained sufficient to maintain the very short telomeres throughout the investigation period.

To test the hypothesis that short telomeres in these cancer cell lines precluded the cloning efficiency, *hTERT* was overexpressed in Calu6 cells prior to DR8 deletion using CRISPR/Cas9. Exogenous overexpression of *hTERT* resulted in a 4.3-fold increase in the number of heterozygous clones and a 1.75-fold increase in the number of successful DR8 deletion clones compared to the DR8 deletion experiment described above (Supplemental Table 3.2; Supplemental Figure 3.2H), indicating that a significant number of DR8 deletion clones die in culture due to telomere shortening prior to being genotyped. These data also indicate that rare clones can emerge with alternative (non-DR8) mechanisms of promoting FL *hTERT* and telomerase activity, but that most of the cells in the culture depend on DR8 to generate sufficient FL *hTERT* and telomerase activity.

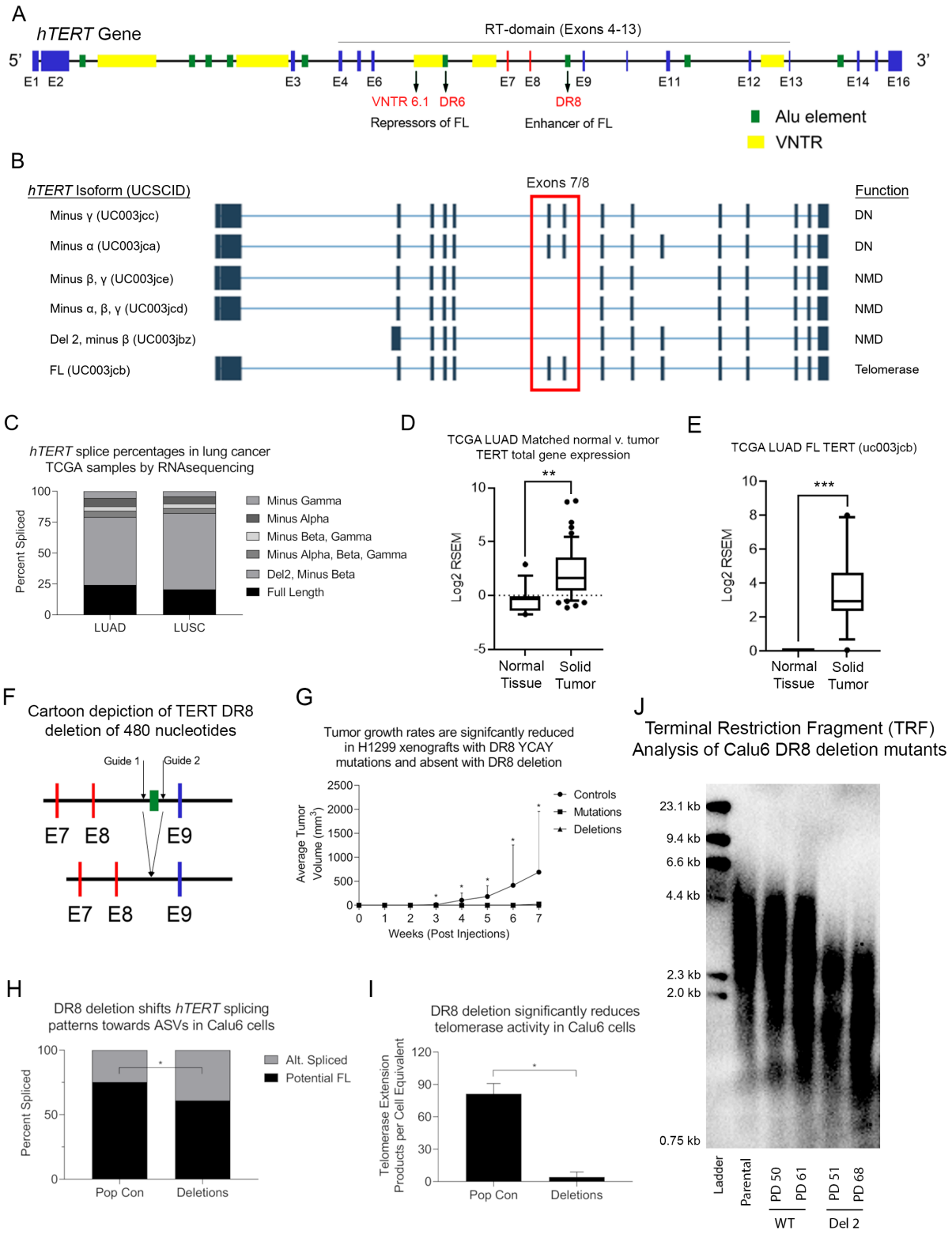

Figure 3.1. FL *hTERT* expression in lung cancers is regulated by an intronic element in *hTERT* (DR8) and deletion/mutation of this element prevents tumor growth in vivo.

A. Cartoon of the complete *hTERT* gene (5p15.33) and important alternative splicing *cis*-elements. **B.** Isoforms of *hTERT* identified from TCGA LUAD RNA sequencing of patient tumor samples. The skipping of exons 7-8 (minus β) is indicated by the red box. **C.** *hTERT* FL and alternative splicing variants observed in LUAD and LUSC patients. **D**. *hTERT* gene expression determined via TCGA LUAD RNA seq. in matched tumor adjacent (normal tissue) compared to tumor samples (solid tumors; n = 12 pairs). **E.** Expression of FL *hTERT* isoform (UC003jcb) in tumor samples compared to normal tissue as determined by TCGA LUAD RNA seq. data. **F.** Cartoon of *hTERT* CRISPR/Cas9 deletion strategy to remove intronic *cis*-element DR8. A two-guide strategy was used to delete a 480-nucleotide region in intron 8 of *hTERT* that contains DR8. **G.** Tumor growth rates are significantly attenuated in mice injected with H1299 mutation clones and completely absent in mice injected with H1299 DR8 deletion clones compared to mice injected with H1299 control clones. **H.** *hTERT* splicing ratio in Calu6 cells with DR8 deleted compared to controls (n = 3 clones [Del. 2, 3, and 4] measured in biological duplicates). **I.** Calu6 telomerase enzyme activity measured by ddTRAP in control and DR8 deleted lines (n = 3 clones [Del. 2, 3, and 4] measured in biological duplicates). **J.** Terminal restriction fragment length Southern blotting determination of telomere length in Calu6 parental, wild-type controls (early and late population doubling) and Del. 2 early and late population doublings. The *, ** and *** indicate statistical significance by Student's *t*-test at $p < 0.05$. Supplemental data associated with this figure can be found in Supplemental Figures 3.1 and 2. Abbreviations: DN: dominant negative; LUAD: lung adenocarcinoma; LUSC: lung squamous cell carcinoma; NMD: nonsense mediated decay; PD: population doublings; TCGA: The Cancer Genome Atlas. VNTR: variable number tandem repeats

Cell Line	Plated Clones →	6-Well Plate →	10 cm Dish →	Genotyped	
Calu6	384	43	23	Wild Types	7
				Heterozygous	6
				Deletions	4

Table 3.1. DR8 CRISPR/Cas9 Clone Progression

3.4.4. SF3B4 in NSCLC Cells Promotes FL *hTERT* Splicing

To identify potential *trans*-acting factors that interact with DR8 and manipulate *hTERT* splicing, we analyzed our previously performed *hTERT* splicing minigene loss of function (siRNA) screen [26]. The entire SF3B spliceosomal complex was significantly related to changes in FL *hTERT* splicing ratios in our minigene screen (Figure 3.2A). Since the SF3B complex is a seven-protein complex, a single target gene was determined by analyzing LUAD patient survival and expression differences for each SF3B protein between matched normal and tumor samples. The majority of SF3B complex members were overexpressed in patient tumor samples compared to normal (paired *t*-test: all $p < 0.05$; Supplemental Table 3.3), and survival analysis revealed that SF3B2, SF3B4, SF3B6 and PHF5A were significantly associated with reduced patient survival at various thresholds (Supplemental Table 3.3). To further narrow down our candidate gene list, SF3B4 was identified as having the largest difference in mRNA expression between normal and patient samples (Supplemental Table 3.3). SF3B4 is a U2 pre-mRNA spliceosomal protein that aids in normal splicing processes due to its recognition of an intron's branch point [194]. The predicted SF3B4 binding motif is 5'-GUGUGA [195], and *in silico* analysis demonstrates that the SF3B4 binding motif is located at the 3' end of DR8 in *hTERT*. SF3B4 gene expression levels are increased 2-

fold in solid primary tumors of LUAD patients compared to matched normal adjacent tissue controls (n = 58; $t_{(114)}$ = 8.840, $p \leq 0.001$), and associated with reduced survival outcomes in LUAD patients (n = 503; Log-Rank test: p = 0.009, Hazard Ratio 1.4 (1.1-1.8) at 10th percentile; Figures 3.2B and C). Additional thresholds were tested and generally trended towards reduced survival association with varying significance (Supplemental Figures 3.3A-D). Consistent with these findings, SF3B4 protein expression was shown to be significantly elevated in NSCLC cell lines compared to primary HBECs (Figure 3.2D and E).

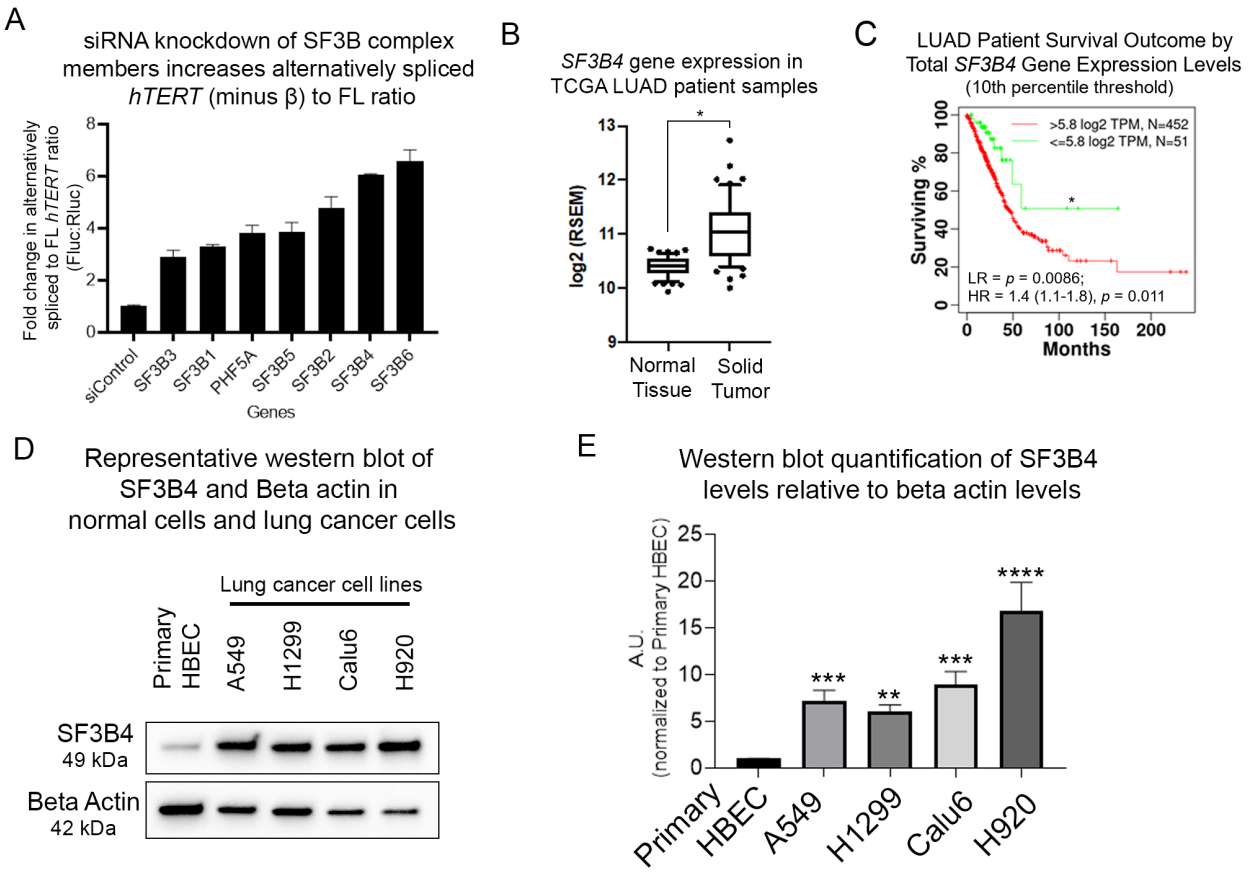

Figure 3.2. Higher *SF3B4* expression in lung cancer stratifies normal versus diseased tissue and is related to poorer patient survival in the TCGA cohort.

A. *hTERT* minigene data showing SF3B complex genes regulate FL *hTERT.* **B.** Log2-transformed (RSEM values) *SF3B4* gene expression levels (n = 58 matched patient samples). **C.** Greater levels of *SF3B4* gene expression are significantly associated with lower overall survival outcomes in LUAD patients (10^{th} percentile threshold; n = 503 patients). **D.** SF3B4 protein expression is higher in lung cancer cell lines compared to normal lung cells (primary human bronchial epithelial cells (HBECs). **E.** Western blot quantification of SF3B4 relative to beta actin protein levels in lung cancer cells and normalized to normal lung cells (primary HBECs; n = 3 for each cell line). Student's *t*-test set at * $p \leq 0.05$ for significance compared to normal tissue controls (B). The * indicates significant *(*$p < 0.05$) log rank (LR) test of the Hazard ratios between high and low expression groups at different thresholds (C). Following one-way analysis of variance (ANOVA), uncorrected Fisher's LSD test was carried out to compare lung cancer cells to normal lung cells (E; ** $p < 0.01$; *** $p < 0.001$; **** $p < 0.0001$). Data are presented as means ± standard deviations where applicable. Supplemental data associated with this figure can be found in Supplemental Figure 3.3. Abbreviations: LUAD: lung adenocarcinoma.

To confirm the impact of SF3B4 on *hTERT* splicing in NSCLC cell lines, H1299, Calu6, and A549 cells were transfected with siRNAs (pool of 3 siRNAs, 10 nM) targeting *SF3B4*; achieving ≥ 85% knockdown efficiency for each cell line (Figures 3.3A and B). Transient SF3B4 knockdown significantly decreased the percentage of potential FL *hTERT* transcripts relative to the minus β ASV (all lines $p < 0.05$) and reduced telomerase activity (Calu6 and H1299 $p < 0.05$, A549 $p = 0.067$) across NSCLC cell lines compared to siRNA control treated cells (Figures 3.3C and D, Supplemental Figures 3.4A-C). Next, we aimed to determine the minimal dose of SF3B4 siRNA necessary to impact *hTERT* splicing levels and cell viability. In addition to the 10 nM siRNA concentration previously tested, a dilution series ranging from 5 nM down to 0.1 nM was performed. Significant SF3B4 knockdown was achieved after transient (72 hours) treatment at the 10, 5, and 1 nM concentrations in Calu6 cells (Figure 3.3E). Likewise, a significant reduction in cell viability was observed in Calu6 cells following 72-hour siRNA treatment at 10, 5, 1, and 0.5 nM concentrations (Supplemental Figure 3.4D). In addition to 10 nM treatments (shown in Figure 3.3D), 5 nM and 1 nM siRNA concentrations significantly reduced FL *hTERT* splicing percentage compared to control treatments (Figure 3.3F, $p < 0.05$; Supplemental Figure 3.4E).

SF3B4 is a constitutive splicing factor, and its depletion may impact many splicing events in cancer cells. To rule out generalized splicing effects following SF3B4 depletion, we measured several cancer-related splicing events in Calu6 and H1299 cells (Supplemental Figures 3.4F and G). Specifically, the PKM1 (mutually exclusive exon 9-10 switching), PKM2 (cancer related isoform with mutually exclusive exon 9-11 switching) and PKM exons 5-6 (internal expression control of PKM) were measured

[196]. In addition, NUMB (exon 9 splicing event; inclusion is associated with certain cancers) [197, 198], and Bcl-xL/Bcl-xS (two alternative 5′ splice sites downstream of exon 2 in Bcl-x pre-mRNA; Bcl-xL is antiapoptotic and related to lung cancer cell survival) [199] were measured. Housekeeping gene TATA-binding protein (TBP) was also included as a loading control [200]. Knockdown of SF3B4 at siRNA concentrations of 10 nM and 5 nM did not significantly impact splicing of these genes within Calu6 and H1299 NSCLC lines, suggesting that the observed altered *hTERT* splicing events are unlikely to be caused by generalized splicing effects induced by SF3B4 depletion.

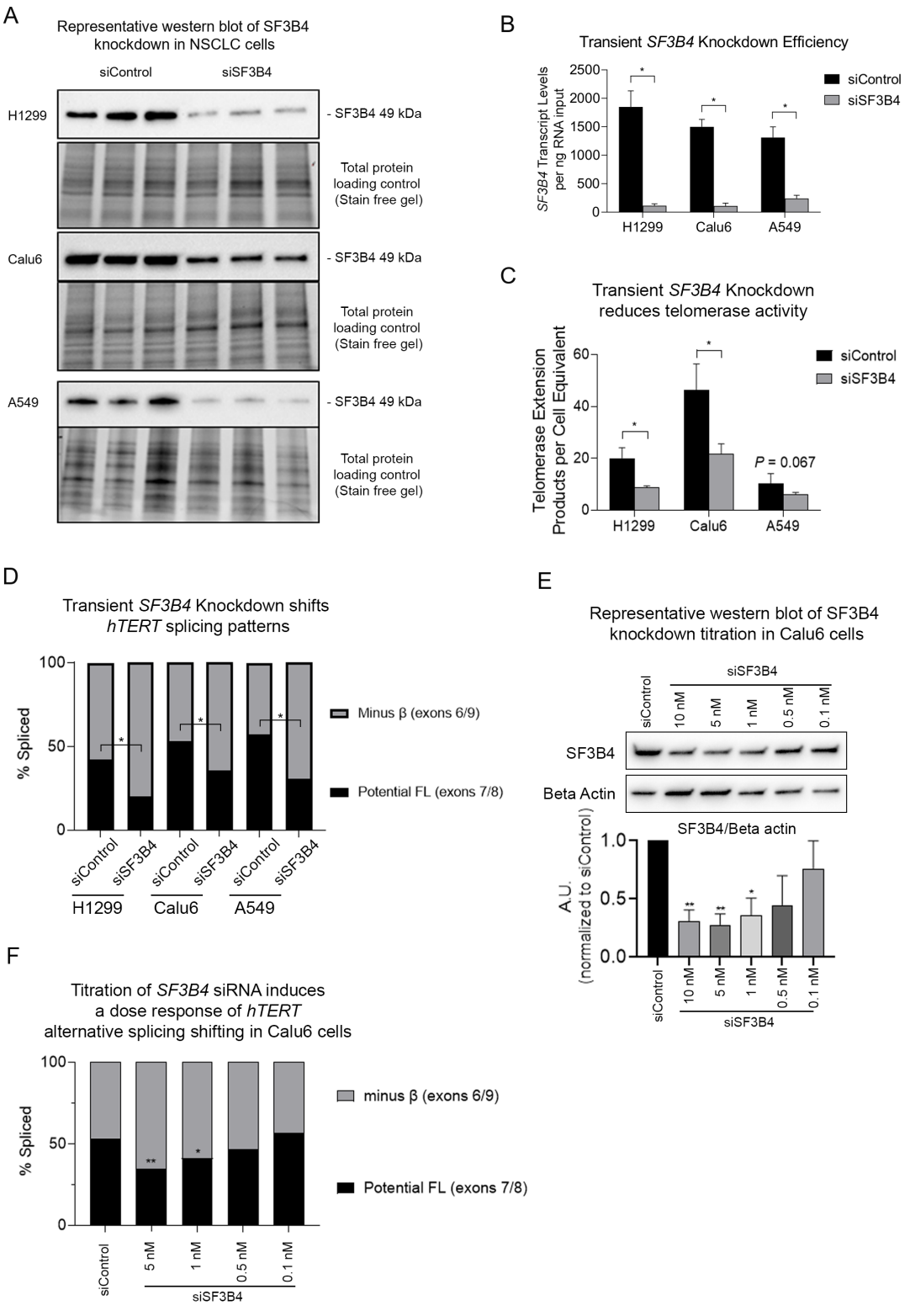

Figure 3.3. SF3B4 knockdown reduces FL *hTERT* and telomerase activity in NSCLC cell lines.

A. SF3B4 protein by western blot and **B.** quantitative mRNA expression by ddPCR following a 72-hour transfection of H1299, Calu6, and A549 NSCLC cell lines with a control siRNA or siRNAs targeting *SF3B4* (10 nM, n = 6 for each cell line). **C.** Transient *SF3B4* knockdown significantly reduced telomerase enzyme activity in H1299, Calu6, and A549 NSCLC cells (determined by ddTRAP; n = 3 biological replicates per cell line). **D.** Transient siRNA induced *SF3B4* knockdown significantly shifted *hTERT* gene expression from potential FL, exon 7-8 containing transcripts, to alternatively spliced, exon 7-8 skipping ASVs in H1299, Calu6, and A549 NSCLC cells (determined by ddPCR; n = 3 biological replicates per cell line)**. E.** Titration of siRNA dose results in differential SF3B4 protein knockdown in Calu6 cells following 72-hours treatment (n = 3 biological replicates per siRNA concentration). **F.** Dose dependent *hTERT* splicing shift in response to a 72-hour siRNA treatment against SF3B4 in Calu6 cells (n = 3 biological replicates per concentration). Student's *t*-test set at * $p < 0.05$ for significance compared to siRNA control conditions. For siRNA titration assay (E and F), ANOVA with uncorrected Fisher's LSD for post hoc comparisons of treatments was used to compare siRNA treated conditions to siControl (* $p < 0.05$; ** $p < 0.01$). Data are presented as means ± standard deviations where applicable. Supplemental data associated with this figure can be found in Supplemental Figure 3.4.

3.4.5. Ectopic Expression of SF3B4 and hTERT Rescue SF3B4 Depletion Phenotypes in Calu6 Cells

To rule out potential off target effects from siRNA treatment, an siRNA resistant SF3B4 construct with a Flag tag on the C-terminus (SF3B4-Flag) was expressed in SF3B4 depleted Calu6 cells. Exogenous SF3B4 expression was confirmed by western blotting using c-terminus SF3B4 and Flag antibodies (Figure 3.4B). The reduction of the percentage of potential FL *hTERT* transcripts (relative to the minus β ASV; $p < 0.01$) and telomerase activity ($p < 0.01$) in response to siSF3B4 were rescued by SF3B4-Flag expression (Figures 3.4A and C; Supplemental Figure 3.5A). Cell viability measured by Alamar blue assay was also rescued by SF3B4-Flag expression ($p < 0.01$, Figure 3.4D).

Since we determined that SF3B4 siRNAs were on-target for *hTERT*, we performed colony formation assays to study the effect of SF3B4 depletion on proliferation of Calu6 cells. SF3B4 depletion in Calu6 WT reduced the number of colonies dramatically compared to control treated cells ($p < 0.01$; Figures 3.4E and F). In addition, we evaluated whether TERT expression was sufficient to rescue the impact of SF3B4 knockdown on proliferation. Using Calu6 cells with stable TERT overexpression (Calu6 TERT OE), we found that TERT overexpression rescued colony formation of Calu6 cells with SF3B4 depletion (Figures 3.4E and F). These data indicate that TERT can partially rescue the effects of SF3B4 on viability and colony formation ability, providing evidence of a direct effect of SF3B4 on TERT. Since the TERT cDNA does not depend on SF3B4 to be spliced to full-length TERT to generate telomerase, these data indicate the observed effects are likely mediated by telomerase active TERT (or full length TERT).

Since SF3B4 is an essential splicing factor (DepMap data), it is also important to understand the impact of SF3B4 knockdown on viability in primary HBEC cells. Other TERT overexpressing cell lines (Calu6 TERT OE and HBEC-3KT) were utilized to test the impact of SF3B4 depletion in the context of TERT expression. Knockdown of SF3B4 was confirmed by western blotting in the primary HBECs and TERT overexpressing cell lines and a statistically significant knockdown was achieved compared to control cells for all lines (greater than 50%; all $p < 0.05$; Supplemental Figures 3.5B-D). Reduction of SF3B4 transcripts was also confirmed by ddPCR in the primary HBECs (Supplemental Figure 3.5E). As expected, the amount of *hTERT* transcripts and telomerase activity were very low and unaffected by SF3B4 depletion in primary HBECs (Supplemental Figures 3.5F and G). Among the four cell lines (Calu6 WT, Calu6 TERT OE, HBEC-3KT and primary HBEC), only WT Calu6 cells showed significantly reduced cell viability measured by Alamar blue (20% reduction compared to siRNA control Calu6 WT; $p < 0.05$; Supplemental Figure 3.5H) or trypan blue (only HBEC-3KT; Supplemental Figure 3.5I). These data indicate that partial reduction of SF3B4 in primary HBECs or TERT overexpressing cells is tolerable (the cells survive and continue to proliferate), but that cancer cells that depend on higher rates of cell turnover for survival more strongly depend on SF3B4 to promote FL *hTERT* splicing and telomerase activity for proliferation and survival.

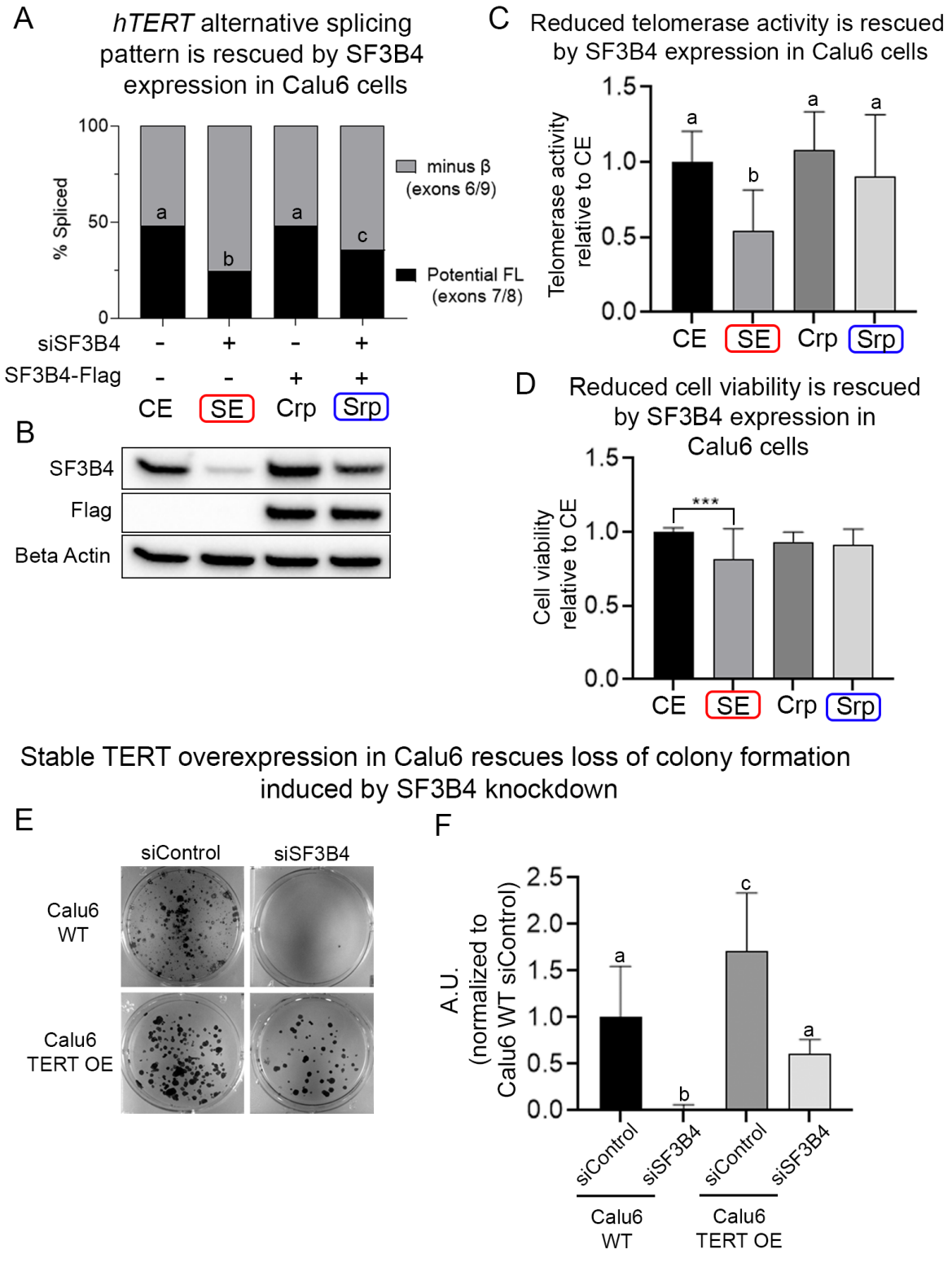

Figure 3.4. siRNA resistant SF3B4 expression and TERT overexpression rescues SF3B4 depletion phenotypes.

A. siRNA resistant SF3B4 (SF3B4-Flag) expression rescues *hTERT* splicing shift caused by SF3B4 knockdown (ddPCR determined *hTERT* splicing isoform levels in upper panel, n = 5). **B.** Western blot of SF3B4 C-terminus endogenous antibody and Flag tag antibody. **C.** Telomerase activity is rescued by siRNA resistant SF3B4 over expression (n = 5). **D.** Cell viability determined by Alamar blue assay is rescued by siRNA resistant SF3B4 over expression (n = 5). **E and F.** TERT overexpression rescues the number of colonies in SF3B4 depleted Calu6 cells (n = 9). **E.** Representative image of the colony formation assay. **F.** Quantification of the number of colonies relative to scrambled siRNA (siControl) treated Calu6 WT cells. For multiple group comparisons (A, C, D and F) *p*-value was calculated using one-way ANOVA with Tukey's multiple comparison test compared to every other condition. When $p < 0.05$ to every other condition, it is grouped and indicated by an alphabet (a,b or c). Otherwise, it is denoted by asterisk (D; *** $p < 0.001$). Data are presented as means ± standard deviations where applicable. Abbreviations: CE: siControl + Empty control vector; SE: siSF3B4 + Empty control vector; Crp: siControl + SF3B4-Flag plasmid; Srp: siSF3B4 + SF3B4-Flag plasmid; Calu6 WT: Calu6 wild-type cell line; Calu6 TERT OE: Calu6 TERT overexpression cell line. Supplemental data associated with this figure can be found in Supplemental Figure 3.5.

3.4.6. Long-Term Reduction of SF3B4 in Cancer Cells Altered Growth and Telomerase

To test for progressive changes in telomere length, growth, *hTERT* expression, and telomerase activity, stable cell lines expressing shRNAs to SF3B4 (three different shRNAs) or control (scrambled shRNA) in HBEC-3KT (normal cell control) and Calu6 cells were generated. In HBEC-3KTs, SF3B4 knockdown was between 40 and 50% compared to non-silencing scramble control cells (all $p < 0.01$ compared to scrambled shRNA control; Figure 3.5A). Cell growth rates were measured and no significant differences between any of the shRNAs were observed (Figure 3.5B). Calu6 cells with stable reductions in SF3B4 using the same shRNAs were also generated. SF3B4 protein levels were measured in cells across several population doublings post selection and shown to be significantly reduced compared to the scrambled controls (representative western blot image shows early post selection knockdown, average reduction in SF3B4 was as follows, shRNA 1 = 20% KD, shRNA 2 = 41% KD, and shRNA 3 40% KD; all $p < 0.05$; Figure 3.5C). In contrast to stable knockdown observed in shRNA 1, knockdown efficiency in shRNA 2 (44% to 32%) and shRNA 3 (42% to 33%) decreased from early to late passages (Supplemental Figures 3.6A and B). Nonetheless, growth rates across all of these stable cell lines were slowed over the course of 35 days compared to control shRNA cells (Figure 3.5D). Next, we measured telomerase enzyme activity and observed reductions in telomerase enzyme activity (all $p < 0.01$; Figure 3.5E), which was confirmed by significantly reduced splicing of FL *hTERT* levels (all $p < 0.05$; Figure 3.5F; Supplemental Figure 3.6C). Similar to the fluctuation in SF3B4 knockdown levels, changes in FL *hTERT* and telomerase activity

were observed throughout the experiment (Supplemental Figures 3.6D and E). In shRNA 1 cells, FL *hTERT* increased by midway through the experiment and exhibited significantly higher telomerase activity by the end of the experiment compared to cells measured during the middle phase. This could indicate that a rare clone emerged and took over the population that was resistant to knockdown of SF3B4 and found an alternative way to generate high levels of telomerase. In shRNA lines 2 and 3, FL *hTERT* and telomerase progressively increasing through the time of investigation. Finally, we analyzed early and late passage cells for changes in telomere length and observed two different phenotypes (Figure 3.5G). In the control cell line (shRNA scramble), telomeres were maintained overtime in culture (0.2 kb reduction over 40 population doublings or a shortening rate of 10 bp per doubling). In SF3B4 shRNA 1, modest telomere shortening was observed (0.6 kb over 29 population doublings or a shortening rate of 20.7 bp per doubling), whereas in shRNAs 2 and 3 cells, telomeres were elongated (~ 0.2 kb over 29 and 28 population doublings, respectively) over time in culture despite extremely low *hTERT* gene expression levels and telomerase activity at the beginning of the culture. A potential explanation could be that the initial selection of clones that could grow with SF3B4 knockdown resulted in a population of clones with very short telomeres, low telomerase, and slow growth. For example, very slow growth and low viability of shRNA 2 cells was observed initially, but overtime, growth rates and viability increased to suggest a shift in the dominant clones within the population (Supplemental Figure 3.6F). However, this result could also arise from a rare clone with poor or no knockdown of SF3B4 and higher telomerase/longer telomeres that was mixed in with the selected population, a hypothesis supported by the observed shift in

knockdown efficiency overtime (Supplemental Figures 3.6A and B). Under this scenario, this clone could have become dominant and took over the culture population with the short telomere cells dying off in culture. In shRNA 3 treated cells, high viability was initially observed, but by mid-phase, the viability of the culture began to suffer, followed by higher viability at the late phase (Supplemental Figure 3.6F). We hypothesize that similar to shRNA 2, a new dominant set of clones might have emerged from the pool of selected cells that had longer telomeres, higher telomerase/FL *hTERT,* and were more resistant to knockdown of SF3B4 (Figure 3.5 and Supplemental Figure 3.6). These data highlight the heterogeneity of cancer cell lines and further point out that the selective pressures associated with reduced telomerase activity induced by manipulation of *hTERT* alternative splicing factors such as SF3B4 could result in rare surviving clones with the ability to re-grow their telomeres. This will be important to consider as we move towards determining if targeting telomerase via alternative RNA splicing is a viable therapeutic target.

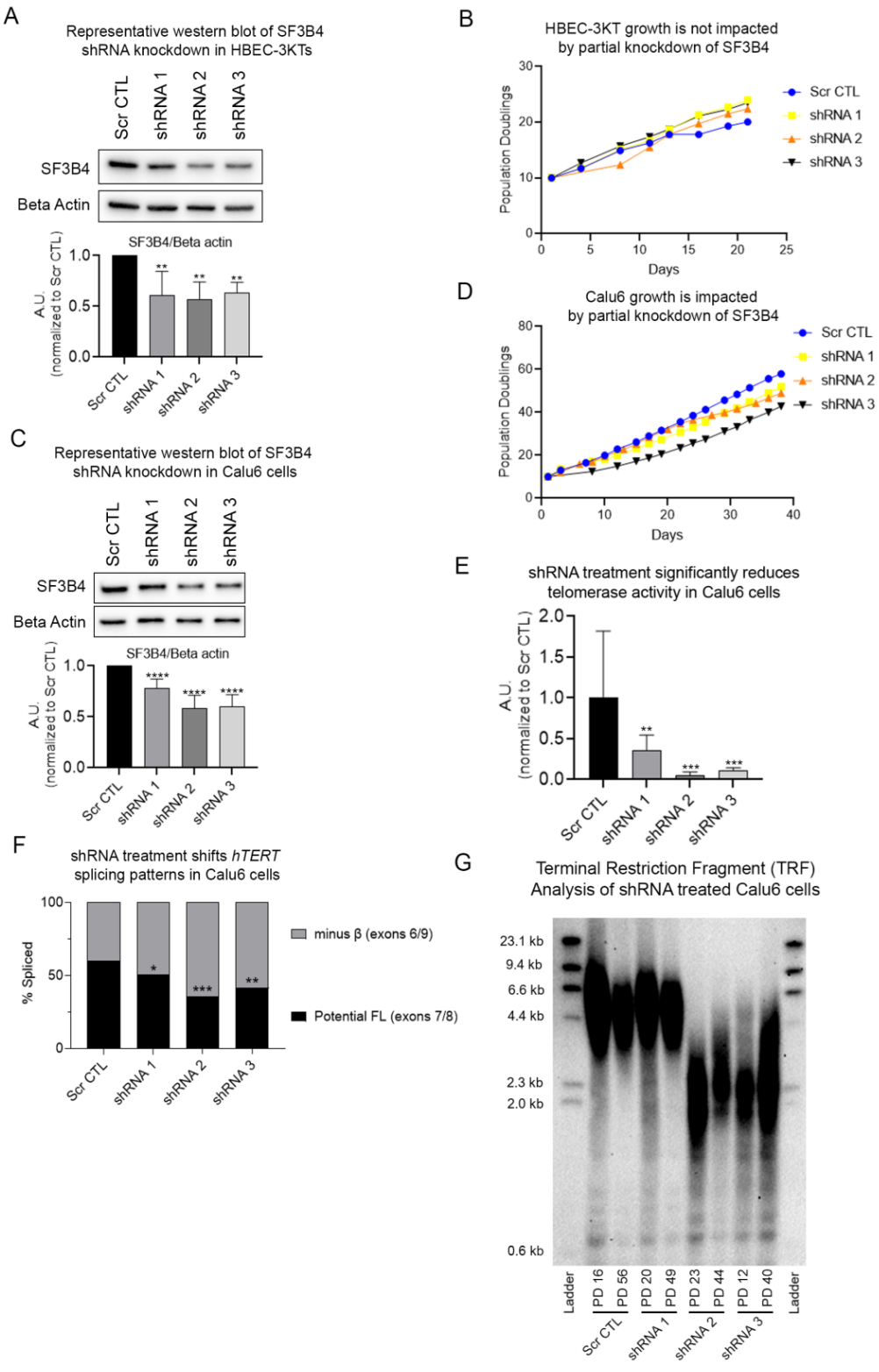

Figure 3.5. SF3B4 depletion differentially impacts normal lung cell growth compared to cancer cells and shortens telomeres in telomerase positive lung cancer cells.

A. Western blot image and quantification of shRNA induced SF3B4 knockdown in human bronchial epithelial cells (HBEC3-KT; n = 3 for each shRNA line). **B.** HBEC-3KT growth curves (population doublings) in SF3B4 shRNA stable cell lines. **C.** Western blot image (representative image of early passage cells) and quantification of shRNA induced SF3B4 knockdown in Calu6 cells (n = 12 for each shRNA line). **D.** Calu6 growth curve (population doublings) in SF3B4 shRNA stable cell lines. **E.** Telomerase enzyme active determined by ddTRAP (n = 3 for each shRNA line, early passage cells shown). **F.** *hTERT* splicing determined by ddPCR shifted significantly in shRNA cell lines (n = 3 for each shRNA cell line). **G.** Terminal restriction fragment length Southern blotting analysis (representative image, blot was repeated twice with similar results). Following one-way analysis of variance (ANOVA), uncorrected Fisher's LSD test was carried out to compare treatment means to scramble Control (Scr CTL, * $p < 0.05$, ** $p < 0.01$, *** $p < 0.001$, **** $p < 0.0001$). Data are presented as means ± standard deviations where applicable. Supplemental data associated with this figure can be found in Supplemental Figure 3.6.

3.4.7. SF3B4 Binds DR8 in NSCLC Cells and Promotes FL *hTERT* Splicing

To determine whether or not SF3B4 binds to DR8, a short (24-nt) RNA bait was generated that spans the 5'-GUGUGA binding motif within the DR8 region (3' end) of *hTERT* pre-mRNA (Figure 3.6A). H1299 and Calu6 protein lysates were incubated with the desthiobiotinylated 3'-end labeled RNA baits attached to streptavidin beads and the enrichment of SF3B4 bound to DR8 was confirmed by western blot analysis (Figures 3.6B-E, Supplemental Figures 3.7A and B). In addition, an RNA bait with a mutated binding motif 5'-UUUUUU was utilized to prevent the interaction of SF3B4 with DR8. Indeed, a significant reduction of SF3B4 binding to the DR8 region within the *hTERT* gene was confirmed in both H1299 and Calu6 NSCLC cell lines with mutations to the SF3B4 binding motif. Combining all data, we propose a working model that SF3B4 binds to DR8 to promote FL *hTERT* splicing, telomerase enzyme activity and cancer cell growth and survival in NSCLC cell lines (Figure 3.6F).

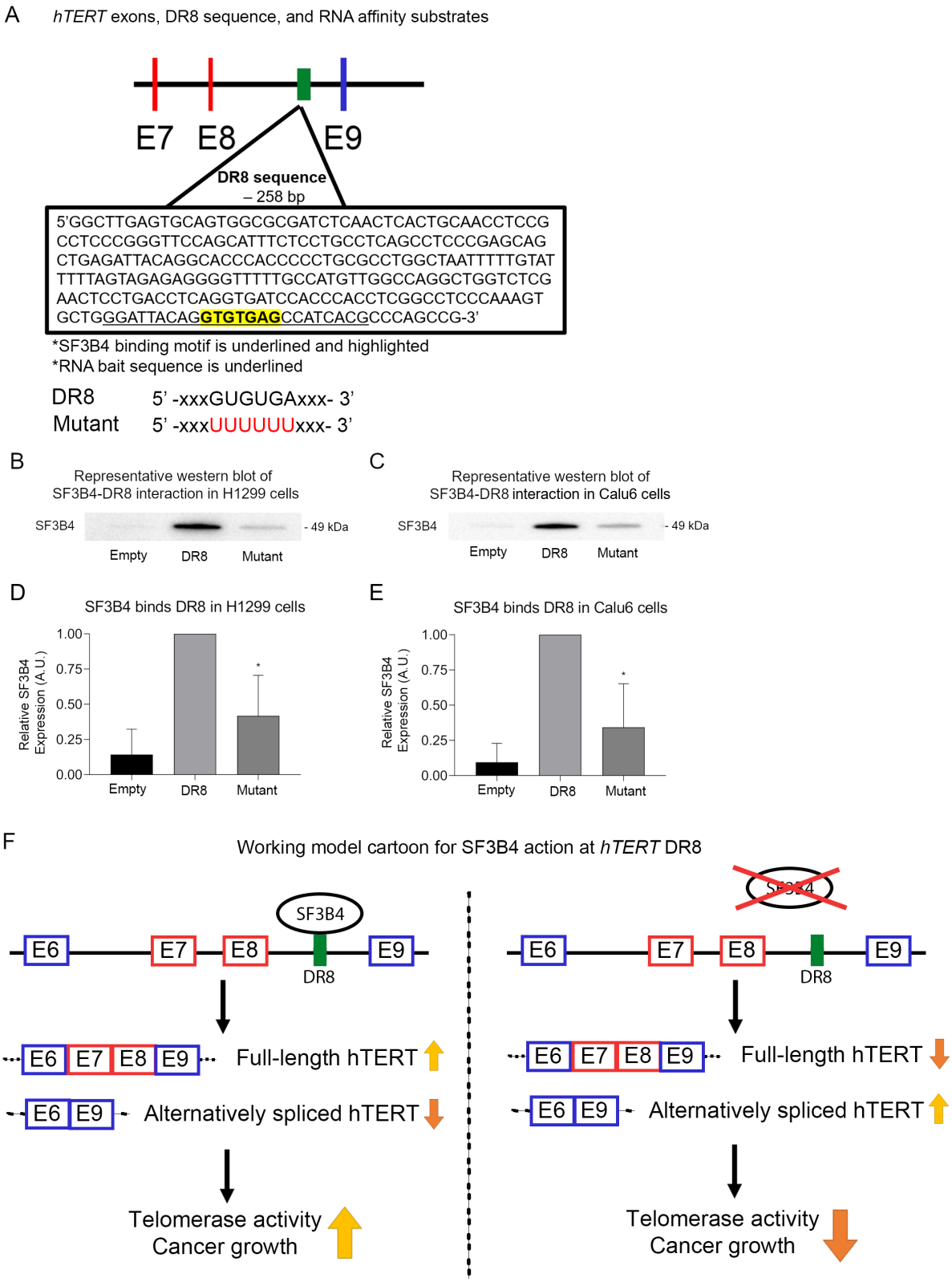

Figure 3.6. SF3B4 binds DR8 *hTERT* sequences in RNA pull down assay.

A. Cartoon schematic displaying the predicted SF3B4 binding motif within the DR8 region (3' end) of *hTERT* pre-mRNA (DNA sequence is shown). The mutated SF3B4 binding motif (highlighted) is included as a control bait. RNA bait sequence underlined. **B and C.** Representative western blot images demonstrating significant enrichment of SF3B4 protein bound to a 24-nt RNA bait containing the predicted SF3B4 binding motif located at the 3' end of DR8. **D and E.** Graphical depiction of SF3B4 protein enrichment bound to wild-type and mutated RNA baits (n = 3). Band intensities are normalized to the WT bait containing the SF3B4 binding motif. An empty bead control was also included. **F.** Working model cartoon for SF3B4 action at *hTERT* DR8. Student's *t*-test set at $p \leq 0.05$ for significance compared to empty bead controls that did not have RNA oligonucleotides attached (indicated by *). Data are presented as means ± standard deviations where applicable. Supplemental data associated with this Figure are found in Supplemental Figure 3.7.

3.5. Discussion

A thorough understanding of FL *hTERT* splicing regulation is vital to elucidating the mechanisms leading to cancer cell telomerase reactivation and cellular immortality. Consistent with *hTERT* splice variant expression patterns across 31 cancer types [25], FL *hTERT* comprises about 21% and 24% of total *hTERT* transcripts in patients with NSCLC (LUAD and LUSC, respectively). Increased levels of FL *hTERT*, but not total *hTERT* gene expression (increased gene level read counts), is predictive of adverse survival outcomes in LUAD patients. These findings suggest that in addition to transcriptional regulation of *hTERT,* alternative RNA splicing is a critically important regulatory mechanism that enables NSCLC cells to “fine-tune” the amount of FL *hTERT* to produce the “correct” amount of telomerase enzyme necessary to either prevent the shortening of telomeres, which would lead to the loss of replicative immortality, or to prevent runaway telomere lengthening that has been shown to induce genomic instability and reduce survival [201].

Alternative RNA splicing involves both *cis*- and *trans*-acting RNA binding proteins to regulate exon inclusion and exclusion within the final protein coding isoform. To determine the functional role of several deep intronic *cis*-elements in *hTERT* splicing, Wong et al. [181] utilized an *hTERT* minigene and we previously demonstrated that DR8 manipulation (mutation or deletion) within H1299 cells shift *hTERT* splicing from FL to minus β ASV, reduces telomerase, and progressively shortens telomeres [26]. In the present study, we further demonstrate that DR8 is also critical for promoting H1299 growth and survival in a xenograft model, as mice injected with H1299 cells containing DR8 mutations or deletions failed to form tumors up to seven weeks post injection (1 out

of 30). We further demonstrate that DR8 appears to be a universal intronic *cis*-element vital for the regulation of FL *hTERT* splicing across NSCLC cells lines, as CRISPR/Cas9-mediated DR8 deletion in Calu6 NSCLC cells inhibited cellular growth and survival by shifting in *hTERT* splicing to ASVs, reducing telomerase enzyme activity, and shortening telomeres. Confirming these results, rescue experiments achieved by the overexpression of *hTERT* in Calu6 cells promoted significantly greater clonal survival following DR8 deletion by CRISPR/Cas9 (Supplemental Table 3.2). These results demonstrate that the DR8 region is vital for promoting FL *hTERT* and telomerase enzyme activity, which in turn, enables cancer cells to maintain their already shortened telomeres necessary for continued proliferation.

It is important to note that changes in FL *hTERT* splicing percentage can result from various combinations of altered steady-state FL and/or alternatively spliced transcript levels and that some of the *hTERT* isoforms not directly measured by our assays are dominant-negative inhibitors of telomerase. For example, minus β is thought to be targeted for degradation by the NMD pathway, and thus, concentrations are potentially higher than measured. Minus β maybe a dominant-negative inhibitor of telomerase [116]. In addition, the presence of the minus α, minus γ, and INS3 and INS4 ASVs (isoforms that retain portions of intron 14) are likely to be included within exon 7 and 8 containing transcripts. Thus, their likely inclusion contributes to an overestimation of total FL *hTERT.* Although the minus α, minus γ, INS3, and INS4 ASVs account for a small percentage of total *hTERT,* they act as dominant-negative telomerase inhibitors and help to explain how slight decreases in FL *hTERT* splicing percentages contribute to decreases in telomerase enzyme activity.

The recruitment of *trans*-acting RNA binding proteins that bind to *hTERT* DR8 dictates *hTERT* splicing choice. To determine which splicing factors might be binding DR8 we analyzed our previous screening data and observed that reduction in all seven members of the SF3B spliceosome complex resulted in increased *hTERT* alternative splicing (Figure 3.2A). Through TCGA patient data analysis (Figure 3.2B-C, Supplemental Figure 3.3, and Supplemental Table 3.3), we narrowed down our candidates to SF3B4 as an essential splicing factor involved in branchpoint recognition, activation of the splicing reaction, and intron removal [202]. Recent studies have shown that SF3B4 overexpression promotes tumorigenesis in hepatocellular carcinoma, whereas SF3B4 knockdown inhibits hepatocellular carcinoma (HCC) proliferation and metastasis [203]. Consistent with these findings, we demonstrate that transient knockdown of SF3B4 shifts *hTERT* splicing from FL towards the minus β ASV and reduces telomerase enzyme activity across three NSCLC cells lines analyzed (Figures 3.3C and D). We also demonstrated in rescue experiments that the phenotypes of SF3B4 depletion are directly related to *hTERT* and are not caused by off target effect of siRNA treatment (Figure 3.4). SF3B4 was further shown to bind the 3' end of DR8 to promote the inclusion of exons 7 and 8 into the *hTERT* mRNA, and thus, the formation of FL *hTERT* and telomerase activity in the absence (e.g., Calu6 cells) and presence of NOVA1 (e.g., H1299 cells; Figure 3.6). This is interesting since our previous data demonstrated that the 5' end of DR8 was bound by NOVA1/PTBP1 [26]. Understanding the role SF3B4 plays in cell biology and telomere length regulation is an important step in determining if this protein or protein complex could be a viable cancer therapy target.

Since SF3B4 is an essential gene and homozygous knockout of SF3B4 is lethal during embryogenesis, but the heterozygous animals survive to adulthood [204], it is important to test how normal human lung cells would respond to knockdown of SF3B4 in culture. To this end, we first demonstrate that *hTERT* transcripts and telomerase activity of normal lung cell (primary HBECs), are not affected by SF3B4 depletion (Supplemental Figures 3.5F and G). We also show that primary HBEC viability is not significantly impacted by SF3B4 knockdown (Supplemental Figure 3.5H). In contrast, SF3B4 knockdown in Calu6 cells significantly reduced viability (Figure 3.4D, Supplemental Figures 3.4D and 5H) and clonogenic growth compared to control cells (Calu6 in Figures 3.4E and F). On the other hand, viability (HBEC-3KT and Calu6 TERT OE) and clonogenic growth (Calu6 TERT OE) was rescued by ectopic TERT expression (Figures 3.4E and F, Supplemental Figures 3.5H and I). Thus, there appears to be a survival difference or an ability to tolerate or compensate for reduced SF3B4 in normal lung cells, compared to rapidly dividing, telomerase expressing lung cancer cells, such as Calu6. Our stable cell lines with knockdown of SF3B4 demonstrate the heterogeneity of Calu6 cells in response to the selective pressure of reduced SF3B4 protein levels. The selection pressure of SF3B4 knockdown in shRNA 2 and 3 was likely strong and only rare very short telomere, low telomerase clones were able to survive and proliferate. This emergence of rare clones could have re-elongated their telomeres (Figure 3.5G). Thus, it is likely that rare clones within the Calu6 cell line that can survive the strong selective pressure of SF3B4 depletion were studied.

The present investigation helps to further elucidate the splicing code involved in the generation of FL *hTERT* in NSCLC. More importantly, the DR8 region serves as a

binding hub for RNA-binding proteins, including SF3B4, NOVA1, and PTBP1. Our data highlight that manipulation of essential splicing factors such as SF3B4 can manipulate telomerase activity and *hTERT* alternative splicing. Further they point out that rare resistant clones can emerge from depletion of essential splicing factors that can maintain and even elongate their telomeres. Thus, more precise strategies need to be developed to force alternative splicing of *hTERT* pre-mRNA towards catalytically inactive variants that reduce telomerase enzyme activity, shorten telomere length, and prevent long term NSCLC cancer cell growth and survival. Furthermore, the emergence of rare, resistant clones must be overcome before this type of therapeutic approach can move forward towards clinical relevance.

Chapter 4 – Dynamics of TERT Regulation via Alternative Splicing in Stem Cells and Cancer Cells

Kim, J. J., Sayed, M. E., Ahn, A., Slusher, A. L., Ying, J. Y., & Ludlow, A. T. (2023). Dynamics of TERT regulation via alternative splicing in stem cells and cancer cells. *Plos one*, *18*(8), e0289327.

4.1. Abstract

Part of the regulation of telomerase activity includes the alternative splicing (AS) of the catalytic subunit telomerase reverse transcriptase (*TERT*). Although a therapeutic window for telomerase/TERT inhibition exists between cancer cells and somatic cells, stem cells express TERT and rely on telomerase activity for physiological replacement of cells. Therefore, identifying differences in *TERT* regulation between stem cells and cancer cells is essential for developing telomerase inhibition-based cancer therapies that reduce damage to stem cells. In this study, we measured *TERT* splice variant expression and telomerase activity in induced pluripotent stem cells (iPSCs), neural progenitor cells (NPCs), and non-small cell lung cancer cells (NSCLC, Calu-6 cells). We observed that a NOVA1-PTBP1-PTBP2 axis regulates *TERT* alternative splicing (AS) in iPSCs and their differentiation into NPCs. We also found that splice-switching of *TERT*, which regulates telomerase activity, is induced by different cell densities in stem cells but not cancer cells. Lastly, we identified cell type-specific splicing factors that regulate

TERT AS. Overall, our findings represent an important step forward in understanding the regulation of *TERT* AS in stem cells and cancer cells.

4.2. Introduction

Telomeres are a repeated DNA sequence (5'-TTAGGGn-3') at the ends of linear chromosomes [11]. During DNA replication the lagging strand of telomeric DNA is not fully copied resulting in telomere shortening with each cell division [12]. After many cell divisions, a critically shortened telomere length is reached by a subset of telomeres resulting in a DNA damage response at chromosome ends and cell cycle withdraw (i.e., the induction of cellular senescence). This barrier to replication is important in somatic cells because it acts as a potent tumor suppressive mechanism preventing continued cell growth of damaged or mutant cells [205]. However, in stem cells, improper telomere maintenance results in aging-related phenotypes and telomeropathies [206]. In certain cell types, an enzyme, telomerase, can maintain or even elongate the shortest telomeres resulting in continued cell divisions [165]. Stem cells possess telomerase activity to maintain chromosome ends so that normal physiological cell replacement can occur [207]. In a sense this is regulated telomerase activity. However, cancer cells must overcome telomere shortening to keep proliferating and 85% of cancer cells rely on the reactivation of telomerase to maintain telomere length [13]. We refer to this type of telomerase as dysregulated telomerase activity. Additionally, most somatic cells lack detectable telomerase activity [166]. The expression pattern of telomerase activity, off in most somatic cells but on in most cancer cells, has led to telomerase inhibition being sought after as a potential cancer therapeutic option [208]. While some success on this front has been made, additional biochemical information about telomerase regulation will lead to better and more efficacious therapeutic options.

Telomerase is a ribonucleoprotein enzyme minimally consisting of two parts: telomerase reverse transcriptase (TERT) and telomerase RNA component (TERC or TR) [78]. Telomerase activity is regulated by transcriptional and post-transcriptional regulation [26, 28, 108, 110, 116, 181]. One aspect of post-transcriptional regulation is alternative splicing (AS) of *TERT*. AS is a post-transcriptional mechanism that enhances proteome diversity by generating multiple isoforms of the same transcriptional unit or pre-mRNA [103, 209]. *TERT* is a gene that consists of 16 exons with 15 introns, in which only the full-length (FL) *TERT* can be translated to form active telomerase with all 16 exons [179]. Regulation of telomerase by AS has been reported in various contexts. For instance, during fetal kidney development, both FL *TERT* (exons 7/8 including *TERT*) and minus beta *TERT* (exons 7/8 excluding *TERT*) are co-expressed in early stages, but FL *TERT* is not expressed in later stages leading to loss of telomerase activity [104]. Minus beta *TERT*, despite there being a frame shift and a premature termination codon in frame in exon 10, has also been reported to form a protein and to have dominant-negative effects in certain cancer cells [116]. Additionally, minus beta TERT has also been observed to protect breast cancer cells from chemotherapeutic insults [210]. In embryonic stem cell differentiation, exon 2 is spliced out (Del2 *TERT*) when cells are differentiated to fibroblasts resulting in loss of FL TERT and telomerase activity [108]. In addition to the role that AS plays in turning off telomerase activity-coding FL *TERT*, isoforms generated by AS have different functions. Minus alpha (exon 6 partial exclusion) TERT is a dominant-negative isoform by sequestering TERC from FL TERT [106]. It has been proposed that minus gamma (exon 11 exclusion) TERT has dominant-negative effects on telomerase activity [107]. INS3 (159 bp insertion of intron

14 at the end of exon 14) and INS4 (600 bp insertion of the entire intron 14) are also dominant-negative isoforms of telomerase [211]. Delta 4-13 (exons 4-13 exclusion) was shown to stimulate cell proliferation seemingly by interacting with WNT/beta-catenin pathway [28]. Moreover, intron 11 retention appeared to be the driving force for nuclear detention of unspliced *TERT* mRNAs and to regulate telomerase activity to only dividing cells [102].

Measurement of *TERT* splice variants by RT-PCR is a challenge that must be addressed. Short fragment PCR detects exon splicing events quantitatively, but the detection and quantification of full-length intact mRNA splice variants (5' mRNA cap to poly A tail) remains difficult to do. Further, most PCR methods that detect *TERT*, capture multiple splice variants rather than a single splice variant. For instance, the assay we use to quantify exons 7/8 including *TERT* captures more than just FL *TERT*. This assay also detects other *TERT* splice variants such as intron 11 retention, minus and plus gamma, minus alpha, INS3 and INS4. However, it should be noted that the exons 7/8 assay is moderately correlated to telomerase enzyme activity [26]. The best estimates of the number of molecules per cell of telomerase coding *TERT* mRNA indicate that FL *TERT* is a minor splice variant and the majority of the transcripts are alternatively spliced to either degraded, dominant-negative, or splice variants with unknown functions [174]. Despite the difficulties of measuring *TERT* splice variants, we can very carefully quantify specific exon events (exons 7/8, exons 6/9, etc.) and we call the exons 7/8 including *TERT*, "potential full-length *TERT*" due to the correlation with telomerase enzyme activity measures. We also measure minus beta *TERT* using an assay that detects the novel exon junction made between exons 6 and 9, which we refer to as

exons 6/9 minus beta or exons 7/8 exclusion. While our assays only detect single exon events, they do not rule out the significance of full-length mRNAs with multiple combinations of these events together. Using these assays, we explore the regulatory mechanisms of *TERT* AS (i.e., inclusion of exons 7/8 or exclusion of exons 7/8) in multiple contexts (i.e., differentiation to specific cell types, specific tumor types and under different growth stresses) as they remain elusive.

In this study, we set out to identify regulated and dysregulated *TERT* splice variant expression as a means to identify a potential cancer therapeutic window. We first determined if the *TERT* AS was regulated by NOVA1-PTBP1-PTBP2 axis, during stem cell differentiation into neural progenitor cells, and indeed observe it was. We previously identified in cancer cells that *TERT* AS was regulated by NOVA1-PTBP1-PTBP2 axis [26, 27]. Next, we made a serendipitous observation that stem cell density impacted *TERT* splice variant expression but that cancer cells did not seem to utilize this mechanism. Finally, based on public database analysis, correlational analysis, and experimental observations, we identified splicing factors (SFs) that may have cell type-specific roles in *TERT* AS regulation and telomerase activity.

4.3. Materials and methods

4.3.1. Cell culture and cell lines

Calu-6 cells (RRID:CVCL_0236) were cultured at 37 °C in 5% CO2 in 4:1 DMEM:Medium 199 containing 10% calf serum (HyClone, Logan, UT). Cell lines were obtained as a kind gift from Drs. John Minna and Adi Gazdar.

4.3.2. iPSC culture and NPC differentiation protocol

Cellartis® Human iPSC Lines from Takara (ChiPSC22, Cat. No. Y00320) were cultured with strict adherence to manufacturer's protocols and manuals. Cellartis® DEF-CS 500 (Y30017) culture system was employed to maintain iPSC cultures (thawing, passages, media changes and cryopreservation).

Generation and culturing of Neural Progenitor Cells (NPCs) was achieved with the STEMdiff® Neural System from STEMCELL Technologies. Briefly, STEMdiff® SMADi Neural Induction kit (Cat. No. 08581) was used to treat iPSC in culture according to manufacturer's protocol that generates CNS-type NPCs. Following induction, NPC cultures were maintained with STEMdiff® Neural Progenitor Medium system (Cat. No. 05833). We performed the induction and selection according to the "monolayer culture protocol". We considered Day 10 post-NPC induction as early-stage NPCs and day 29 as late-stage NPCs. Pellets were collected and population doublings were determined post-differentiation (~Day 15-20).

4.3.3. Transient siRNA experiments

iPSCs were plated in 6-well plates (450,000 cells per well) and were transfected with non-silencing controls (Santa Cruz Biotechnology, sc-37007) or a pool of siRNAs targeting (Santa Cruz Biotechnology, PTBP1 sc-38280, NOVA1 sc-42142, PTBP2 sc-

78824, SRSF2 sc-38317, U2AF2 sc-37667, and HNRNPM sc-38286). The iPSCs and Calu-6 cells were plated 24 h prior to transfections and transfection complexes were prepared with 10 nM of siRNAs using Opti-MEM (Gibco) and RNAi max (Invitrogen) following the manufacturer's procedures. Following 72 h of exposure to siRNAs, cells were washed, trypsinized, counted and pelleted for downstream assays.

4.3.4. Cell density experiments

iPSCs were plated on 6-well plates with 6 different cell densities: 250,000 cells; 400,000 cells; 500,000 cells; 750,000 cells; 1,000,000 cells; and 1,500,000 cells. Calu-6 cells were plated on 10-cm plates with three different cell densities: 816,000 cells; 1,600,000 cells; and 3,200,000 cells. After 48 hours, cell pellets were collected for analysis.

4.3.5. Western blot analysis

Cell pellets were collected and lysed in 40 µL of lysis buffer (NP40 based buffer) per 1 x 10^6 cells. Total protein lysates were further treated with 40 µL of 2 x Laemmli buffer (Bio-Rad) and boiled for 10 mins at 95 °C. Each protein lysate was loaded onto a polyvinylidene fluoride (PVDF) membrane by equal volume. Each blot was probed for beta-actin and based upon beta-actin band densitometry, lysate loading volumes were adjusted for all subsequent target protein westerns. Prepared lysates were resolved by SDS-polyacrylamide gel electrophoresis, transferred to PVDF membranes, and detected with antibodies for NOVA1 (rabbit monoclonal [EPR13847], Abcam, ab183024, 1:1000 dilution in 5% NFDM), PTBP1 (rabbit monoclonal [EPR9048B], Abcam, ab133734, 1:10,000 dilution in 5% NFDM), PTBP2 (Abcam, EPR9891, ab154853, 1:1000 dilution in 5% NFDM), SRSF2 (rabbit polyclonal [EPR12238], Abcam, ab204916,

1:1000 in 5% BSA), U2AF2 (rabbit polyclonal, Sigma-Aldrich, HPA041943, 1:1000 in 5% BSA), SRPK1 (rabbit polyclonal, Abcam, ab90527, 1:1000 in 5% BSA), CDC40 (rabbit monoclonal [EPR12539], Abcam, ab175924, 1:1000 in 5% BSA), HNRNPA1 (mouse monoclonal [9H10], Sigma-Aldrich, R4528, 1:1000 in 5% BSA), HNRNPA2B1 (mouse monoclonal [DP3B3], Abcam, ab6102, 1:1000 in 5% BSA), HNRNPCL1 (rabbit polyclonal, Abcam, ab129762, 1:1000 in 5% BSA), HNRNPH/HNRNPH1 (rabbit polyclonal [50-249], Acris Antibodies, AP19044PU-N, 1:2000 in 5% BSA), and HNRNPM (mouse monoclonal [1D8], Thermo Fisher Scientific, MA1-34981, 1:1000 in 5% BSA). Protein loading was determined with antibodies against histone H3 (Anti-Histone H3 antibody produced in rabbit, H0164; Sigma) for Figure 4.1, and beta-actin (mouse monoclonal [8H10D10], Cell Signaling Technology, 3700, 1:1000 in 5% BSA) and GAPDH (rabbit monoclonal [14C10], Cell Signaling Technology, 2118, 1:1000 in 5% BSA) for the rest experiments. Blots were imaged with Bio-Rad ChemiDoc XRS+ Molecular Imager and quantified with Bio-Rad Image Lab software. Normalized splicing factor (SF) protein expression levels were used for correlational assays (Figure 4.5 and Supplemental Figure 4.4). Once all lysates were probed for target genes, stripped membranes were probed for beta-actin or GAPDH to confirm equal loading. Values from the loading control blots were averaged and used to normalize the target protein quantification. These normalized protein expression values were expressed relative to the 400,000-cell density condition to generate the final values analyzed in the correlations.

4.3.6. Droplet digital TRAP assay (telomerase activity)

Droplet digital telomerase repeated amplification protocol (ddTRAP) assay was performed as described in Ludlow et al. [212]. Briefly, cells were lysed, diluted, and added to the extension reactions for 60 min followed by a 5-min heat inactivation of telomerase at 95 °C. An aliquot of the extension product was amplified in a droplet digital PCR (ddPCR) for 40 cycles. Fluorescence intensity was measured, and droplets were counted on the droplet reader (QX200, Bio-Rad). Data was then calculated to represent telomerase extension products per cell equivalent or normalized.

4.3.7. Reverse transcription-ddPCR

RNA was extracted from frozen cell pellets using RNeasy® Plus Universal Mini Kit (Qiagen, 73404) according to manufacturer's protocol. For TERT splicing analyses we used SuperScript IV First-Strand Synthesis System (Thermo Fisher) to generate cDNAs and used within 48 hours of production in ddPCR measures. 1 µg of RNA was used to synthesize cDNAs. All cDNAs were diluted to 1:4 (20 µL of cDNA + 60 µL nuclease-free water) before use and stored at -20 °C. Primer sequences to target *TERT* splice variants (potential FL, minus beta, minus alpha, INS3, and INS4) and methods for calculating percent spliced *TERT* transcripts are from Ludlow et al. [26]. Total amount of *TERT* transcript was estimated by summing transcript level of exons 7/8 including (potential FL) and excluding (minus beta) *TERT*. Primers to measure intron 11 retention and intron 14 retention of *TERT* are from Dumbović et al. [102]. Primers to target minus gamma are Forward: 5'-ACATGGAGAACAAGCTGTTTGCG-3' targeting exon 9 and Reverse: 5'-CGGGCATAGCTGAGGAAGGT-3' targeting exons 10/12 junction. Primers to target plus gamma are Forward: 5'-ACATGGAGAACAAGCTGTTTGCG-3' targeting

exon 9 and Reverse: 5’-GGAAGTTCACCACTGTCTTCCGC-3’ targeting exon 11. Primers to measure Del2 *TERT* are Forward: 5’-TACCGCGAGGTGCTGCCGCTGGCCACGTTC-3’ targeting exon 1 and Reverse: 5'-CAGGATCTCCTCACGCAGCA-3’ targeting exon 3. To quantify skipping of *TERT* exon 2 (Del2 *TERT*) we used two separate PCR reactions with 5' hydrolysis probes targeting either the exons 1/3 junction to detect Del2: 5' 6-FAM-TCCTTCCGC/ZEN/CAGGGGTTGGCTGTG/blackhole quencher or a probe targeting exon 2: 5' HEX-CAGCCGAAG/ZEN/TCTGCCGTTGCCCAAGA/black hole quencher. Primer validations using 2x EmeraldAmp® MAX HS PCR Master Mix (TaKaRa, RR330) are included in supporting information (S1 File in [31]). cDNAs for OCT4, NANOG, NES, and SOX1 were generated using iScript Advanced (Bio-Rad) and used in the same manner as mentioned above for *TERT* (except cDNAs for quantification of OCT4 and NANOG which cDNAs were diluted 1:50).

4.3.8. Telomere length analysis

The average length of telomeres (terminal restriction fragment lengths) was measured as described in Mender and Shay’s study [185] with the following modifications: DNA was transferred to Hybond-N+ membranes (GE Healthcare, Piscataway, NJ) using overnight gravity transfer. The membrane was briefly air-dried and DNA was fixed by UV-crosslinking. Membranes were then probed for telomeres using a digoxigenin (DIG)-labeled telomere probe generated in-house [213] detected with a horseradish peroxidase-linked anti-DIG antibody (Roche, Cat. No. 11093274910), and exposed with CDP-star (Roche, Cat. No. 11759051001) and were imaged with Bio-Rad ChemiDoc XRS+ Molecular Imager.

4.3.9. Bioinformatics and statistical analyses

Unless otherwise noted, one-way ANOVA with uncorrected Fisher's LSD for post hoc comparisons were used to determine statistical significance between experimental groups. For bioinformatics analysis, RSEM values of each gene from 58 patients were downloaded from The Splicing variant Database [192] and Log2-transformed to generate box plots. Paired Student's *t* test was used for two group comparisons (normal tissue versus solid tumor in Figure 4.4 and Supplemental Figure 4.3). Pearson's correlations were utilized to examine the relationship of two factors (Supplemental Figure 4.2, ratio of exons 7/8 including *TERT* vs telomerase activity; Figure 4.5 and Supplemental Figure 4.4, ratio of exons 7/8 including *TERT* and expression levels of SF proteins). Statistical significance was defined as a p value ≤ 0.05.

4.4. Results

4.4.1. NOVA1-PTBP1-PTBP2 axis regulates *TERT* exons 7/8 alternative splicing during differentiation of induced pluripotent stem cells to neural progenitor cells.

Sayed et al. [27] previously elucidated an alternative splicing (AS) regulatory mechanism of *TERT* by a NOVA1-PTBP1-PTBP2 axis in NSCLC cells. Briefly, NOVA1 recruits PTBP1 to DR8 (*cis*-element of *TERT* located in intron 8, direct repeat 8 (DR8)) to promote full-length (FL) *TERT* production. When PTBP1 is reduced, PTBP2 becomes abundant due to reciprocal regulation of PTBP2 by PTBP1 (PTBP1 represses expression of PTBP2 in non-neuronal tissues [214]). Then NOVA1 recruits PTBP2 to DR8 instead of PTBP1 to induce exon skipping of *TERT* resulting in reduced FL *TERT* splicing and reduced telomerase activity. We investigated whether this *TERT* AS regulatory mechanism is conserved during differentiation of induced pluripotent stem cells (iPSCs) to neural progenitor cells (NPCs) because NOVA1 and PTBP2 are highly expressed in neuronal cells [215-217]. Differentiation of iPSC to NPC was confirmed by loss of stem cell pluripotency markers (OCT4 and NANOG) and increased NPC markers (SOX1 and NES) using immunocytochemistry (Supplemental Figure 4.1A) and RT-PCR (Supplemental Figures 4.1B-E). Differentiation increased NOVA1 as expected, PTBP1 expression decreased, and PTBP2 expression increased in NPCs compared to iPSCs (Figure 4.1A). We observed fewer exons 7/8 including (potential FL) *TERT* transcripts with higher expression of NOVA1 and PTBP2 (Figure 4.1B). In addition, both total *TERT* expression (Supplemental Figure 4.1F) and telomerase activity decreased during differentiation (Figure 4.1C and Supplemental Figure 4.1G). We also measured Del2 *TERT* during differentiation and observed a significant increase in Del2

(Supplemental Figure 4.1H). Next, we measured telomere length using terminal restriction fragment (TRF) analysis from the first day of differentiation until ~40 population doublings of NPCs. While iPSCs were able to maintain their telomeres at around 18 kb, telomere length started to shorten as they progressed into the NPC lineage (Figure 4.1D). To mechanistically confirm that the NOVA1-PTBP1-PTBP2 axis regulates *TERT* AS in iPSCs, loss-of-function (siRNA) experiments were performed. We confirmed siRNA knockdown efficiency by western blotting, indicating robust reduction in target protein levels (Figure 4.1E, Supplemental Figures 4.1I-K). When NOVA1 is reduced by 80%, PTBP1 expression also significantly decreased by 39% (Supplemental Figures 4.1I and J). When PTBP1 was reduced by 82%, PTBP2 expression significantly increased by 6.5-fold compared to control-treated iPSCs, as expected (Supplemental Figures 4.1J and K) [214]. When PTBP2 is reduced by 84%, NOVA1 and PTBP1 expressions also significantly decreased by 42% and 47%, respectively (Supplemental Figures 4.1I-K). When treated with PTBP1- or NOVA1-targeting siRNAs, the ratio and transcript level of potential FL *TERT* (exons 7/8 including *TERT*) were also significantly reduced compared to control-treated cells (Figure 4.1F, Supplemental Figure 4.1L). Only PTBP1 knockdown resulted in significantly reduced telomerase activity compared to control-treated iPSCs (Figure 4.1G). On the other hand, we did not observe significant changes of *TERT* or telomerase when PTBP2 was knocked down (Figures 4.1F and G, Supplemental Figures 4.1L and M). In summary, these results support that the NOVA1-PTBP1-PTBP2 axis regulates *TERT* AS in iPSCs and during differentiation of iPSCs to NPCs.

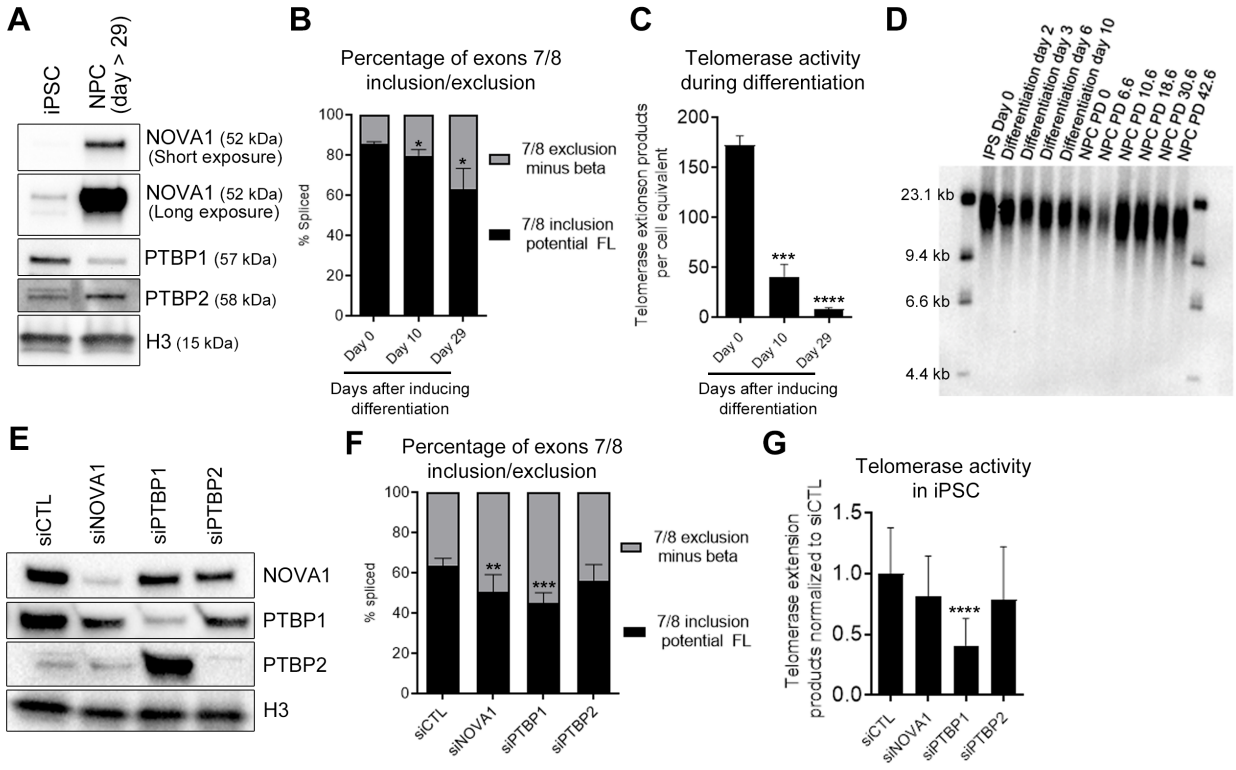

Figure 4.1. NOVA1-PTBP1-PTBP2 axis regulates *TERT* splice variant expression in differentiation of induced pluripotent stem cell (iPSC) to neural progenitor cell (NPC).

A) Western blot of NOVA1, PTBP1 and PTBP2 in iPSC differentiation into NPC. H3 protein expression was used as a loading control for western blots. B) Reduction of exons 7/8 including *TERT* splice variant expression during differentiation compared to iPSCs (day 0) (determined by ddPCR; n = 3 biological replicates per condition). C) Reduction of telomerase activity during differentiation compared to iPSCs (day 0) (determined by ddTRAP; n = 3 biological replicates per condition). D) Terminal restriction fragment (TRF) Southern blot analysis displaying telomere lengths in iPSC at day 0 through NPCs PD 42.6. First and last lanes are molecular weight markers used to determine the sizes of TRFs in samples during the differentiation time course. iPSC was fully differentiated into NPC by day 10. E) Western blot image of siRNA-induced NOVA1, PTBP1 and PTBP2 knockdown in human iPSC. F) Transient siRNA-induced knockdown of NOVA1 and PTBP1, but not PTBP2, significantly shifted *TERT* gene expression from potential FL *TERT* (exons 7/8 included) to alternatively spliced minus beta *TERT* (exons 7/8 excluded) in iPSCs (determined by ddPCR; n = 5 biological replicates per condition). G) Transient knockdown of

PTBP1, not NOVA1 nor PTBP2, significantly reduced telomerase enzyme activity in iPSCs (determined by ddTRAP; n = 5 biological replicates per condition). One-way ANOVA with uncorrected Fisher's LSD for post hoc comparisons of treatments were used to compare Day 10 and Day 29 with Day 0 (B, C) and siRNA-treated conditions with siControl (F, G; *, $P < 0.05$; **, $P < 0.01$; ***, $P < 0.001$; ****, $P < 0.0001$). Data are presented as means ± standard deviations where applicable.

4.4.2. Impact of iPSC cell density on expression of *TERT* splice variants.

Understanding the regulation of *TERT*'s reverse transcriptase domain (exons 4-13) is important for understanding the generation of telomerase active *TERT*. Therefore, in the following experiments, we focused on alternative splicing within this region. While we were testing different cell seeding densities of iPSCs for siRNA knockdown experiments, we noticed that the ratio of exons 7/8 including *TERT* appeared to change depending on cell density. We hypothesized that higher cell density resulted in higher percentage of exons 7/8 including *TERT*. To test our hypothesis, we seeded different numbers of iPSCs and collected 48 hours after (Figure 4.2A). Although the amount of total *TERT* transcripts (sum of exons 7/8 inclusion (potential FL) and exons 7/8 exclusion (minus beta)) did not change significantly (Figure 4.2B), the ratio of exons 7/8 including *TERT* increased along with cell density (Figure 4.2C). With higher cell density, telomerase activity was also increased and positively correlated to the ratio of exons 7/8 including *TERT* (Figure 4.2D, Supplemental Figure 4.2H), supporting that the increase of exons 7/8 including *TERT* transcripts represents increased production of FL *TERT* transcripts (i.e., telomerase coding *TERT*). We also measured other known *TERT* splice variants that include exons 7/8 such as minus alpha (exon 6 partial exclusion), INS3, INS4, minus gamma (exon 11 exclusion), plus gamma (exon 11 inclusion), intron 11 retention, and intron 14 retention to rule out changes in other splice variants explaining our observations. Expression of the tested splice variants that also contain exons 7/8 were not impacted significantly by cell density (Supplemental Figures 4.2A-G). In summary, these data suggest that alternative splicing regulation of exons 7/8 skipping in iPSC is impacted by cell density. Higher cell densities induce higher

expression of FL *TERT* resulting in higher telomerase activity without an increase in total *TERT* expression.

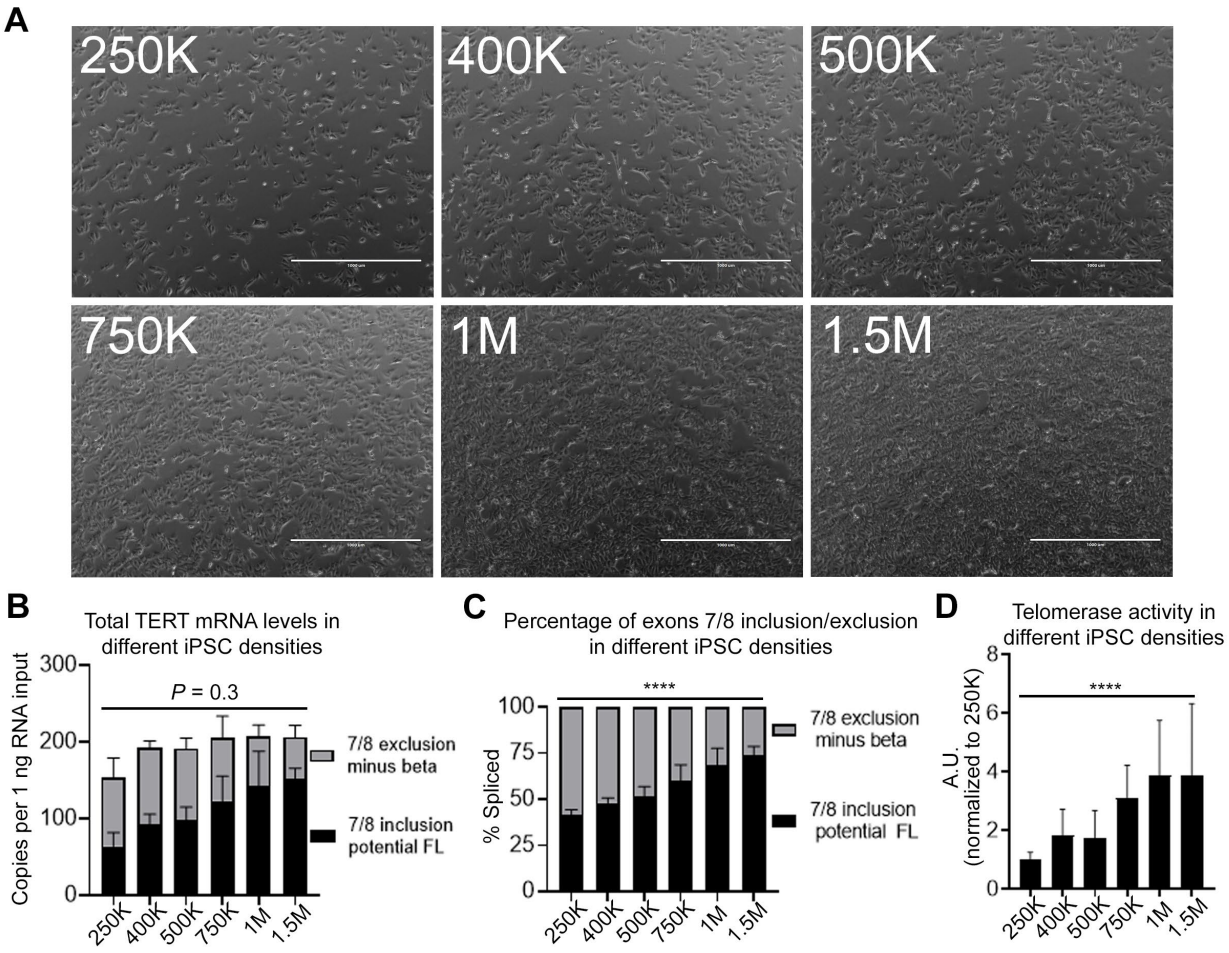

Figure 4.2. Impact of iPSC cell density on expression of *TERT* splice variants.

A) Representative phase contrast micrograph, 24 hours after seeding. The number of seeded iPSCs are indicated. Scale bar for image is 1000 µm. B and C) *TERT* gene expression is shifted from alternatively spliced, exons 7/8 excluding *TERT* (minus beta), to exons 7/8 including *TERT* (potential FL) with higher iPSCs density (determined by ddPCR; n = 4 biological replicates per condition). Transcript copies per 1 ng RNA input (B) and splicing ratio (C) were quantified. D) Telomerase activity significantly increased with higher iPSC density compared to lowest cell density condition (determined by ddTRAP; n = 4 biological replicates per condition). One-way ANOVA was performed to compare total amount of *TERT* including/excluding exons 7/8 (B), ratio of exons 7/8 including *TERT* splice variants (C), and telomerase activity (D) of all conditions (****, $P < 0.0001$). Data are presented as means ± standard deviations where applicable.

4.4.3. Impact of Calu-6 cell density on expression of *TERT* splice variants.

Next, we aimed to determine if cell density impacted cancer cell *TERT* splice variant expression similar to iPSCs. To test our hypothesis, we seeded different numbers of Calu-6 lung cancer cells and collected 48 hours after (Figure 4.3A). We observed significant reduction in both exons 7/8 including and excluding *TERT* transcripts (Figures 4.3B and C) while we did not observe significant changes in the splicing ratio of exons 7/8 (Figure 4.3D). Next, we measured the same *TERT* splice variants that we measured in iPSCs, and all splice variants were decreased in the medium and high-density conditions compared to the low-density condition (Figures 4.3E-K). Telomerase activity was significantly reduced in medium density compared to low-density, but low- and high-density were not significantly different from each other (Figure 4.3L). Clearly, overall *TERT* transcripts decreased with an increased cell density in Calu-6 cells. Also, higher cell density resulted in reduction of telomerase activity in Calu-6 cells, which is opposite to our observations in iPSCs.

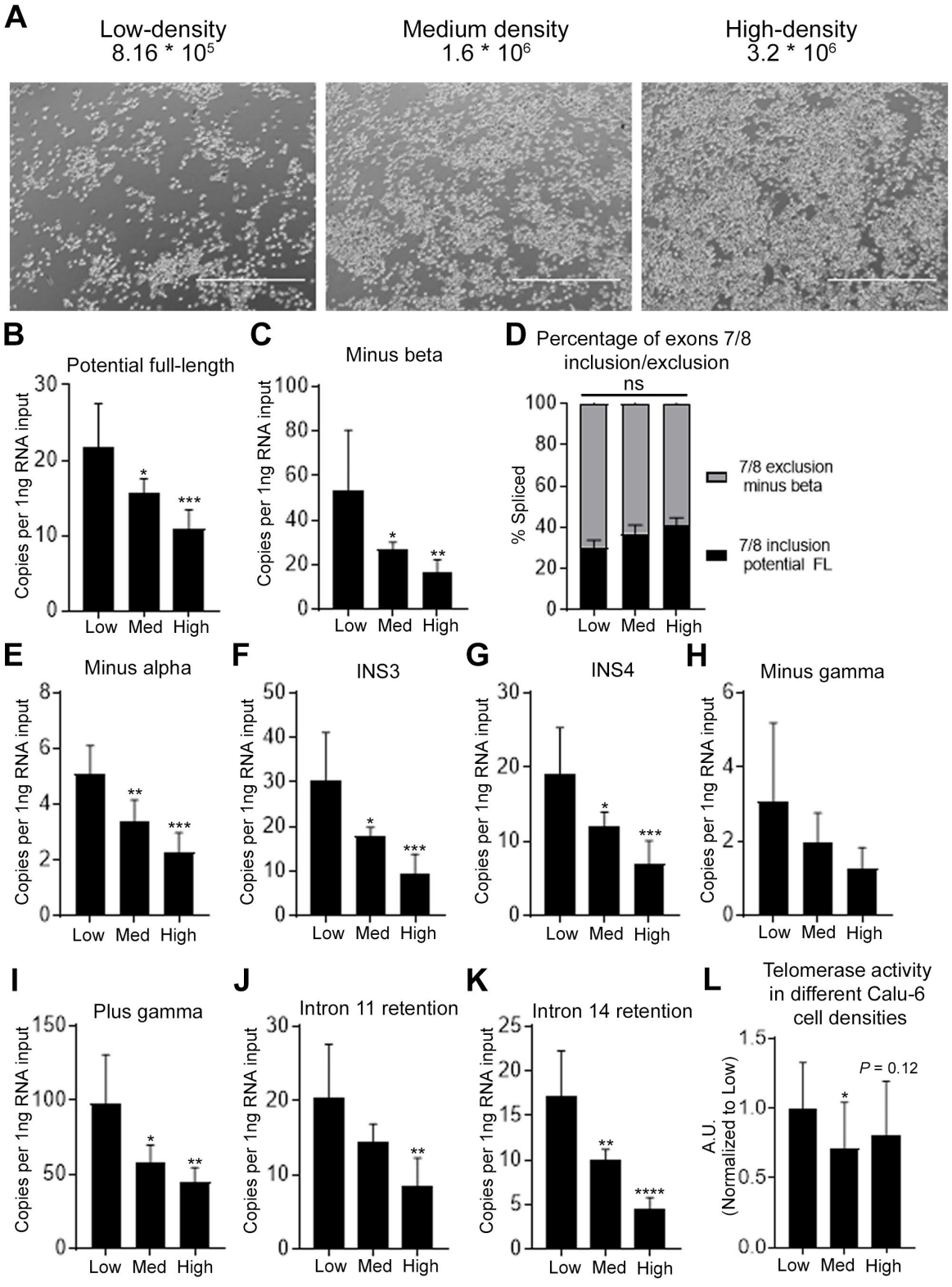

Figure 4.3. Impact of Calu-6 cell density on expression of *TERT* splice variants.

A) Representative phase contrast micrograph images 24 hours after seeding. The number of seeded Calu-6 cells are indicated. Scale bar for image is 1000 μm. B,C, and E-K) Expression of *TERT* splice variants are reduced with higher cell density. Potential FL (B), minus beta (C), minus alpha (E), INS3 (F), INS4 (G), minus gamma (H), plus gamma (I), intron 11 retention (J), and intron 14 retention (K) transcripts were quantified (determined by ddPCR; n = 6 biological replicates per condition). D) Exons 7/8 alternative splicing ratio did not change significantly in different cell densities. L) Telomerase activity in different cell densities (determined by ddTRAP; n = 6 biological replicates per condition). One-way ANOVA with uncorrected Fisher's LSD for *post hoc* comparisons were used to compare medium (Med) and high-density (High) conditions with low-density (Low) condition (B-L; ns, $P > 0.05$; *, $P < 0.05$; **, $P < 0.01$; ***, $P < 0.001$; ****, $P < 0.0001$). Data are presented as means ± standard deviations where applicable.

4.4.4. Identification of candidate splicing factors that potentially regulate *TERT* splice variant expression differently between iPSCs and lung cancer cells.

We utilized our *TERT* minigene loss-of-function (siRNA) screening data in HeLa cells from Ludlow et al. [26] and publicly available TCGA (The Cancer Genome Atlas) data from LUAD (lung adenocarcinoma) patients [192] to select candidates regulating *TERT* AS for further study. Briefly, Ludlow et al. [26] measured the ratio of luciferase expression that indicated inclusion or exclusion of exons 7/8 from a *TERT* reporter minigene after siRNA knockdown of splicing factors in HeLa cells to find enhancers/repressors of telomerase. From the minigene data, we selected three SFs (SRSF2, U2AF2, and CDC40) that promoted FL *TERT* production more than 2-fold and had predicted binding sites in the *TERT* gene between exons 5-9. We also selected two SFs (HNRNPA1 and HNRNPM) because they promoted minus beta *TERT* production more than 2-fold and have predicted binding sites in the *TERT* gene between exons 5-9 (Figure 4.4A). We also included four additional splicing regulatory genes (HNRNPA2B1, HNRNPH1, HNRNPCL1, and SRPK1) because they are either related to cancer in general or have been associated with telomere biology (HNRNPA2B1: [218]; HNRNPH1: [219]; HNRNPCL1: [220]; SRPK1: [221]).

The TCGA data provides gene expression levels (RSEM values from RNA-Seq) from tumor tissues and tumor-adjacent normal tissues of LUAD patients. Since we recently published that only TCGA LUAD tumor samples express FL *TERT* and tumor adjacent normal tissues do not express FL *TERT* [30], we surmised that highly expressed splicing factors would be related to the re-emergence of FL *TERT* in the cancerous tissue. Using this logic we investigated the expression of the minigene-

selected SFs in the paired-normal-tumor-samples from the TCGA data (Figures 4.4B-F). Among the selected SFs, we identified five SFs that had significantly increased expression in the tumor samples compared to normal tissues (SRSF2 ($P < 0.01$), U2AF2 ($P < 0.01$), HNRNPA2B1 ($P < 0.01$), SRPK1 ($P < 0.01$), and HNRNPA1 ($P < 0.01$), Figures 4.4B-F). Four SFs were not significantly different between matched normal and tumor samples (CDC40, HNRNPH1, HNRNPCL1, and HNRNPM, Supplemental Figures 4.3A-D). We used these data as the foundation for an antibody expression screen of the same proteins in our cell density experiments with the iPSCs as a means to identify SFs that regulate TERT differently or similarly between stem and cancer cells.

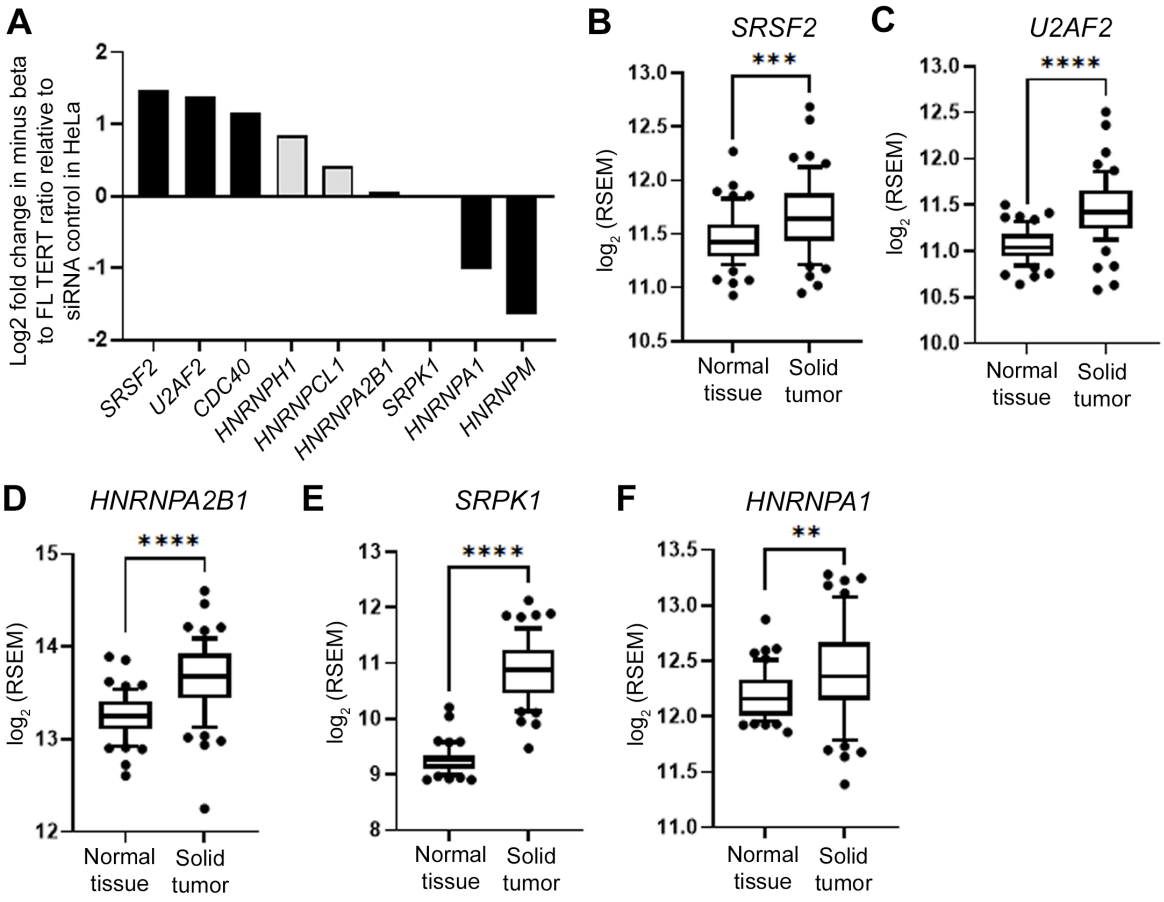

Figure 4.4. Analysis of *TERT* AS minigene loss-of-function screen and patient tumor expression profiles of splicing factors identifies top candidate SF related to *TERT* splicing in lung cancer cells.

A) *TERT* minigene data of selected SFs showing effect of SF knockdown on *TERT* exons 7/8 splicing in HeLa cells [26]. B-F) Log2-transformed RSEM values of SFs gene-expression levels (n = 58 matched LUAD patient samples). SRSF2 (B), U2AF2 (C), HNRNPA2B1 (D), SRPK1 (E), and HNRNPA1 (F) are significantly upregulated in tumor tissues from LUAD patients compared to tumor-adjacent normal tissues. Paired Student's *t* test set at $P \leq 0.05$ for significance compared with normal tissue controls (B-F; ** $P < 0.01$; *** $P < 0.001$; **** $P < 0.0001$). In the box plots, the lower boundary of the box indicates the 25th percentile, a line within the box marks the median and the higher boundary of the box indicates the 75th percentile. Whiskers above and below the box indicate the 10th and 90th percentiles. Points above and below the whiskers indicate data outside the 10th and 90th percentiles.

4.4.5. Impact of iPSC cell density on SF expression of *TERT* regulating candidate SFs.

Since *TERT* AS was significantly altered in the iPSC cell density experiment, we surmised that SFs that correlated with changes in potential FL *TERT* would potentially regulate *TERT* AS in stem cells. We measured protein levels of the nine SFs (SRSF2, U2AF2, CDC40, HNRNPA1, HNRNPM, HNRNPA2B1, HNRNPH1, HNRNPCL1, and SRPK1) in the iPSCs cell density experiment. Using SF protein level data and the *TERT* mRNA splice variant expression data we carried out correlational analysis to reveal potential relationships between percentage of exons 7/8 including *TERT* and SFs. Expression level of six splicing factors (HNRNPA2B1, HNRNPCL1, HNRNPH, HNRNPM, SRSF2, and SRPK1) showed significant positive correlations with the percentage of exons 7/8 inclusion (potential FL *TERT*; Pearson's correlation $r = 0.5747$, $P = 0.0033$; $r = 0.4992$, $P = 0.013$; $r = 0.6230$, $P = 0.0011$; $r = 0.5589$, $P = 0.0045$; $r = 0.6651$, $P = 0.0004$; $r = 0.6597$, $P = 0.0005$, respectively; Figures 4.5A-F), whereas three splicing factors (HNRNPA1, U2AF2, and CDC40) did not show significant correlation (Supplemental Figures 4.4A-C).

Based on the *TERT* minigene study in HeLa cells, TCGA data in LUAD patients, and iPSC data, we classified the SFs into either FL *TERT*-promoting (green color), minus beta *TERT*-promoting (red color), or non-effector (no color) to summarize their predicted behavior in iPSCs and cancer cells (Supplemental Table 4.1). From this table, we selected HNRNPM as a stem cell-specific FL *TERT* promoter because it was only related to FL *TERT* expression in stem cells; SRSF2 as a FL *TERT* promoter in both stem cells and cancer cells because it was related to FL *TERT* expression in all three

data sets; and U2AF2 as a cancer cell specific FL *TERT* promoter because it was only related to FL *TERT* expression in the minigene and TCGA data (yellow color highlighted in Supplemental Table 4.1). We also investigated correlation between the percentage of exons 7/8 including *TERT* and three RNA binding proteins: PTBP1, NOVA1, and PTBP2. However, we could not find correlation in different cell densities (Supplemental Figures 4.4E-G).

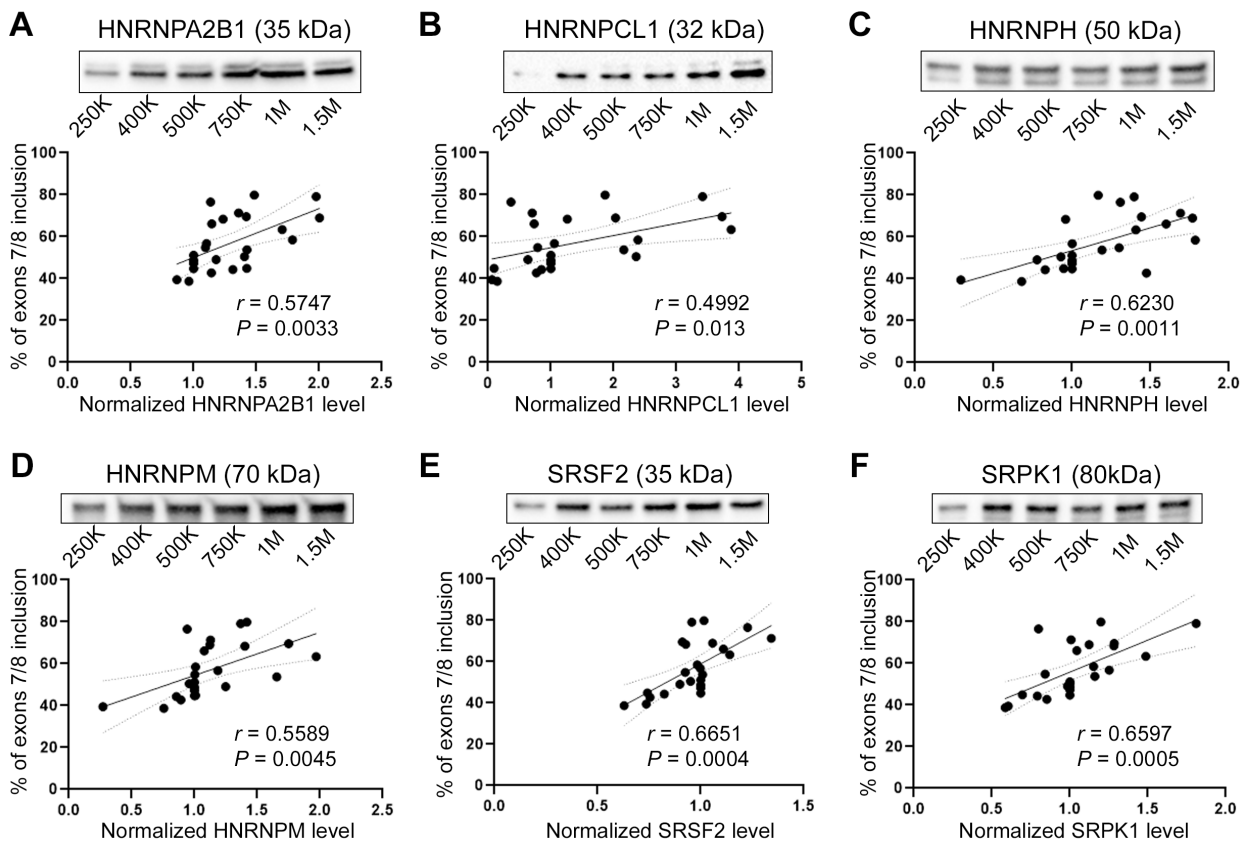

Figure 4.5. Impact of iPSC cell density on SF expression of *TERT* AS candidate SFs.

A-F) Western blots of splicing factors and correlation analyses in different iPSC density. Top are representative images and bottom are scatter plots showing correlations between housekeeping gene-normalized SF expression levels and percentage of *TERT* exons 7/8 inclusion (n = 4 biological replicates per condition). Antibodies targeting HNRNPA2B1 (A), HNRNPCL1 (B), HNRNPH (C), HNRNPM (D), SRSF2 (E), and SRPK1 (F) were used for the western blots. 95% Confidence bands, Pearson's correlation coefficient (*r*) and *p* values are shown. For the correlation analysis, 24 data points are included (six conditions x four replicates).

4.4.6. Knockdown of candidate splicing factors (SFs) in cancer cells (Calu-6) results in expected shifts in *TERT* AS.

Based on our candidate selection process, three SFs are expected to be FL *TERT* promoters (HNRNPM in iPSCs; SRSF2 in both iPSCs and cancer cells; U2AF2 in cancer cells). To confirm our predictions, we performed loss-of-function (siRNA) studies in Calu-6 lung cancer cells. Knockdown by siRNAs of each splicing factor in Calu-6 cells was confirmed by western blotting (Figures 4.6A-C). When HNRNPM expression was reduced, the ratio of exons 7/8 including *TERT* to exons 7/8 excluding *TERT* expression did not change significantly compared to control-treated cells, matching our predictions (Figure 4.6D). When expression of SRSF2 or U2AF2 was reduced, the ratio of exons 7/8 including *TERT* to exons 7/8 excluding *TERT* was reduced, indicating a reduction in FL *TERT* expression (Figure 4.6D). These outcomes of *TERT* AS also matched our predictions that SRSF2 and U2AF2 were FL *TERT* promoters in cancer cells, while HNRNPM would not impact splicing of *TERT* exons 7/8. The absolute expression of exons 7/8 including *TERT* transcripts were reduced with knockdown of all SFs compared to the scramble siRNA-treated cells (Supplemental Figure 4.5A). Exons 7/8 excluding *TERT* transcripts were significantly reduced in HNRNPM and SRSF2 knockdown cells, while U2AF2 cells had similar expression levels compared to controls (Supplemental Figure 4.5B). When compared to the scramble siRNA-treated cells, telomerase activity was significantly reduced by knockdown of all splicing factors (Supplemental Figure 4.5C). This indicates that HNRNPM knockdown was indirectly reducing *TERT* expression, while SRSF2 or U2AF2 knockdown was likely more directly shifting *TERT* splice variant expression ratio, resulting in reduced telomerase activity.

When protein expression levels of the three SFs were compared in iPSCs to NPCs, SRSF2 expression increased significantly whereas HNRNPM or U2AF2 expression did not change significantly (Supplemental Figures 4.5D-F).

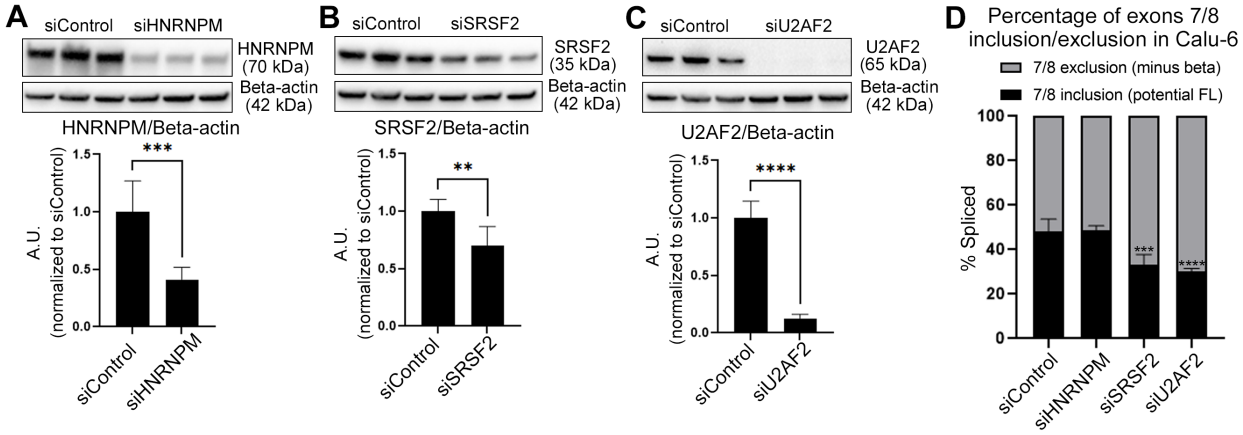

Figure 4.6. Knockdown of candidate splicing factors (SFs) in cancer cells (Calu-6) resulted in expected shifts in *TERT* splice variant expression.

A-C) Knockdown of HNRNPM (A), SRSF2 (B), and U2AF2 (C) was confirmed by western blot. Representative images of selected SFs and beta-actin (loading control) (top panel). Knockdown was quantified by normalization with beta-actin then expressed relative to siRNA control (n = 6 biological replicates per condition; bottom panel). D) *TERT* splice variant expression ratio of exons 7/8 inclusion (potential FL) to exons 7/8 exclusion (minus beta) was reduced by knockdown of SRSF2 and U2AF2, not HNRNPM (determined by ddPCR; n = 6 biological replicates per condition). Student's t test set at $P \leq 0.05$ for significance compared with siRNA-treated conditions with siControl (A-C; **, $P < 0.01$; *** $P < 0.001$; **** $P < 0.0001$). One-way ANOVA with uncorrected Fisher's LSD for *post hoc* comparisons of

siRNA treatments were used to compare siRNA-treated conditions with siControl (D; ***, $P < 0.001$; ****, $P < 0.0001$). Data are presented as means ± standard deviations where applicable.

4.5. Discussion

Understanding the precise control and regulation of telomerase activity is critical to both cancer and regenerative biology. Recent evidence from our laboratory and others has pointed out that in addition to transcriptional regulation, post-transcription mechanisms such as alternative RNA splicing are critical to the generation of telomerase-active TERT. Specifically, *TERT* pre-mRNAs are alternatively spliced to form various splice variants and only full-length *TERT* with all 16 exons can be translated into active telomerase (Figure 4.7A). On the other hand, other splice variants (such as minus beta *TERT*) are degraded by nonsense-mediated decay or translated into inactive telomerase that cannot synthesize telomeres [25]. In this research, we confirmed that *TERT* AS is regulated by the NOVA1-PTBP1-PTBP2 axis in iPSCs and iPSC differentiation into NPC. Next, we determined that *TERT* AS is impacted by cell density in stem cells (iPSCs) but not in cancer cells (Calu-6). Lastly, we identified splicing factors that are predicted to impact *TERT* splice variant expression only in cancer cells, only in stem cells, or in both cell types. Overall, our findings indicate that we may be able to decipher a regulated *TERT* AS code that controls telomerase in stem cells, and that cancer cells probably use several different codes to induce FL *TERT* and telomerase via alternative RNA splicing factor expression.

NOVA1 and PTBP2 are brain- and neural-specific splicing factors that help determine neural cell fate, while PTBP1 is a more ubiquitous splicing factor. While PTBP1 and PTBP2 share overlapping target genes, they also have separate targets and may induce opposite effects on shared target genes [222]. We have previously shown that when PTBP1 is knocked down, FL *TERT* and telomerase levels are reduced

in non-small cell lung cancer (NSCLC) cells [27]. Specifically, we determined that PTBP1 interacts with NOVA1 to promote FL *TERT* and telomerase activity in lung cancer cells. However, when PTBP1 was knocked down in lung cancer cells, PTBP2 levels went up to compensate for reduced PTBP1 levels, and PTBP2 interacts with NOVA1 [223] and resulted in reduced FL *TERT* and telomerase. When we differentiated stem cells into NPCs we also observed increased NOVA1, increased PTBP2, reduced PTBP1, and reduced *TERT*. The amount of total *TERT* transcripts, the amount and percentage of exons 7/8 including *TERT* (FL *TERT*), and telomerase activity decreased with the differentiation (iPSC differentiation in Figure 4.7B), mimicking what we observed in NSCLC cells when PTBP1 was knocked down. We then tested this observation in loss-of-function studies in stem cells. We were able to replicate that when PTBP1 is reduced, PTPB2 is increased and likely interacts with NOVA1 to repress TERT and telomerase activity. In addition to PTBP1 knockdown, we also knocked down NOVA1 and PTBP2 by siRNA treatment in iPSCs. Compared to PTBP1 knockdown result that replicates our previous study in cancer cells [27], NOVA1 knockdown did not result in significant reduction of telomerase activity in iPSCs despite the significant reduction of NOVA1 expression level. It only resulted in the reduction of the amount and percentage of exons 7/8 including *TERT*. When NOVA1 was knocked down, PTBP1 level also decreased significantly (~39%) whereas PTBP2 level did not change significantly. Considering the abundance of PTBP1 and NOVA1 in iPSCs, the reduction of exons 7/8 including *TERT* is likely to be mainly associated with PTBP1 reduction induced by indirect effects from NOVA1 knockdown. It also can be interpreted that either 1) reduced level of NOVA1 expression is still sufficient to recruit PTBP1 to promote FL

TERT or 2) NOVA1 does not affect the recruitment of PTBP1 in iPSCs. Further studies (e.g., overexpression of NOVA1 in iPSCs) are needed to confirm the recruitment of PTBP1 by NOVA1 in iPSCs. Overall the importance of PTBP1 regarding *TERT* AS in iPSCs remains. When PTBP2 was knocked down, it resulted in non-significant changes in telomerase activity or *TERT* AS. In addition to the decrease in PTBP2 expression level, expression levels of NOVA1 and PTBP1 were also modestly reduced by PTBP2 knockdown. No reduction in exons 7/8 including *TERT* was observed despite the significant reduction of NOVA1 and PTBP1 expression, likely due to there being enough PTBP1 and NOVA1 protein remaining to maintain FL *TERT* expression levels. This indicates that there is likely a threshold of PTBP1 or NOVA1 reduction that must be reached before FL *TERT* is impacted. Despite the challenges of data interpretation due to apparent interdependent protein expression between NOVA1-PTBP1-PTBP2 the following conclusions can be still made: 1) a threshold of exons 7/8 including *TERT* reduction is needed to result in significant telomerase activity reduction. 2) PTBP1 is a major FL *TERT* promoter in iPSCs. 3) The increase in NOVA1 and PTBP2 with neuronal cell lineage differentiation is likely a strong cell fate determining mechanism that results in repressed *TERT* in neural tissues of humans (left panel in Figure 4.7C).

When we were empirically determining the cell density to seed stem cells at for siRNA loss-of-function studies, we noted that FL *TERT* splice variant expression tended to track with cell density. Indeed, when we tested different densities, we observed a striking switching in splice variant expression from mostly minus beta (exons 7/8 excluded) to mostly potential FL *TERT* (exons 7/8 included) with little changes in total *TERT* transcripts of the reverse transcriptase domain (exons 4-13) (iPSC density in

Figure 4.7B). Next, we wanted to confirm if this cell density dependent switch in splicing was conserved in lung cancer cells. We observed reduced *TERT* total transcripts with little to no switching in splice variant expression in higher cell density of Calu-6 lung cancer cells (Calu-6 density Figure 4.7B). These data indicate that regulation of *TERT* expression in stem cells may rely more heavily on *TERT* splice variant ratios compared to the lung cancer cells that relies more on transcriptional regulation to promote or repress TERT. This observation should be tested in more cancer cell lines to determine a general versus cell line specific phenomenon.

Next, we wanted to build upon the idea that there is a regulated *TERT* splicing code in stem cells and a dysregulated *TERT* splicing code in cancer cells. To do this we utilized our previously published *TERT* minigene splicing factor loss-of-function screen [26], TCGA public RNA-Seq data of splicing factor expression, and an antibody screen of *TERT* related splicing factors in stem cells. Of the nine splicing factors that we screened to be potential *TERT* regulatory factors, we observed that five splicing factors were related to *TERT* expression in lung cancer patient samples. Then we counter screened all nine factors in our stem cell density model by measuring their protein expression and correlated *TERT* expression to splicing factor expression. This analysis revealed that six splicing factors were correlated with FL *TERT* expression. The combination of these analyses revealed stem cell- and cancer cell-specific TERT regulatory factors (Supplemental Table 4.1). Based on our current (Figure 4.1) and previous observations, we also investigated the correlation between *TERT* expression and NOVA1, PTBP1, and PTBP2. However, the expression of these *TERT* AS regulators was not correlated to the expression of *TERT* in different stem cell densities.

This indicates that the shifting of *TERT* AS in different cell density is not dictated by the NOVA1-PTBP1-PTBP2 axis.

Based on our screening data we next wanted to test our predictions of *TERT* cell type-specific regulators. We performed loss-of-function experiments in Calu-6 lung cancer cells. Our data revealed that our methods accurately predicted splicing factors that would impact *TERT* splice variant expression ratios in cancer cells (right panel in Figure 4.7C). To investigate whether the three splicing factors (HNRNPM, SRSF2, U2AF2) regulate *TERT* AS in stem cell differentiation into NPC, we compared protein expression levels of the splicing factors in iPSCs and NPCs. However, differentiation did not induce significant changes in the expression levels of HNRNPM and U2AF2. Moreover, increased SRSF2 expression in NPC indicates that SRSF2 is unlikely a FL *TERT*-promoting splicing factor in NPC. In addition to the three splicing factors we tested, other splicing factors and RNA binding proteins that regulate *TERT* alternative splicing have been identified by other studies. In studies using cancer cells, splicing of the *TERT* reverse transcriptase domain has been focused on because of its importance in telomerase activity [25, 30]. In stem cells, it was shown that skipping of *TERT* exon 2 is a developmental switch for TERT expression and is regulated by the splicing co-factor SON [108]. Finding conserved or different *TERT* AS regulation in multiple cell and tissue types will result in the identification of therapeutic approaches by which specific manipulation of telomerase activity can be achieved in certain cell types (e.g., cancer cells versus stem cells). For example, we recently published that knockdown of SF3B4 induces reduction of FL *TERT* in NSCLC cells resulting in decreased telomerase activity, cell viability, and proliferation of cancer cells [30]. Conversely, when SF3B4 was

knocked down in non-cancerous cells (human bronchial epithelial cells, HBECs) it did not reduce viability or proliferation of cells proposing a new approach for cancer cell specific therapy.

These data point out that *TERT* AS is regulated by both tissue specific and general RNA binding proteins. By prediction and or empirical identification of where these RNA binding proteins interact with their motifs on the *TERT* pre-mRNAs, we might be able to develop antisense oligonucleotide (ASO) type drugs to block the binding of the RNA binding proteins to switch the splicing of *TERT* from telomerase coding TERT to degraded or dominant-negative type TERTs. Indeed, research has already pointed out that SRSF2 binding is predicted at the intron 6/exon 7 boundary and groups have targeted this region using ASOs to induce minus beta splicing [224]. Further, we and others have utilized the binding motif of NOVA1 in direct repeat 8 to develop ASOs as well [26, 181, 225]. As we continue to elucidate the RNA binding proteins of *TERT* we will identify additional and potentially more potent motifs to target with splicing switching ASOs aimed at reducing telomerase activity for anticancer purposes. A provocative idea would be to target FL *TERT* repressor motifs with ASOs to promote FL *TERT* splicing and increase telomerase activity for regenerative medicine purposes.

Our data are not without limitations. Since we only tested a single stem cell line and a single cancer cell line, our data should therefore be interpreted with caution, and further research including additional cell lines should be performed to see if our predictions and models hold. Moreover, although we measured multiple *TERT* splice variants in this study, we did not measure all known *TERT* splice variants. To date, 21 *TERT* splice variants have been identified [28] and determining expression levels of all

different splice variants is extremely challenging. Measurement of other known *TERT* splice variants or novel splice variants in different cell types will provide insights to fully understand *TERT* AS regulation. Another limitation of this study is that we did not perform the siRNA loss-of-function studies in the stem cells. Since our laboratory is mainly focused on inhibition of telomerase activity as a cancer therapeutic approach, we focused on dysregulated telomerase in this research. For future research, identification of the *TERT* splicing code should be performed as well as functional outcomes (telomerase activity, telomere length, cell survival, etc.) in different cell types that are characterized by regulated (i.e., stem cells) or dysregulated (i.e., cancer cells) alternative splicing.

Overall, our data represent an advance in our understanding of *TERT* regulation in stem cells and cancer cells. We utilized a novel model to investigate *TERT* splicing regulation in stem cells and contrasted this with associations of SFs in cancer cells. Our data revealed that certain SFs are dysregulated in cancer and do not seem to play a role in *TERT* regulation in stem cells. These data and subsequent studies may reveal a splicing factor(s) or their binding site(s) that could be targeted with small molecule drugs or antisense oligonucleotides, respectively, to reduce telomerase activity in cancer cells and promote durable cancer remissions.

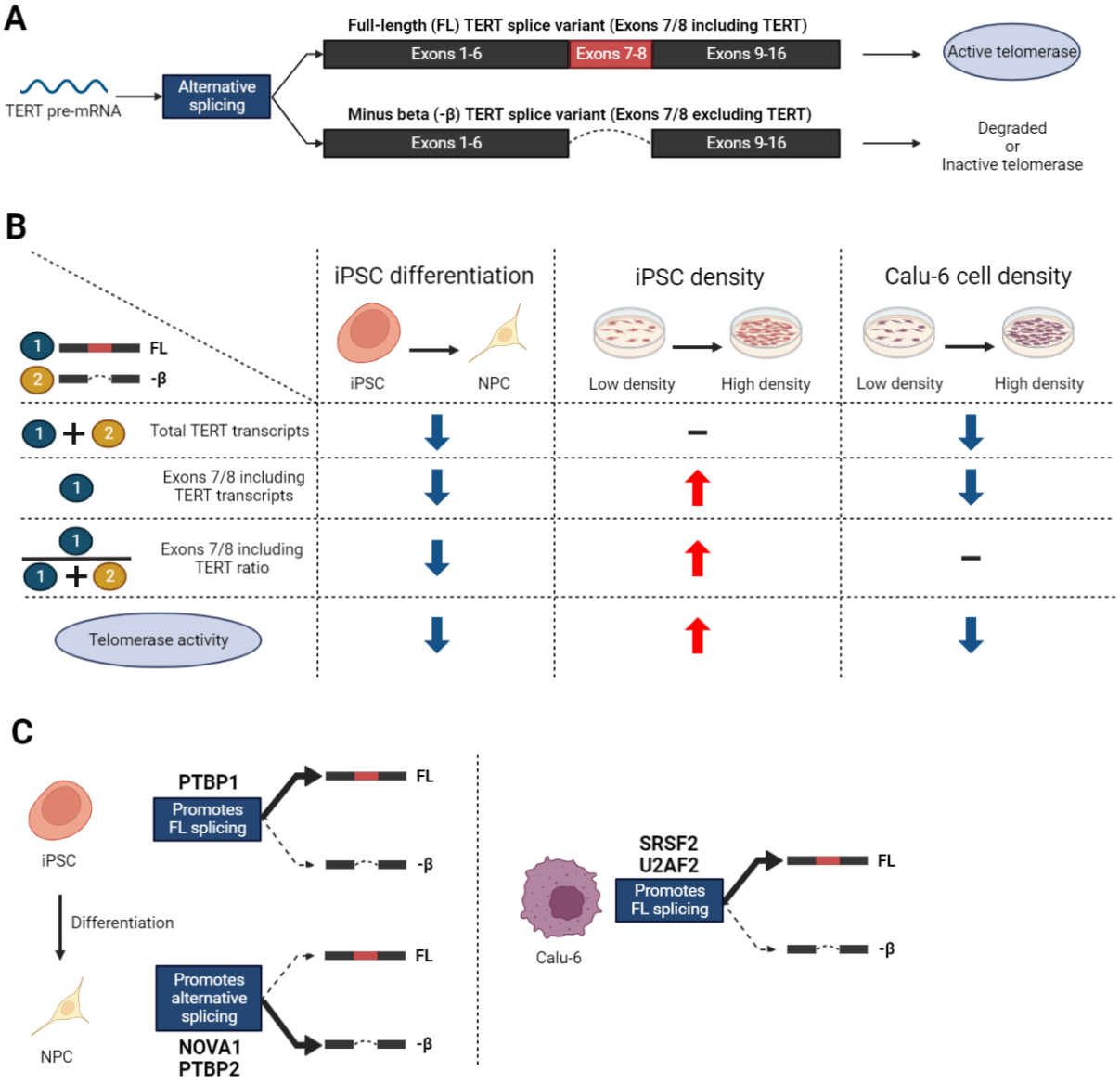

Figure 4.7. Working model figure describing splicing events of *TERT* observed in this study.

A) Alternative splicing of *TERT* pre-mRNA produces splice variants. Only full-length *TERT* with all 16 exons can be translated into active telomerase. When exons are spliced out (e.g., exclusion of exons 7-8 in red box), transcripts are degraded or form inactive telomerase. B) *TERT* expression and telomerase activity in three different contexts (iPSC differentiation into NPC, increase in iPSC density, and Calu-6 cell density). Increase (red arrow) or decrease (blue arrow) or no change (—) are indicated for total *TERT* transcripts (FL *TERT* (7/8 included) plus minus beta *TERT* (7/8 excluded); ①+②), absolute amount of FL

TERT transcript (7/8 included, ①), percentage of FL *TERT* transcripts compared to total (①/(①+②)), and telomerase activity. C) (Left panel) *TERT* AS regulators in iPSC differentiation into NPC or in calu-6 cells. PTBP1 promotes FL *TERT* in iPSCs whereas NOVA1 and PTBP2 promote minus beta *TERT* in NPCs. (Right panel) Three splicing factors were selected as cell type specific FL *TERT*-promoting candidates (HNRNPM in iPSCs; SRSF2 in both iPSCs and cancer cells; U2AF2 in cancer cells). *TERT* AS in Calu-6 cells was not affected by HNRNPM knockdown. On the other hand, SRSF2 or U2AF2 knockdown significantly reduced the amount and percentage of FL *TERT* (7/8 included). This figure was created with BioRender.com.

Chapter 5 – Effect of Aging and Exercise on hTERT Expression in Thymus Tissue of hTERT Transgenic Bacterial Artificial Chromosome Mice

5.1. Abstract

Introduction: Telomere shortening occurs with aging due to telomerase insufficiency and exercise interventions can upregulate telomerase activity. The impact of aging and exercise on *hTERT* alternative splicing (AS) in the thymus is unknown.

Purpose: This study aimed to examine *hTERT* AS in response to aging and exercise in thymus tissue.

Methods: Transgenic mice expressing the human TERT (hTERT) called hTERT-BAC (bacterial artificial chromosome) mice were utilized in two different exercise models. For the first model, the mice were divided into three different groups depending on their age (young (6 months), middle-aged (12 months), and old (18-22 months)) and further assigned into either an individual sedentary cage (no wheel access) or an individual exercise cage (wheel access) for three weeks prior to thymus tissue excision. For the second exercise model, the thymus tissues from middle-aged mice (16 months) were excised before (Pre, n = 5), immediately post (IPE, n = 5), and 1-hour post (1h-Post, n = 5) treadmill running (30 min at 60% maximum speed). Exons 7/8 containing *hTERT* and the "minus beta" (-β) *hTERT* AS variant (exons 7 and 8 skipping) were quantified by droplet digital reverse transcription-polymerase chain reaction.

Results: The amount of *hTERT* transcripts decreased with aging (r = -0.7511, p < 0.0001) and three weeks of voluntary wheel running did not counteract this reduction. The ratio of exons 7/8 containing *hTERT* increased with aging (r = 0.3669, p = 0.0423) but three weeks of voluntary wheel running attenuated this aging-driven effect (r = 0.2013, p = 0.4719). 30 minutes of acute treadmill exercise did not induce and significant changes in thymus *hTERT* expression or AS variant ratio (p > 0.05).

Conclusions: Thymic *hTERT* expression is reduced with aging. We speculated that this reduction could be a primary aging effect since exercise did not counteract the reduction of expression. We also showed that the increased percentage of exons 7/8 containing *hTERT* transcripts during sedentary aging is attenuated by exercise indicating that *hTERT* AS regulation is impacted by secondary aging as well as primary aging.

5.2. Introduction

Aging is a complex and inevitable process that occurs throughout an organism's life. Aging consists of both chronological aging and biological aging, each with distinct characteristics. Chronological aging is the straightforward measurement of an organism's age in years, starting from birth. However, it does not necessarily reflect the individual's physical or physiological state accurately. In contrast, biological aging refers to the gradual deterioration of an organism's cells, tissues, and organs over time resulting in decline in physical and mental function, increase in risk of diseases, and ultimately death. This type of aging is influenced by a combination of genetic, environmental, and lifestyle factors, such as diet, exercise, and exposure to toxins. Biological aging is governed by two major aging process: primary aging and secondary aging. Primary aging is a collection of processes leading to loss of physiological resilience that are determined by an individual's genetics. Secondary aging is the collection of age-related processes that enhance the risk of disease and can be slowed down with lifestyle factors such as diet and exercise [57].

At a cellular level, the accumulation of senescent cells is a part of an organism's aging. Many factors can induce cellular senescence, such as epigenetic factors, mitochondrial dysfunction, DNA damage, proteostatic dysfunction, nutrient signaling dysfunction, and telomere erosion or telomere DNA damage signaling. Among these factors, telomere induced senescence plays a significant role in aging [226]. Telomeres are regions of repeated 5'-TTAGGG-3' DNA sequences at each end of chromosomes [11]. The major function of telomeres is to prevent the ends of chromosomes from being recognized as DNA double strand breaks [227]. By preventing DNA damage signaling at

chromosome ends, this prevents fusions of the chromosome ends by non-homologous end joining DNA repair mechanism thus preserving genomic stability [36]. However, telomere length shortens with cell division due to the inability of DNA polymerase to fully replicate the lagging strand of DNA [12]. When one or a subset of telomeres become critically short by repeated cell divisions, a DNA damage response will be triggered, and cells will become replicatively senescent [10]. Since the number of cell divisions in multicellular organisms will accumulate during aging, populations of senescent cells will increase overtime resulting in aging-related phenotypes [226]. However, some cells (i.e., male germline cells, adult stem cells, activated immune cells, etc.) can slow down telomere shortening with the expression of the enzyme telomerase.

Telomerase is a ribonucleoprotein enzyme that can elongate or maintain telomeres by *de novo* telomere synthesis [228]. Telomerase consists of an enzyme subunit TERT (telomerase reverse transcriptase), RNA component TERC (Telomerase RNA component, also known as TR), and accessary proteins. In human cells, TERT expression is the rate limiting factor of the telomerase complex [35, 78]. For this reason, the transcriptional level of TERT has been studied as a key regulatory mechanism of telomerase activity. In addition to transcriptional regulation, post-transcriptional regulation such as alternative splicing (AS) of *TERT* also regulates telomerase activity. The human *TERT* (*hTERT*) gene has 16 exons and 15 introns and the *hTERT* pre-mRNAs undergo RNA splicing to form *hTERT* full-length (FL) mRNA with all 16 exons with four functional domains (TEN: telomerase N-terminal; TRBD: telomerase RNA-binding domain; RT: reverse transcriptase; CTE: C-terminal extension) or alternatively spliced *hTERT* mRNA variants (Figure 5.1) [25, 229]. Since all four functional domains

are required for telomerase to be able to synthesize telomeres, only FL *hTERT* mRNA can be translated into active telomerase (Figure 5.1) [179]. In contrast, alternatively spliced minus beta (-β) *hTERT* lacking exons 7-8 for example, cannot form active telomerase and is expected to be degraded by nonsense-mediated decay or to form a truncated hTERT protein with dominant-negative function [106, 174]. Since FL *hTERT* and minus beta *hTERT* have been shown to be the most abundant *hTERT* mRNA variants [116], we focused on splicing of *hTERT* exons 7/8 in this study.

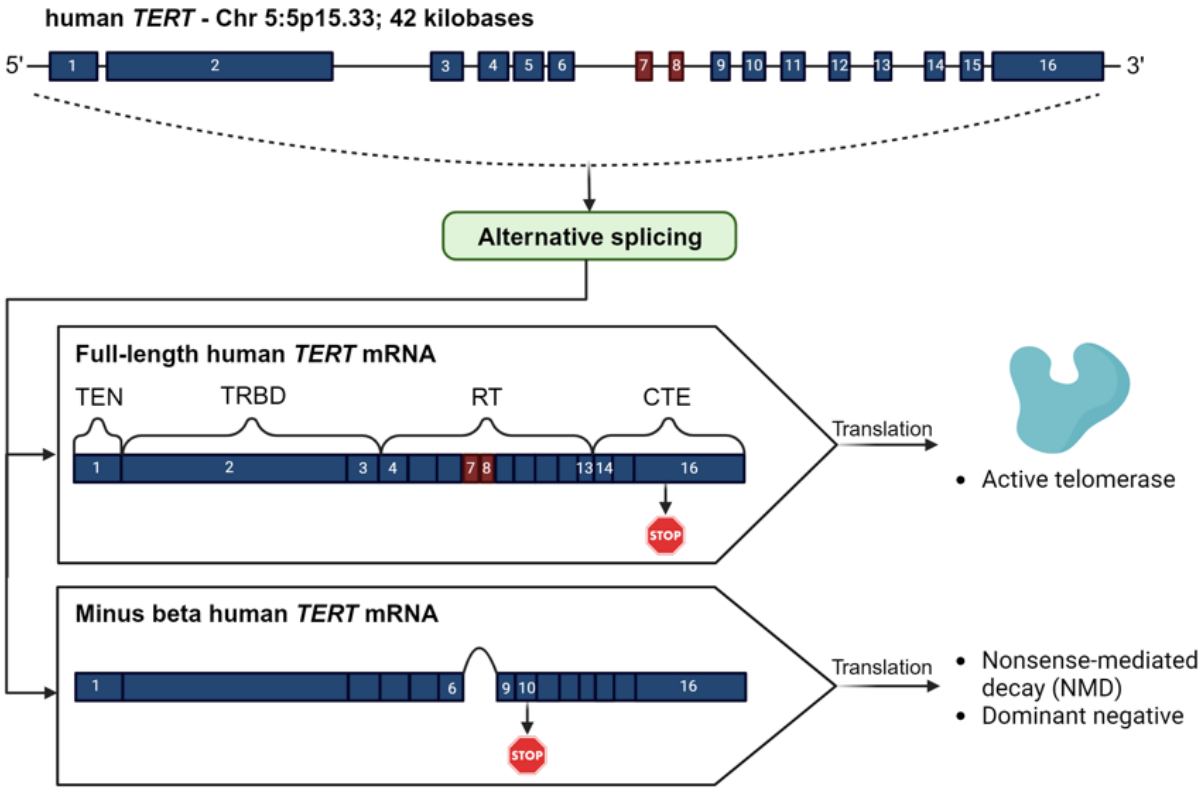

Figure 5.1. Cartoon of alternative splicing regulation of human *TERT* (*hTERT*) genes.

hTERT consists of 16 exon genes (colored box with numbers) and 15 introns (solid black line between exons). After transcription of *hTERT* gene, pre-mRNA undergo alternative splicing to form mature mRNA. Two main mRNA variants are depicted: full-length *hTERT* with all 16 exons and minus beta *hTERT* lacking exons 7-8 (highlighted in red). Four functional domains (TEN: telomerase N-terminal; TRBD: telomerase RNA-binding domain; RT: reverse transcriptase; CTE: C-terminal extension). Stop codon is located in exon 16 of full-length *hTERT*. Minus beta *hTERT* has premature stop codon in exon 10, induced by frameshifting from exons 7-8 skipping. Only full-length *hTERT* can be translated into active telomerase, whereas minus beta *hTERT* is predicted to be degraded by nonsense-mediated decay or translated to form dominant negative hTERT that may inhibit telomerase activity. This figure was created with BioRender.com.

In this study, we utilized transgenic mice expressing the human *TERT* (*hTERT*) gene, called hTERT-BAC mice (Bacterial Artificial Chromosome), to study the effect of aging and exercise on *hTERT* expression in thymus [121]. Our rationale for using transgenic mice is that the regulation of mouse *Tert* is different from the regulation of human *TERT*, especially AS regulation of *TERT* [29]. For example, more than 85% of mouse *Tert* is FL *Tert*, whereas about 40% of human *TERT* is FL *hTERT* [27]. We chose to study thymus because a large portion of previous studies of telomerase and *hTERT* regulation was performed with immune cells (especially T cells) and the thymus is the organ that matures T cells [19]. Previous research has indicated that thymus tissues [230, 231] and thymocytes [232] from humans express robust levels of *hTERT* and have telomerase activity, making studying *hTERT* expression regulation in this tissue more accessible compared to other tissues such as skeletal muscle. When telomerase activity was measured in PBMCs, telomerase activity progressively declined with age up

to 40 years of age whereby it reached a low but steady level [233]. However, this study used very few younger samples and should be interpreted cautiously. Thus, much is left to be understood about *hTERT* expression and telomerase regulation in immune tissues. Since immune tissues play an important role in aging biology (inflammation, antitumor protection), it is important to understand telomerase regulation with aging and how a healthy lifestyle factor may be able to intervene on any changes observed. Since alternative splicing regulation of *hTERT* has not been investigated in previous studies focusing on immune cells and aging, we collected thymus from hTERT-BAC mice to study *hTERT* AS regulation. In addition to the above rationale, we chose thymus to study the impact of aging on *hTERT* regulation because thymus is known to involute with aging. We were interested in *hTERT* expression during aging of the thymus and if exercise could counteract any observed expression or splicing changes. We hypothesized that expression of *hTERT* and ratio of FL *hTERT* to minus beta *hTERT* would decrease with aging and exercise would counteract the age-driven decrease. To test our hypothesis, we measured the expression level of exons 7/8 containing *hTERT* (potential FL *hTERT*) and minus beta *hTERT* in thymus tissues from hTERT-BAC mice of different ages, and mice that exercised or not. In fact, we found that *hTERT* expression (including both potential FL *hTERT* and minus beta *hTERT*) was reduced by aging regardless of exercise. In the case of *hTERT* AS, contrary to our hypothesis, we observed an increase in the ratio of potential FL *hTERT* with aging, and exercise appeared to attenuate this age-driven effect. Our results support that *hTERT* expression decreases likely due to primary aging and exercise cannot counteract the decrease of

hTERT expression in thymus, whereas *hTERT* AS is dysregulated with likely due to secondary aging and exercise counteracted this dysregulation.

5.3. Materials and Methods

5.3.1. Animals

All animal experiments were approved by the University of Michigan Institutional Animal Care and Use Committee (IACUC) and conducted as per the institutional guidelines. C57BL/6-Tg(TERT)C10Hode/J (~ 8-weeks old) were purchased from The Jackson Laboratory (Bar Harbor, ME, USA). The transgenic hTERT+ founder mice were housed at 25°C on a 12:12-h light-dark cycle, fed ad libitum laboratory mouse chow (Prolab RMH 3000, 5P00, LabDiet by Purina, Nestlé, Vevey, Switzerland), and given free access to water. Following a 2-week acclimation period, breeding pairs were established for the hTERT-BAC mouse colony that maintain the C57BL/6 background and express the *hTERT* gene [121]. Following each litter, pups were weaned after three weeks, and PCR genotyping was carried out using tail DNA (KAPA Biosystems, Wilmington, MA, USA). hTERT-BAC mice that were hTERT+ were confirmed from extracted tail DNA using transgene hTERT (F: 5'-GGAAGGCAGGAGGCTCTTGG-3'; R: 5'-TGCACACACTTGTGCCCTTGC-3'; 431-bp) and control primer pairs (F: 5'-CAAATGTTGCTTGTCTGGTG-3'; R: 5'-GTCAGTCGAGTGCACAGTTT-3'; 200-bp) in EmeraldAmp MAX PCR Master Mix (Takara Bio, Mountain View, CA, USA) on a C1000 Touch Thermal Cycler (Bio-Rad Laboratories, Hercules, CA, USA) under the following conditions: heat activation at 98°C for 5 minutes, followed by 35 cycles of denaturation at 95°C for 10 seconds, annealing at 60°C for 30 seconds, and an extension at 72°C for 1 minute. A final extension step at 72°C for 5 minutes was also performed. The results were confirmed on a 1.2% agarose gel.

5.3.2. Voluntary wheel running protocol

Confirmed hTERT+ transgenic male and female hTERT-BAC mice were divided into three different groups depending on their age (young (6 months)/middle-aged (12 months)/old (18-22 months)) and further assigned into either an individual sedentary cage (no wheel access) or an individual exercise cage (wheel access). The exercise cage was equipped with a low-profile wireless running wheel (ENV-047, MED Associates, Fairfax, VT). The number of wheel revolutions were obtained by a wireless device USB hub (DIG-807, MED Associates, Fairfax, VT) and running distance was calculated with wheel analysis software (SOF-861, MED Associates, Fairfax, VT). Body mass and food consumption were measured weekly. Animals had access to running wheels until immediately before their tissues were sampled 3 hours prior to the beginning of dark cycle (animals were maintained on a 12:12 hour light: dark cycle with lights on at 6am and lights off at 6pm).

5.3.3. Treadmill Acclimation and Exercise Testing Protocol

Confirmed hTERT+ transgenic male and female hTERT-BAC mice were aged to 69-weeks before undergoing a 10-day treadmill acclimation protocol as previously described [29, 143, 157]. In brief, the treadmill was set at a 7% incline for all treadmill sessions and mice were introduced to gradual increases in speed during each session on the treadmill. Mice were motivated to run by prodding with a bristled brush. Forty-eight hours after the last acclimation session, each mouse completed an incremental exercise test to determine their peak treadmill running speed. The peak treadmill running speed test was initiated with each mouse being placed on a motionless

treadmill for 2 minutes before increasing the belt speed to 5 meters per minute for minutes 2 through 5. At minute 5, the treadmill speed was increased at a consistent pace of 1 meter per minute until the running ability of each mouse was impaired (determined by the animal's refusal to run even when provoked for ≥ 30 seconds). The final speed at which the mouse refused to run was recorded as the peak treadmill running speed.

5.3.4. Acute Treadmill Exercise Protocol

Forty-eight hours after peak treadmill running speed test, the mice were exposed to 30 minutes of submaximal treadmill running at 60% of their peak speed. Mice were separated into three experimental groups (n = 5 per group; number of males is indicated in Table 5.2). The no exercise resting control group (Pre, n = 5) were exposed to a motionless treadmill for 30 minutes before being euthanized for tissue processing. This is important as the rodents might have developed a stress response associated with the treadmill resulting from the maximal speed test only 48-hours prior, and the exposure to the motionless treadmill would serve to control for any potential physiological responses that would otherwise confound subsequent measures. The remaining 10 mice underwent a 30-min treadmill exercise bout and were euthanized either immediately following acute treadmill exercise (IPE: Immediately post exercise, n = 5) or at 1 hour into recovery from the exercise bout (1h-Post, n = 5).

5.3.5. Cell and Tissue Processing

Thymus tissues were dissected and flash frozen in liquid nitrogen for future analysis from hTERT-BAC mice. Prior to analysis for specific biomolecules, tissues were minced with a razor blade on ice. The minced samples were either processed immediately or stored at −80°C until further analysis.

5.3.6. Droplet Digital reverse transcription PCR

Thymus tissue RNA was extracted using QIAzol and RNeasy® Universal Mini Kit (Qiagen, Hilden, Germany). Isolated RNA was quantified by spectrophotometry using a NanoDrop 2000 and cDNA was synthesized using SuperScript IV First-Strand cDNA Synthesis System primed with oligo dT and random hexamers at a 1:1 ratio (Invitrogen, Carlsbad, CA). All cDNAs were diluted 1:4 using nuclease-free water and stored at −20 °C until analysis of *hTERT* expression levels quantitatively by RT-droplet digital PCR (ddPCR).

Species specific primers (i.e., human) were utilized for total *hTERT* gene quantification by RT-ddPCR. Total *hTERT* gene expression levels were determined by summing the absolute quantification of the potential FL, exons 7/8 containing transcripts (determined by PCR of exons 7/8 – Forward primer exon 7: 5'-ACAGTTCGTGGCTCACCTG-3'; Reverse primer exon 8: 5'-GCGTAGGAAGACGTCGAAGA-3'; universal probe #52 [Roche; Basal, Switzerland] in exon 8) plus the minus beta (−β), exon 7–8 skipping ASV (determined by PCR of exon 6–9 containing transcripts – Forward primer exon 6/9 junction: 5'-CAAGAGCCACGTCCTACGTC-3'; Reverse primer exon 10: 5'-

CAAGAAATCATCCACCAAACG-3'; universal probe #58 [Roche; Basal, Switzerland] in exon 9; 28). The summation of exon 7/8 containing and exon 7–8 skipping transcripts has been shown to account for ≥ 95% of total *hTERT*, suggesting that this strategy should provide a good estimate of total cellular *hTERT* transcripts [25]. It is possible that exon 7/8 containing transcripts, such as the minus α (skipping of the first 36 nucleotides at the 5' end of exon 6) and minus γ (exon 11 skipping) transcripts that yields hTERT catalytically inactive, could be included in this analysis. However, these transcripts account for < 5% of total *hTERT* [25]. A 2 µL sample of cDNA (equivalent to 25ng of RNA input) was combined with primers and probe sets, and 2x ddPCR Supermix for Probes (Bio-Rad Laboratories) in a 20 µL final volume mix. Droplets were generated using 70 µL of Droplet Generation Oil for Probes using the QX200 Droplet Generator (Bio-Rad Laboratories). Generated droplets were loaded into a 96-well plate and amplified under the following thermocycling conditions: initial denaturation at 95° for 10 minutes, followed by 40 cycles of denaturation at 94°C for 30 seconds and annealing at 60°C for 1 minute. A final enzyme denaturation step at 98°C for 5 minutes was also performed. Droplets were analyzed using the QX200 Droplet Reader and QuantaSoft software systems, respectively (Bio-Rad Laboratories). Full length and alternatively spliced *hTERT* percentages were determined as previously described [27] and according to the following formulas: Percent Potential FL = Exon 7/8 containing transcript / Total transcript (total transcripts = exon 7/8 containing transcripts + exon 7–8 lacking transcripts); Percent alternatively spliced = 100 – Percent Potential FL.

5.3.7. Statistical Analyses

For the voluntary wheel running study (Figure 5.2 and Figure 5.3), a two-way ANOVA and Pearson's correlations were utilized to evaluate the effects of exercise and aging on the total amount of potential full-length *hTERT*, minus beta *hTERT* and total *hTERT* (potential full-length + minus beta) transcripts, and ratio of potential full-length *hTERT* transcripts. For the two-way ANOVA, *post hoc* comparisons were performed (Tukey's multiple comparison) when the interaction between age and exercise or the effect of age was statistically significant (p-value < 0.05). When a significant effect of age was found, main age effect was evaluated by a simple main effect analysis. When a significant effect of exercise was observed, post hoc comparisons were not conducted because there were only two conditions for the exercise variable (sedentary or exercise), and the main effect already encompasses the relevant comparisons. When a significant interaction between age and exercise was found, each group was compared to all the other groups. For Pearson's correlations, relationships of two factors (Figure 5.3, absolute amount of *hTERT* transcripts or ratio of potential full-length *hTERT* vs Age) were evaluated and correlation coefficient (r) and p-value were calculated.

For the acute treadmill study (Figure 5.4), a one-way ANOVA was performed to compare the total amount of potential full-length *hTERT*, minus beta *hTERT,* and total *hTERT* (potential full-length + minus beta) transcripts, and ratio of potential full-length *hTERT* transcripts. Statistical significance was defined as a p-value < 0.05.

5.4. Results

5.4.1. Effect of exercise and aging on *hTERT* AS regulation in thymus from hTERT-BAC mice.

To study the effect of exercise and aging on *hTERT* expression, we divided hTERT-BAC male and female mice into three different age groups. Average ages were 6 months for the young group, 15 months for the middle-aged group, and 22-23 months for the old group (Table 5.1). For the exercise intervention, we provided mice in the exercise group with an individual running wheel for three weeks because previous studies have shown that telomerase activity, mouse *Tert* expression, and telomerase regulating genes in cardiac tissue and circulating leukocytes were significantly changed by three weeks of voluntary wheel running intervention [154, 158]. A two-way ANOVA was performed to analyze the effect of age and exercise on the phenotypes (Table 5.1). As expected, age from three groups were significantly different ($p < 0.0001$). Neither significant effect of age nor exercise was found from food consumption or final body weight of groups, supporting that all groups consumed similar amount of food and weighed similar compared to the other groups, respectively. When running distances in exercise group were compared to each other by a one-way ANOVA, no significant difference was found ($p = 0.0659$) although average daily running distance was similar between young and middle-aged mice and was four times higher than the daily running distance of old mice (Table 5.1).

Table 5.1 - Animal Weights and Other Phenotypes

Phenotype	Sedentary			Exercise			*p* values		
	Young (n=8; 3M5F)	Middle-aged (n=4; 4F)	Old (n=4; 2M2F)	Young (n=7; 2M5F)	Middle-aged (n=4; 1M3F)	Old (n=4; 2M2F)	Interaction	Age	Exercise
Age (Months)	6 (1.2)	14.8 (1)	22.3 (1.5)	6.1 (1.3)	15.3 (1.3)	23.5 (2.6)	0.7040	**<0.0001**	0.1777
Food consumption per day (g/day)	2.7 (0.3)	3.2 (0.5)	2.9 (0.5)	2.5 (0.3)	2.5 (0.3)	3.1 (0.2)	0.0618	0.0576	0.1140
Final body weight (g)	30.1 (5.2)	33.5 (3.4)	31.5 (2.5)	27.9 (5.4)	32.5 (2.4)	34.5 (3.3)	0.3928	0.0539	0.9568
Distance per day (m/day)	0	0	0	2455.8 (1713.0)	2594.0 (1689.6)	616.7 (521.3)	NA	NA	0.0659

Note : Data are presented as mean (SD). A two-way ANOVA was used to calculate *p*-values, except for running distance per day (m/day), for which a one-way ANOVA was used. Significant *p*-values (<0.05) are bolded. The numbers of male and female mice are represented using the letters 'M' or 'F' followed by the respective counts.

After identifying characteristics of our mice from different age and exercise groups, we quantitatively measured the absolute amount of total *hTERT* transcripts (potential full-length (FL) *hTERT* + minus beta *hTERT*; Figure 5.2A), potential FL *hTERT* (Figure 5.2B), and minus beta *hTERT* (Figure 5.2C). Then we converted the quantified values into the ratio of potential FL *hTERT* and minus beta *hTERT* (Figure 5.2D) showing the percentage of exons 7-8 skipping. To determine the effect of age and exercise, a two-way ANOVA was performed for the amount of total *hTERT* (FL + minus beta), potential FL *hTERT*, minus beta *hTERT*, and ratio of potential FL *hTERT* (Table 5.2). The two-way ANOVA revealed that there were statistically significant interactions between the effects of age and exercise on the absolute amount of minus beta *TERT* ($F(2, 25) = 3.559$, $p = 0.0436$) and ratio of potential FL *TERT* ($F(2, 25) = 3.624$, $p = 0.0415$). Simple main effects analysis showed that age had a statistically significant effect on absolute amount of total *hTERT* ($p < 0.0001$), potential FL *hTERT* ($p < 0.0001$), minus beta *hTERT* ($p < 0.0001$), and ratio of potential FL *hTERT* ($p = 0.0289$).

This supports that age is the major driver of expression *hTERT*. In addition, the simple main effects analysis showed that exercise had a statistically significant effect on absolute amount of minus beta *hTERT* (p = 0.0441). Since effect of exercise was determined by a comparison of two combined groups (three sedentary groups vs three exercise groups), the result suggested that the expression of minus beta decreased with exercise intervention (Figure 5.2C). To further understand the effect of age and exercise, p*ost hoc* comparisons were performed. It confirmed that young mice expressed significantly higher total *hTERT* and potential FL *hTERT* in thymus compared to middle-aged or old mice (Supplemental Table 5.1). Notably, although young mice expressed significantly higher minus beta *hTERT* compared to middle-aged or old mice, exercise significantly reduced expression of minus beta *hTERT* in young mice (Figure 5.2C). When ratio of potential FL *hTERT* was evaluated by *post hoc* comparisons, significant differences were found from comparisons between sedentary groups (Figure 5.2D).

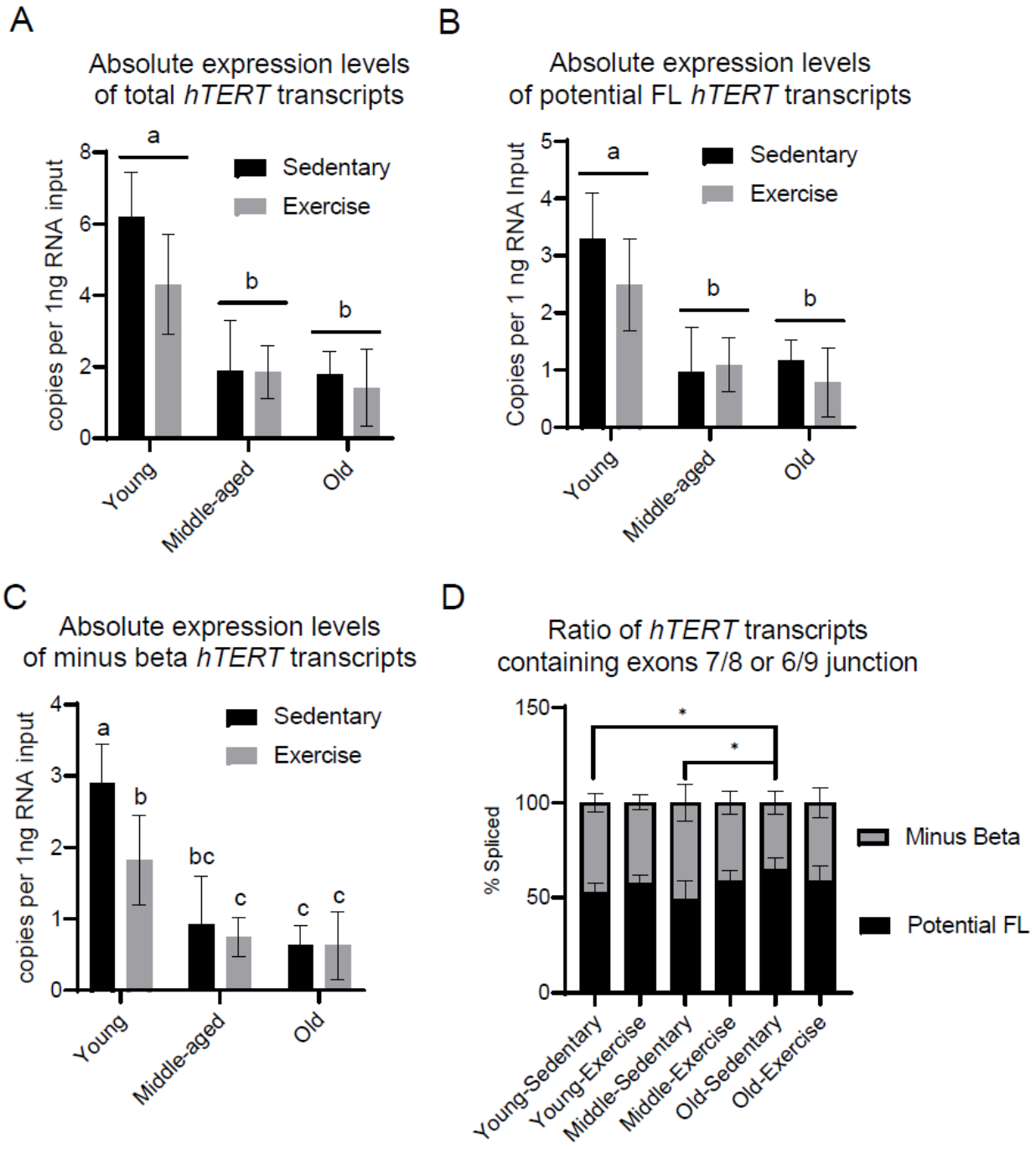

Figure 5.2. Effect of exercise and aging on *hTERT* AS regulation in thymus from hTERT-BAC mice.

A-C. Absolute amount of total *hTERT* (A; potential full-length + minus beta), potential full-length *hTERT* (B), and minus beta *hTERT* (C) transcripts in 6 different conditions. **D**. Ratio of potential full-length *hTERT* (exons 7/8 containing *hTERT*) and minus beta *hTERT* (with exons 6/9 junction) transcripts in 6 different conditions. ddPCR assay was used to determine the amount of transcripts (n = indicated in Table 5.1). A

two-way ANOVA was performed to evaluate the effect of age and exercise on total amount of total *hTERT* (potential full-length + minus beta), potential full-length *hTERT*, and minus beta *hTERT*. *Post hoc* comparisons of total *hTERT* (A) and potential full-length *hTERT* (B) showed only young mice (grouped as "a") had significantly higher ($p < 0.0001$) total *hTERT* and potential full-length *hTERT* transcripts than the other age groups (grouped as "b"). *Post hoc* comparisons of minus beta *hTERT* (C) revealed that sedentary-young mice (grouped as "a") had significantly higher ($p < 0.01$) minus beta *hTERT* transcripts than all the other groups and exercised-young mice (grouped as "b") had significantly higher ($p < 0.05$) minus beta *hTERT* transcripts than all the other groups (grouped as "c") except sedentary-middle-aged mice ($p = 0.1026$; grouped as "bc"). *Post hoc* comparisons of potential full-length *hTERT* ratio (D) showed significantly different ratio from two comparisons (*, $p < 0.05$). Statistical analysis results are in Table 5.2 and Supplemental Table 5.1.

Table 5.2 – Statistical analysis (ANOVA table) from Figure 5.2

	Values	*F* (DFn, DFd)			*p* values		
		Interaction *F* (2, 25)	Age *F* (2, 25)	Exercise *F* (1, 25)	Interaction	Age	Exercise
Figure 2A	Absolute amount of total *hTERT* (Potential FL + Minus beta)	2.016	34.59	3.025	0.1543	**<0.0001**	0.0943
	Absolute amount of potential FL *hTERT*	1.160	27.96	1.773	0.3298	**<0.0001**	0.1950
	Absolute amount of minus beta *hTERT*	3.559	37.47	4.495	**0.0436**	**<0.0001**	**0.0441**
Figure 2B	Ratio of exons 7-8 splicing	3.624	4.095	1.241	**0.0415**	**0.0289**	0.2760

Note : A two-way ANOVA was used for statistical analysis (F: F-statistic; DFn: Degrees of freedom for the numerator; DFd: Degrees of freedom for the denominator). Significant *p*-values ($p < 0.05$) are bolded.

5.4.2. Aging dictates *TERT* expression and effect of aging on *TERT* AS regulation depends on exercise

Since we observed a decrease in *hTERT* expression with aging regardless of exercise, and changes in *hTERT* AS ratio with aging only from sedentary mice, we carried out correlation analyses between age with absolute amount of total *hTERT* or splicing ratio of *hTERT* exons 7/8. As expected, expression of total *hTERT* transcripts showed significant negative correlation with age when all mice were used (Figure 5.3A), only sedentary groups were used (Figure 5.3B), and only exercise groups were used (Figure 5.3C). These correlation analyses clearly support that *hTERT* expression is downregulated with aging regardless of exercise. On the other hand, when it comes to *hTERT* alternative splicing, percentage of potential FL *hTERT* showed significant positive correlation with age when all mice were used (r = 0.3669, p = 0.0423; Figure 5.3D). Although neither of correlation analysis using only sedentary group nor only exercise group showed statistically significant correlation, correlation from sedentary group showed stronger positive correlation (r = 0.4878, p = 0.0552) compared to exercise group (r = 0.2013, p = 0.4719). This result supports the idea that *TERT* splicing is shifted towards inclusion of exons 7/8 with aging, but exercise counteracts the effect of aging.

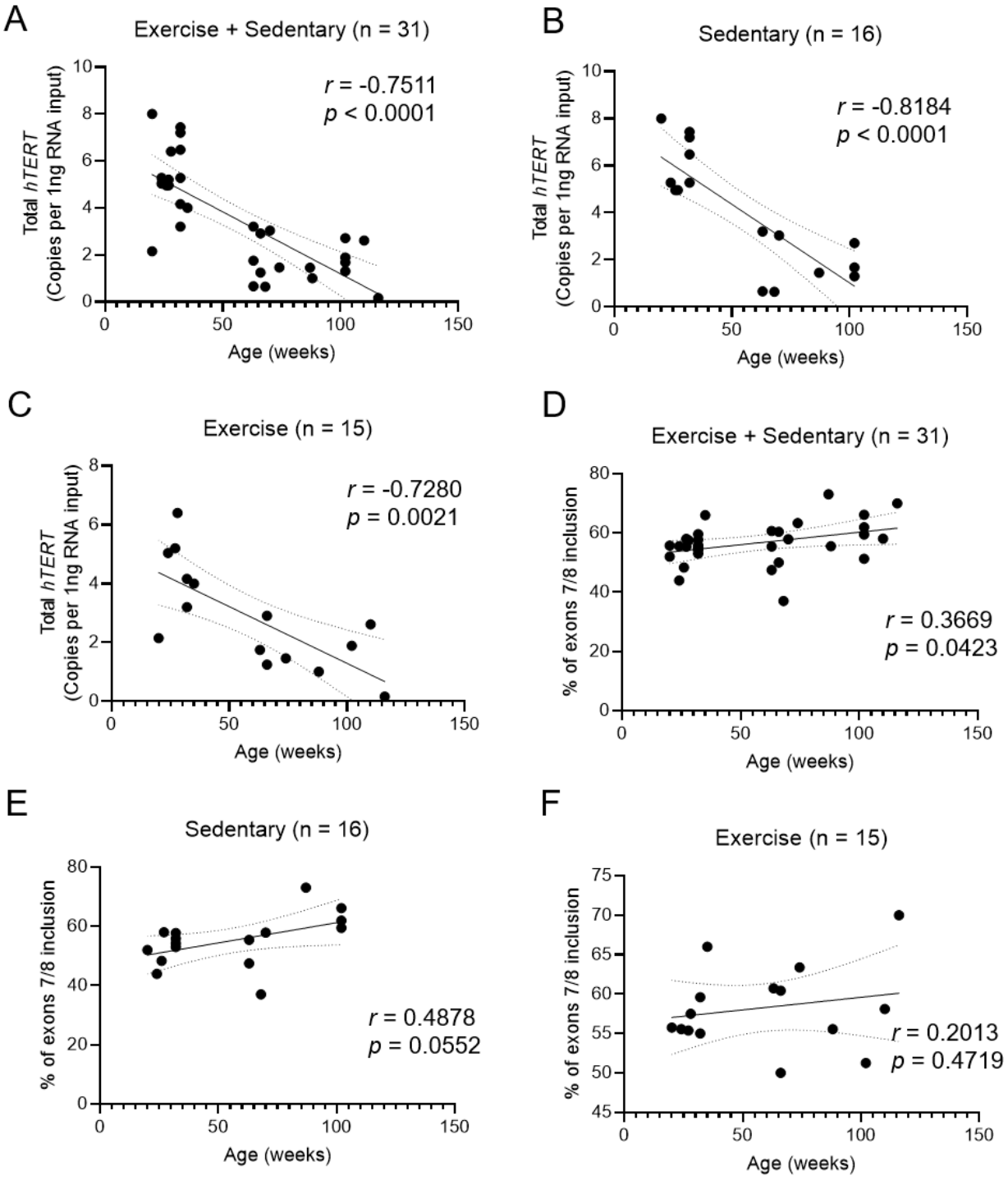

Figure 5.3. Aging dictates *hTERT* expression and effect of aging on *hTERT* AS regulation depends on exercise.

(**A,B,C**) Scatter plots showing correlations between Age (weeks; x-axis) and absolute amount of total *hTERT* (potential full-length + minus beta) transcripts (y-axis) in all mice (A; n = 31), sedentary mice (B; n = 16), and exercised mice (C; n = 15). (**D,E,F**) Scatter plots showing correlations between Age (weeks; x-axis) and percentage of *hTERT* exons 7/8 inclusion (y-axis) in all mice (D; n = 31), sedentary mice (E; n = 16), and exercised mice (F; n = 15). 95% Confidence bands, Pearson's correlation coefficient (*r*) and *p* values are shown.

5.4.3. Neither *hTERT* expression nor AS is impacted by acute treadmill exercise in thymus from hTERT-BAC mice

Next, we wanted to test the impact of acute exercise in older mice on *hTERT* mRNA expression and AS. To do this, we compared three groups of middle-aged hTERT-BAC mice exposed to a single bout of treadmill running. Since all mice were aged until 69 weeks in sedentary condition, we hypothesized that the acute treadmill exercise would induce significant changes in *hTERT* expression. We compared maximum running speeds and body weights to the other groups, and statistical analysis showed no significant difference between the groups supporting that the mice were equally well distributed into the groups (Table 5.3). From collected thymus tissues from pre-, immediately post- and 1-hour post-exercise conditions, we did not observe statistical significance between any groups for *hTERT* expression (Figure 5.4A). Also, we did not find significant differences in *TERT* AS with acute exercise intervention (Figure 5.4B).

Table 5.3 – Animal Weights and Other Phenotypes of 71-week-old hTERT-BAC mice

Phenotype	Exercise			p values
	Pre (n=5; 2M3F)	Immediately Post (n=5; 1M4F)	1-hour post (n=5; 1M4F)	
Max speed (m/min)	22.8 (3.4)	23.1 (2.5)	23.4 (3.2)	0.9531
Body weight (g)	30.0 (3.4)	29.0 (2.0)	28.0 (3.7)	0.6138

Note : Data are presented as mean (SD). p values were calculated by one way ANOVA. The numbers of male and female mice are represented using the letters 'M' or 'F' followed by the respective counts.

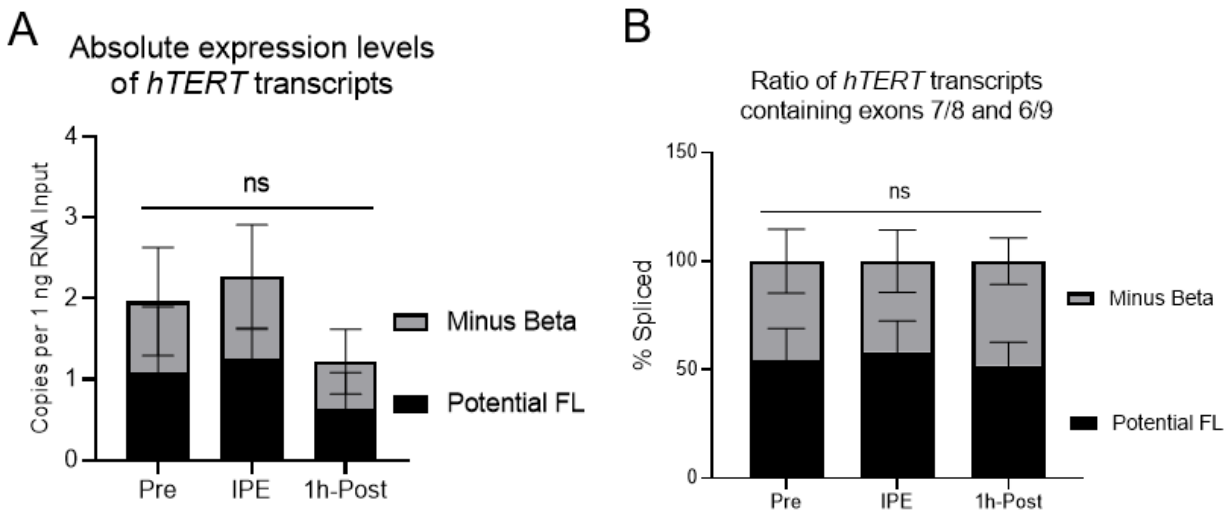

Figure 5.4. *hTERT* AS regulation by acute treadmill exercise in thymus from hTERT-BAC mice.

A. Absolute amount of potential full-length *hTERT* and minus beta *hTERT* transcripts in pre-, immediately post-, and 1-hour post-exercise (n = 5 per condition). **B**. Ratio of potential full-length *hTERT* and minus beta *hTERT* transcripts in pre-, immediately post-, and 1-hour post-exercise (n = 5 per condition). One-way ANOVA was performed to compare total amount of potential full-length *hTERT*, minus beta *hTERT* and total *hTERT* (potential full-length + minus beta) transcripts (A) and ratio of potential full-length *hTERT* transcripts (B) in all conditions, however statistical significance was not found ($p > 0.05$).

5.5. Discussion

Understanding the regulation of telomerase in aging and determining lifestyle factors that can impact telomere maintenance in a variety of tissues and organs is critical to developing novel healthy life expectancy-extending strategies. Previous studies have shown that exercise can robustly increase *hTERT* gene expression and telomerase activity and maintains or slows telomere shortening in immune cells, cardiac tissues, endothelial cells, and skeletal muscle [19]. Specifically, three weeks of voluntary wheel running upregulated mouse *Tert* expression and mouse telomerase activity in left ventricle [158] and aorta [154] from eight-week-old male C57/Bl6 mice. Our group has recently observed that acute treadmill exercise induced changes in *TERT* AS in gastrocnemius, left ventricle, and brain from 8-week-old hTERT-BAC mice [29]. In the present study, we used the same mouse model to determine the impact of age and exercise on *hTERT* expression and splicing ratio. Unexpectedly, the absolute amount of total *hTERT* and exons 7/8 containing *hTERT* (potential FL *hTERT*) transcripts did not change significantly by three weeks of voluntary wheel running regardless of age in thymus tissue. Instead, the expression of minus beta *hTERT* significantly decreased by exercise intervention (determined by a simple main effect analysis). From *post hoc* comparisons, a significant reduction of minus beta *hTERT* by exercise was found in young mice. This was an unexpected result because the previous studies using three weeks of voluntary wheel running observed increases in telomerase activity and mouse *Tert* gene expression in cardiac muscle and circulating leukocytes from wildtype C57/Bl6 mice [154, 158]. The impact of exercise on the thymus is underexplored but

could have important impacts on immunosenescence. Overall, our data indicate that the impact of age and exercise on *TERT* expression and AS are tissue specific.

AGE: When the effect of aging on *hTERT* expression was investigated, we observed a major reduction in *hTERT* transcripts in the thymus. We speculate that the reduction of *hTERT* expression in the thymus is likely to be driven by primary aging factors. To determine if primary aging is indeed responsible for reduced *hTERT* expression additional experimental data would be needed utilizing a known intervention that slows primary aging, such as caloric restriction. The thymus is known to involute with aging which results in lower naïve T-cell production [17]. The reduction of *hTERT* expression with aging could be related to age-related thymic involution. The loss of *hTERT* expression in the thymus could be due to the de-methylation of the *hTERT* promoter since methylation of the *hTERT* promoter upregulates transcription of the *hTERT* gene [92-95], or it could be changes in epigenetics such as histone modification that represses expression of *hTERT* [96, 97]. Also, since animal transcriptomes undergo extensive remodeling during aging [52], altered transfactor expression with aging could be a reason for the reduction of *hTERT* expression (i.e., decrease in *hTERT* transcription activators or increase in *hTERT* transcription repressors [234]). Interestingly, we found that alternative splicing of *hTERT*, specifically the ratio of exons 7/8 containing *hTERT* tended to increase with aging, and the effect of aging was stronger in thymus from sedentary mice. Since regulation of RNA processing has been known to be disrupted by aging [235], *hTERT* alternative splicing also could be dysregulated by aging resulting in higher percentage of exons 7/8 inclusion.

EXERCISE: Previous studies of exercise and indirect indicators of thymus output have indicated that humans with long exposure to cycling activity [23] or with higher VO_2 peak values [236] have greater numbers of naïve T cells and fewer senescent T cells compared to individuals that are less active or have lower VO_2 peak, respectively, indirectly indicating greater thymic function. Direct investigations of the impact of exercise on thymus tissues are sparse in the literature and mainly indirect methods have been utilized such as those in references above [23, 236, 237]). In our study, three weeks of voluntary wheel running was observed to decrease minus beta *hTERT* in young mice (Figure 5.2C). However, neither absolute amount of total *hTERT*, potential FL *hTERT*, nor ratio of *hTERT* variants changed significantly with exercise in young mice. We speculate that this could support increased telomerase activity in thymus with exercise if the reduction of minus beta *hTERT* results in less inhibition of telomerase activity (minus beta hTERT is a dominant-negative telomerase). In addition, the increase in exons 7/8 inclusion ratio observed with sedentary aging was counteracted by exercise training (three weeks of voluntary wheel running – Figure 5.3D-F). We speculate that exercise may repress changes in the alternative splicing machinery that could have caused the increase in the ratio of exons 7/8 containing *hTERT* to minus beta *hTERT*, as supported by previous research [29, 238]. In addition to three weeks of voluntary wheel running, we used acute treadmill exercise to study the response of *hTERT* AS in middle-aged hTERT-BAC mice. Although we did not find significant changes in any of our measurements (total *hTERT*, potential full-length *hTERT*, minus beta *hTERT*, and ratio of potential full-length *hTERT*), we were able to observe similar *hTERT* expression patterns compared to our previous study based on the same

exercise intervention but with much younger mice [29]. In our previous study, *hTERT* mRNA expression increased at immediately post exercise and went back down then decreased even further than sedentary resting condition in recovery phase in gastrocnemius and left ventricle. This pattern was observed in thymus from middle-aged mice (Figure 5.4A). Regarding *hTERT* AS ratio, it is hard to interpret the changes of the ratio because of very small differences between the groups.

TRIIM: A recent clinical trial, TRIIM (Thymus Regeneration, Immunorestoration, and Insulin Mitigation), in humans indicated that thymus involution can be reversed by treatment with growth hormone (GH), metformin and DHEA [239]. Age-related changes in GH levels and insulin resistance could be related to thymic involution, declining immune system function, and reduced *hTERT* expression. Interestingly, GH has been observed to increase *hTERT* expression in various tissues and cells [158, 240]. Further, certain types of exercise are known to increase GH concentration in blood [241], which could impact thymus aging and involution. With our voluntary wheel running model, which is unlikely to be a potent enough metabolic stress to induce significant GH levels, may explain why we did not see changes in our aged animals. Exercise also maintains insulin sensitivity, similar to treatments with DHEA and metformin, mimicking aspects of the TRIIM trial intervention. Further the treadmill running may not have been intense enough to induce GH in our mice and thus induce changes in *hTERT* expression levels. Future experiments would be needed to test if GH treatment or TRIIM trial-like treatments in hTERT-BAC mice could increase thymus *hTERT* expression, insulin sensitivity, T cell *hTERT* expression, and reverse or slow immunosenescence.

Limitations: We used mixed sex cohort, which limited our ability to detect sex differences. We used two types of exercise intervention: one is three weeks of voluntary wheel running, and the other is acute treadmill exercise at 60% of maximum speed that could have been insufficient to induce increase in GH secretion. In our aging model, we observed *hTERT* expression decreased with aging. However, we did not identify the underlying mechanisms; one potential mechanism is epigenetic changes of the *hTERT* promoter. In addition, we did not measure changes in expression of any transcription factors or splicing factors. With transcriptomics analyses, transfactors driving age-related *hTERT* expression reductions would be determined. We did not identify the *hTERT* transcripts that increased with aging and were repressed by exercise that contained exons 7/8 such as minus gamma, INS3 or INS4. Lastly, although we speculated whether the changes effect of *hTERT* expression was driven by either primary aging or secondary aging based on the effect of exercise, exercise does not alter all aspects of secondary aging and lack of an exercise does not necessarily indicate that it is driven by primary aging. Thus, other types of interventions, such as caloric restriction, should be used to determine whether the changes of *hTERT* expression was driven by primary aging, secondary aging, or both. Future work should clarify these important questions.

Overall, our data revealed the age-driven reduction of thymic *hTERT* expression and this reduction is likely to be caused by primary aging since exercise did not counteract the reduction of expression. We also showed that the increased expression of potential full-length *hTERT* during sedentary aging is attenuated by exercise indicating that *hTERT*

expression is impacted by secondary aging as well. Despite these findings, future studies are required to identify the underlying mechanisms and functions of these changes in TERT expression.

Chapter 6 – Discovery and Characterization of a Novel Telomerase Alternative Splicing Isoform That Protects Lung Cancer Cells From Chemotherapy Induced Cell Death

6.1. Abstract

All cancer cells must adopt a telomere maintenance mechanism to achieve replicative immortality. Most human cancer cells utilize the enzyme telomerase to maintain telomeres. Alternative splicing of *TERT* regulates the amount and function of telomerase, however many alternative splicing isoforms of TERT have unknown functions. Here we used single molecule long read sequencing of *TERT* and observed 45 *TERT* mRNA variants including 13 known and 32 novel variants. Among the variants, *TERT* Delta 2-4, which lacks exons 2-4 but retains the original protein domains and open reading frame, was selected for the further functional studies. We find that induced pluripotent stem cells and cancer cells express higher levels of *TERT* Delta 2-4 compared to primary human bronchial epithelial cells. Neither overexpression nor knockdown of TERT Delta 2-4 induced changes in telomerase activity, growth rate or telomere length. Instead, overexpression of TERT Delta 2-4 enhanced clonogenicity and resistance to cisplatin-induced apoptosis of both telomerase expressing cancer cells (Calu-6) and telomerase deficient cancer cells (U-2 OS). Knockdown of TERT Delta 2-4 reduced clonogenicity and resistance to cisplatin of Calu-6 cells. Our results suggest that TERT Delta 2-4 is a cancer cell specific isoform of TERT that enhances

cells' resistance to intrinsic apoptosis. Overall, we suggest TERT Delta 2-4 as a novel therapeutic target to improve cancer drug efficiency.

6.2. Introduction

Telomerase is a ribonucleoprotein enzyme composed of a protein subunit TERT (Telomerase reverse transcriptase), RNA template TERC (Telomerase RNA component; also called TR), and accessary proteins [78]. The primary function of telomerase is to maintain or elongate telomeres by *de novo* telomere synthesis [228]. TERT has four functional domains (N-terminal extension, TEN, DNA binding; RNA binding domain, TRBD binds TERC RNA; reverse transcriptase domain, RT, enzyme activity; C-terminal extension, CTE, DNA binding) and all four are required for telomerase to be able to synthesize telomere repeats [229, 242]. Three localization signals are embedded in *TERT*'s exons: mitochondrial targeting signal (MTS) in exon 1 [243], nuclear localization signal (NLS) in exon 2 [244], and nuclear export signal (NES) in exon 12 [245] (Figure 6.1A). These signals play important roles in dictating the function of TERT proteins in different cell types and under different physiological conditions.

TERT is a 16-exon gene that when spliced to full-length *TERT* (FL *TERT*) generates active telomerase [179]. However, *TERT* pre-mRNAs undergo alternative splicing (AS) and can form *TERT* mRNA variants in addition to full-length *TERT* [25]. Previously studied *TERT* mRNA variants are minus beta (exons 7-8 skipping), minus alpha (use of a cryptic splice site skipping 36 nucleotides at the 5' end of exon 6), minus gamma (exon 11 skipping), INS3 (159 bp insertion of intron 14 (622-781) at the end of exon 14 followed by a stop codon), INS4 (600 bp insertion of the entire intron 14, followed by a stop codon), Del2 (exon 2 skipping), and delta 4-13 (exons 4-13 skipping). Although these alternatively spliced TERT isoforms cannot form active telomerase,

different functions of the isoforms have been studied. For example, minus beta *TERT* has been reported to be translated into protein and inhibit telomerase activity (dominant-negative effect) in certain cancer cells, despite a premature termination codon (PTC) in exon 10 induced by frameshifting [116]. In addition, overexpression of minus beta TERT resulted in protection of breast cancer cells from chemotherapeutic insults [210]. Minus alpha TERT has also been observed to act as a dominant-negative telomerase [106]. Splicing outside of the exons 5-9 such as minus gamma [107], INS3, and INS4 [211] also generate dominant-negative TERT isoforms. *TERT* exon 2 spicing event produces *TERT* Del2 mRNA variant which has two tandem PTCs in exon 3 when exon 2 is skipped, has been reported as a developmental switch to limit telomerase activity by reducing the number of pre-mRNAs that can splice to FL *TERT* when embryonic stem cells are differentiated into fibroblasts [108]. Delta 4-13 TERT was shown to interact with the WNT/beta-catenin pathway to promote cell proliferation in telomerase negative human fibroblasts [28]. In addition to these seven isoforms/variants, there are 14 additional *TERT* mRNA variants have been reported for a total of 21 mRNA variants [28]. *TERT* AS not only produces *TERT* mRNA variants and protein isoforms, but also regulates subcellular localization of *TERT* mRNAs. It has been observed that retained introns (e.g., intron 11 and intron 14) sequestered *TERT* pre-mRNAs in the nucleus but during mitosis these retained introns are spliced out to form FL *TERT* and the mRNA is exported to the cytoplasm for translation [102]. Despite the literature presented above, the functions of many TERT isoforms still remain unknown. Another limitation from previous studies is the lack of single molecule techniques detecting multiple splicing events on individual mRNA molecules. For example, although exon splicing events

(e.g., exon 2, exons 7-8, and exon 11) can be detected individually by RT-PCR, whether all these splicing events occurs on the one same mRNA or on three independent mRNAs is unknown. Thus, different methods are required to capture the full catalogue of *TERT* mRNA variants. Further, technological advancements have increased the throughput of full-length single molecule sequencing allowing for multiple cell lines to be profiled at once compared to the single cell lines that have been used in the past to study *TERT* alternative splicing variants [28, 108]. By deciphering the catalogue of *TERT* mRNA variants across various cell types and determining the functions of TERT protein isoforms, it may allow us to determine a means to target TERT specifically in cancer cells while sparing TERT functions in normal adult stem cells and other TERT positive cell types.

To begin to catalogue *TERT* mRNA variants, we used single molecule long-read RNA sequencing with *TERT* specific sequencing libraries from four telomerase positive human cell lines. As a result, we discovered 45 variants including 13 known and 32 novel *TERT* mRNA variants. Among the variants, we chose one newly identified *TERT* mRNA lacking exons 2-4 (we call TERT Delta 2-4) that maintained the original open reading frame of TERT, was specifically expressed in lung cancer cells, and identified the function of the isoform based on loss of function and gain of function approaches. We identified that TERT Delta 2-4 isoform functions to promote colony formation and protect cells from apoptosis inducing chemotherapy (cisplatin).

6.3. Materials and Methods

6.3.1. MinION TERT Sequencing Library Preparation and Sequencing

Total RNA was extracted (Qiazol) from four human cell lines (iPSCs CHiPs 22 Takara, H1299, Calu-6, A549) that utilize telomerase enzyme activity to maintain telomeres and cellular immortality. Triplicate first strand cDNAs were synthesized with 2 µg of RNA input with oligo dT priming to capture potential protein coding transcripts using SuperScript IV First-Strand Synthesis System (Thermo Fisher). Following cDNA synthesis, cDNAs were amplified with a forward primer that contained the ONT library preparation sequence SSP plus *TERT* Exon 1 (5'-TTT CTG TTG GTG CTG ATA TTG C *CGGCCACCCCCGCGATG*, (TERT sequence is italicized)) and a reverse primer that contained the ONT library preparation sequence VNP plus *TERT* Exon 16 (5'-ACT TGC CTG TCG CTC TAT CTT CT *GGGCGGGTGGCCATCAGT*, (TERT sequence is italicized)) for a total 30 cycles. Following confirmation of successful amplification via agarose gel, bands in the 2.5 kb – 4 kb range (upper bands; upper TERT) and bands below 2.5 kb to 0.5 kb (lower bands; lower TERT) were excised and purified via gel extraction (Qiagen). Next, size binned fractions were amplified with ONT bar coded primers 1-12 (4 cells lines by 3 replicates by 2 size bins) for 20 cycles and then excess primers were removed via Ampure XP beads. Following clean up, library preparation was completed by rapid adaptor addition and quantification (agarose gel and qubit DNA) to ensure equal loading. Following flow cells were primed and loaded. Each size bin was sequenced on its own flow cell (R9.4.1). Data was generated for each run using the most up-to-date methods and protocols available at the time of sequencing. The Mk1C MinION device was used for data acquisition. Sequencing was performed with

the standard 72 h sequencing protocol run on the MinION Mk1C, using the MinKNOW software (v 3.3.2). From lower TERT, 21.8 million reads were obtained and 16.4 million reads passed from all 12 samples. From upper TERT, 14.1 million reads were obtained and 12.2 million reads were passed from all 12 samples. Base-calling from read event data was performed by Guppy (v 3.1.5). Fastq files which were classified as pass by the MinKNOW software were subsequently processed and analyzed.

6.3.2. Bioinformatics Analyses of TERT Sequencing Library

Passed fastq files were aligned to human genome (GRCh38.p13) using minimap2 (v 2.14; [246, 247]) in SAM MD-tag aware mode. Generated sam files were aligned with SAMtools (v 1.13; [248]) followed by transcriptClean (v 2.0.2; [249]) for correction of read microindels (< 5 bp), mismatches, and noncanonical splice junctions (< 5 bp). Read annotation was performed with TALON (v 5.0; [250]), using the human Gencode v.38 reference annotation gtf with minimum alignment identity = 0.5 and coverage = 0.5. Identified transcripts were subsequently filtered using a minimum count threshold of N = 35 reads in K = 2 samples. Based on the quantification, Swan (v 2.0; [251]) was used to further process the data. First, Swan report was generated to screen transcript model. Second, all transcripts were manually binned based on the appearance of their transcript model (visual inspection of inclusion or exclusion of introns or exons). Third, sequences from all transcripts were obtained and confirmed that transcripts were binned correctly. Based on the binned transcripts, count number (from TALON abundance) of transcripts in the same bin were aggregated and a heatmap was generated using log2-transforemd values. Analyses of the data were

performed using python (v 3.9) and R studio (v 2022.07.01; [252]) with the reshape2 package (v1.4.4;[253]), dplyr package (v 1.0.6; [254]), and ggplot2 package (v 3.3.6; [255]).

6.3.3. Cell Culture and Cell Lines

Cellartis® Human iPSC Lines from Takara (ChiPSC22, Cat. No. Y00320) were cultured with strict adherence to manufacturer's protocols and manuals. Cellartis® DEF-CS 500 (Y30017) culture system was employed to maintain iPSC cultures (thawing, passages, media changes and cryopreservation). NSCLC cell lines (A549 (RRID:CVCL_0023), Calu6 (RRID:CVCL_0236), NCI-H1299 (RRID:CVCL_0060), and NCI-H920 (RRID:CVCL_1599)) and Human Bone Osteosarcoma Epithelial Cells (U-2 OS (RRID:CVCL_0042)) were maintained in culture at 37°C in 5% CO_2 in 4:1 DMEM:Medium 199 supplemented with 10% cosmic calf serum (HyClone, Logan, UT). All unmodified cell lines were obtained from American Type Culture Collection (ATCC, Manassas, VA). Human bronchial epithelial cells (HBEC, primary ATCC - PCS-300-010) were maintained in bronchial epithelial growth media (ATCC - PCS-300-030) supplemented with a bronchial epithelial cell growth kit (ATCC - PCS-300-040) on collagen coated plates (porcine gelatin, Millipore Sigma). Cell line identity was verified by the vendor (ATCC). All cell lines were confirmed to be myocoplasma free at the start of the culture and several clean vials were frozen back for subsequent use (e-Myco kit, Bulldog-Bio) and no further testing was completed. Cells were continuously cultured for 70 passages or up to three months' time, whichever occurred first, at which point a new mycoplasma free vial was obtained, thawed and cultured.

6.3.4. Plasmid

A codon-optimized Delta 2-4 construct was generated by GeneArt Gene Synthesis (Invitrogen) based on the *TERT* mRNA sequence (NM_198253.3). The Delta 2-4 was initially inserted in pDONR221 donor vector, then cloned into pLenti6.2-3xFLAG-V5-ccdB plasmid by Gateway cloning LR recombination reaction (Cat no. 11791019, Invitrogen™) to produce 3xFLAG-V5-Delta 2-4 plasmid. pLenti6.2-3xFLAG-V5-ccdB was a gift from Susan Lindquist & Mikko Taipale (Addgene plasmid # 87072 ; http://n2t.net/addgene:87072 ; RRID:Addgene_87072; [256])

6.3.5. Stable Cell Line Generation

Stable cell lines expressing Flag-V5-Delta 2-4 were generated for Calu-6 and U-2 OS cells. Lentivirus was produced by transfecting 293T cells (RRID:CVCL_0063) with either pLenti6.2-3xFLAG-V5-ccdB (Control empty vector) or 3xFLAG-V5-Delta 2-4 plasmid, and helper plasmids (psPAX, pMD). Viral supernatants were collected, and target cells (Calu-6 and U-2 OS) were infected. Following 24 hours of infection, and 24 hours of recovery, cells were treated with Blasticidin (Cat no. R210-01, Gibco) and populations of stably selected cells were cultured and analyzed in subsequent experiments. Expression of 3xFLAG-V5-Delta 2-4 was confirmed by western blot analysis (Figure 6.2D).

6.3.6. Transient siRNA experiments

Calu-6 cells were plated in 6-well plates (300,000 cells per well) and were transfected with non-silencing controls (Santa Cruz Biotechnology, sc-37007) or siRNAs targeting *TERT* exons 1/5 junction (IDT Integrated DNA Technologies, siD2-4 (12:12): 5'- UCCUUCCGCCAGGCCGAGCGUCUC-3', siD2-4 (8:16): 5'-UCCGCCAGGCCGAGCGUCUCACCU-3', siD2-4 (16:8): 5'-CCCCUCCUUCCGCCAGGCCGAGCG-3'). Calu-6 cells were plated 24 h prior to transfections and transfection complexes were prepared with siRNAs using Opti-MEM (Gibco) and RNAi max (Invitrogen) following the manufacturer's procedures. Final concentration of siRNAs were 10 nM. Following either 48-or-72 hours of exposure to siRNAs, cells were washed, trypsinized, counted and pelleted for downstream assays.

6.3.7. Reverse transcription-ddPCR

RNA was extracted from frozen cell pellets using RNeasy® Plus Universal Mini Kit (Qiagen, 73404) according to manufacturer’s protocol. We used SuperScript IV First-Strand Synthesis System (Thermo Fisher) to generate cDNAs and used within 48 hours of production in ddPCR measures. 1 µg of RNA was used to synthesize cDNAs. All cDNAs were diluted 1:4 (20 µL of cDNA + 60 µL nuclease-free water) before use and stored at -20 °C. Primer sequences to target *TERT* splice variants (potential FL and minus beta) and methods for calculating percent spliced *TERT* transcripts are from Ludlow et al. [26]. Primers to measure SRSF3 PTC+ and SRSF3 PTC- are from Kano et al. [257]. Primers to measure intron 11 retention and intron 14 retention of *TERT* are

from Dumbović et al. [102]. Primers to measure *TERT* transcript with exons 3 to 5 are Forward: 5’- CCGGAAGAGTGTCTGGAGCAAGTTGCAAAGC-3’ targeting exon 3 and Reverse: 5’- ACCCTCGAGGTGAGACGCTCGGC-3’ targeting exon 5. For SRSF3 PTC+, SRSF3 PTC-, intron 11 retention, intron 14 retention, and *TERT* with exons 3 to 5, EvaGreen Supermix (Cat no. 186-4034, BIORAD) was used and annealing/elongation temperature at 60 °C for a minute.

For the delta 2-4 assays, primers to target *TERT* total delta 2-4 (Delta 2-4 and delta 2-4/ delta 7-8) are Forward: 5’- CAGTGCCTGGTGTGCGTG-3’ targeting exon 1 and Reverse: 5’- ACGCTGAACAGTGCCTTCAC-3’ targeting exon 5. Primers to target Delta 2-4 are Forward: 5’- CAGTGCCTGGTGTGCGTG -3’ targeting exon 1 (same as total delta 2-4) and Reverse: 5’- GCTGGAGGTCTGTCAAGGTAGAG -3’ targeting exon 7. To quantify skipping of *TERT* exons 1/5 junction we used 5' hydrolysis probes: 5'-6-FAM/TTCCGCCAGGCCGAGCGTCT/3BHQ_1/-3'. For the delta 2-4 assays, primer concentration was 900 nM and probe concentration was 250 nM. Optimized PCR thermal cycling specifically for delta 2-4 assays is: an initial incubation at 95°C for 10 min, 45 cycles of 1 min at 94°C and 2 min at 64.1°C, followed by a final incubation at 98°C for 5 min and holding at 12°C until reading time. The amplification signals were read using the QX200™ Droplet Reader and analyzed using its associated QuantaSoft software (Bio-Rad).

6.3.8. Cloning method to identify *TERT* mRNA variants

Using oligo dT primed cDNAs from A549 cells (total RNA input 2 µg, Superscript IV), PCR was performed with *TERT* exon 1 (5’-CGGCCACCCCCGCGATG-3’) and exon

16 (5’-GGGCGGGTGGCCATCAGT-3’) targeting primers with a high-yield and high-fidelity polymerase (Advantage® GC 2 PCR Kit, Cat. No. 639120, TaKaRa). The PCR products were TA cloned into TOPO™ TA and transformation was performed using TOP 10 E.coli (Termo Fisher). We use EcoRI to do digest plasmids from colonies to identify clones shorter than FL *TERT*. Then we used M13 F and M13 R to sequence from both ends which captured the complete Delta 2-4 sequence.

6.3.9. Nucleus and Cytoplasm fragmentation

Triplicates of Calu-6 cells were used to obtain cytoplasmic RNA and nuclear RNA fractions using PARIS™ Kit (Cat no. AM1921, Invitrogen™). Following RNA extraction, TURBO DNA-free™ Kit (Cat no. AM1907, Invitrogen™) was used to remove trace DNA contamination.

6.3.10. Gel-based PCR

Cytoplasmic and nuclear localization of MALAT1 and GAPDH were measured by gel-based PCR using 2 µL of cDNA (equivalent to 25 ng of RNA input) and 2x EmeraldAmp® MAX HS PCR Master Mix (Cat no. RR330, TaKaRa). Primers to target MALAT1 were Forward: 5’- GAATTGCGTCATTTAAAGCCTAGTT-3’ and Reverse: 5’-GTTTCATCCTACCACTCCCAATTAAT-3’. Primers to target GAPDH were Forward: 5’-AGCCACATCGCTCAGACAC-3’ and Reverse: 5’-GCCCAATACGACCAAATCC -3’. Annealing temperature was 60 °C for 30 seconds for both targets, and cycle numbers were 12 for MALAT1 and 18 for GAPDH.

6.3.11. Droplet Digital TRAP Assay for Telomerase Activity

Quantification of telomerase enzyme activity was determined by the droplet digital TRAP assay [183, 184]. In brief, a 1.0 x 10^6 cell pellet was lysed in 40 µL of NP-40 lysis buffer, diluted to a final concentration of 1.25 x 10^3 cells/µL, and 2 µL added to an extension reaction (50 cell equivalents per µL) for 60 min followed by a 5 min heat inactivation of telomerase at 95°C. An aliquot (2 µL) of extension products containing an equivalent of 100 cells was amplified in a droplet digital PCR for 40 cycles. Droplet fluorescence intensity and number were read and counted on the QX200 Droplet Reader (Bio-Rad). Data were calculated to represent telomerase extension products per cell equivalent.

6.3.12. Terminal Restriction Fragment Assay for Telomere Length Analysis

The average length of telomeres (terminal restriction fragment lengths) was measured as previously described [185] with the following modifications: A DIG-labeled DNA molecular weight marker II ladder was loaded on either side of the samples (Millipore Sigma, St. Louis, MO). DNA was transferred to Hybond-N+ membranes (GE Healthcare, Piscataway, NJ) using overnight transfers. The membrane was briefly air-dried and DNA was fixed by UV-crosslinking. Membranes were then probed for telomeres using a digoxigenin (DIG)-labeled telomere probe, detected with a horseradish peroxidase-linked anti-DIG antibody (Cat no. 11093274910; Roche, Basel, Switzerland, RRID:AB_2734716), exposed with CDP-star (Cat no. 11759051001; Roche), and imaged (Chemidoc XRS + Molecular Imager, Bio-Rad).

6.3.13. Clonogenic Assay

Calu-6 and U-2 OS cells with or without TERT Delta 2-4 overexpression were used for clonogenic assays. siRNA was treated in duplicate only for Calu-6 cells as described above (10 nM siRNA). After 24 hours of siRNA and treatments, cells were trypsinized, counted, and plated in triplicate at densities of 100 cells resulting in 6 replicates for each condition. Media was changed every four days, and once clearly visible clones were present (~11 days), they were fixed and stained with Crystal violet. Plates were imaged (Chemidoc XRS + Molecular Imager, Bio-Rad) and the number of colonies were counted by ColonyCountJ [186].

6.3.14. Alamar Blue cell viability Assay

To determine the viability of cells with overexpression of Delta 2-4, RNAi and cisplatin treatment, we used Alamar blue assays. In TERT Delta 2-4 expressing U-2 OS and Calu-6 cells, 1.0 x 10^4 cells were plated on 96-well plates in 180 µL of growth media. Immediately after plating the cells, 20 µL of either PBS (vehicle) or cisplatin (Cat. No. 232120-50MG, Millipore Sigma) dissolved in PBS were treated with 6 different concentrations (U-2 OS: 6.25-4.69-3.52-2.64-1.98-0.39 µg/mL; Calu-6: 100-25-6.25-1.56-0.39-0.1 µg/mL). After 44 hours of treatment exposure, 20 µL of 10X Alamar blue was added to the media. After 4 hours of incubation, the fluorescence of each well was determined on a plate reader (Molecular Devices SpectraMax iD3) at 545 nM excitation and 590 nM emission. Values from cisplatin treated cells were divided by averaged

values from PBS treated of cells (same cell line) to calculate percentage of alive cells (with the vehicle condition assumed to be 100% viable).

For siRNA/rescue experiment in Calu-6, reverse transfection was performed [258]. Transfection complexes were prepared with siRNAs (siD2-4 (8:16)) using Opti-MEM (Gibco) and RNAi max (Invitrogen) following the manufacturer's procedures and 20 µL of the complex was plated in 96-well plate and incubated for 20 minutes. 1.0 x 10^4 cells were plated on each well in 160 µL of growth media, followed by 20 µL of either PBS or cisplatin (1.59 µg/mL) dissolved in PBS. Final concentration of siRNA was 30 nM in 200 µL. After 44 hours, 20 µL of 10X Alamar blue (Cat. No. DAL1025, Invitrogen™) was added. After 4 hours of incubation, the fluorescence of each well was determined on a plate reader (Molecular Devices SpectraMax iD3) at 545 nM excitation and 590 nM emission. Viability was calculated as describe above.

6.3.15. Western Blot Analysis

Cell pellets (1 x 10^6 cells) were collected and lysed in 100 µL of lysis buffer (NP40 based buffer – 10 mM Tris-HCl pH 8.0, 1mM $MgCl_2$, 1mM EDTA, 1% NP-40, 0.25 mM Sodium deoxycholate, 10% Glycerol, 150 mM NaCl, 0.036% 2-mercapto ethanol, 0.2 mM). Total protein lysates were further treated with 100 µL of 2 x Laemmli buffer (Bio-Rad) and boiled for 10 mins at 95°C. Each protein lysate was loaded by equal volume and resolved by SDS-polyacrylamide gel electrophoresis, transferred to polyvinylidene fluoride (PVDF) membranes, and detected with antibodies for TERT

(rabbit monoclonal, Y182, Cat. No. ab32020, Abcam, 1:1000 dilution in 5% BSA), FLAG (rabbit monoclonal, D6W5B, Cat. No. 14973, Cell Signaling, 1:1,000 dilution in 5% BSA), and V5 (mouse monoclonal, SV5-Pk1, Cat. No. R960-25, 1:1000 dilution in 5% BSA). Protein loading was determined with antibodies against beta-actin (mouse monoclonal [8H10D10], 3700, Cell Signaling Technology, 1:1000 in 5% BSA). Blots were imaged with Bio-Rad ChemiDoc XRS+ Molecular Imager and quantified with Bio-Rad Image Lab software.

6.3.16. Growth Curve – Population Doubling (PD)

To track and compare growth rates of stable cells lines of control vector and TERT Delta 2-4 overexpressing cells, population doublings were calculated based on the formula below. PD values were started from 10 doublings, after 2 weeks of blasticidin selection and PD values were calculated accumulatively per subculture based on the formula: new PD = (LOG([the number of trypsinized cells]/[the number of previously plated cells])/0.3)+ [the number of previous PD].

6.3.17. Statistical analysis

For *TERT* transcript subcellular localization experiment (Figure 6.1G) and siRNA testing experiments (Supplemental Figure 6.4B-D), one-way ANOVA with uncorrected Fisher's LSD for post hoc comparisons were used to determine statistical significance between experimental groups. For knockdown and rescue experiments (Figure 6.3D and E; Supplemental Figure 6.5D and E), p-value was calculated using one-way

ANOVA with Tukey's multiple comparison test compared to every other condition. When a *p*-value from a comparison between two groups was $p < 0.05$, the two groups were assigned different letters of the alphabet (i.e., a vs. b). When the *p*-value was $p \geq 0.05$, two groups were assigned to the same letter (a vs. a). To compare two conditions, unpaired two-tailed t-test was used to calculate *p*-values.

6.4. Results

6.4.1. Long-read sequencing identifies the catalogue of *TERT* mRNA variants.

To capture the *TERT* mRNA variant expression profile, TERT specific sequencing libraries were prepared from four different types of cells: human induced pluripotent stem cells (iPSCs), and three non-small cell lung cancer (NSCLC) cells (A549, Calu-6, and H1299). Then single molecule long-read RNA sequencing was performed on an Oxford Nanopore Technology (ONT) MinION Mk1C (Figure 6.1B). We observed 45 *TERT* mRNA variants and generated a heatmap to show log2-transformed expression levels in the four cell lines (Supplemental Figure 6.1). In addition to the heatmap, characteristics of the TERT isoforms were determined such as the open reading frame (ORF), premature termination codon (PTC), novelty, and transcript model (exons and introns) (Supplemental Figure 6.2). Among the discovered *TERT* mRNA variants, we focused on relatively more abundant variants according to the heatmap (Supplemental Figure 6.1). Most of the abundant *TERT* variants were known mRNAs, such as delta 2 *TERT* (also known as Del2 which lacks exon 2), delta 2 excluding exons 7-8 (delta 2/delta 7-8), FL *TERT* (full-length with all 16 exons), delta 7-8 *TERT* (known as minus beta, skipping of exons 7-8), and delta 5'E6 *TERT* (known as minus alpha, use of a cryptic splice site in exon 6 that removes that first 36 nucleotides of exon 6) (Figure 6.1C and D). However, we also discovered a relatively abundant novel *TERT* splicing event: delta 2-4 *TERT* that lacks exons 2-4 (Figure 6.1C and D). We observed two abundant delta 2-4 mRNA variants. One that has an exons 2-4 skipping event that included exons 7/8 and retained the original protein domains and open reading frame (referred to herein as Delta 2-4, note the capital D); and a second one with exons 2-4

skipping was also observed to be combined with the beta deletion (exons 7-8 skipping event; delta 2-4/delta 7-8 in Figure 6.1C and D). We also identified Delta 2-4 isoform from an independent approach based on traditional cDNA cloning. Delta 2-4 was identified in several clones by restriction enzyme digests and validated by Sanger sequencing, supporting our findings from the long-read RNA sequencing (Figure 6.1E). To quantitatively measure the expression level of delta 2-4 mRNA variants, we developed two droplet digital PCR (ddPCR) assays. One assay detects “total delta 2-4” which includes quantification of Delta 2-4 (with exons 7/8) and delta 2-4 /delta 7-8 (without exons 7/8) by using *TERT* exon 1 and exon 5 targeting primers. The second assay detects only Delta 2-4 by using *TERT* exon 1 and exon 7 targeting primers (Supplemental Figure 6.3A). An exon 1/5 junction targeting 5’hydrolysis probe was used for both assays to make the assays specific to the exons 2-4 skipping event. We applied the assays to quantify delta 2-4 expression in a cell panel, and the results showed that total delta 2-4 (including both Delta 2-4 and delta 2-4/ delta 7-8) expression was higher than Delta 2-4 expression in the cell panel as expected, supporting the validity of our new assays (Figure 6.1F). iPSCs showed the highest total delta 2-4 and Delta 2-4 expression compared to the other cell lines, followed by A549, Calu-6, H1299, H920, and HBEC (human bronchial epithelial cell). The detection of total delta 2-4 or Delta 2-4 in HBECs was very minimal. Based on our observations we conclude that lung cancer cells and telomerase positive iPSCs express a novel TERT isoform called Delta 2-4 that retains the original open reading frame and potentially codes for a new protein and that HBECs that lack telomerase activity do not express Delta 2-4 isoform making Delta 2-4 isoform a developmental and cancer specific TERT isoform.

Next, we wanted to determine if TERT Delta 2-4 codes for a novel protein. Since antibodies to TERT are difficult to work with and the low abundance of TERT proteins make protein detection challenging, we needed to take several complimentary approaches to indirectly provide evidence of TERT Delta 2-4 protein coding capacity. Since previous reports have indicated that the majority of *TERT* mRNAs are sequestered in the nucleus, we considered the cellular localization of *TERT* delta 2-4 mRNAs. Additionally, our rationale was that RNA transcripts that are to be translated into proteins, should have higher cytoplasmic localization ratio than transcripts that lack protein coding capacity and are expected to be degraded by RNA decay mechanisms. We separated Calu-6 cells into nuclear or cytoplasmic fractions, extracted RNAs, and produced cDNAs with oligo dT priming (Figure 6.1G; Supplemental Figure 6.3B). We measured MALAT1, which is a nuclear non-coding RNA (as a control for nuclear RNA fractionation validity), GAPDH (as a control for cytoplasmic RNA fractionation validity), total delta 2-4 (Delta 2-4 and delta 2-4 /delta 7-8), Delta 2-4, potential FL (exons 7-8 containing *TERT*), minus beta (exons 7-8 excluding *TERT*), i11 (intron 11 retained *TERT*), and i14 (intron 14 retained *TERT*). We observed that *TERT* mRNA variants except i11 and i14 had significantly higher cytoplasmic localization ratio compared to MALAT1. When compared to GAPDH, which is protein-coding gene, total delta 2-4, potential FL, minus beta, i11, and i14 *TERT* mRNA variants had significantly lower cytoplasmic localization ratios. As shown in Dumbović et al. [102], intron 11 or 14 retained *TERT* transcripts were mostly localized in nucleus. Despite the protein coding capacity of full-length *TERT* (active telomerase), potential FL *TERT* still had lower cytoplasmic localization ratio than GAPDH or Delta 2-4. This is because expression of

potential FL is determined by measuring expression of *TERT* exons 7/8. Although exons 7/8 containing *TERT* transcripts measured in cytoplasm are likely to be the FL *TERT* mRNA, other non-full-length exons 7/8 containing *TERT* mRNA variants (e.g., minus gamma, INS3, INS4, Del2, i11 or i14 retained *TERT* transcripts in nucleus) are also detected in the nuclear fraction. Total delta 2-4 includes both Delta 2-4 and delta 2-4 /delta 7-8, and delta 2-4 /delta 7-8 contains premature termination codon (PTC) in exon 10 so it is expected to be degraded by non-sense mediated decay in the cytoplasm. Thus, we hypothesized that degradation of delta 2-4 /delta 7-8 would result in lower cytoplasmic localization ratio of total delta 2-4 compared to Delta 2-4, and this was confirmed by our observations (Fig 1G). To further support the protein coding capacity of Delta 2-4, we also carried out a non-sense mediated decay inhibition assay. Knockdown of SMG1 resulted in a significant increase in a PTC containing transcript of SRSF3 (control for validity of assay) as expected [257]. However, Delta 2-4 did not increase (i.e., remained at steady state levels) when SMG1 was knocked down compared to control (Figure 6.1H) suggesting that Delta 2-4 likely forms a protein.

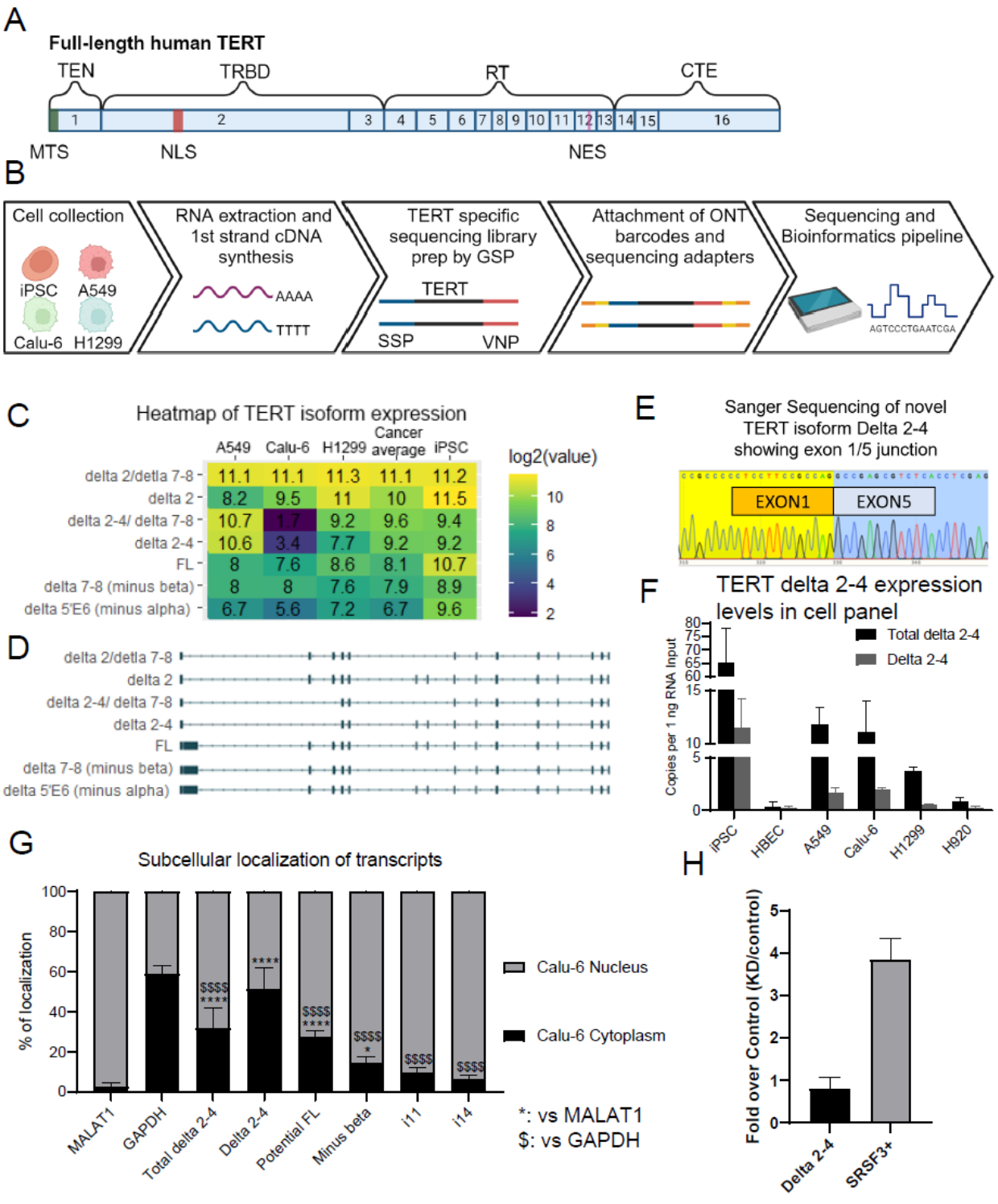

Figure 6.1. Long-read sequencing pipeline to discover novel TERT Delta 2-4 isoform and validation of Delta 2-4 expression.

A. Cartoon of full-length TERT exons. Four functional domains (TEN: telomerase N-terminal; TRBD: telomerase RNA-binding domain; RT: reverse transcriptase; CTE: C-terminal extension) and three localization signals (MTS: mitochondrial-targeting signal in exon 1; NLS: nuclear localization signal in exon2; NES: nuclear export signal in exon 12) are shown. **B**. Long-read sequencing pipeline to discover novel TERT isoforms. Four cell lines: induced pluripotent stem cells (iPSCs), Calu-6, A549, and H1299 were pelleted from three biological replicates and RNA was extracted from each pellet. First cDNA strand was synthesized with oligo dT using superscript 4, followed by PCR with gene specific primer (GSP; *TERT* exons targeting primers) tailed with SSP or VNP (SSP-Exon 1 or VNP-Exon 16). After purification of TERT specific cDNA library, ONT (Oxford nanopore technology) barcodes and rapid 1D sequencing adapters were attached sequentially. Samples were loaded into MinION Mk1C and generated raw sequence files were processed by bioinformatics pipeline consisting of minimap2, TranscriptClean, TALON, SWAN, and R. **C**. Heatmap showing expression levels of relatively abundant TERT isoforms. Numeric values are Log2-transformed TPM values and colors indicate expression level. Cancer average is averaged value of A549, Calu-6, and H1299. **D**. Transcript models of the isoform (Left to right: 5' to 3'). Boxes indicate exons and solid lines between exons indicate introns. **E**. Sanger Sequencing result confirmed *TERT* exon 2-4 splicing event. **F**. *TERT* Delta 2-4 expression levels in cell panels (determined by ddPCR; n = 3 biological replicates per condition). Total D2-4 indicates total *TERT* Delta 2-4 including delta 2-4 and delta2-4/ delta 7-8, and D2-4 indicates *TERT* Delta 2-4 with exon 7/8 (determined by ddPCR; n = 3 biological replicates per condition). **G**. Percentage of localization between cytoplasm and nucleus was determined for nuclear non-coding RNA MALAT1, GAPDH, and TERT isoforms. Total Delta 2-4: Delta 2-4 and Delta 2-4/ Delta 7-8; Delta 2-4: Delta 2-4 with exons 7/8; Potential FL: exons 7/8 including *TERT*; Minus beta: exons 6/9 junction containing *TERT*; i11: intron 11 retained *TERT*; i14: intron 14 retained *TERT* (TERT mRNA variants: determined by ddPCR; MALAT1 and GAPDH: determined by gel-based PCR; n = 3 biological replicates). Unpaired t-test was performed to compare *TERT* mRNA variants' percentage of localization compared to MALAT1 or GAPDH. ($$$$: $p < 0.0001$ compared to MALAT1; ****: $p < 0.0001$ and *: $p < 0.05$ compared to GAPDH) **H**. SMG1 knockdown indirectly indicates that Delta 2-4 *TERT* is likely translated into a protein. H1299 cells were treated with either 10nM of siRNA control or siRNA targeting SMG1. Droplet digital PCR was used to measure gene expression of *TERT* Delta 2-4 including exons 7/8. As a positive control that our non-sense mediated decay manipulation worked, we measured SRSF3 containing a premature termination codon that is known to regulate levels of SRSF3. Three independent replicates were performed.

6.4.2. Impact of Delta 2-4 on growth rate, telomere length and telomerase activity.

Having partially established the protein capacity of *TERT* Delta 2-4 mRNA, we were interested in determining the functional role of this new protein isoform. To identify the function of the Delta 2-4 isoform, we performed loss of function studies using custom designed siRNAs. First, three siRNAs (siD2-4 (12:12), siD2-4 (8:16), and siD2-4 (16:8)) targeting different regions of *TERT* exons 1/5 junction and mixture of the same three siRNAs (siD2-4 (mix)) were tested (Supplemental Figure 6.4A). Our goal of this experiment was to find an siRNA that specifically reduces Delta 2-4 while leaving the remainder of *TERT* mRNA variants at or near steady state expression levels. Following 72 hours of siRNA treatment, *TERT* Delta 2-4 expression was significantly reduced by siD2-4 (12:12) and siD2-4 (8:16) treatment compared to control (scrambled siRNA) treated Calu-6 cells (Supplemental Figure 6.4C). During the same treatment, total *TERT* delta 2-4 was not significantly reduced by any siRNAs (Supplemental Figure 6.4B). This supports that Delta 2-4 was targeted with siRNAs better than delta 2-4/ delta 7-8 likely due to higher cytoplasmic localization of Delta 2-4 than delta 2-4/ delta 7-8 (Figure 6.1G). The expression level of *TERT* transcripts containing exons 3-5 was measured to determine if total *TERT* transcripts without exons 1/5 junctions were reduced by exons 1/5 junction targeting siRNAs (i.e., off-target). We found that siD2-4 (12:12) significantly reduced the expression level of *TERT* exons 3-5 containing transcripts indicating that this siRNA was not suitable for further study (Supplemental Figure 6.4D), while siD2-4 (8:16) did not reduce the expression level of *TERT* transcripts containing exons 3-5. As a result, siD2-4 (8:16) was selected for further siRNA experiments. With 48 hours of siRNA treatment in Calu-6 cells, we observed statistically significant 25% reduction of

total delta 2-4 (Delta 2-4 and delta 2-4/ delta 7-8) and 50% reduction of Delta 2-4 were achieved by siD2-4 (8:16) suggesting that siRNA targeted mostly Delta 2-4 rather than delta 2-4/ delta 7-8, without affecting exons 3-5 containing *TERT* transcripts in comparison to control treated Calu-6 cells (Figure 6.2A and B, Supplemental Figure 6.4E). Despite the reduction of *TERT* Delta 2-4 expression, telomerase activity, growth rate, and cell viability did not change after 48 hours of siD2-4 (8:16) treatment in comparison to control (Figure 6.2C, Supplemental Figure 6.4F and G). These data indicate that Delta 2-4 is not necessary for telomerase to be active or for cell proliferation when other TERT isoforms are expressed.

Having established a loss of function model we next tested gain of function by expressing Delta 2-4. We performed gain of function studies by establishing TERT Delta 2-4 expressing cell lines. We generated a codon optimized Delta 2-4 construct so that it would have good expression in mammalian cells, and it would also be siRNA resistant for rescue experiments. To avoid endogenous TERT antibody issues [79], we added two N-terminal tags, FLAG and V5 tags allowing for reliable detection of the exogenously expressed Delta 2-4 protein (Supplemental Figure 6.4H). N-terminal tags do not impact TERT function as shown in previous studies [259-262]. Stable cell lines were successfully established in two different cell types (Calu-6 and U-2 OS) and expression of ectopic TERT Delta 2-4 was confirmed by antibodies targeting C-terminus of TERT (TERT Y182 antibody) and tags (FLAG and V5 antibodies) (Figure 6.2D). The use of these two cells lines allowed us to test telomerase dependent phenotypes and telomerase independent phenotypes. Calu-6 cell is telomerase expressing human non-small cell lung cancer cell line. It was used to determine the function of TERT delta 2-4

in the presence of telomerase and other TERT isoforms, such as inhibition of telomerase activity via dominant-negative actions. U-2 OS cell is telomerase deficient human bone osteosarcoma epithelial cell line relying on alternative lengthening of telomere (ALT) mechanisms to maintain its telomeres. We used U-2 OS to identify functions of TERT Delta 2-4 independent to other telomerase or TERT isoforms. Overexpression of TERT Delta 2-4 did not affect telomerase activity in Calu-6 cells, and telomerase activity was not detected from TERT Delta 2-4 expressing U-2 OS cells, as expected (Figure 6.2E). In addition, expression of TERT Delta 2-4 did not change growth rate for over 50 days for both Calu-6 or U-2 OS, despite 50 and 30 population doublings (PDs), respectively, from the end of stable cell line selection (Supplemental Figure 6.4I). Lastly, telomere length did not change in either cell line during our growth period as determined by terminal restriction fragment (TRF) analysis (Figure 6.2F and G). Overall, the functional studies based on loss of function and gain of function approaches showed that TERT Delta 2-4 functions are likely not related to telomerase activity, growth rate or telomere length.

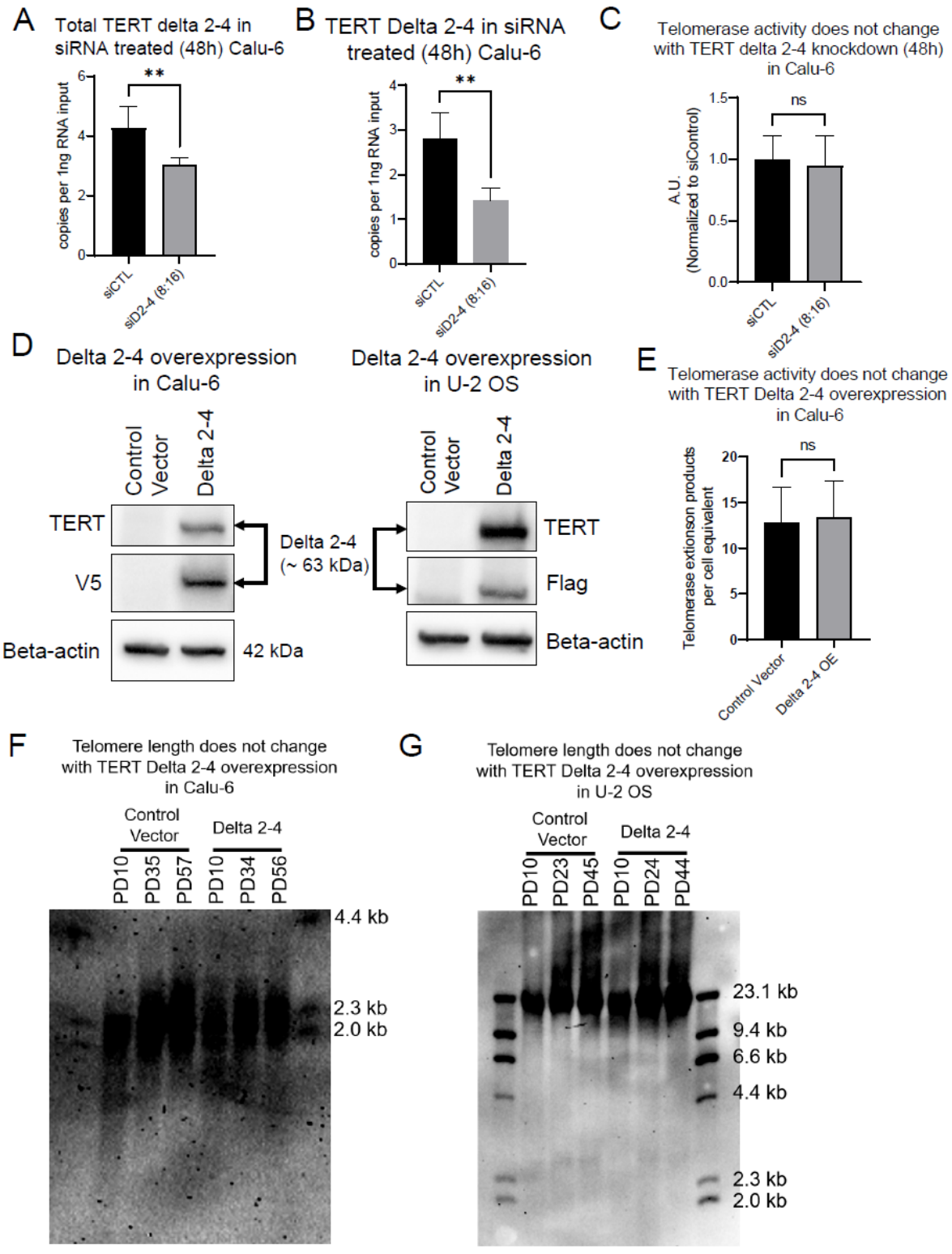

Figure 6.2. Impact of TERT Delta 2-4 isoform on growth rate, telomere length, and telomerase activity.

A. Total TERT Delta 2-4 (Delta 2-4 and Delta 2-4/ Delta 7-8) was measured following 48 hours after siRNA treatment (determined by ddPCR; n = 6 biological replicates). **B**. TERT Delta 2-4 expression level was measured following 48 hours after siRNA treatment (determined by ddPCR; n = 6 biological replicates). **C**. Telomerase activity did not change with TERT Delta 2-4 knockdown (48 hours) in Calu-6 cells. Telomerase activity was determined by ddTRAP (n = 6 biological replicates per condition). **D**. Flag-V5-Delta 2-4 expression was confirmed by TERT Y182 antibody, V5 antibody, and Flag antibody in Calu-6 cells (left) and U-2 OS cells (right). Beta-actin was loading control. **E**. Telomerase activity did not change with TERT Delta 2-4 overexpression in Calu-6 cells. Telomerase activity was determined by ddTRAP (n = 11 biological replicates per condition). **F** and **G**. Telomere length did not change with TERT Delta 2-4 overexpression in Calu-6 (F) and U-2 OS (G) (determined by terminal restriction fragment (TRF) assay).

6.4.3. Impact of Delta 2-4 on clonogenicity and resistance to cisplatin.

To continue to explore the functional roles of TERT Delta 2-4 isoform, we hypothesized that since this isoform lacks the typical *TERT* nuclear localization signal (exon 2) and the telomerase RNA-binding (TRBD) domain due to skipping of exons 2-4 (Figure 6.1A), but still possess mitochondrial targeting signal (MTS; in exon 1) and other functional domains, it could be functioning in the mitochondria in some capacity. Since mitochondrial localization of TERT is known to protect cells from apoptosis and it is independent to telomerase RNA template (TR, also known as TERC) [263, 264], we hypothesized that TERT Delta 2-4 would make cells more resistant to apoptosis by protection of mitochondrial DNA. We used a classic assay of apoptosis resistance, the clonogenic assay, to test our hypothesis. In fact, we observed that expression of TERT Delta 2-4 enhanced clonogenicity (47% increased total area; 30% increased average size; 16% increased number of colonies) in comparison to empty vector expressing U-2 OS cells (Total area of colonies = Average size of colonies x Number of colonies). This observation supports the idea that the enhancement of clonogenicity by Delta 2-4 overexpression is telomerase independent (Figure 6.3A and B, Supplemental Figure 6.5A and B). When TERT Delta 2-4 is expressed in Calu-6 cells, clonogenicity was also enhanced (72% increased total area; 42% increased average size; 18% increased number of colonies) compared to empty vector expressing cells. In addition, siRNA targeting TERT Delta 2-4 (siDelta2-4) treatment reduced clonogenicity (46% decreased total area; 18% decreased average size; 36% decreased number of colonies) and it was rescued by siRNA resistant Delta 2-4 expression (Supplemental Figure 6.5C) supporting

that the reduced clonogenicity by siRNA targeting TERT Delta 2-4 was on-target (Figure 6.3C and D, Supplemental Figure 6.5D, E).

In a follow up experiment, we tested the impact of cisplatin, a common lung cancer chemotherapy, on our gain of function cells. Cisplatin, which is a platinum-based chemotherapeutic, binds to DNA and induces DNA damage resulting in mitochondria-mediated intrinsic apoptosis of cells [265]. Thus, we hypothesized that overexpression of TERT Delta 2-4 would enhance the cells' resistance to cisplatin treatment in comparison to control. We first tested various concentrations of cisplatin with serial dilutions of drug in TERT Delta 2-4 expressing U-2 OS and Calu-6 cells. Supporting our hypothesis, expression of TERT Delta 2-4 indeed enhanced cells' resistance to cisplatin in both U-2 OS (25% enhanced at cisplatin concentration 4.69 μg/mL) and Calu-6 (31% enhanced at cisplatin concentration 1.56 μg/mL) cells (Supplemental Figure 6.5F and G). In a rescue experiment, Calu-6 cells with TERT Delta 2-4 knockdown were 26% more sensitive to cisplatin treatment, whereas cells with ectopic expression of TERT Delta 2-4 were 40% more resistant to cisplatin treatment (Figure 6.3E). Moreover, reduced resistance to cisplatin by siRNA knockdown was rescued by siRNA resistant TERT Delta 2-4 expression, supporting that the effect of siRNA knockdown on reduced resistance to cisplatin was an on-target effect of siRNA treatment. Overall, reduced clonogenicity and resistance to cisplatin treatment by TERT Delta 2-4 knockdown and increased clonogenicity and resistance to cisplatin treatment by TERT Delta 2-4 overexpression support our hypothesis: TERT Delta 2-4 enhances cells' resistance to intrinsic apoptosis.

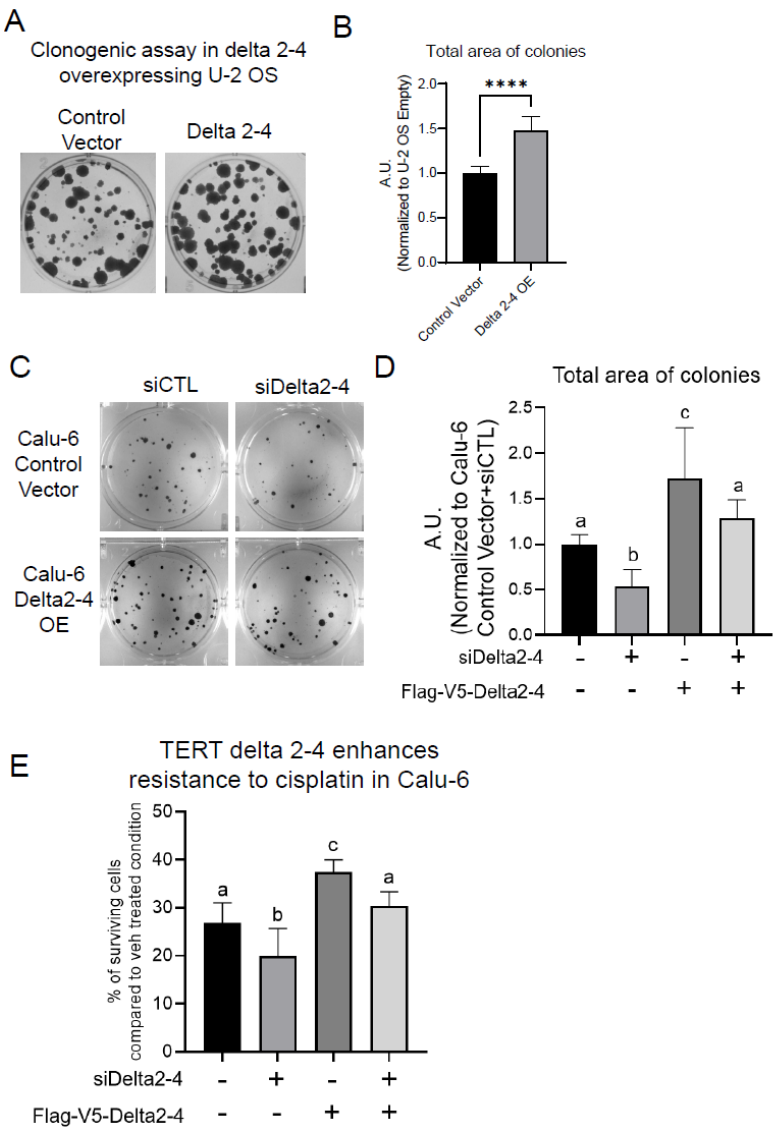

Figure 6.3. Impact of TERT Delta 2-4 isoform on clonogenicity and resistance to cisplatin.

A and **B**. Overexpression Delta 2-4 in telomerase deficient cell U-2 OS enhanced clonogenicity. Representative image (A) and quantified graph (B) are shown. **C** and **D**. Knockdown of TERT Delta 2-4 reduced clonogenicity in telomerase positive cells Calu-6, whereas overexpression of TERT Delta 2-4 enhanced clonogenicity in Calu-6. Knockdown effect was rescued by siRNA resistant Delta 2-4 overexpression. Representative image (C) and quantified graph (D) are shown. **E**. Calu-6 cells became more sensitive to cisplatin treatment (1.59 ug/mL, 48 hours) by TERT Delta 2-4 knockdown and more resistant by TERT Delta 2-4 overexpression. Knockdown effect was rescued by siRNA resistant Delta 2-4 overexpression.

6.5. Discussion

Increased telomerase activity is associated with greater than 85% of human cancers, including lung cancers [13]. Significant advances have been made in understanding of telomerase composition, biogenesis, trafficking, and regulation. However, fundamental questions remain about the alternative splicing isoforms separation of function from FL TERT that codes for active telomerase and maintains telomeres in cancer cells. Further, several reports have indicated off-telomere functions of FL TERT that appear to be difficult to interpret because many of these functions have been observed only in the ectopically expressed TERT context. Due to the low abundance and tight regulation of FL *TERT* mRNA levels, it appears unlikely that FL TERT functions as both a telomere maintaining telomerase and a TERC independent mitochondrial protective enzyme. We hypothesized that alternative splicing isoforms of TERT perform most or all of the non-telomere functions that have been ascribed to overexpressed FL TERT. Here we report the catalogue of *TERT* mRNA variants from four cells lines. In particular, we focused on a novel TERT isoform that we called TERT Delta 2-4. Based on our experimental data we determined that Delta 2-4 does not function in telomere biology but ascribed its function to protecting cells from apoptosis, likely via mitochondrial protection. These results shift the paradigm in the field from the idea that mitochondrial TERT is FL TERT to a new idea that mitochondrial TERT is an alternative splicing isoform: Delta 2-4. This new model supports the idea that FL TERT is low abundant and only functions in telomere synthesis via active telomerase and that alternative splicing of *TERT* creates functional isoforms that aid in cancer development. This final point is critical because our data suggests that Delta 2-4 is cancer specific and

thus, we may be able to target Delta 2-4 in cancer cells while sparing the function of FL TERT in adult somatic tissues that express functionally relevant levels of TERT.

Previous reports have identified TERT alternative splicing isoforms from a variety of cell types [28, 108, 175, 179, 266]. These studies utilized either traditional cDNA cloning followed by Sanger sequencing to identify AS variants or short read RNA sequencing following by mathematical reconstruction of isoforms based on overlapping reads and probability modeling [108]. While these methods are valid and do identify some transcript variants, newer and more advanced sequencing modalities allow for richer investigation of the transcript landscape of TERT in cells. To directly investigate full length cDNA molecules which might contain multiple splicing events in combination we chose to use single molecule long read sequencing. This technology avoids potential bias of short read sequencing in the mathematical modeling of isoforms. Among long read sequencing technologies, we used Oxford Nanopore Technologies MinION MK1C. While other technologies (e.g., Pacific Biosciences Iso-Seq) allow for robust long read sequencing, the flexibility, reduced cost, and ability to rapidly test multiple different library preparations in the laboratory lead to our decision to use the MinION MK1C. The flexibility of the MinION allowed us to optimize a library preparation for a low abundant and extensively spliced gene such as *TERT*. *TERT* is low abundant gene that is expressed only 1-40 transcript copies in a cell [267]. To ensure robust detection of *TERT* we prepared *TERT* specific sequencing libraries using gene specific primers targeting exon 1 and 16. We discovered 32 *TERT* mRNA transcripts that have not been reported previously to our knowledge.

We focused on TERT Delta 2-4 because of its abundance and potential to code for a new protein isoform with potentially new functions in cell biology. Exons 2 to 4 are mainly translated into telomerase RNA template binding domain (TRBD in Figure 6.1A) and skipping of these exons does not induce a premature stop codon. Since exon 1 contains a mitochondrial targeting signal (MTS), Delta 2-4 is likely to be localized to mitochondria. In fact, localization of TERT protein in the mitochondria and the roles of mitochondria localized TERT have been reported by previous studies. In 2004, Santos et al.[243] first determined that MTS was in *TERT* exon 1 and confirmed that overexpressed TERT localized to the mitochondria by immunocytochemistry and immunoblot of mitochondrial fractions from epithelial cell lines and fibroblasts from humans. To date, the main paradigm of mitochondrial TERT has focused on the shuttling of full-length TERT from the nucleus to the cytoplasm or mitochondria induced by certain stresses (e.g., oxidative stress) [113, 243, 264, 268-273]. However, we suggest that due to the low abundance of FL TERT (i.e., not enough molecules to be able to perform nuclear functions and mitochondrial functions at the same time), mitochondrial TERT is more likely an alternative splicing isoform of TERT. Delta 2-4 is an ideal candidate because it lacks the TRBD, and retains the RT domain and the MTS. We confirmed that Delta 2-4 expression enhances cells' clonogenicity, which is an indicator of resistance to apoptosis. Since intrinsic apoptosis is mediated by the mitochondria this evidence provides support for our hypothesis that Delta 2-4 is the mitochondrial TERT.

Our results showed that Calu-6 cells with Delta 2-4 reduction were 26 percent more sensitive to cisplatin treatment. This supports the idea that higher cancer drug efficiency can be achieved by reduction of Delta 2-4 expression. As we only tested cisplatin and there are other drugs that robustly induce intrinsic mitochondrial regulated apoptosis (such as Raptinal, Staurosproine, or Bcl-2 inhibitor HA14-1 [274]), testing other drugs while simultaneously reducing TERT Delta 2-4 expression may result in more significant improvements in drug efficiency. Also, the siRNA treatment method we used can be improved. Although we already tested three different sequence of siRNAs, different oligonucleotide chemistries (e.g., RNase H inducing modified DNA nucleotide Gapmers) or different sequences of targeting the exon 1/5 junction can be tested to achieve better knockdown. In addition, different mRNA targeting methods, such as CRISPR/cas7-11, may improve efficiency of reducing TERT Delta 2-4 and thus achieving more significant sensitization of cancer cells. A different angle of manipulating TERT Delta 2-4 expression would be to increase Delta 2-4 expression to improve fitness of normal cells. For example, a previous study has shown that overexpression of full-length TERT with additional mitochondria targeting signal (mitoTERT) in cardiomyocytes improved the fitness of cells [275]. We hypothesize that overexpression of TERT Delta 2-4 would improve the fitness of cardiomyocytes as much as mitoTERT or even better than mitoTERT because mitoTERT still contains nuclear localization signal in exon 2 that is not present in Delta 2-4 so that Delta 2-4 could have even greater mitochondrial localization.

Our study is not without limitations. First of all, when we prepared the TERT specific sequencing library, we used PCR which may have skewed the expression levels shown in the heatmap (Supplemental Figure 6.1). Thus, validation of *TERT* transcripts must be done before performing the functional studies for novel TERT isoforms. Another limitation is that *TERT* transcripts that do not contain exons 1 or 16 were not included in our list of isoforms because we used exons 1 and 16 targeting primers. However, we were looking for mRNA variants that retained the original open reading frame and coded for proteins. Although we discovered many TERT isoforms in induced pluripotent stem cells and three non-small cell lung cancer cells, further discovery may be made by using different types of cells, such as embryonic stem cells, somatic cells, adult stem cells, and cells from other types of cancers. We showed robust expression of *TERT* Delta 2-4 mRNA by long-read sequencing, sanger sequencing, and ddPCR assays. However, we were not able to show endogenous protein expression of Delta 2-4 isoform due to the low efficiency of TERT antibodies [79]. Also, we did not provide direct evidence of interaction between Delta 2-4 and mitochondria or mitochondrial localization of Delta 2-4.

In conclusion, we show that TERT Delta 2-4 has functions outside of telomere synthesis, that are to enhance clonogenicity of cells and to make lung cancer cells more resistant to cisplatin treatment. Implications of our data are 1) follow-up studies for different TERT isoforms can be performed based on newly discovered TERT isoforms 2) better cancer drug efficiency could be achieved by targeting specifically TERT Delta 2-4 that is likely to have less toxicity compared to targeting FL TERT isoform, and 3) better

mitochondrial protective effect against ROS may be achieved by overexpression of TERT Delta 2-4. Overall, our study not only provides a steppingstone to study functions of novel TERT isoforms, but also suggests a novel therapeutic target to either improve cancer drug efficiency or increase the fitness of normal cells.

Chapter 7 – Conclusion and Potential Future Directions

The focus of my dissertation was the alternative splicing (AS) regulation of *TERT* and the functional outcomes of TERT AS isoforms. The goal of this research was to decipher the regulatory mechanisms of telomerase in different contexts including exercise to treat aspects of cancer and aging. All four studies included in the dissertation were performed with this aim in mind: to understand *TERT* AS, but each study has unique conclusions, limitations, and potential future directions.

In the first study, *TERT* AS regulation of SF3B4 was studied in non-small cell lung cancer (NSCLC) cells. We chose NSCLC cells because *TERT* AS was dysregulated in tumor tissues from lung cancer patients. We selected SF3B4 as a potential full-length (FL) TERT promoting transfactor based on *TERT* minigene screening [26], and TCGA data showing upregulated SF3B4 expression in tumor tissues from lung cancer patients. Our model shows that SF3B4 binds to DR8 to promote the production of FL *TERT* resulting in higher telomerase activity in NSCLC cells, thus telomerase activity and growth of NSCLC cells can be inhibited by targeting SF3B4 to shift splicing away from FL *TERT*. Another important point of the study is that viability of primary HBEC was not reduced with SF3B4 knockdown although SF3B4 is a general splicing factor and likely to be essential in normal cells as well. The results suggested that SF3B4 is a potential cancer therapeutic target. These data implicate the SF3B complex as being a key part of lung cancer survival. However, we only suggested

SF3B4 as a potential cancer therapeutic target and did not directly inhibit SF3B4 to confirm the idea. In fact, there are already clinical trials underway using SF3B inhibiting molecules to treat cancers [276, 277]. A key future direction would be to test these molecules (spliceostatin, E7107, pladienolide B, herboxidiene, etc.) to shift *TERT* splicing towards non-telomerase coding transcripts, reduce telomerase, shorten telomeres, and kill lung cancer cells. Next, these compounds could be used with standard of care lung cancer treatments to test for additive and synergistic effects.

In the second study, telomerase regulation was examined in various contexts. From iPSC to NPC differentiation model, we confirmed that *TERT* AS regulating NOVA1-PTBP1-PTBP2 axis, which was identified in NSCLC cells [27], is conserved in the differentiation process. From the iPSC density model, we found that telomerase activity was mainly regulated by *TERT* AS in different iPSC densities. We predicted stem cell specific FL TERT promoting splicing factors based on correlation analyses. To identify cancer specific FL TERT promoting splicing factors, we utilized our *TERT* minigene screening data [26] and public TCGA data from lung cancer patients. Based on siRNA knockdown in Calu-6 cells, we validated predictions in Calu-6 cells. The results also supported that cell type specific *TERT* AS regulating mechanisms exist. Despite these important findings, our study still has limitations and additional studies will make our findings more meaningful. First of all, even though we found that telomerase activity increased with higher cell density and that *TERT* AS mainly governed the increase telomerase activity, we did not find the underlying mechanisms. We hypothesize that nutrition deprivation (reduced glucose or amino acids per cell in the media due to high density of cells) or increased acidity (i.e., lactate and H+ ions) of the

media could drive the *TERT* AS switching. We could test this by subjecting cell cultures to controlled conditions of reduced glucose or amino acids and altered pH levels in the media. An alternative hypothesis is that higher cell density might recreate conditions similar to when stem cells require maximal telomere elongation during population expansion before differentiation. To investigate this, we could measure the expression of stem cell proliferation markers, conduct cell cycle analysis, and assess changes in telomere length in cell cultures exposed to different cell densities. If the underlying mechanisms of the observed changes in *TERT* AS in higher iPSC density are defined, it will result in not only further understanding of telomerase regulation in developmental processes, but also understanding of telomerase regulation under certain physiological stress (e.g., exercise interventions). For instance, if lactate in the media is responsible for the shift in splicing of *TERT* towards FL, this information could lead to experiments testing the hypothesis that lactate induced by exercise could shift the splicing of *TERT* toward FL *TERT* during and following exercise in specific cell types and tissues (i.e., immune cells or vascular tissues). Second, we examined expression levels of limited number of splicing factors to figure out *TERT* AS regulating transfactors. To overcome, high-throughput approaches could be used to determine the splicing factors that regulate FL *TERT* splicing in the iPSC density model. For example, CRISPR knockout screen in the iPSC cell density model could determine additional *TERT* AS regulators. The discovered *TERT* AS regulating candidate genes could then be tested in both stem cells and cancer cells and confirmed as cell type specific *TERT* AS regulators. Ultimately this would lead to more precise understanding of *TERT* splicing regulation in

stem cells and cancer cells, potentially identifying therapeutic targets for regenerative medicine and/or cancer therapy purposes.

In the third study, we measured expression of human *TERT* transcripts in thymus from human TERT expressing transgenic hTERT-BAC mice in three different age groups (young/middle-aged/old) with or without access to a running wheel for three weeks. Our results showed that *hTERT* expression declined with aging and three weeks of voluntary wheel running did not counteract age-driven decline, supporting primary aging mechanisms (i.e., epigenetic changes) as the cause of the decline of *hTERT* expression. However, we did not examine any potential underpinning mechanisms for the reduction of *hTERT* expression. For instance, we did not measure any expression levels of transcription factors that are potentially related to age-driven reduction of *hTERT* expression. Also, we did not measure any epigenetics markers such as histone modification or *hTERT* promoter methylation. A logical extension to overcome the limitations would be to test the hypothesis that changes in transcription factor expression or epigenetic changes in the histone or DNA methylation of the *hTERT* promoter resulted in the repression of *hTERT* transcription with aging. Expression of transcription factors that are known to regulate *hTERT* transcription could be measured in different age groups to identify key players regulating *hTERT* transcription during aging. To determine how age impacts promoter epigenetics of *hTERT* we could measure DNA methylation changes and changes in histone activation and repressive marks that would help elucidate causes of the repressed *hTERT* transcripts. When it comes to *hTERT* AS, three weeks of voluntary wheel running counteracted the increase in percentage of exons 7/8 containing *hTERT* transcripts with aging, supporting that

secondary aging drives the increase in exons 7/8 containing *hTERT* transcripts. Although our data support that the decrease in *hTERT* expression and changes in *hTERT* AS are primarily regulated by primary aging and secondary aging, respectively, it cannot be assured solely by the effect of exercise. To support our conclusion, other factors affecting aging such as caloric restriction, which is well known to slow primary biological aging, should be performed to determine whether *hTERT* expression and hTERT AS are regulated by primary aging or secondary aging. When it comes to *hTERT* mRNA variants, we defined the exons 7/8 containing *hTERT* transcript as a potential FL *hTERT* because FL hTERT is relatively abundant isoform compared to alternatively spliced isoforms. However, the limitation was that the hTERT isoform expression profile has never been examined in thymus and more studies are needed to identify the source transcripts of the increased exons 7/8 containing *hTERT* transcripts with aging. One immediate next step would be to measure additional *hTERT* transcripts that contain exons 7/8 such as such as minus gamma, INS3, INS4, Delta 2-4, or delta 2 or some combination of these. We hypothesize that the increase in exon 7/8 containing transcripts was not due to FL *hTERT* but was actually due to other *hTERT* transcripts that contain exons 7/8 as mentioned above. Such data would indicate that exercise prevented an increase in these dominant-negative and degraded transcripts providing evidence of a positive effect of exercise with aging on the expression profile of *hTERT* transcripts in the thymus. We also did not directly measure the protein levels of hTERT and the correlation of *hTERT* mRNA levels with telomerase activity (surrogate for FL hTERT protein levels) is modest at best (Ludlow et al., 2018 [26] showed 0.35 correlation between exons 7/8 and ddTRAP in a panel of lung cancer cells). A major

limitation in the field of telomerase biology is the lack of commercially available antibodies that reliably detect hTERT protein levels. Further, the abundance of hTERT proteins is estimated at 200-700 in telomerase positive cancer cells [79], and is likely lower in telomerase positive somatic cells such as the thymus tissue. The measurement of other *hTERT* mRNA variants that contain exons 7/8 will improve our confidence that our *hTERT* measurements will be indicative of the protein levels of hTERT in the thymus. However, this will still be a limitation that we will have to address in the manuscript. We also measured *hTERT* AS in thymus from middle-aged TERT-BAC mice before, immediately post, and 1-hour post 30 minutes of acute treadmill exercise at 60% of maximum speed. We did not find significant changes in *hTERT* AS expression but we found similar expression pattern in *hTERT* expression that expression increased immediately after exercise and decreased even further than pre-exercise at 1-hour post exercise as we observed previously in gastrocnemius, left ventricle, and brain from young TERT-BAC mice [29]. When *hTERT* expression level was measured in thymus, two main challenges to find statistically significant difference were heterogeneity of *hTERT* expression resulting in large standard deviation and low *TERT* expression in aged mice. Using a post hoc power analysis (group A mean = 1.1, group B mean = 1.25, standard deviation = 0.59) indicated that we were significantly underpowered to detect a statistically significant difference. Using these same values, a sample size estimate was calculated for the same input values as above and we would need 243 animals per group to be sufficiently powered (Beta = 0.8, alpha 5%) to detect differences. Clearly, this is not a practical future direction and likely indicates that the acute exercise intervention that we used is not a sufficient stimulus to impact *hTERT*

expression in aged thymus. Also, another limitation was the inability to determine the origin of hTERT transcripts due to the presence of multiple cell types in thymus tissue. Single cell RNA sequencing (scRNA-Seq) could be used to unravel the heterogeneity within thymus tissue, but it will still be challenging to detect robust *hTERT* signal due to its low abundance. Alternatively, we could use flow cytometry with cell surface antigen markers to sort populations of cells from single cell suspensions of thymus (T cells, B cells, thymocytes, and adipocytes) and measure *hTERT* expression to overcome the abundance issues associated with single cell measures of TERT expression. In addition to these approaches, different types and intensities of exercise intervention could be used for future studies as the intervention we used could have been insufficient to induce significant changes of *hTERT* AS in thymus. Lastly, limitation of mouse model (e.g., human TERT in mice cannot form active telomerase due to incompatibility with murine telomerase complex components) will be ultimately overcome if samples are obtained from humans.

In the last study, we identified 45 TERT alternatively spliced mRNA variants including 13 known and 32 novel variants and carried out functional studies for a selected novel TERT isoform: Delta 2-4. According to our data, the Delta 2-4 TERT is likely to be a mitochondrial TERT that prevents mitochondrial DNA damage to makes cells more resistant to apoptosis. Despite the low abundance of TERT expression, mitochondrial TERT has been considered to be shuttled FL TERT from nucleus for about 20 years. Because of this “shuttling of FL TERT” paradigm, research groups started to use subcellular localization modified TERT, such as mitochondria localization TERT (mitoTERT) or nuclear localization TERT (nucTERT) by removing and adding

mitochondria targeting signal (MTS) or nuclear localization signal (NLS) to study the effect of full-length TERT at different locations [113, 264, 272, 273, 275]. Thus, a key future direction would be to provide evidence that mitochondrial TERT is not FL TERT but alternatively spliced TERT isoform, Delta 2-4. The major limitation of our study is that we did not show any direct evidence of interaction between Delta 2-4 and mitochondria. Thus, mitochondrial localization and binding to mitochondrial DNA of Delta 2-4 should be confirmed. Chromatin-immunoprecipitation (ChIP) followed by PCR of mitochondrial DNA targets using Delta 2-4 overexpressing cell lines can be used to determine the binding of mitochondrial DNA to overexpressed delta 2-4. Localization of Delta 2-4 could be determined by immunocytochemistry with mitochondria targeting antibody and ectopic tag antibody for Delta 2-4. Mitochondria extracts can be used for immunoblotting to detect Delta 2-4 expression. After confirming the mitochondrial localization, the role of Delta 2-4 TERT in binding TERT mitochondrial DNA would need to be determined. Since Delta 2-4 retains the TEN, RT, and CTE domains of TERT, it is highly likely that TERT can bind DNA (TEN and CTE) and potentially has enzyme activity. We could use a heterologous expression system to purify Delta 2-4 protein and perform in vitro enzyme activity and binding assays as well as structural studies. These follow-up studies will support that Delta 2-4 is the mitochondrial TERT. However, it is also possible that Delta 2-4's function does not involve a direct interaction with mitochondria. An alternative explanation for Delta 2-4's role in enhancing cell viability could be that it serves as a co-factor that regulates the expression of genes responsible for improving mitochondrial fitness. This hypothesis could be examined through transcriptomic analyses to further support the biological function of Delta 2-4. Using

either scrambled siRNA or Delta 2-4 targeting siRNA on wild-type or Delta 2-4 overexpressing Calu-6 cells, the effect of Delta 2-4 knockdown, overexpression, and rescue on global gene expression will be determined and the list of differentially expressed genes will be used for gene set enrichment analysis. Lastly, additional types of cells should be used to elucidate the regulation and function of Delta 2-4. For example, the expression pattern of Delta 2-4 could be measured in adult tissues or other types of cancer cells. Also, knockdown or overexpression of Delta 2-4 could be tested in normal cells such as fibroblasts. In knockdown experiments we would expect little to no effects because our evidence indicates low or undetectable expression of Delta 2-4 in somatic cells. Overexpression of Delta 2-4 we would expect to provide somatic cells with enhanced resistance to apoptosis without impacting telomere biology or growth kinetics. We suspect and need to test if this protective effect of Delta 2-4 is through mitochondrial related pathways.

TERT Delta 2-4 is a potential therapeutic target for two different reasons. First, as our data showed that Delta 2-4 knockdown made cancer cells more sensitive to cisplatin treatment, Delta 2-4 expression could be reduced with other cancer drug treatment to enhance the efficiency of the drugs. Second, Delta 2-4 overexpression could be used to improve fitness of certain tissues. A recent study showed that overexpression of mitoTERT in cardiomyocytes was critical for mitochondrial respiration and during ischemia/reperfusion injury in mouse models [275]. We expect that overexpression of Delta 2-4 TERT would result in at least similar, or even better protection effects than mitoTERT, considering that mitoTERT is artificially modified TERT and still contains nuclear localization signal.

Overall, the studies included in my dissertation have clarified *TERT* AS regulation and function of new isoforms in various contexts including 1) Developmental stage cells, 2) Differentiated cells, and 3) Cancer cells. Based on the results, my dissertation offer therapeutic insights based on the regulation of telomerase activity. My research advanced understanding of *TERT* AS regulation as a step toward achieving a “complete decoding of telomerase regulation” and provides a foundational basis for further studies on telomerase regulation. The figure below integrates all four of my dissertation studies (Figure 7.1). In the working model below, we describe developmental stage cells that have high telomerase activity, maintain telomeres, express FL TERT and Delta 2-4. In this scenario, we predict that there would only be a sufficient quantity of FL TERT in cells to maintain telomeres, and there would not be enough FL TERT to adequately protect mitochondria. Since previous research has observed that TERT can co-localize with mitochondria and act in a protective way [113, 243, 264, 268-273], we think we have a premise that could explain how cells achieve enough TERT for both nuclear and mitochondrial functions. Since Delta 2-4 lacks the nuclear localization signal in exon 2 [244] but retains the mitochondrial localization signal in exon 1 [243], we think Delta 2-4 translocates to the mitochondria in telomerase positive cells to help maintain mitochondrial fitness. Thus, this idea would shift the paradigm in the field and provide a novel observation to rectify the conflicting data concerning the abundance of TERT in cells being limiting to perform both nuclear and mitochondrial functions. We think that Delta 2-4 could be needed in the mitochondrial to promote cell survival because cells in a state of high glycolytic flux exhibit elevated reactive oxygen species (ROS) generation compared to cells with low glycolytic flux [278-280]. This idea integrates well with germ

line cells, the inducible telomerase situation in immune cells and endothelial cells, as well as with cancer cells. In all these various cell types, they share the ability to express FL TERT to maintain telomere length and are also in states of cell division and high glycolytic flux, resulting in elevated levels of mitochondrial ROS. Thus Delta 2-4 is also needed to promote cell survival and mitochondrial fitness. In other somatic cells, such as neurons and muscle cells, which express no telomerase and very little, if any, FL TERT or other TERT isoforms, we suspect that mitochondria health is promoted by utilizing beta-oxidation as the primary metabolic system for energy production. Additionally, we speculate that other pathways are employed to enhance mitochondrial fitness in these telomerase and TERT null cells. This figure and new working model offer many places for future investigation, such as how Delta 2-4 is regulated, whether Delta 2-4 is induced by stimuli that induce expression of FL TERT in immune cells (such as exercise or antigen stimulation), if germ line cells and adult stem cells also co-express FL TERT and Delta 2-4, whether Delta 2-4 is targetable in cancer cells or impacts adult stem cells, if Delta 2-4 is co-localized to the mitochondria of telomerase-positive cells, what its mechanism of action is in promoting mitochondrial fitness if it is indeed in the mitochondria, and whether Delta 2-4 forms a functional protein in endogenous cells. All of these fundamental questions will advance the field of telomerase biology forward and provide a paradigm shifting explanation for the observations that FL TERT protects mitochondria.

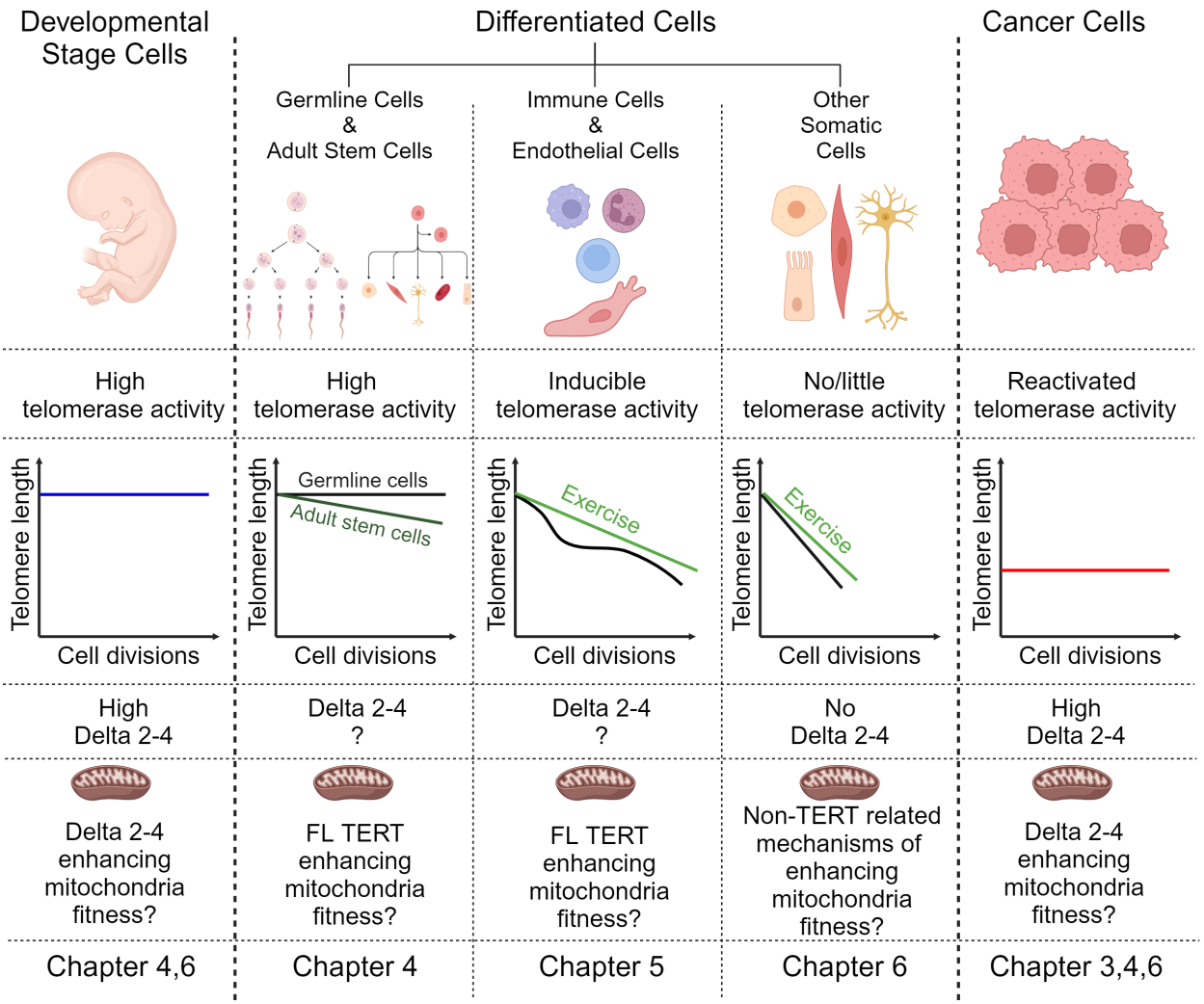

Figure 7.1. Focus of my dissertation on telomerase and TERT regulation in various contexts.

My dissertation focused on telomerase and TERT regulation in various contexts including developmental stage cells, differentiated cells, and cancer cells. Developmental stage cells such as embryonic stem cells have high telomerase activity that can maintain the telomere length. Differentiated cells differ based on the cell types. Germline cells have high telomerase activity to maintain telomere length. However adult stem cells have modest telomerase activity to only slow down telomere shortening. Immune cells and endothelial cells are telomerase inducible in response to external factors such as immune stimulation, changes in blood flow, and even endurance exercise. Thus, telomere shortening can be slowed down when telomerase is induced. Other somatic cells have very little or lacks telomerase activity resulting in

fastest telomere shortening. But exercise could result in adaptations such as telomere protective shelterin expression changes, anti-inflammatory, improved mitochondrial function, and antioxidant expression that could result in less telomere DNA damage and longer telomeres. Cancer cells reactivate telomerase and maintain short telomere length. Delta 2-4 was highly expressed in induced pluripotent stem cells (iPSCs) and cancer cells. However somatic cells (HBEC: human bronchial epithelial cells) had very low Delta 2-4 expression. We hypothesize that mitochondrial fitness is enhanced by Delta 2-4 in Developmental stage cells and cancer cells, and by full-length (FL) TERT in somatic cells. Currently Delta 2-4 expression in germline cells, adult stem cells, immune cells, and endothelial cells is unknown. In chapter 3, we focused on cancer cells. In chapter 4, we focused on iPSCs, cancer cells, and neural progenitor cells. In chapter 5, we focused on thymus tissue, which has immune cells. In chapter 6, we focused on iPSCs, cancer cells, and HBECs.

Appendix A - Supplemental Data for Chapter 3

Assay	Primer Pair	Gene and Exon Location	Primer Sequence 5' → 3'	Roche UPL #
ddPCR	1	hTERT Exon 7 For.	ACAGTTCGTGGCTCACCTG	52
	1	hTERT Exon 8 Rev.	GCGTAGGAAGACGTCGAAGA	
	2	hTERT Exon 6/9 For.	CAAGAGCCACGTCCTACGTC	58
	2	hTERT Exon 9 Rev.	CAAGAAATCATCCACCAAACG	
	3	SF3B4 Exon 3 For.	TCAGCAGCCGAACGACTT	14
	3	SF3B4 Exon 3 Rev.	GAGGAGGTGCATCTGCAAAC	
Gel Based	4	hTERT Exon 5 For.	GCCTGAGCTGTACTTTGTCAA	
	4	hTERT Exon 9 Rev.	AGGCTGCAGAGCAGCGTGGAGAGG	
	5	hTERT DR8 Deletion For.	GGCTTGAGTGCAGTGGCGCG	
	5	hTERT DR8 Deletion Rev.	TTTCGGGAAGCGCTATAG	
	6	PKM1 Exon 9 For.	CTTCTTATAAGTGTTTAGCAGCAGCT	
	7	PKM2 Exon 10 For.	GGGGCCATAATCGTCCTCACCA	
	6,7	PKM Exon 11 Rev.	CAGGTGGGCCTGACGAGCTG	
	8	PKM Exon 5 For.	CCTGTGGCTGGACTACAAGA	
	8	PKM Exon 6 Rev.	CCATATCAACATCCTGCTCGACC	
	9	NUMB Exon 8 For.	ACCTGAGGACCCCTTCTCAT	
	9	NUMB Exon 10 Rev.	CGGACGCTCTTAGACACCTC	
	10	Bcl-x Exon 2 For.	CATGGCAGCAGTAAAGCAAG	
	10	Bcl-x Exon 3 Rev.	GCATTGTTCCCATAGAGTTCC	
	11	TBP Exon 3 For.	GGAGAGTTCTGGGATTGTAC	
	11	TBP Exon 5 Rev.	CTTATCCTCATGATTACCGCAG	
ddTRAP	12	TS Primer	AATCCGTCGAGCAGAGTT	Evergreen
	12	ACX Primer	GCGCGGCTTACCCTTACCCTTACCCTAACC	

Supplemental Table 3.1. Primers and Probes

Cell Line	Plated Clones →	6-Well Plate →	10 cm Dish →	Genotyped	
Calu6	384	101	84	Wild Types	50
				Heterozygous	27
				Deletions	7

Supplemental Table 3.2. hTERT Overexpression DR8 CRISPR/Cas9 Clone Progression

Gene	Survival in LUAD	Over expression in tumor v. normal (matched patient samples, paired *t* test)
SF3B1	Not significant	Yes, ($p < 0.0001$), diff = 0.1776 log2 RSEM
SF3B2	Significant at (25, 50 and 75)	Yes, ($p < 0.0001$), diff = 0.2246 log2 RSEM
SF3B3	Not significant	Yes, ($p < 0.0001$), diff = 0.5813 log2 RSEM
SF3B4	Significant at (10 and 25)	Yes, ($p < 0.0001$), diff = 0.6766 log2 RSEM
SF3B5	Not significant	Single exon gene, RNA seq. Data not reliable
SF3B6	Significant at (10 and 25)	Yes, ($p < 0.0001$), diff = 0.5643 log2 RSEM
PHF5A	Significant at (25 and 50)	Yes, ($p = 0.0236$), diff = 0.1933 log2 RSEM

Supplemental Table 3.3. *hTERT* minigene siRNA screen identifies SF3B complex as a potential telomerase inhibitor target in LUAD

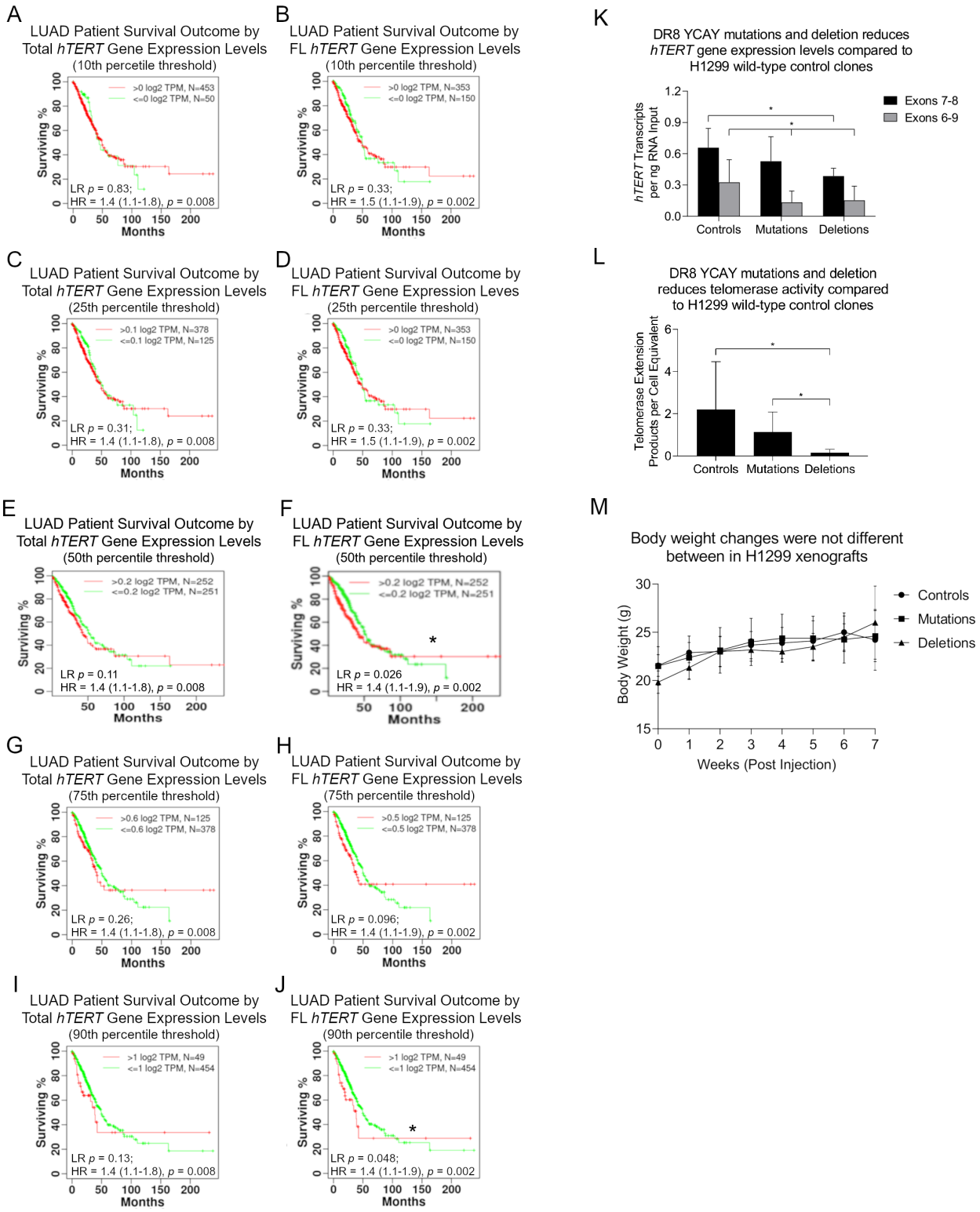

Supplemental Figure 3.1. related to Figure 3.1. Patient data indicates poor survival in lung cancers with high levels of FL *hTERT* isoform expression.

A, C, E, G and I. Gene level analysis indicates that greater total *hTERT* gene expression levels do not predict overall LUAD patient survival (10^{th}, 25^{th}, 75, and 90^{th} percentile threshold; n = 503 patients). **B, D, F, H and J.** Increased expression levels of the FL *hTERT* isoform (NM_198253) are significantly associated with lower overall survival outcomes in LUAD patients at the 90^{th} percentile threshold and tended towards significance at the 75^{th} percentile threshold. No significance was observed at the 10^{th} or 25^{th} percentile thresholds (n = 503 patients). Note: 150 patients have "0" values for *hTERT* FL from TCGA RNA-seq. data, thus the plots for B and D are the same at the 10^{th} or 25^{th} percentile thresholds. **K.** Grouped averages for *hTERT* gene expression levels in H1299 clones determined by ddPCR (n = 2 cDNAs per clonal cell line in technical triplicates). **L.** Grouped averages for telomerase activity analysis determined by ddTRAP (in technical triplicates). **M.** Body weight was not different in mice injected with H1299 control, DR8 mutation, or DR8 deletion clones throughout the seven-week post injection period. The * indicates significant ($p < 0.05$) log rank (LR) test of the Hazard ratios between high and low expression groups at different thresholds (F and J). Student's *t*-test set at $p \leq 0.05$ for significance compared to wild-type control clones; denoted by *. Data are presented as means ± standard deviations where applicable (K-M). Abbreviations: LUAD: lung adenocarcinoma.

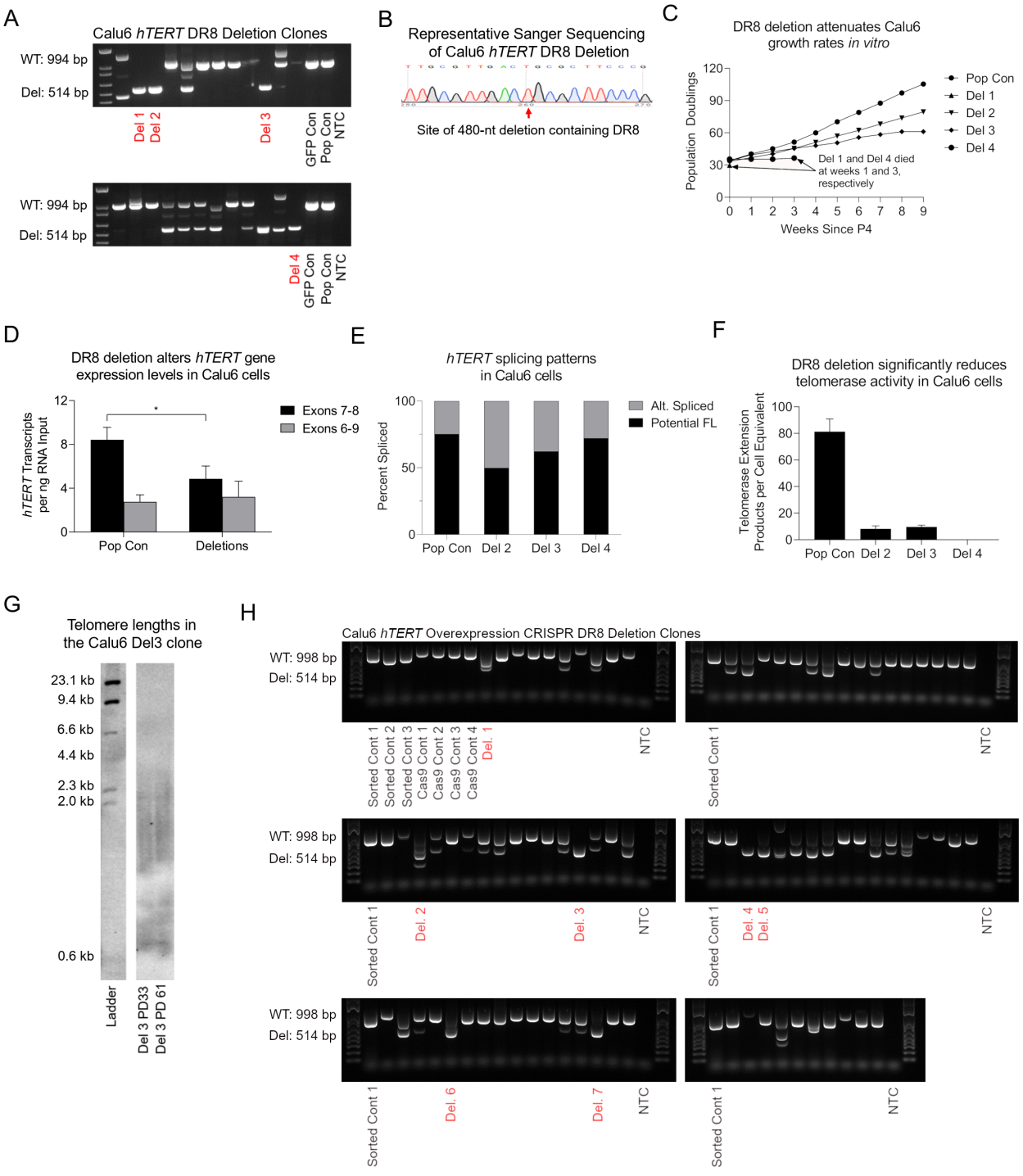

Supplemental Figure 3.2. related to Figure 3.1. Characteristics of individual Calu6 wild-type clones and Calu6 TERT overexpression clones following DR8 deletion with CRISPR/Cas9.

A. Representative agarose gel of Calu6 clones highlighting (in red) four single cell clones with complete deletion of the 480-nt sequence containing DR8. **B.** Representative Sanger sequencing confirming gel analysis of DR8 deletion. **C.** Cell growth rates were significantly attenuated in Calu6 DR8 deletion compared to wild-type control clones. DR8 deletion clones 1 and 4 died *in vitro* at weeks 1 and 3 (post passage 4), respectively. **D.** Average *hTERT* gene expression levels determined by ddPCR in Calu6 wild-type control and DR8 deletion clones (average of Del. 2, 3, and 4). **E.** *hTERT* splicing percentage analysis calculated from *hTERT* transcript levels in Calu6 wild-type control and individual DR8 deletion clones. **F.** Telomerase activity analysis determined by ddTRAP in Calu6 wild-type control and individual DR8 deletion clones. **G.** Calu6 Del. 3 clone telomere length; representative image. **H.** Representative agarose gel images of all *hTERT* overexpressing Calu6 cells CRISPR/Cas9-mediated deletion of the 480-nt sequence within intron 8 containing the DR8 *cis*-element. Highlighted lanes represent the seven successful DR8 deletions. Panels D-F: Analysis performed on 3 biological replicates derived from each clone. Student's *t*-test set at $p \leq 0.05$ for significance compared to population controls; denoted by *. Data are presented as means ± standard deviations where applicable. Abbreviations: GFP Con: green fluorescent protein control; Pop Con: Calu6 parental cells.

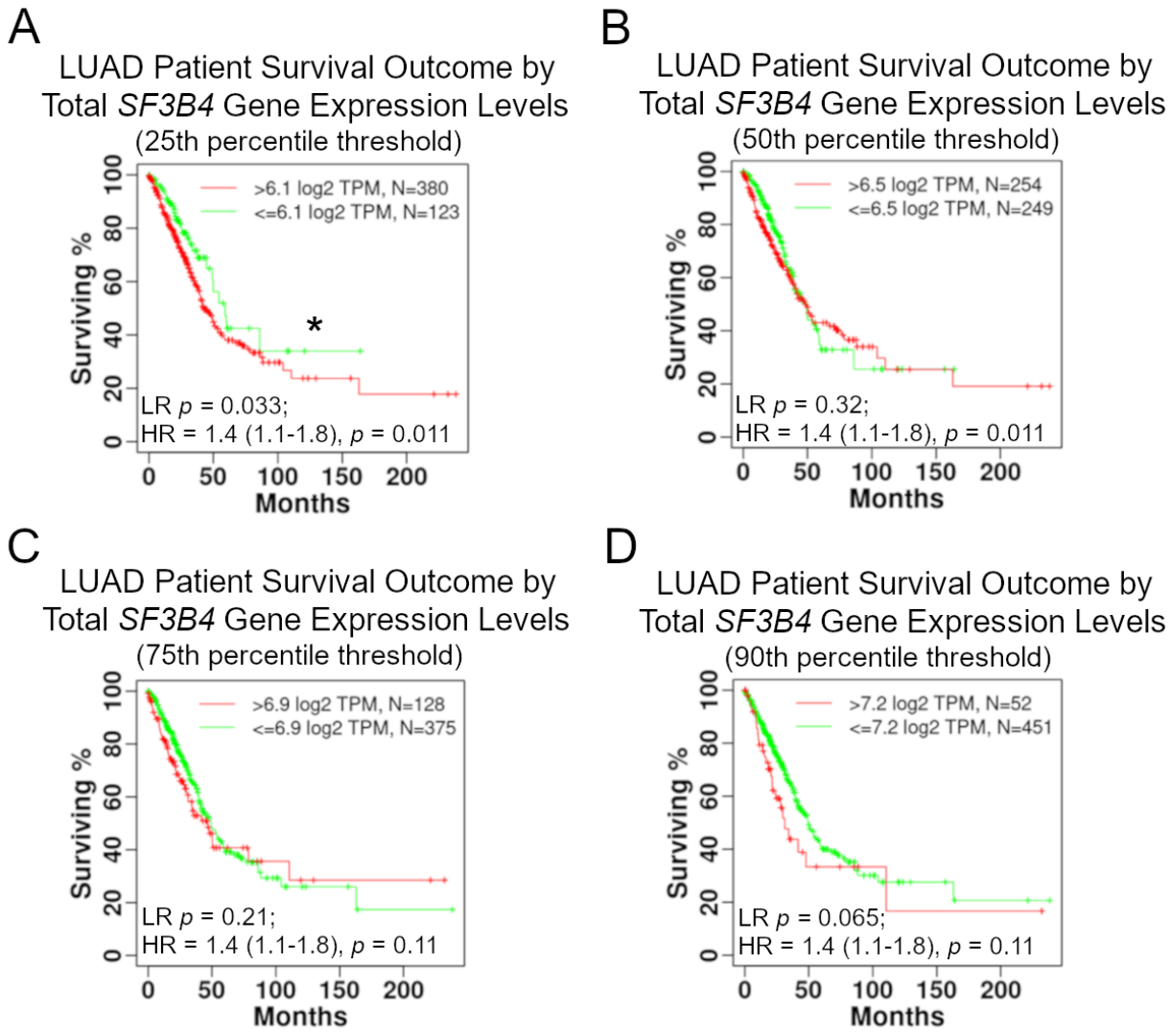

Supplemental Figure 3.3. related to Figure 3.2. Higher *SF3B4* expression in Lung cancer is related to poorer patient survival in the TCGA cohort.

A-D. Greater levels of *SF3B4* gene expression are significantly associated with lower overall survival outcomes in LUAD patients at the 25th and tended towards significance at the 90th percentile thresholds. No significance was observed at the 50th or 75th percentile thresholds. The * indicates significant (p < 0.05) log rank (LR) test of the Hazard ratios between high and low expression groups at different thresholds. Abbreviations: LUAD: lung adenocarcinoma.

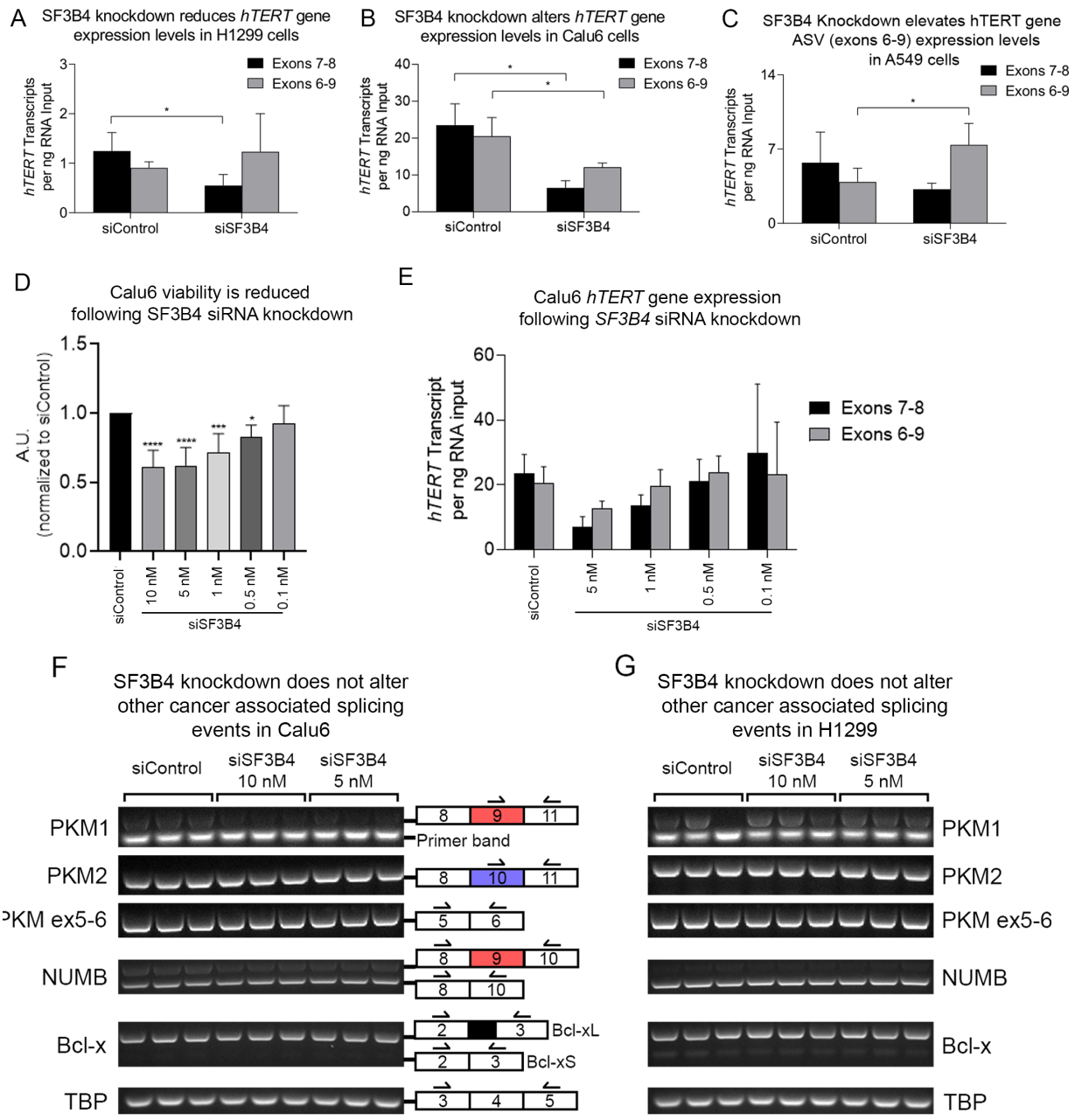

Supplemental Figure 3.4. related to Figure 3.3. SF3B4 knockdown in NSCLC cell lines.

A-C. Average *hTERT* gene expression levels following transient *SF3B4* knockdown in H1299, Calu6, and A549 NSCLC cells (determined by ddPCR in biological triplicates). **D and E.** Calu6 cells treated for 72-hours with various concentrations (10 and 5 nM) of siRNAs against either non-targeting scrambled control (siControl control was 10 nM) or SF3B4 (concentrations indicated in the Figure) to determine

viability by trypan blue staining (D) and average *hTERT* gene expression by ddPCR (E). **F and G** Splicing events linked to cancer progression are minimally altered by depletion of SF3B4 in Calu6 (F) and H1299 (G). Student's *t*-test for two group comparisons. For multiple group comparisons *p*-value was calculated using one-way ANOVA with uncorrected Fisher's LSD test compared to siControl (* $p < 0.05$; ** $p < 0.01$; *** $p < 0.001$; **** $p < 0.0001$). Data are presented as means ± standard deviations where applicable.

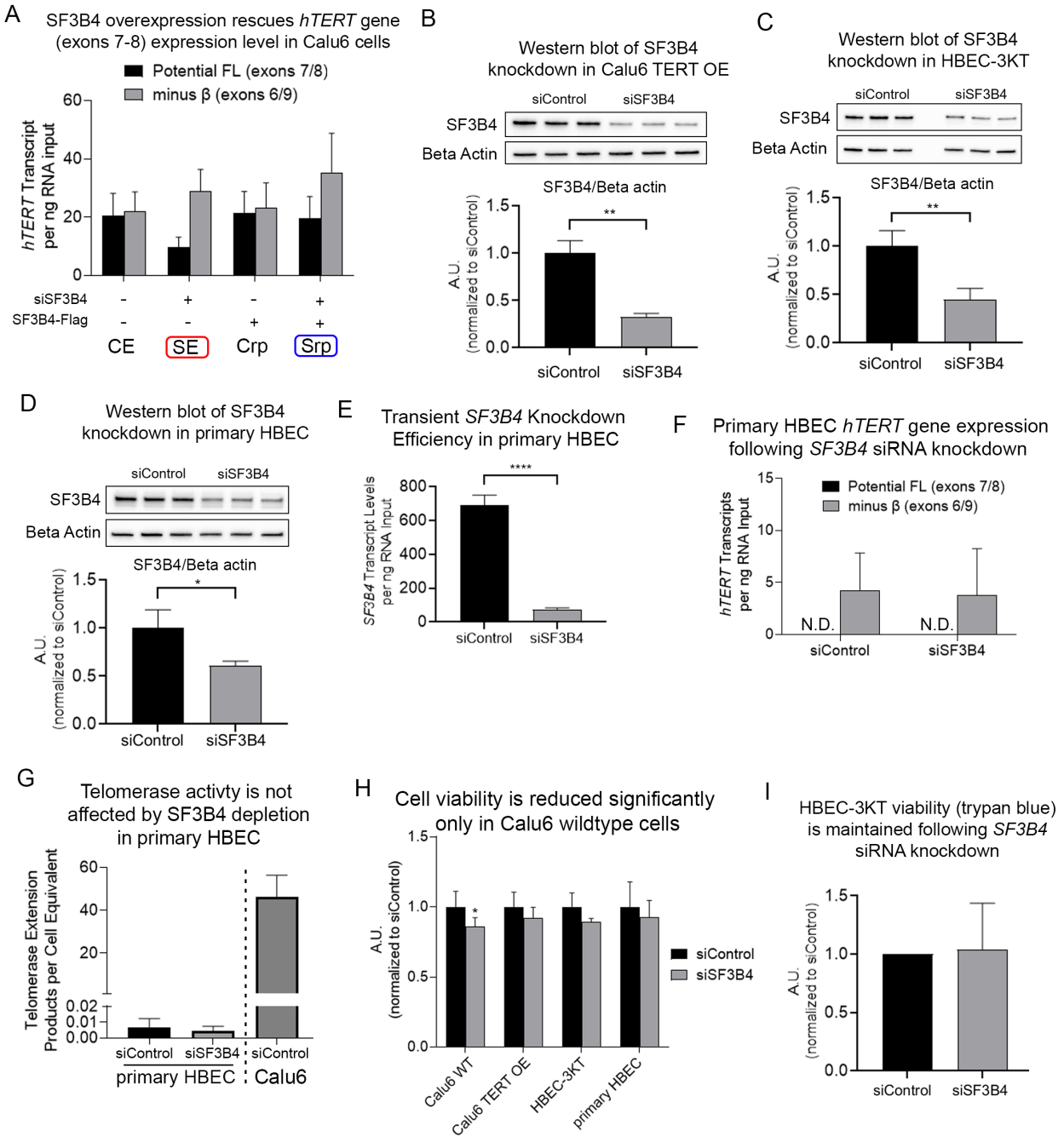

Supplemental Figure 3.5. related to Figure 3.4. SF3B4 knockdown and rescue in Calu6, and knockdown in TERT overexpression cells (Calu6 TERT OE, HBEC-3KT) and primary HBEC.

A. Transient over expression of siRNA resistant SF3B4 rescues TERT ASV (exons 7-8) level (n = 5 each condition). **B-D.** Representative western blot image and quantification (densitometry) of SF3B4 knockdown in Calu6 TERT overexpression cells (B), HBEC-3KT (C) and primary HBECs (D; n = 3

biological replicates per each cell line). **E.** SF3B4 transcripts levels measured by ddPCR in primary HBECs (n = 3 biological replicates). **F.** *hTERT* transcripts levels were determined in primary HBECs with or without SF3B4 depletion (n = 3 biological replicates). **G.** Telomerase activity was measured in primary HBECs with or without SF3B4 depletion (n = 3 biological replicates). siControl treated Calu6 data from Figure 3C is shown for comparison. **H.** Only Calu6 wild-type shows statistically significant reduction of cell viability in SF3B4 depleted condition (each cell line n = 4 biological replicates, siRNA treatments for 72-hours). **I.** HBEC-3KT viability following treatment siRNAs against either non-targeting scrambled control (siControl) or SF3B4 as measured by trypan blue staining. Student's *t*-test for two group comparisons (C-K; * $p < 0.05$; ** $p < 0.01$; **** $p < 0.0001$). For multiple group comparisons (A) p-value was calculated using one-way ANOVA with Tukey's multiple comparison test compared to every other condition. Data are presented as means ± standard deviations where applicable. Abbreviations: CE: siControl + Empty control vector; SE: siSF3B4 + Empty control vector; Crp: siControl + SF3B4-Flag plasmid; Srp: siSF3B4 + SF3B4-Flag plasmid; Calu6 WT: Calu6 wild-type cell line; Calu6 TERT OE: Calu6 TERT Over expression cell line; N.D.: Not Detected.

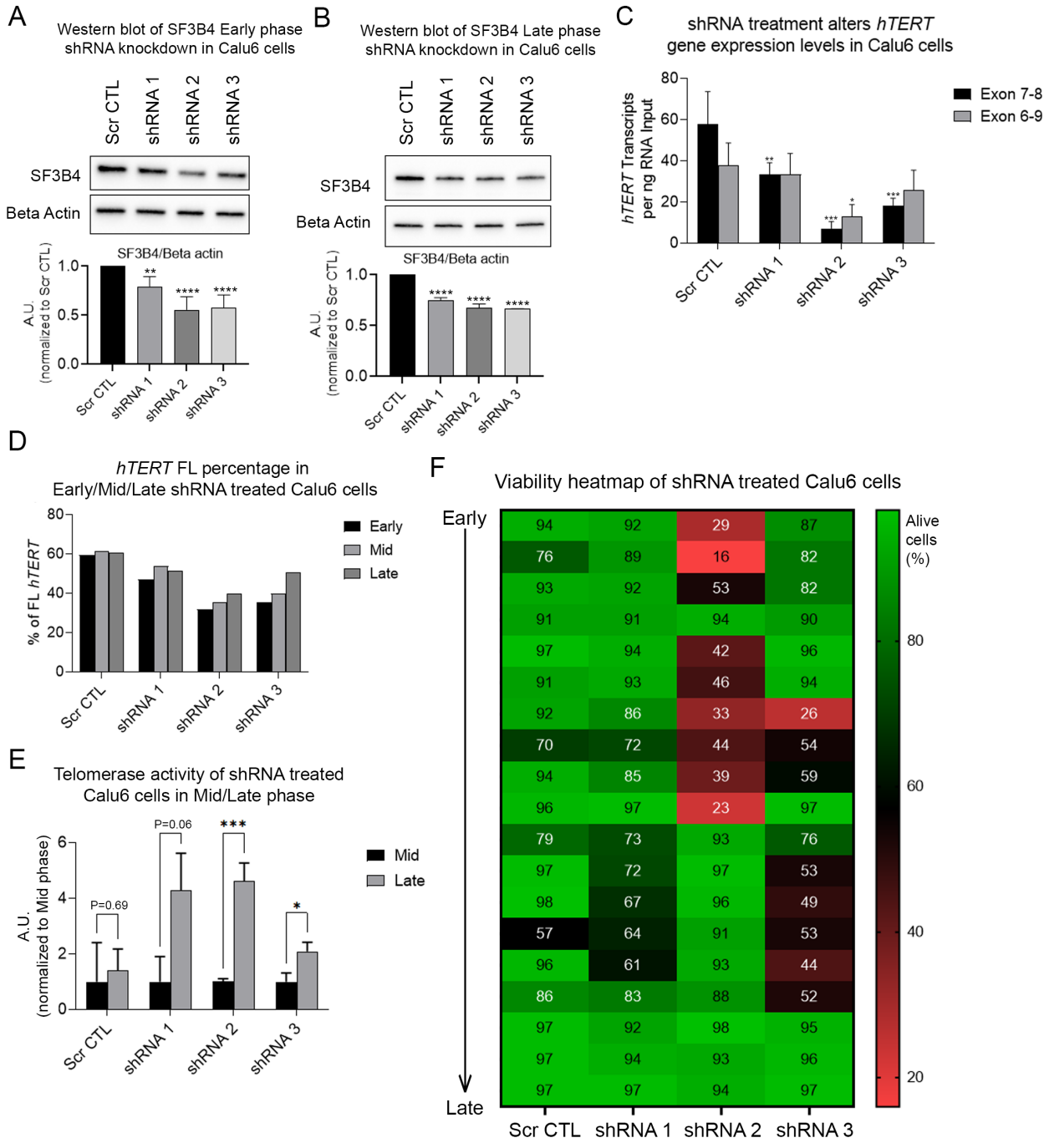

Supplemental Figure 3.6. related to Figure 3.5. SF3B4 depletion using short hairpin RNA (shRNA) in Calu6 cells.

A. Western blot of SF3B4 and beta actin early phase cells (n = 9 for each condition). **B.** Western blot of SF3B4 and beta actin late phase cells (n = 3 for each condition). **C.** Average *hTERT* gene expression

levels following stable *SF3B4* knockdown in Calu6 NSCLC cells (determined by ddPCR; n = 3 in biological triplicates). **D.** *hTERT* FL percentage graphed for early, middle (mid), and late phase cells. **E.** Telomerase activity re-graphed for middle (mid) and late phase cells. **F.** Viability heatmap determined by trypan blue staining of shRNA cells throughout the experiment. Student's *t*-test for two group comparisons. For multiple group comparisons (A-C) *p*-value was calculated using one-way ANOVA with uncorrected Fisher's LSD test compared to Scr CTL (Scramble control); * $p < 0.05$; ** $p < 0.01$; *** $p < 0.001$; **** $p < 0.0001$). Data are presented as means ± standard deviations where applicable.

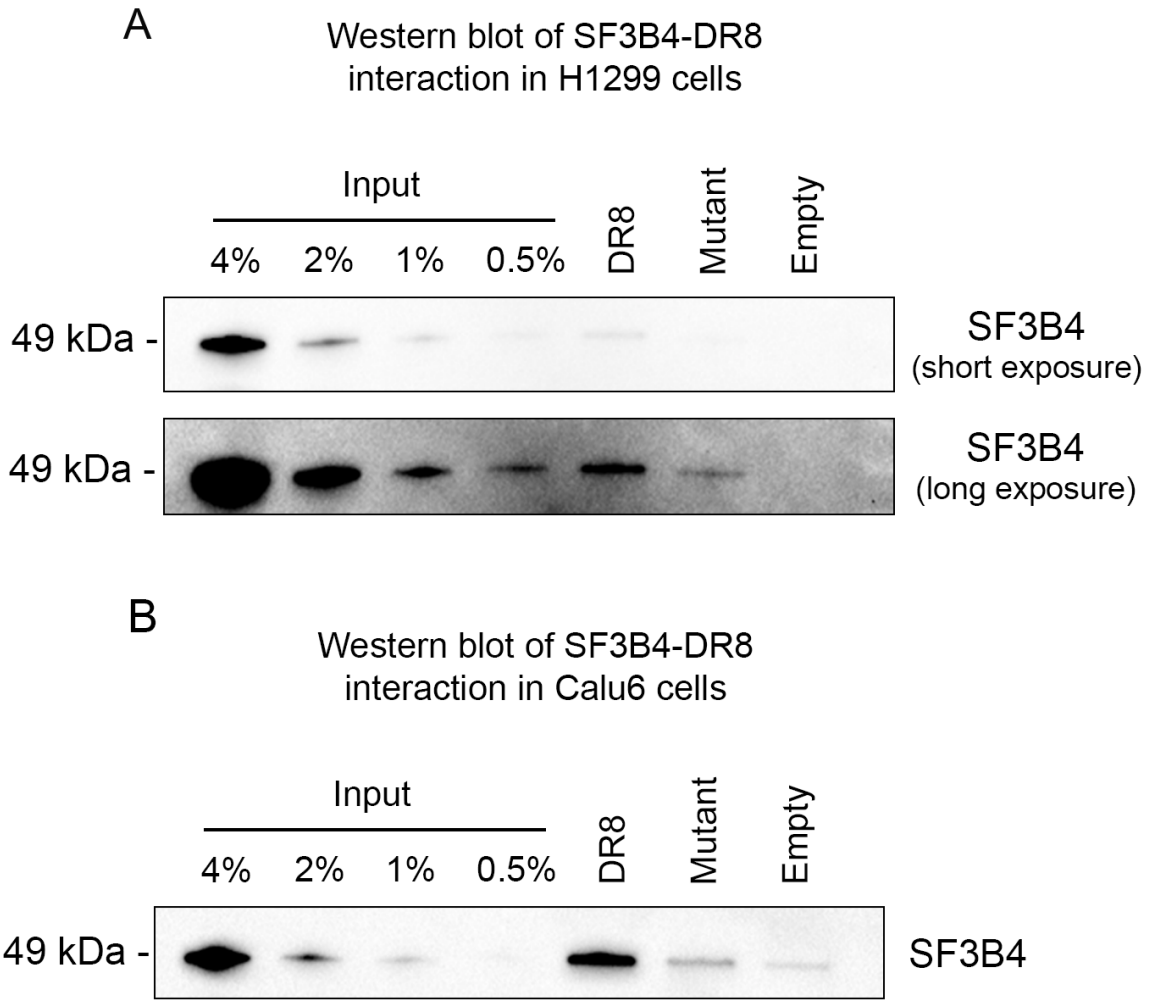

Supplemental Figure 3.7. related to Figure 3.6. RNA pulldown assay in Calu6 and H1299 cells.

A. RNA affinity western blot of SF3B4 enrichment in H1299 cells. Various lysate input percentages were compared against DR8, mutant, and empty beads. **B.** RNA affinity western blot of SF3B4 enrichment in Calu6 cells. Various lysate input percentages were compared against DR8, mutant, and empty beads.

Appendix B - Supplemental Data for Chapter 4

Green (SFs potentially promote FL)
SFs that have positive correlation with potential FL TERT in iPSC ($p < 0.05$)
SFs that increase exon 7/8 skipping more than 2-fold when KD in HeLa
SFs that are upregulated significantly in LUAD

Red (SFs potentially promote minus beta)
SFs that have negative correlation with potential FL TERT in iPSC ($p < 0.05$)
SFs that decrease exon 7/8 skipping more than 2-fold when KD in HeLa
SFs that are downregulated significantly in LUAD

Splicing Factors	iPSC density	Minigene in HeLa	LUAD patients data of TCGA	Type
hnRNP-CL1	P <0.05	x	NS	1
hnRNP-H1	P < 0.01	x	NS	1
SRPK1	P < 0.01	x	Up in LUAD	2
hnRNP-A2B1	P < 0.01	x	Up in LUAD	2
hnRNP-M	P < 0.01	Promote -beta	NS	3
SRSF2	P < 0.01	Promote FL	Up in LUAD	4
U2AF2	NS	Promote FL	Up in LUAD	5
hnRNP-A1	NS	Promote -beta	Up in LUAD	6
CDC40	NS	Promote FL	NS	7

Supplemental Table 4.1. Summary of SFs from three different approaches.

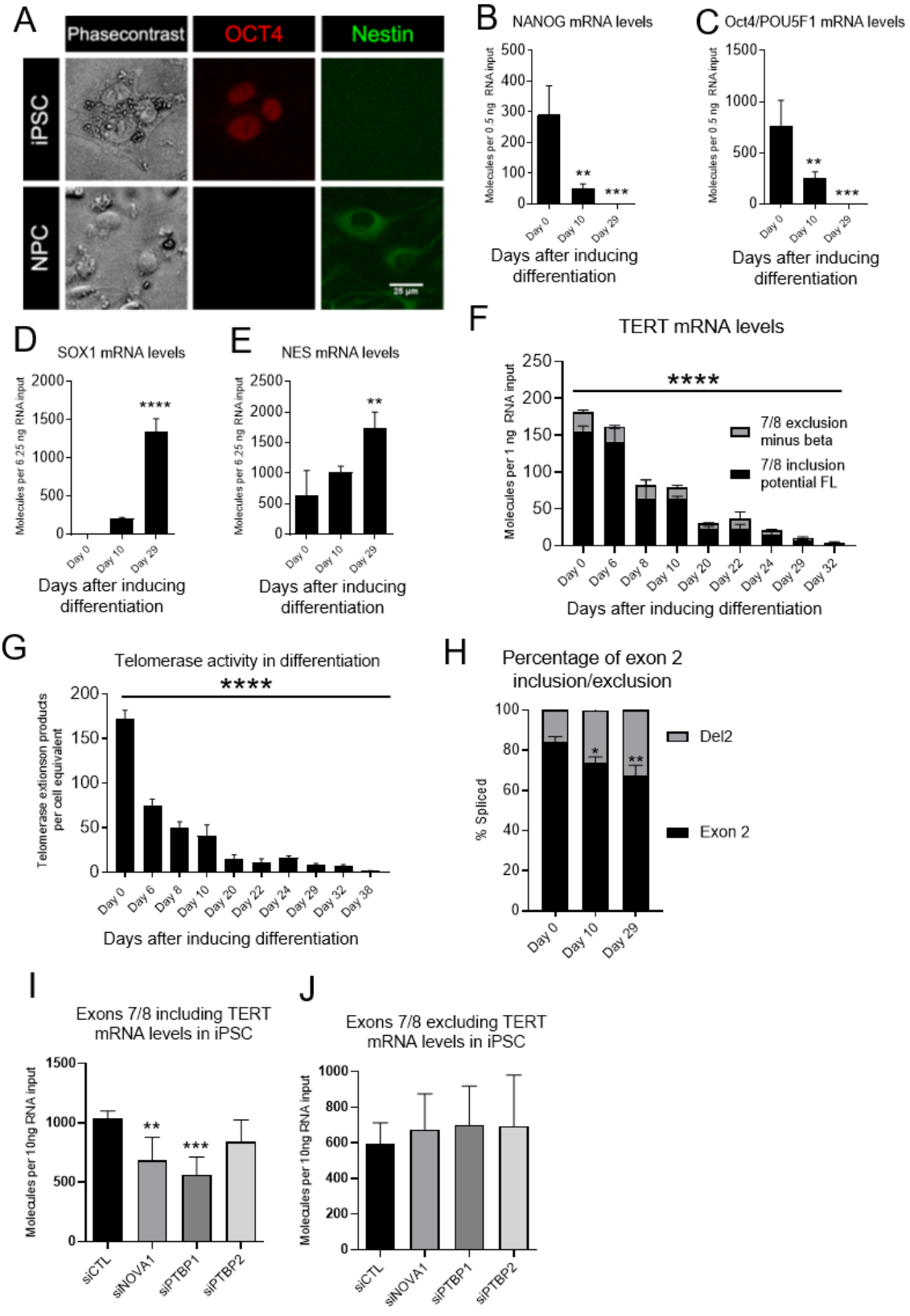

Supplemental Figure 4.1.

A Representative phase contrast and fluorescent microscopy images support iPSC differentiation into NPC. **B-E** mRNA expression levels of stem cell pluripotency markers (B,C) and NPC markers (D,E) support iPSC differentiation into NPC (determined by ddPCR; n = 3 biological replicates per condition). **F** mRNA expression level of potential FL *TERT* (exons 7/8 inclusion) and minus beta (exons 7/8 exclusion) were measured in differentiation (determined by ddPCR; n = 3 biological replicates per condition). **G** Reduction of telomerase activity in differentiation (determined by ddTRAP; n = 3 biological replicates per condition). **H** Del 2 *TERT* (exon 2 exclusion) isoform expression during differentiation increased compared to iPSCs (day 0) (determined by ddPCR; n = 3 biological replicates per condition). **I** and **J** Average *TERT* gene expression levels determined by ddPCR (n = 6 biological replicates per condition) in siRNA treated iPSC. Exons 7/8 including *TERT* (potential FL; I) and exons 7/8 excluding *TERT* (minus beta; J) isoforms were measured. One-way ANOVA with uncorrected Fisher LSD for post hoc comparisons were used to compare Day 10 and Day 29 with Day 0 (B-E, H; *, $P < 0.05$; **, $P < 0.01$; ***, $P < 0.001$; ****, $P < 0.0001$). For F and G, only One-way ANOVA was performed on the number of total *TERT* transcripts including/excluding exons 7/8 (F) and telomerase activity (G). One-way ANOVA with uncorrected Fisher LSD for post hoc comparisons were used to compare siRNA-treated conditions with siControl (I and J; **, $P < 0.01$; ***, $P < 0.001$). Data are presented as means ± standard deviations where applicable.

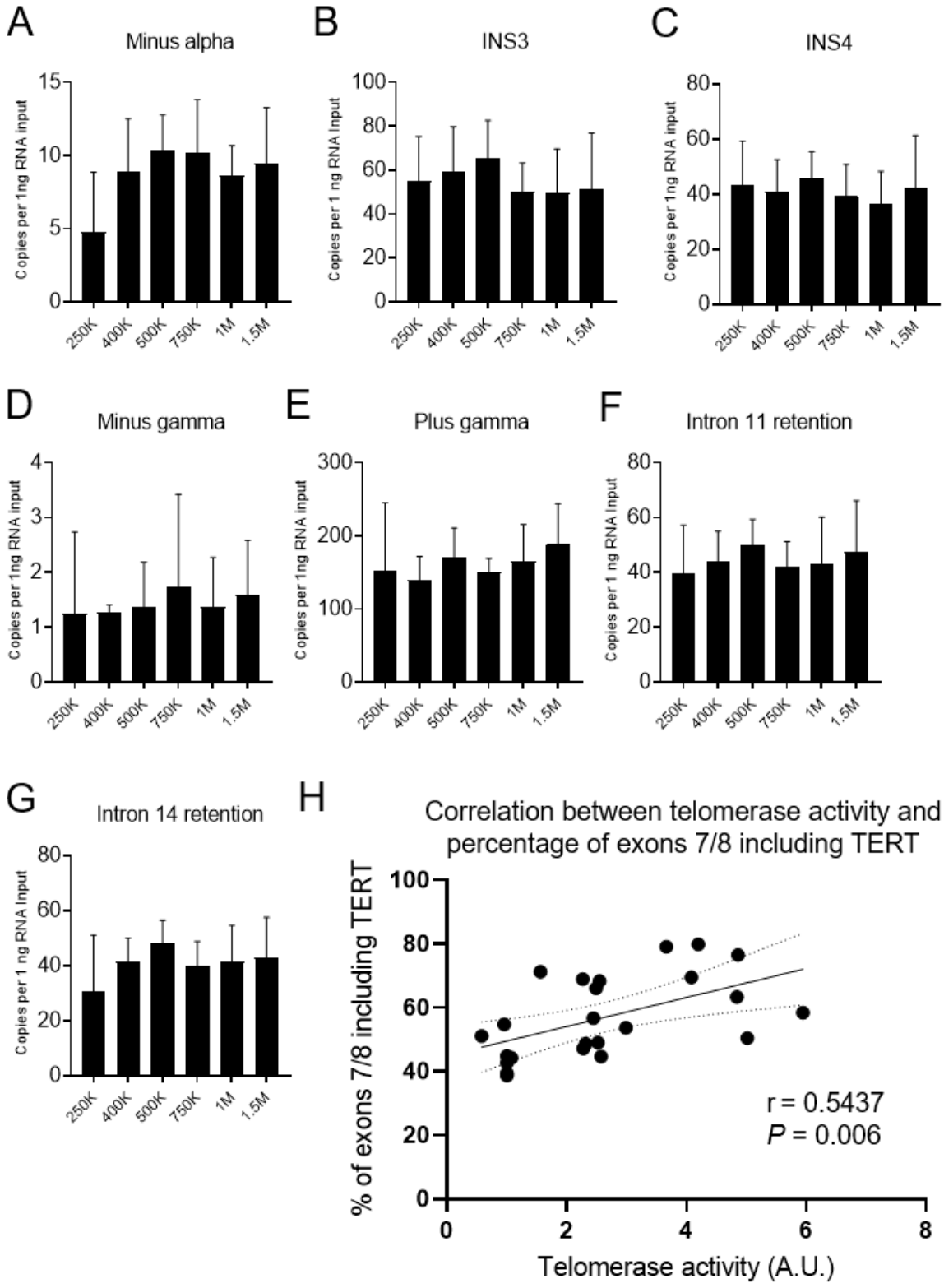

Supplemental Figure 4.2.

A-G Average *TERT* mRNA variant expression levels determined by ddPCR. minus alpha (A), INS3 (B), INS4 (C), minus gamma (D), plus gamma (E), intron 11 retention (F), and intron 14 retention (G) transcripts were quantified (determined by ddPCR; n = 4 biological replicates per condition). **H** Pearson correlation analysis shows that changes of telomerase activity and ratio of exons 7/8 inclusion (potential FL) by iPSC cell density are positively and significantly correlated. 95% Confidence bands, Pearson's correlation coefficient (r) and p value are shown. One-way ANOVA was performed to compare total amount of *TERT* mRNA variants from all conditions, but none of them had significantly different expression (A-G). For correlation analysis, 24 data points are included (H; six conditions x four replicates). Data are presented as means ± standard deviations where applicable.

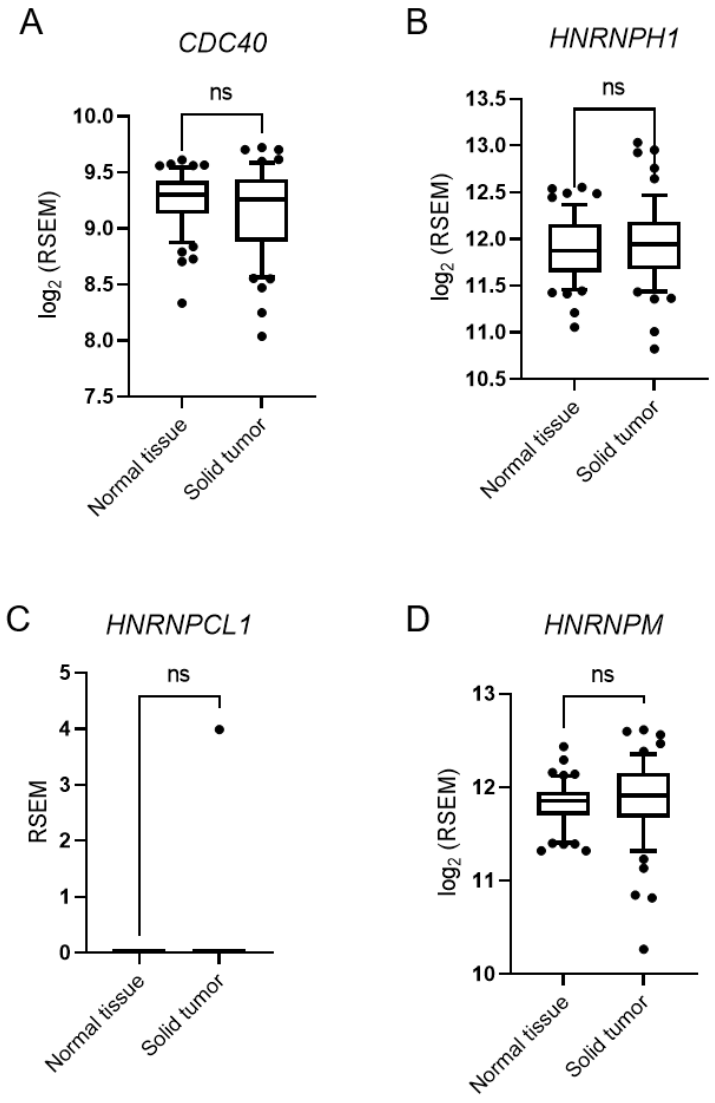

Supplemental Figure 4.3.

A-D Log2-transformed (A,B, and D) or raw (C) RSEM values of SFs gene-expression levels (n = 58 matched patient samples). CDC40 (A), HNRNPH1 (B), HNRNPCL1 (C), and HNRNPM (D) are not significantly differentially expressed in tumor tissue from LUAD patients. HNRNPCL1 was detected in only one sample out of 116 samples (C; 58 tumors and 58 normal tissue). Student t test set at $P \leq 0.05$ for significance compared with normal tissue controls (all $P > 0.05$). In the box plots, the lower boundary of the box indicates the 25 th percentile, a line within the box marks the median and the higher boundary of the box indicates the 75 th percentile. Whiskers above and below the box indicate the 10 th and 90 th percentiles. Points above and below the whiskers indicate outliers outside the 10 th and 90 th percentiles.

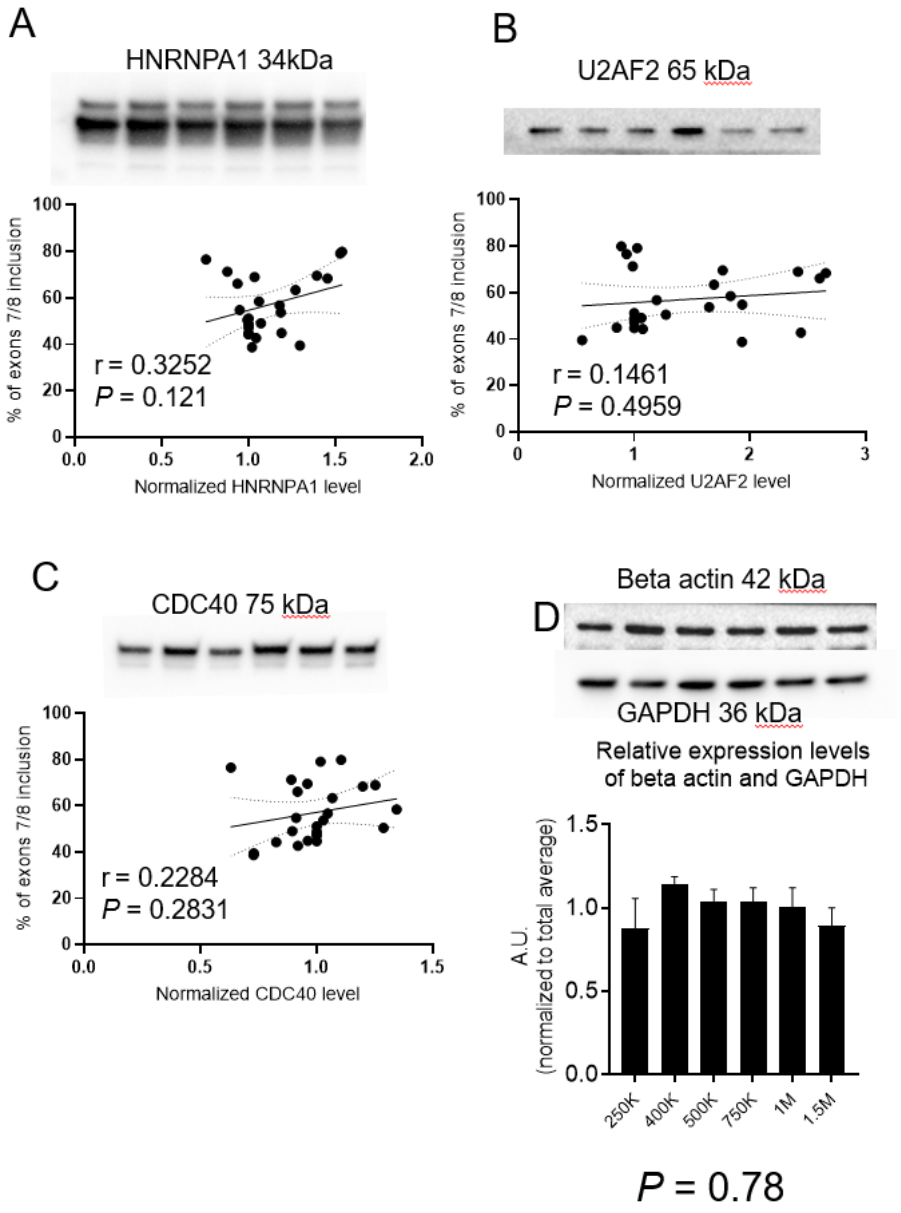

Supplemental Figure 4.4.

A-C Western blot of splicing factors and correlation analyses in different iPSC density. Top are representative images and bottoms are scatter plots showing correlation. 95% Confidence bands, Pearson's correlation coefficient (r) and p value are shown. Antibodies targeting HNRNPA1 (A), U2AF2 (B), CDC40 (C), and beta actin or GAPDH (D; loading control) were used for western blot (n = 4 biological replicates per condition). Pearson's linear correlational analysis was performed between splicing factors and *TERT* exons 7/8 inclusion expression percentage of total *TERT*. **D**, Western blot of beta actin and

GAPDH used for normalization of target genes. Bottom panel shows quantifications of beta actin and GAPDH normalized by average of six conditions (D). Statistical significance was not found by one-way analysis of variance (ANOVA) comparing all conditions (D; $P = 0.78$). Data are presented as means ± standard deviations where applicable. For correlation analysis, 24 data points are included (A-C; six conditions x four replicates).

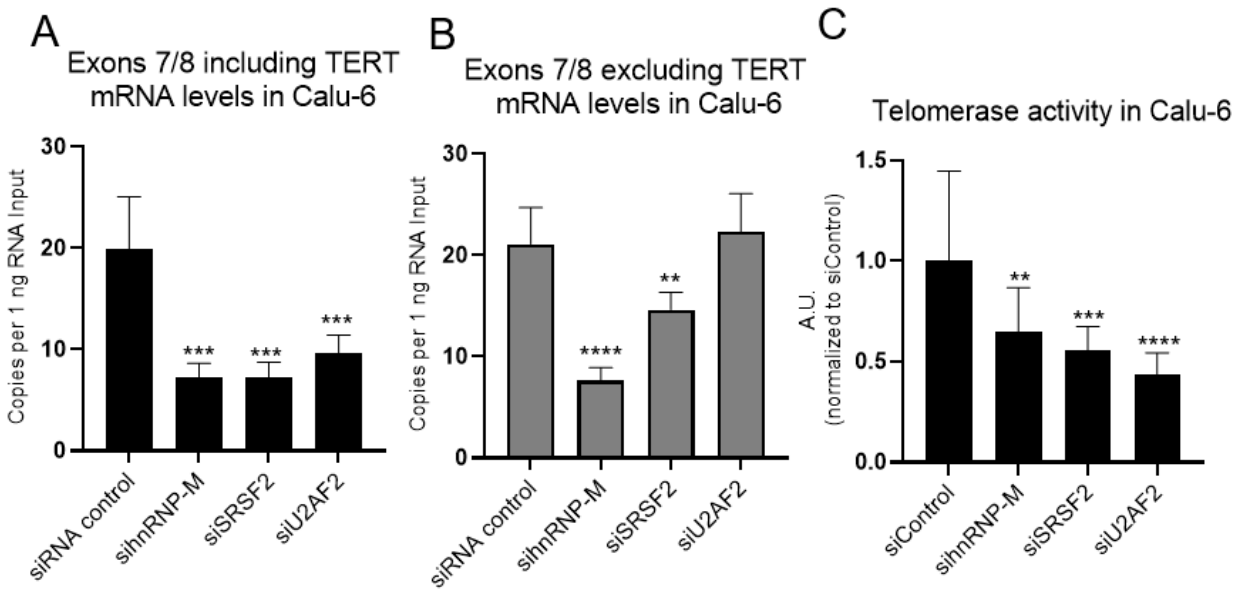

Supplemental Figure 4.5.

A-B the expression of *TERT* transcripts with exons 7/8 (potential FL; A) and without exons 7/8 (minus beta; B) were measured after knockdown using siRNAs (determined by ddPCR; n = 6 biological replicates per condition). **C**, Telomerase activity was reduced by all siRNA treatment (determined by ddTRAP; n = 6 biological replicates per condition). One-way ANOVA with uncorrected Fisher LSD for post hoc comparisons of siRNA treatments were used to compare siRNA-treated conditions with siControl (A-C; **, $P < 0.01$; ***, $P < 0.001$; ****, $P < 0.0001$). Data are presented as means ± standard deviations where applicable.

Appendix C - Supplemental Data for Chapter 5

Supplemental Table 5.1. Post hoc comparisons for Table 5.2.

	Tukey's multiple comparisons test	Predicted (LS) mean diff.	95.00% CI of diff.	Summary	Adjusted P Value
Absolute amount of total *hTERT*	Young vs. Middle-aged	3.388	2.102 to 4.673	****	<0.0001
	Young vs. Old	3.651	2.365 to 4.936	****	<0.0001
	Middle-aged vs. Old	0.2630	-1.204 to 1.730	ns	0.8963
Absolute amount of potential FL *hTERT*	Young vs. Middle-aged	1.863	1.095 to 2.630	****	<0.0001
	Young vs. Old	1.922	1.154 to 2.689	****	<0.0001
	Middle-aged vs. Old	0.05900	-0.8170 to 0.9350	ns	0.9846
Absolute amount of minus beta *hTERT*	Young:Sedentary vs. Young:Exercise	1.084	0.2475 to 1.920	**	0.0060
	Young:Sedentary vs. Middle-aged:Sedentary	1.984	0.9943 to 2.974	****	<0.0001
	Young:Sedentary vs. Middle-aged:Exercise	2.150	1.160 to 3.140	****	<0.0001
	Young:Sedentary vs. Old:Sedentary	2.270	1.280 to 3.260	****	<0.0001
	Young:Sedentary vs. Old:Exercise	2.272	1.282 to 3.262	****	<0.0001
	Young:Exercise vs. Middle-aged:Sedentary	0.9000	-0.1130 to 1.913	ns	0.1026
	Young:Exercise vs. Middle-aged:Exercise	1.066	0.05299 to 2.079	*	0.0350
	Young:Exercise vs. Old:Sedentary	1.186	0.1730 to 2.199	*	0.0151
	Young:Exercise vs. Old:Exercise	1.188	0.1750 to 2.201	*	0.0149
	Middle-aged:Sedentary vs. Middle-aged:Exercise	0.1660	-0.9768 to 1.309	ns	0.9975
	Middle-aged:Sedentary vs. Old:Sedentary	0.2860	-0.8568 to 1.429	ns	0.9699
	Middle-aged:Sedentary vs. Old:Exercise	0.2880	-0.8548 to 1.431	ns	0.9690
	Middle-aged:Exercise vs. Old:Sedentary	0.1200	-1.023 to 1.263	ns	0.9995
	Middle-aged:Exercise vs. Old:Exercise	0.1220	-1.021 to 1.265	ns	0.9994
	Old:Sedentary vs. Old:Exercise	0.002000	-1.141 to 1.145	ns	>0.9999

Ratio of exons 7-8 splicing	Young:Sedentary vs. Young:Exercise	-4.902	-14.61 to 4.802	ns	0.6327
	Young:Sedentary vs. Middle-aged:Sedentary	3.466	-8.015 to 14.95	ns	0.9348
	Young:Sedentary vs. Middle-aged:Exercise	-5.710	-17.19 to 5.771	ns	0.6474
	Young:Sedentary vs. Old:Sedentary	-12.25	-23.73 to -0.7704	*	0.0316
	Young:Sedentary vs. Old:Exercise	-5.803	-17.28 to 5.678	ns	0.6321
	Young:Exercise vs. Middle-aged:Sedentary	8.368	-3.384 to 20.12	ns	0.2753
	Young:Exercise vs. Middle-aged:Exercise	-0.8084	-12.56 to 10.94	ns	>0.9999
	Young:Exercise vs. Old:Sedentary	-7.350	-19.10 to 4.402	ns	0.4098
	Young:Exercise vs. Old:Exercise	-0.9016	-12.65 to 10.85	ns	0.9999
	Middle-aged:Sedentary vs. Middle-aged:Exercise	-9.176	-22.43 to 4.081	ns	0.3034
	Middle-aged:Sedentary vs. Old:Sedentary	-15.72	-28.97 to -2.460	*	0.0135
	Middle-aged:Sedentary vs. Old:Exercise	-9.269	-22.53 to 3.988	ns	0.2933
	Middle-aged:Exercise vs. Old:Sedentary	-6.541	-19.80 to 6.716	ns	0.6549
	Middle-aged:Exercise vs. Old:Exercise	-0.09315	-13.35 to 13.16	ns	>0.9999
	Old:Sedentary vs. Old:Exercise	6.448	-6.809 to 19.71	ns	0.6680

Note : p-values are calculated by Tukey's multiple comparisons

Appendix D - Supplemental Data for Chapter 6

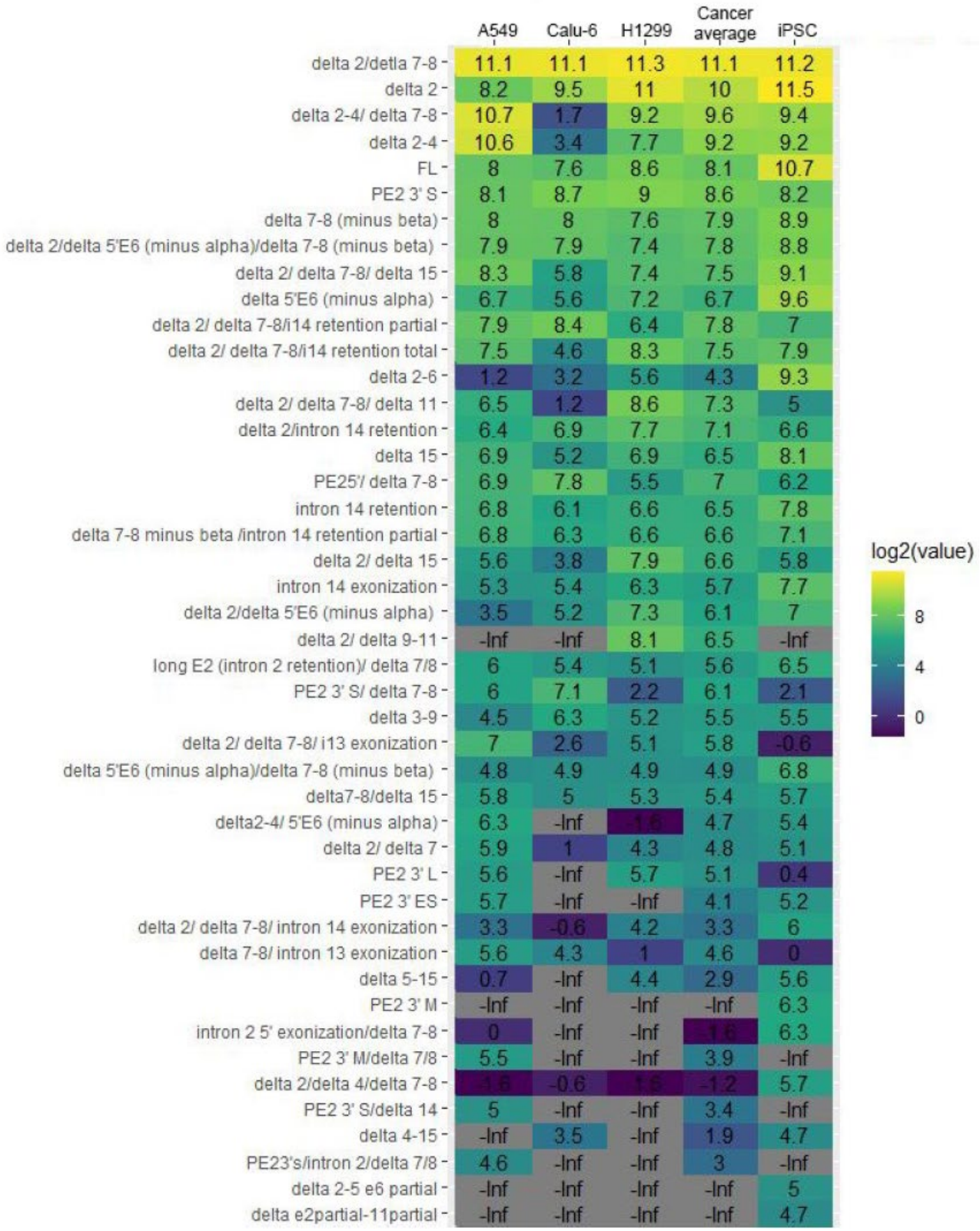

Supplemental Figure 6.1. Heatmap of 45 *TERT* mRNA variants.

Transcript Name	ORF	Premature stop codon	Novelty	Transcript model
delta 2; delta 7-8	291 bp	In exon 3	Known	
delta 2	291 bp	In exon 3	Known (Del2)	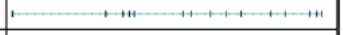
delta 2-4; delta 7-8	693 bp	In exon 10	Novel	
delta 2-4	1671 bp	In-frame	Novel	
FL	3405 bp	In-frame	Known	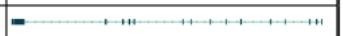
PE2 3' S	636 bp	In exon 3	Novel	
delta 7-8	2013 bp	In exon 5	Known (-β)	
delta 2; delta 5'E6; delta 7-8	291 bp	In exon 3	Known	
delta 2; delta 7-8; delta 15	291 bp	In exon 3	Novel	
delta 5'E6	3273 bp	In-frame	Known (-α)	
delta 2; delta 7-8; i14 ret part	291 bp	In exon 3	Novel	
delta 2; delta 7-8; i14 ret tot	291 bp	In exon 3	Novel	
delta 2-6	1368 bp	In-frame	Novel	
delta 2; delta 7-8; delta 11	291 bp	In exon 3	Known	
delta 2; i14 ret part	291 bp	In exon 3	Known	
delta 15	3261 bp	In-frame	Novel	
PE2 5'; delta 7-8	450 bp	In exon 3	Novel	
i14 retention	3291 bp	In retained intron 14	Novel	
delta 7-8; i14 ret part	2424 bp	In exon 10	Novel	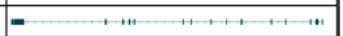
delta 2; delta 15	291 bp	In exon 3	Novel	
i14 exonization	3483 bp	In-frame	Known	
delta 2; delta 5'E6	291 bp	In exon 3	Known	
delta 2; delta 9-12	291 bp	In exon 3	Novel	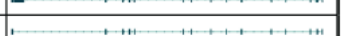
long E2 (i2 ret); delta 7-8	1725 bp	In retained intron 2	Known	
PE2 3'S; delta 7-8	264 bp	In exon 2	Novel	
delta 3-8	1725 bp	In exon 10	Novel	
delta 2; delta 7-8; i13 exon	291 bp	In exon 3	Novel	
delta 5'E6; delta 7-8	2388 bp	In exon 10	Known	
delta 7-8; delta 15	2424 bp	In exon 10	Novel	
delta 2-4; 5'E6	1650 bp	In-frame	Novel	
delta 2; delta 8	291 bp	In exon 3	Novel	
PE2 3'L	171 bp	In exon 2	Novel	
PE2 3' ES	2202 bp	In-frame	Novel	
delta 2; delta 7-8; i14 exon	291 bp	In exon 3	Known	
delta 7-8; i13 exon	2424 bp	In exon 10	Novel	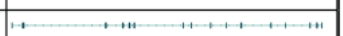
delta 5-15	1920 bp	In-frame	Novel	
PE2 3' M	279 bp	In exon 2	Novel	
i2 5' exon; delta 7-8	153 bp	In retained intron 2	Novel	
PE2 3'M; delta 7-8	828 bp	In exon 3	Novel	
delta 2; delta 4; delta 7-8	291 bp	In exon 3	Novel	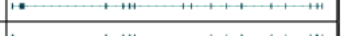
PE2 3'S; delta 15	594 bp	In exon 3	Novel	
delta 4-15	1806 bp	In-frame	Novel	
PE2 3'S; i2; delta 7-8	282 bp	In retained intron 2	Novel	
delta 2-5; E6 part	282 bp	In exon 8	Novel	
delta E2-E11 part	1632 bp	In-frame	Novel	

Supplemental Figure 6.2. Characteristics of 45 *TERT* mRNA variants.

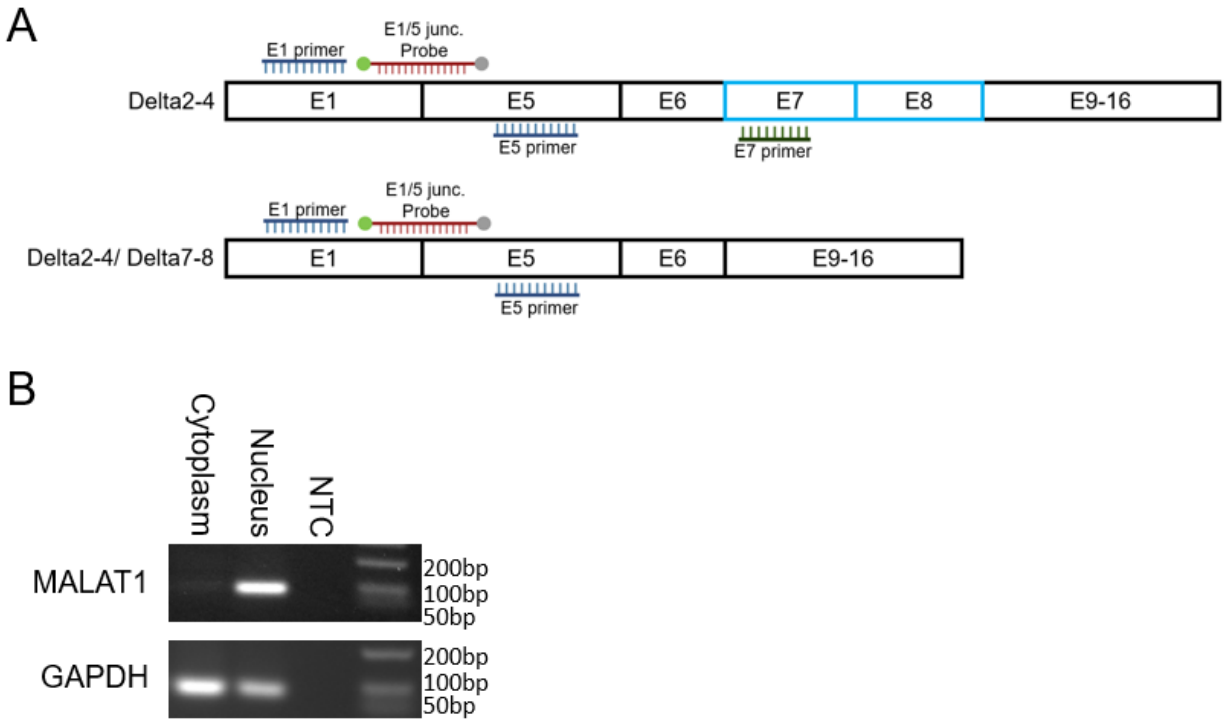

Supplemental Figure 6.3. delta 2-4 ddPCR assays and validation of cytoplasm and nucleus fractionation.

A. Two assays are shown. One assay uses E1 primer (*TERT* Exon 1 targeting primer), E5 primer (*TERT* Exon 5 targeting primer), and E1/5 junc. probe (*TERT* exons 1/5 junction targeting probe) to measure total *TERT* (Delta 2-4 and delta 2-4/ delta 7-8). The other assay uses E1 primer, E7 primer (*TERT* exon 7 targeting primer), and E1/5 junc. probe to measure only Delta 2-4. **B**. To validate cytoplasm and nucleus fractionation, gel based RT-PCR was performed to target MALAT1 or GAPDH.

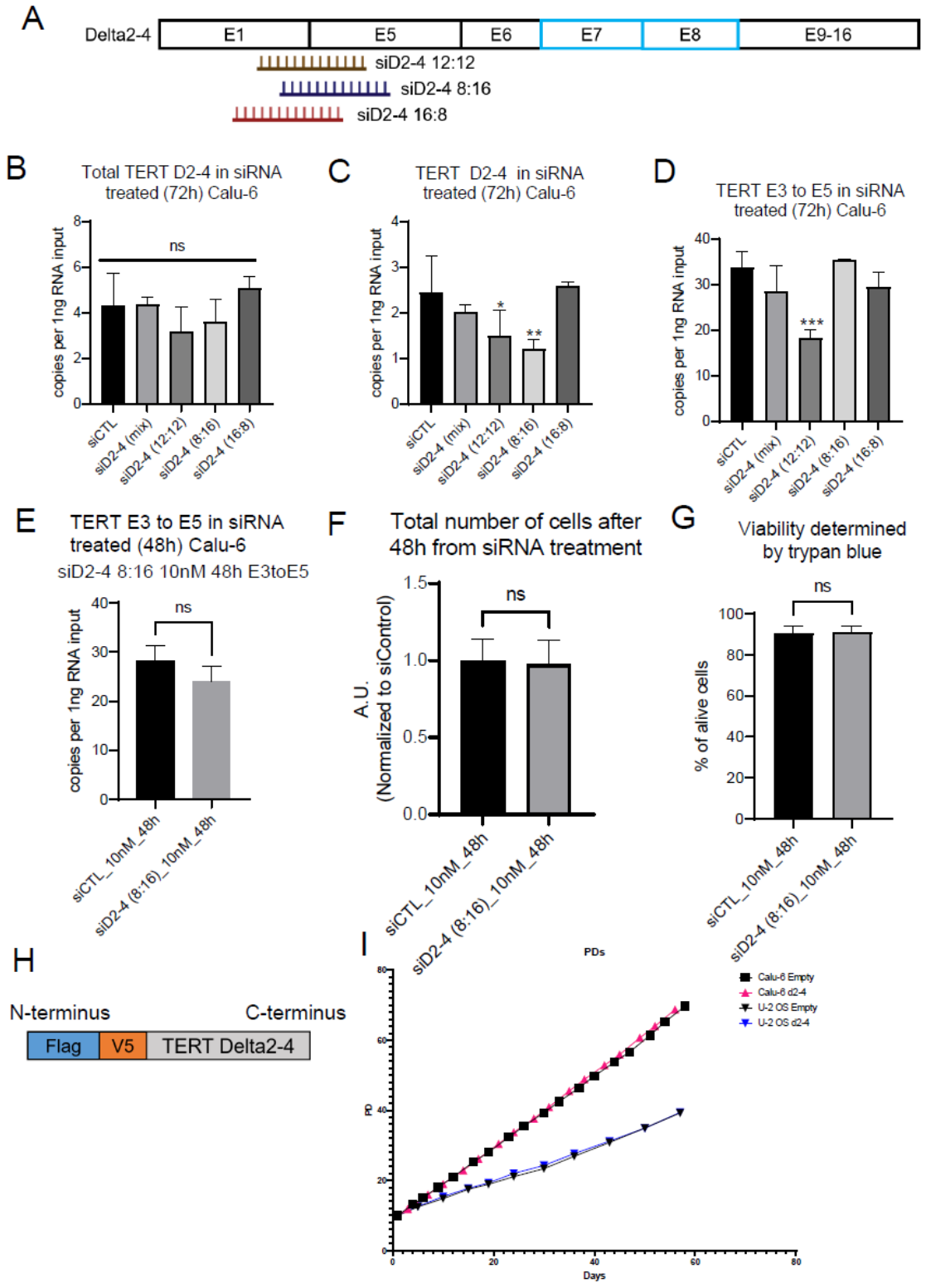

Supplemental Figure 6.4. related to Figure 6.2.

A. Three siRNAs targeting *TERT* exon 1/5 junction are shown. (**B-D**) Expression levels of total delta 2-4 *TERT* (B), Delta 2-4 (C), and *TERT* transcripts with exons 3 to 5 following 72 hours of siRNA treatment (n = 3; measured by ddPCR). (**E-G**) Expression levels of *TERT* transcript exons 3 to 5 (E), total number of cells (F), and viability determined by trypan blue (G) were determined following 48 hours of siRNA treatment targeting Delta 2-4 (n = 6). **H**. Cartoon of codon optimized Delta 2-4 with Flag and V5 tags on N-terminus. I. Growth curve showing no difference in growth rate with overexpression of Delta 2-4.

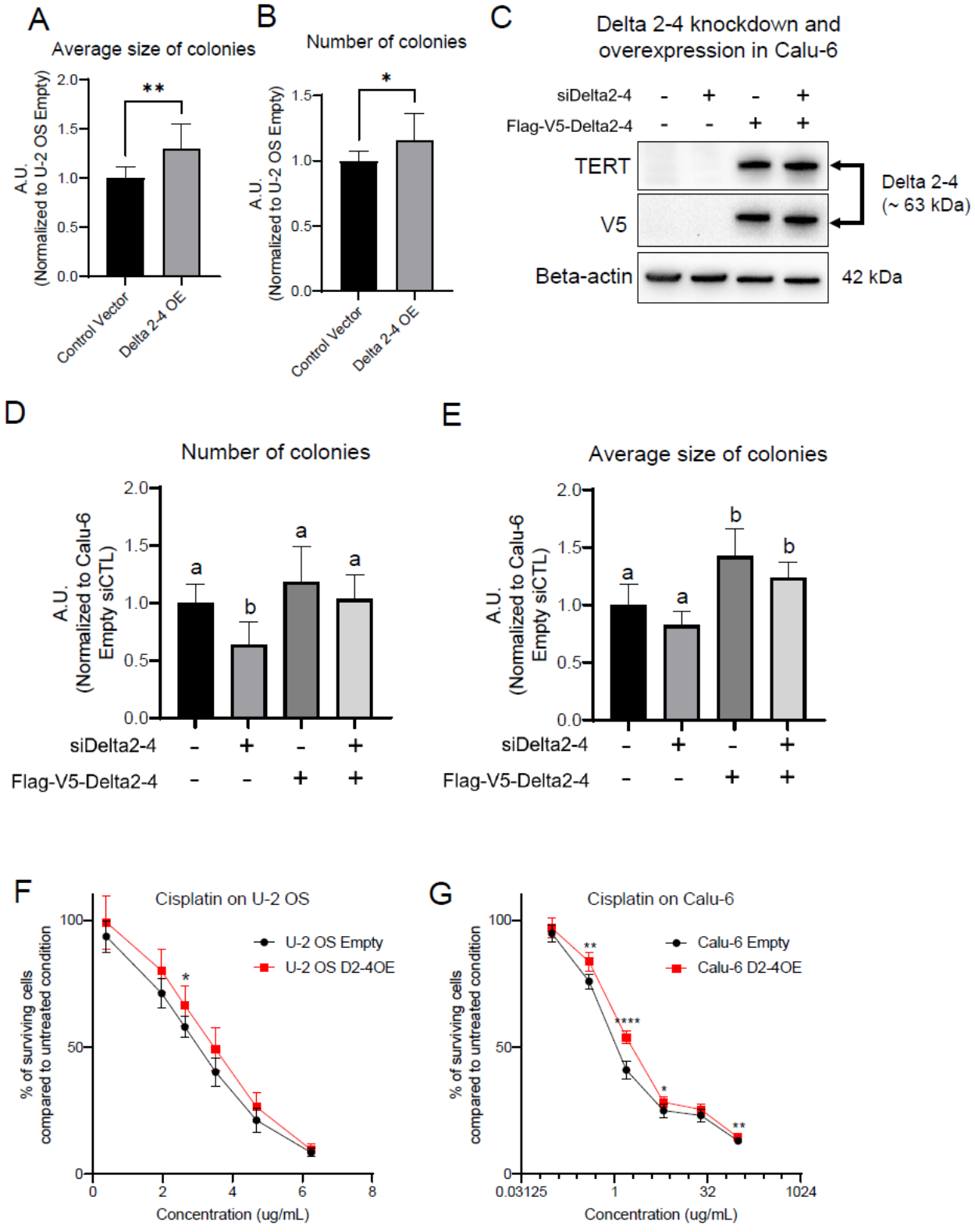

Supplemental Figure 6.5. related to Figure 6.3.

(**A-B**) Average size of colonies (A) and number of colonies (B) from U-2 OS cell line clonogenic assay. **C**. Codon optimized ectopic Delta 2-4 isoform expression did not change by siRNA treatment targeting endogenous Delta 2-4. (**D-E**) Number of colonies (D) and average size of colonies (E) from Calu-6 cell line clonogenic assay. (**F-G**) Percentages of surviving cells with cisplatin treatment on U-2 OS cells (F) and Calu-6 cells (G).

References

1. Lopez-Otin C, Blasco MA, Partridge L, Serrano M, Kroemer G. Hallmarks of aging: An expanding universe. Cell. 2023;186(2):243-78. Epub 20230103. doi: 10.1016/j.cell.2022.11.001. PubMed PMID: 36599349.
2. Lopez-Otin C, Pietrocola F, Roiz-Valle D, Galluzzi L, Kroemer G. Meta-hallmarks of aging and cancer. Cell Metab. 2023;35(1):12-35. doi: 10.1016/j.cmet.2022.11.001. PubMed PMID: 36599298.
3. de Groot P, Munden RF. Lung cancer epidemiology, risk factors, and prevention. Radiol Clin North Am. 2012;50(5):863-76. doi: 10.1016/j.rcl.2012.06.006. PubMed PMID: 22974775.
4. Tas F, Ciftci R, Kilic L, Karabulut S. Age is a prognostic factor affecting survival in lung cancer patients. Oncol Lett. 2013;6(5):1507-13. Epub 20130906. doi: 10.3892/ol.2013.1566. PubMed PMID: 24179550; PubMed Central PMCID: PMCPMC3813578.
5. Venuta F, Diso D, Onorati I, Anile M, Mantovani S, Rendina EA. Lung cancer in elderly patients. J Thorac Dis. 2016;8(Suppl 11):S908-S14. doi: 10.21037/jtd.2016.05.20. PubMed PMID: 27942414; PubMed Central PMCID: PMCPMC5124601.
6. Jeon HS, Choi YY, Choi JE, Lee WK, Lee E, Yoo SS, et al. Telomere length of tumor tissues and survival in patients with early stage non-small cell lung cancer. Mol Carcinog. 2014;53(4):272-9. Epub 20121012. doi: 10.1002/mc.21972. PubMed PMID: 23065897.
7. Fernandez-Marcelo T, Gomez A, Pascua I, de Juan C, Head J, Hernando F, et al. Telomere length and telomerase activity in non-small cell lung cancer prognosis: clinical usefulness of a specific telomere status. J Exp Clin Cancer Res. 2015;34:78. Epub 2015/08/08. doi: 10.1186/s13046-015-0195-9. PubMed PMID: 26250468; PubMed Central PMCID: PMCPMC4528384.
8. Faugeras E, Veronese L, Jeannin G, Janicot H, Bailly S, Bay JO, et al. Telomere Status of Advanced Non-Small-Cell Lung Cancer Offers a Novel Promising Prognostic and Predictive Biomarker. Cancers (Basel). 2022;15(1). Epub 20221231. doi: 10.3390/cancers15010290. PubMed PMID: 36612286; PubMed Central PMCID: PMCPMC9818321.
9. Ferlay J, Colombet M, Soerjomataram I, Parkin DM, Pineros M, Znaor A, et al. Cancer statistics for the year 2020: An overview. Int J Cancer. 2021. Epub 20210405. doi: 10.1002/ijc.33588. PubMed PMID: 33818764.
10. Cong YS, Wright WE, Shay JW. Human telomerase and its regulation. Microbiol Mol Biol Rev. 2002;66(3):407-25, table of contents. doi: 10.1128/MMBR.66.3.407-425.2002. PubMed PMID: 12208997; PubMed Central PMCID: PMCPMC120798.
11. Moyzis RK, Buckingham JM, Cram LS, Dani M, Deaven LL, Jones MD, et al. A highly conserved repetitive DNA sequence, (TTAGGG)n, present at the telomeres of

human chromosomes. Proc Natl Acad Sci U S A. 1988;85(18):6622-6. doi: 10.1073/pnas.85.18.6622. PubMed PMID: 3413114; PubMed Central PMCID: PMCPMC282029.
12. Levy MZ, Allsopp RC, Futcher AB, Greider CW, Harley CB. Telomere end-replication problem and cell aging. J Mol Biol. 1992;225(4):951-60. doi: 10.1016/0022-2836(92)90096-3. PubMed PMID: 1613801.
13. Kim NW, Piatyszek MA, Prowse KR, Harley CB, West MD, Ho PL, et al. Specific association of human telomerase activity with immortal cells and cancer. Science. 1994;266(5193):2011-5. doi: 10.1126/science.7605428. PubMed PMID: 7605428.
14. Cunningham AP, Love WK, Zhang RW, Andrews LG, Tollefsbol TO. Telomerase inhibition in cancer therapeutics: molecular-based approaches. Curr Med Chem. 2006;13(24):2875-88. doi: 10.2174/092986706778521887. PubMed PMID: 17073634; PubMed Central PMCID: PMCPMC2423208.
15. Franceschi C, Garagnani P, Morsiani C, Conte M, Santoro A, Grignolio A, et al. The Continuum of Aging and Age-Related Diseases: Common Mechanisms but Different Rates. Front Med (Lausanne). 2018;5:61. Epub 20180312. doi: 10.3389/fmed.2018.00061. PubMed PMID: 29662881; PubMed Central PMCID: PMCPMC5890129.
16. Childs BG, Durik M, Baker DJ, van Deursen JM. Cellular senescence in aging and age-related disease: from mechanisms to therapy. Nat Med. 2015;21(12):1424-35. doi: 10.1038/nm.4000. PubMed PMID: 26646499; PubMed Central PMCID: PMCPMC4748967.
17. Liang Z, Dong X, Zhang Z, Zhang Q, Zhao Y. Age-related thymic involution: Mechanisms and functional impact. Aging Cell. 2022;21(8):e13671. Epub 20220712. doi: 10.1111/acel.13671. PubMed PMID: 35822239; PubMed Central PMCID: PMCPMC9381902.
18. Foster AD, Sivarapatna A, Gress RE. The aging immune system and its relationship with cancer. Aging health. 2011;7(5):707-18. doi: 10.2217/ahe.11.56. PubMed PMID: 22121388; PubMed Central PMCID: PMCPMC3222953.
19. Kim JJ, Ahn A, Ying J, Hickman E, Ludlow AT. Exercise as a Therapy to Maintain Telomere Function and Prevent Cellular Senescence. Exerc Sport Sci Rev. 2023;51(4):150-60. Epub 20230607. doi: 10.1249/JES.0000000000000324. PubMed PMID: 37288975; PubMed Central PMCID: PMCPMC10526708.
20. McTiernan A, Friedenreich CM, Katzmarzyk PT, Powell KE, Macko R, Buchner D, et al. Physical Activity in Cancer Prevention and Survival: A Systematic Review. Med Sci Sports Exerc. 2019;51(6):1252-61. doi: 10.1249/MSS.0000000000001937. PubMed PMID: 31095082; PubMed Central PMCID: PMCPMC6527123.
21. Rezende LFM, Sa TH, Markozannes G, Rey-Lopez JP, Lee IM, Tsilidis KK, et al. Physical activity and cancer: an umbrella review of the literature including 22 major anatomical sites and 770 000 cancer cases. Br J Sports Med. 2018;52(13):826-33. Epub 20171116. doi: 10.1136/bjsports-2017-098391. PubMed PMID: 29146752.
22. Patel AV, Friedenreich CM, Moore SC, Hayes SC, Silver JK, Campbell KL, et al. American College of Sports Medicine Roundtable Report on Physical Activity, Sedentary Behavior, and Cancer Prevention and Control. Med Sci Sports Exerc. 2019;51(11):2391-402. doi: 10.1249/MSS.0000000000002117. PubMed PMID: 31626056; PubMed Central PMCID: PMCPMC6814265.

23. Duggal NA, Pollock RD, Lazarus NR, Harridge S, Lord JM. Major features of immunesenescence, including reduced thymic output, are ameliorated by high levels of physical activity in adulthood. Aging Cell. 2018;17(2). Epub 20180308. doi: 10.1111/acel.12750. PubMed PMID: 29517845; PubMed Central PMCID: PMCPMC5847865.
24. Roake CM, Artandi SE. Regulation of human telomerase in homeostasis and disease. Nat Rev Mol Cell Biol. 2020;21(7):384-97. Epub 20200402. doi: 10.1038/s41580-020-0234-z. PubMed PMID: 32242127; PubMed Central PMCID: PMCPMC7377944.
25. Slusher AL, Kim JJ, Ludlow AT. The Role of Alternative RNA Splicing in the Regulation of hTERT, Telomerase, and Telomeres: Implications for Cancer Therapeutics. Cancers (Basel). 2020;12(6). Epub 20200610. doi: 10.3390/cancers12061514. PubMed PMID: 32531916; PubMed Central PMCID: PMCPMC7352778.
26. Ludlow AT, Wong MS, Robin JD, Batten K, Yuan L, Lai TP, et al. NOVA1 regulates hTERT splicing and cell growth in non-small cell lung cancer. Nat Commun. 2018;9(1):3112. Epub 20180806. doi: 10.1038/s41467-018-05582-x. PubMed PMID: 30082712; PubMed Central PMCID: PMCPMC6079032.
27. Sayed ME, Yuan L, Robin JD, Tedone E, Batten K, Dahlson N, et al. NOVA1 directs PTBP1 to hTERT pre-mRNA and promotes telomerase activity in cancer cells. Oncogene. 2019;38(16):2937-52. Epub 20181219. doi: 10.1038/s41388-018-0639-8. PubMed PMID: 30568224; PubMed Central PMCID: PMCPMC6474811.
28. Hrdlickova R, Nehyba J, Bose HR, Jr. Alternatively spliced telomerase reverse transcriptase variants lacking telomerase activity stimulate cell proliferation. Mol Cell Biol. 2012;32(21):4283-96. Epub 20120820. doi: 10.1128/MCB.00550-12. PubMed PMID: 22907755; PubMed Central PMCID: PMCPMC3486134.
29. Slusher AL, Kim JJ, Ribick M, Ludlow AT. Acute Exercise Regulates hTERT Gene Expression and Alternative Splicing in the hTERT-BAC Transgenic Mouse Model. Med Sci Sports Exerc. 2022;54(6):931-43. Epub 20220208. doi: 10.1249/MSS.0000000000002868. PubMed PMID: 35135999; PubMed Central PMCID: PMCPMC9117413.
30. Slusher AL, Kim JJ, Ribick M, Pollens-Voigt J, Bankhead A, Palmbos PL, et al. Intronic Cis-Element DR8 in hTERT Is Bound by Splicing Factor SF3B4 and Regulates hTERT Splicing in Non-Small Cell Lung Cancer. Mol Cancer Res. 2022;20(10):1574-88. doi: 10.1158/1541-7786.MCR-21-0058. PubMed PMID: 35852380; PubMed Central PMCID: PMCPMC9532359.
31. Kim JJ, Sayed ME, Ahn A, Slusher AL, Ying JY, Ludlow AT. Dynamics of TERT regulation via alternative splicing in stem cells and cancer cells. PLoS One. 2023;18(8):e0289327. Epub 20230802. doi: 10.1371/journal.pone.0289327. PubMed PMID: 37531400; PubMed Central PMCID: PMCPMC10395990.
32. Morgan TH. Random Segregation Versus Coupling in Mendelian Inheritance. Science. 1911;34(873):384. doi: 10.1126/science.34.873.384. PubMed PMID: 17741940.
33. Creighton HB, McClintock B. A Correlation of Cytological and Genetical Crossing-Over in Zea Mays. Proc Natl Acad Sci U S A. 1931;17(8):492-7. doi:

10.1073/pnas.17.8.492. PubMed PMID: 16587654; PubMed Central PMCID: PMCPMC1076098.
34. Muller HJ. The remaking of chromosomes. Collect Net. 1938;8:182-95.
35. Shay JW, Wright WE. Telomeres and telomerase: three decades of progress. Nat Rev Genet. 2019;20(5):299-309. doi: 10.1038/s41576-019-0099-1. PubMed PMID: 30760854.
36. Shammas MA. Telomeres, lifestyle, cancer, and aging. Curr Opin Clin Nutr Metab Care. 2011;14(1):28-34. doi: 10.1097/MCO.0b013e32834121b1. PubMed PMID: 21102320; PubMed Central PMCID: PMCPMC3370421.
37. Lim CJ, Cech TR. Shaping human telomeres: from shelterin and CST complexes to telomeric chromatin organization. Nat Rev Mol Cell Biol. 2021;22(4):283-98. Epub 20210209. doi: 10.1038/s41580-021-00328-y. PubMed PMID: 33564154; PubMed Central PMCID: PMCPMC8221230.
38. Olovnikov AM. [Principle of marginotomy in template synthesis of polynucleotides]. Dokl Akad Nauk SSSR. 1971;201(6):1496-9. PubMed PMID: 5158754.
39. Watson JD. Origin of concatemeric T7 DNA. Nat New Biol. 1972;239(94):197-201. doi: 10.1038/newbio239197a0. PubMed PMID: 4507727.
40. Ogawa T, Okazaki T. Discontinuous DNA replication. Annu Rev Biochem. 1980;49:421-57. doi: 10.1146/annurev.bi.49.070180.002225. PubMed PMID: 6250445.
41. Robin JD, Ludlow AT, Batten K, Magdinier F, Stadler G, Wagner KR, et al. Telomere position effect: regulation of gene expression with progressive telomere shortening over long distances. Genes Dev. 2014;28(22):2464-76. doi: 10.1101/gad.251041.114. PubMed PMID: 25403178; PubMed Central PMCID: PMCPMC4233240.
42. Srinivas N, Rachakonda S, Kumar R. Telomeres and Telomere Length: A General Overview. Cancers (Basel). 2020;12(3). Epub 20200228. doi: 10.3390/cancers12030558. PubMed PMID: 32121056; PubMed Central PMCID: PMCPMC7139734.
43. Rossiello F, Jurk D, Passos JF, d'Adda di Fagagna F. Telomere dysfunction in ageing and age-related diseases. Nat Cell Biol. 2022;24(2):135-47. Epub 20220214. doi: 10.1038/s41556-022-00842-x. PubMed PMID: 35165420; PubMed Central PMCID: PMCPMC8985209.
44. Mender I, Shay JW. Telomere Dysfunction Induced Foci (TIF) Analysis. Bio Protoc. 2015;5(22). doi: 10.21769/bioprotoc.1656. PubMed PMID: 27500188; PubMed Central PMCID: PMCPMC4972040.
45. Coppe JP, Desprez PY, Krtolica A, Campisi J. The senescence-associated secretory phenotype: the dark side of tumor suppression. Annu Rev Pathol. 2010;5:99-118. doi: 10.1146/annurev-pathol-121808-102144. PubMed PMID: 20078217; PubMed Central PMCID: PMCPMC4166495.
46. Griffith JD, Comeau L, Rosenfield S, Stansel RM, Bianchi A, Moss H, et al. Mammalian telomeres end in a large duplex loop. Cell. 1999;97(4):503-14. doi: 10.1016/s0092-8674(00)80760-6. PubMed PMID: 10338214.
47. Wright WE, Pereira-Smith OM, Shay JW. Reversible cellular senescence: implications for immortalization of normal human diploid fibroblasts. Mol Cell Biol.

1989;9(7):3088-92. doi: 10.1128/mcb.9.7.3088-3092.1989. PubMed PMID: 2779554; PubMed Central PMCID: PMCPMC362778.
48. Shay JW, Van Der Haegen BA, Ying Y, Wright WE. The frequency of immortalization of human fibroblasts and mammary epithelial cells transfected with SV40 large T-antigen. Exp Cell Res. 1993;209(1):45-52. doi: 10.1006/excr.1993.1283. PubMed PMID: 8224005.
49. Lustig AJ. Crisis intervention: the role of telomerase. Proc Natl Acad Sci U S A. 1999;96(7):3339-41. doi: 10.1073/pnas.96.7.3339. PubMed PMID: 10097039; PubMed Central PMCID: PMCPMC34270.
50. Shay JW, Wright WE. Quantitation of the frequency of immortalization of normal human diploid fibroblasts by SV40 large T-antigen. Exp Cell Res. 1989;184(1):109-18. doi: 10.1016/0014-4827(89)90369-8. PubMed PMID: 2551703.
51. Muoio D, Laspata N, Fouquerel E. Functions of ADP-ribose transferases in the maintenance of telomere integrity. Cell Mol Life Sci. 2022;79(4):215. Epub 20220329. doi: 10.1007/s00018-022-04235-z. PubMed PMID: 35348914; PubMed Central PMCID: PMCPMC8964661.
52. Lopez-Otin C, Blasco MA, Partridge L, Serrano M, Kroemer G. The hallmarks of aging. Cell. 2013;153(6):1194-217. doi: 10.1016/j.cell.2013.05.039. PubMed PMID: 23746838; PubMed Central PMCID: PMCPMC3836174.
53. Holloszy JO. The biology of aging. Mayo Clin Proc. 2000;75 Suppl:S3-8; discussion S-9. PubMed PMID: 10959208.
54. Holloszy JO, Schechtman KB. Interaction between exercise and food restriction: effects on longevity of male rats. J Appl Physiol (1985). 1991;70(4):1529-35. doi: 10.1152/jappl.1991.70.4.1529. PubMed PMID: 2055832.
55. Yang JH, Petty CA, Dixon-McDougall T, Lopez MV, Tyshkovskiy A, Maybury-Lewis S, et al. Chemically induced reprogramming to reverse cellular aging. Aging (Albany NY). 2023;15(13):5966-89. Epub 20230712. doi: 10.18632/aging.204896. PubMed PMID: 37437248; PubMed Central PMCID: PMCPMC10373966.
56. Browder KC, Reddy P, Yamamoto M, Haghani A, Guillen IG, Sahu S, et al. In vivo partial reprogramming alters age-associated molecular changes during physiological aging in mice. Nat Aging. 2022;2(3):243-53. Epub 20220307. doi: 10.1038/s43587-022-00183-2. PubMed PMID: 37118377.
57. Cartee GD, Hepple RT, Bamman MM, Zierath JR. Exercise Promotes Healthy Aging of Skeletal Muscle. Cell Metab. 2016;23(6):1034-47. doi: 10.1016/j.cmet.2016.05.007. PubMed PMID: 27304505; PubMed Central PMCID: PMCPMC5045036.
58. Rudolph KL, Chang S, Lee HW, Blasco M, Gottlieb GJ, Greider C, et al. Longevity, stress response, and cancer in aging telomerase-deficient mice. Cell. 1999;96(5):701-12. doi: 10.1016/s0092-8674(00)80580-2. PubMed PMID: 10089885.
59. Munoz-Lorente MA, Cano-Martin AC, Blasco MA. Mice with hyper-long telomeres show less metabolic aging and longer lifespans. Nat Commun. 2019;10(1):4723. Epub 20191017. doi: 10.1038/s41467-019-12664-x. PubMed PMID: 31624261; PubMed Central PMCID: PMCPMC6797762.
60. Bernardes de Jesus B, Schneeberger K, Vera E, Tejera A, Harley CB, Blasco MA. The telomerase activator TA-65 elongates short telomeres and increases health span of adult/old mice without increasing cancer incidence. Aging Cell. 2011;10(4):604-

21. Epub 20110414. doi: 10.1111/j.1474-9726.2011.00700.x. PubMed PMID: 21426483; PubMed Central PMCID: PMCPMC3627294.
61. Thery F, Martina L, Asselman C, Zhang Y, Vessely M, Repo H, et al. Ring finger protein 213 assembles into a sensor for ISGylated proteins with antimicrobial activity. Nat Commun. 2021;12(1):5772. Epub 20211001. doi: 10.1038/s41467-021-26061-w. PubMed PMID: 34599178; PubMed Central PMCID: PMCPMC8486878.
62. Lou Z, Wei J, Riethman H, Baur JA, Voglauer R, Shay JW, et al. Telomere length regulates ISG15 expression in human cells. Aging (Albany NY). 2009;1(7):608-21. Epub 20090717. doi: 10.18632/aging.100066. PubMed PMID: 20157543; PubMed Central PMCID: PMCPMC2806043.
63. Daniali L, Benetos A, Susser E, Kark JD, Labat C, Kimura M, et al. Telomeres shorten at equivalent rates in somatic tissues of adults. Nat Commun. 2013;4:1597. doi: 10.1038/ncomms2602. PubMed PMID: 23511462; PubMed Central PMCID: PMCPMC3615479.
64. Demanelis K, Jasmine F, Chen LS, Chernoff M, Tong L, Delgado D, et al. Determinants of telomere length across human tissues. Science. 2020;369(6509). doi: 10.1126/science.aaz6876. PubMed PMID: 32913074; PubMed Central PMCID: PMCPMC8108546.
65. Barnes RP, Fouquerel E, Opresko PL. The impact of oxidative DNA damage and stress on telomere homeostasis. Mech Ageing Dev. 2019;177:37-45. Epub 20180328. doi: 10.1016/j.mad.2018.03.013. PubMed PMID: 29604323; PubMed Central PMCID: PMCPMC6162185.
66. Mao P, Liu J, Zhang Z, Zhang H, Liu H, Gao S, et al. Homologous recombination-dependent repair of telomeric DSBs in proliferating human cells. Nat Commun. 2016;7:12154. Epub 20160711. doi: 10.1038/ncomms12154. PubMed PMID: 27396625; PubMed Central PMCID: PMCPMC4942568.
67. Anderson R, Lagnado A, Maggiorani D, Walaszczyk A, Dookun E, Chapman J, et al. Length-independent telomere damage drives post-mitotic cardiomyocyte senescence. EMBO J. 2019;38(5). Epub 20190208. doi: 10.15252/embj.2018100492. PubMed PMID: 30737259; PubMed Central PMCID: PMCPMC6396144.
68. Imran SAM, Yazid MD, Cui W, Lokanathan Y. The Intra- and Extra-Telomeric Role of TRF2 in the DNA Damage Response. Int J Mol Sci. 2021;22(18). Epub 20210914. doi: 10.3390/ijms22189900. PubMed PMID: 34576063; PubMed Central PMCID: PMCPMC8470803.
69. Barnes RP, de Rosa M, Thosar SA, Detwiler AC, Roginskaya V, Van Houten B, et al. Telomeric 8-oxo-guanine drives rapid premature senescence in the absence of telomere shortening. Nat Struct Mol Biol. 2022;29(7):639-52. Epub 20220630. doi: 10.1038/s41594-022-00790-y. PubMed PMID: 35773409; PubMed Central PMCID: PMCPMC9287163.
70. Armanios M. The Role of Telomeres in Human Disease. Annu Rev Genomics Hum Genet. 2022;23:363-81. Epub 20220624. doi: 10.1146/annurev-genom-010422-091101. PubMed PMID: 35609925.
71. Aviv A, Anderson JJ, Shay JW. Mutations, Cancer and the Telomere Length Paradox. Trends Cancer. 2017;3(4):253-8. Epub 20170327. doi: 10.1016/j.trecan.2017.02.005. PubMed PMID: 28718437; PubMed Central PMCID: PMCPMC5903276.

72. Feldser DM, Greider CW. Short telomeres limit tumor progression in vivo by inducing senescence. Cancer Cell. 2007;11(5):461-9. Epub 20070412. doi: 10.1016/j.ccr.2007.02.026. PubMed PMID: 17433785; PubMed Central PMCID: PMCPMC1945093.
73. Artandi SE, Chang S, Lee SL, Alson S, Gottlieb GJ, Chin L, et al. Telomere dysfunction promotes non-reciprocal translocations and epithelial cancers in mice. Nature. 2000;406(6796):641-5. doi: 10.1038/35020592. PubMed PMID: 10949306.
74. Ungar RA, Giri N, Pao M, Khincha PP, Zhou W, Alter BP, et al. Complex phenotype of dyskeratosis congenita and mood dysregulation with novel homozygous RTEL1 and TPH1 variants. Am J Med Genet A. 2018;176(6):1432-7. Epub 20180425. doi: 10.1002/ajmg.a.38706. PubMed PMID: 29696773; PubMed Central PMCID: PMCPMC5992073.
75. Walne AJ, Dokal I. Advances in the understanding of dyskeratosis congenita. Br J Haematol. 2009;145(2):164-72. Epub 20090204. doi: 10.1111/j.1365-2141.2009.07598.x. PubMed PMID: 19208095; PubMed Central PMCID: PMCPMC2882229.
76. Jager K, Walter M. Therapeutic Targeting of Telomerase. Genes (Basel). 2016;7(7). Epub 20160721. doi: 10.3390/genes7070039. PubMed PMID: 27455328; PubMed Central PMCID: PMCPMC4962009.
77. Borrell B. Lawsuit challenges anti-ageing claims. Nature. 2012;488(7409):18. doi: 10.1038/488018a. PubMed PMID: 22859181.
78. Cohen SB, Graham ME, Lovrecz GO, Bache N, Robinson PJ, Reddel RR. Protein composition of catalytically active human telomerase from immortal cells. Science. 2007;315(5820):1850-3. doi: 10.1126/science.1138596. PubMed PMID: 17395830.
79. Xi L, Cech TR. Inventory of telomerase components in human cells reveals multiple subpopulations of hTR and hTERT. Nucleic Acids Res. 2014;42(13):8565-77. Epub 20140702. doi: 10.1093/nar/gku560. PubMed PMID: 24990373; PubMed Central PMCID: PMCPMC4117779.
80. Tycowski K.T. KNG, Conrad N.K., Fok V., Steitz J.A.. Gesteland R.F., Cech T.R., Atkins J.F. The RNA World. New York: Cold Spring Harbor Laboratory Press; 2006.
81. Dratwa M, Wysoczanska B, Lacina P, Kubik T, Bogunia-Kubik K. TERT-Regulation and Roles in Cancer Formation. Front Immunol. 2020;11:589929. Epub 20201119. doi: 10.3389/fimmu.2020.589929. PubMed PMID: 33329574; PubMed Central PMCID: PMCPMC7717964.
82. Semenza GL. Hypoxia-inducible factors in physiology and medicine. Cell. 2012;148(3):399-408. doi: 10.1016/j.cell.2012.01.021. PubMed PMID: 22304911; PubMed Central PMCID: PMCPMC3437543.
83. Townsend JR, Stout JR, Jajtner AR, Church DD, Beyer KS, Oliveira LP, et al. Resistance exercise increases intramuscular NF-kappab signaling in untrained males. Eur J Appl Physiol. 2016;116(11-12):2103-11. Epub 20160831. doi: 10.1007/s00421-016-3463-2. PubMed PMID: 27582262.
84. Trenerry MK, Carey KA, Ward AC, Cameron-Smith D. STAT3 signaling is activated in human skeletal muscle following acute resistance exercise. J Appl Physiol

(1985). 2007;102(4):1483-9. Epub 20070104. doi: 10.1152/japplphysiol.01147.2006. PubMed PMID: 17204573.
85. McLean CS, Mielke C, Cordova JM, Langlais PR, Bowen B, Miranda D, et al. Gene and MicroRNA Expression Responses to Exercise; Relationship with Insulin Sensitivity. PLoS One. 2015;10(5):e0127089. Epub 20150518. doi: 10.1371/journal.pone.0127089. PubMed PMID: 25984722; PubMed Central PMCID: PMCPMC4436215.
86. Vinagre J, Almeida A, Populo H, Batista R, Lyra J, Pinto V, et al. Frequency of TERT promoter mutations in human cancers. Nat Commun. 2013;4:2185. doi: 10.1038/ncomms3185. PubMed PMID: 23887589.
87. Killela PJ, Reitman ZJ, Jiao Y, Bettegowda C, Agrawal N, Diaz LA, Jr., et al. TERT promoter mutations occur frequently in gliomas and a subset of tumors derived from cells with low rates of self-renewal. Proc Natl Acad Sci U S A. 2013;110(15):6021-6. Epub 20130325. doi: 10.1073/pnas.1303607110. PubMed PMID: 23530248; PubMed Central PMCID: PMCPMC3625331.
88. McKelvey BA, Umbricht CB, Zeiger MA. Telomerase Reverse Transcriptase (TERT) Regulation in Thyroid Cancer: A Review. Front Endocrinol (Lausanne). 2020;11:485. Epub 20200731. doi: 10.3389/fendo.2020.00485. PubMed PMID: 32849278; PubMed Central PMCID: PMCPMC7412884.
89. Avin BA, Wang Y, Gilpatrick T, Workman RE, Lee I, Timp W, et al. Characterization of human telomerase reverse transcriptase promoter methylation and transcription factor binding in differentiated thyroid cancer cell lines. Genes Chromosomes Cancer. 2019;58(8):530-40. Epub 20190210. doi: 10.1002/gcc.22735. PubMed PMID: 30664813; PubMed Central PMCID: PMCPMC6621557.
90. Zhang A, Zheng C, Lindvall C, Hou M, Ekedahl J, Lewensohn R, et al. Frequent amplification of the telomerase reverse transcriptase gene in human tumors. Cancer Res. 2000;60(22):6230-5. PubMed PMID: 11103775.
91. Barthel FP, Wei W, Tang M, Martinez-Ledesma E, Hu X, Amin SB, et al. Systematic analysis of telomere length and somatic alterations in 31 cancer types. Nat Genet. 2017;49(3):349-57. Epub 20170130. doi: 10.1038/ng.3781. PubMed PMID: 28135248; PubMed Central PMCID: PMCPMC5571729.
92. Lee DD, Leao R, Komosa M, Gallo M, Zhang CH, Lipman T, et al. DNA hypermethylation within TERT promoter upregulates TERT expression in cancer. J Clin Invest. 2019;129(1):223-9. Epub 20181203. doi: 10.1172/JCI121303. PubMed PMID: 30358567; PubMed Central PMCID: PMCPMC6307937.
93. Lewis KA, Tollefsbol TO. Regulation of the Telomerase Reverse Transcriptase Subunit through Epigenetic Mechanisms. Front Genet. 2016;7:83. Epub 20160509. doi: 10.3389/fgene.2016.00083. PubMed PMID: 27242892; PubMed Central PMCID: PMCPMC4860561.
94. Kumari A, Srinivasan R, Vasishta RK, Wig JD. Positive regulation of human telomerase reverse transcriptase gene expression and telomerase activity by DNA methylation in pancreatic cancer. Ann Surg Oncol. 2009;16(4):1051-9. Epub 20090205. doi: 10.1245/s10434-009-0333-8. PubMed PMID: 19194757.
95. Wang N, Kjellin H, Sofiadis A, Fotouhi O, Juhlin CC, Backdahl M, et al. Genetic and epigenetic background and protein expression profiles in relation to telomerase activation in medullary thyroid carcinoma. Oncotarget. 2016;7(16):21332-46. doi:

10.18632/oncotarget.7237. PubMed PMID: 26870890; PubMed Central PMCID: PMCPMC5008288.
96. Xu D, Popov N, Hou M, Wang Q, Bjorkholm M, Gruber A, et al. Switch from Myc/Max to Mad1/Max binding and decrease in histone acetylation at the telomerase reverse transcriptase promoter during differentiation of HL60 cells. Proc Natl Acad Sci U S A. 2001;98(7):3826-31. doi: 10.1073/pnas.071043198. PubMed PMID: 11274400; PubMed Central PMCID: PMCPMC31137.
97. Takakura M, Kyo S, Sowa Y, Wang Z, Yatabe N, Maida Y, et al. Telomerase activation by histone deacetylase inhibitor in normal cells. Nucleic Acids Res. 2001;29(14):3006-11. doi: 10.1093/nar/29.14.3006. PubMed PMID: 11452025; PubMed Central PMCID: PMCPMC55810.
98. Liu C, Fang X, Ge Z, Jalink M, Kyo S, Bjorkholm M, et al. The telomerase reverse transcriptase (hTERT) gene is a direct target of the histone methyltransferase SMYD3. Cancer Res. 2007;67(6):2626-31. doi: 10.1158/0008-5472.CAN-06-4126. PubMed PMID: 17363582.
99. Wu S, Ge Y, Huang L, Liu H, Xue Y, Zhao Y. BRG1, the ATPase subunit of SWI/SNF chromatin remodeling complex, interacts with HDAC2 to modulate telomerase expression in human cancer cells. Cell Cycle. 2014;13(18):2869-78. doi: 10.4161/15384101.2014.946834. PubMed PMID: 25486475; PubMed Central PMCID: PMCPMC4612678.
100. Dvinge H. Regulation of alternative mRNA splicing: old players and new perspectives. FEBS Lett. 2018;592(17):2987-3006. Epub 20180616. doi: 10.1002/1873-3468.13119. PubMed PMID: 29856907.
101. Tellier M, Maudlin I, Murphy S. Transcription and splicing: A two-way street. Wiley Interdiscip Rev RNA. 2020;11(5):e1593. Epub 20200303. doi: 10.1002/wrna.1593. PubMed PMID: 32128990.
102. Dumbovic G, Braunschweig U, Langner HK, Smallegan M, Biayna J, Hass EP, et al. Nuclear compartmentalization of TERT mRNA and TUG1 lncRNA is driven by intron retention. Nat Commun. 2021;12(1):3308. Epub 20210603. doi: 10.1038/s41467-021-23221-w. PubMed PMID: 34083519; PubMed Central PMCID: PMCPMC8175569.
103. Pan Q, Shai O, Lee LJ, Frey BJ, Blencowe BJ. Deep surveying of alternative splicing complexity in the human transcriptome by high-throughput sequencing. Nat Genet. 2008;40(12):1413-5. Epub 20081102. doi: 10.1038/ng.259. PubMed PMID: 18978789.
104. Ulaner GA, Hu JF, Vu TH, Giudice LC, Hoffman AR. Tissue-specific alternate splicing of human telomerase reverse transcriptase (hTERT) influences telomere lengths during human development. Int J Cancer. 2001;91(5):644-9. PubMed PMID: 11267974.
105. Colgin LM, Wilkinson C, Englezou A, Kilian A, Robinson MO, Reddel RR. The hTERTalpha splice variant is a dominant negative inhibitor of telomerase activity. Neoplasia. 2000;2(5):426-32. doi: 10.1038/sj.neo.7900112. PubMed PMID: 11191109; PubMed Central PMCID: PMCPMC1507985.
106. Yi X, White DM, Aisner DL, Baur JA, Wright WE, Shay JW. An alternate splicing variant of the human telomerase catalytic subunit inhibits telomerase activity. Neoplasia. 2000;2(5):433-40. doi: 10.1038/sj.neo.7900113. PubMed PMID: 11191110; PubMed Central PMCID: PMCPMC1507981.

107. Hisatomi H, Ohyashiki K, Ohyashiki JH, Nagao K, Kanamaru T, Hirata H, et al. Expression profile of a gamma-deletion variant of the human telomerase reverse transcriptase gene. Neoplasia. 2003;5(3):193-7. doi: 10.1016/S1476-5586(03)80051-9. PubMed PMID: 12869302; PubMed Central PMCID: PMCPMC1502410.
108. Penev A, Bazley A, Shen M, Boeke JD, Savage SA, Sfeir A. Alternative splicing is a developmental switch for hTERT expression. Mol Cell. 2021;81(11):2349-60 e6. Epub 20210413. doi: 10.1016/j.molcel.2021.03.033. PubMed PMID: 33852895; PubMed Central PMCID: PMCPMC8943697.
109. Haendeler J, Hoffmann J, Diehl JF, Vasa M, Spyridopoulos I, Zeiher AM, et al. Antioxidants inhibit nuclear export of telomerase reverse transcriptase and delay replicative senescence of endothelial cells. Circ Res. 2004;94(6):768-75. Epub 20040212. doi: 10.1161/01.RES.0000121104.05977.F3. PubMed PMID: 14963003.
110. Kim W, Ludlow AT, Min J, Robin JD, Stadler G, Mender I, et al. Regulation of the Human Telomerase Gene TERT by Telomere Position Effect-Over Long Distances (TPE-OLD): Implications for Aging and Cancer. PLoS Biol. 2016;14(12):e2000016. Epub 20161215. doi: 10.1371/journal.pbio.2000016. PubMed PMID: 27977688; PubMed Central PMCID: PMCPMC5169358.
111. Rosen J, Jakobs P, Ale-Agha N, Altschmied J, Haendeler J. Non-canonical functions of Telomerase Reverse Transcriptase - Impact on redox homeostasis. Redox Biol. 2020;34:101543. Epub 20200526. doi: 10.1016/j.redox.2020.101543. PubMed PMID: 32502898; PubMed Central PMCID: PMCPMC7267725.
112. Indran IR, Hande MP, Pervaiz S. hTERT overexpression alleviates intracellular ROS production, improves mitochondrial function, and inhibits ROS-mediated apoptosis in cancer cells. Cancer Res. 2011;71(1):266-76. Epub 20101111. doi: 10.1158/0008-5472.CAN-10-1588. PubMed PMID: 21071633.
113. Singhapol C, Pal D, Czapiewski R, Porika M, Nelson G, Saretzki GC. Mitochondrial telomerase protects cancer cells from nuclear DNA damage and apoptosis. PLoS One. 2013;8(1):e52989. Epub 20130109. doi: 10.1371/journal.pone.0052989. PubMed PMID: 23326372; PubMed Central PMCID: PMCPMC3541395.
114. Chatterjee S, Hofer T, Costa A, Lu D, Batkai S, Gupta SK, et al. Telomerase therapy attenuates cardiotoxic effects of doxorubicin. Mol Ther. 2021;29(4):1395-410. Epub 20210101. doi: 10.1016/j.ymthe.2020.12.035. PubMed PMID: 33388418; PubMed Central PMCID: PMCPMC8058493.
115. Radan L, Hughes CS, Teichroeb JH, Vieira Zamora FM, Jewer M, Postovit LM, et al. Microenvironmental regulation of telomerase isoforms in human embryonic stem cells. Stem Cells Dev. 2014;23(17):2046-66. Epub 20140617. doi: 10.1089/scd.2013.0373. PubMed PMID: 24749509; PubMed Central PMCID: PMCPMC4142780.
116. Listerman I, Sun J, Gazzaniga FS, Lukas JL, Blackburn EH. The major reverse transcriptase-incompetent splice variant of the human telomerase protein inhibits telomerase activity but protects from apoptosis. Cancer Res. 2013;73(9):2817-28. Epub 20130422. doi: 10.1158/0008-5472.CAN-12-3082. PubMed PMID: 23610451; PubMed Central PMCID: PMCPMC3643995.

117. Wright WE, Shay JW. Telomere dynamics in cancer progression and prevention: fundamental differences in human and mouse telomere biology. Nat Med. 2000;6(8):849-51. doi: 10.1038/78592. PubMed PMID: 10932210.
118. Parrinello S, Samper E, Krtolica A, Goldstein J, Melov S, Campisi J. Oxygen sensitivity severely limits the replicative lifespan of murine fibroblasts. Nat Cell Biol. 2003;5(8):741-7. doi: 10.1038/ncb1024. PubMed PMID: 12855956; PubMed Central PMCID: PMCPMC4940195.
119. Newbold RF. The significance of telomerase activation and cellular immortalization in human cancer. Mutagenesis. 2002;17(6):539-50. doi: 10.1093/mutage/17.6.539. PubMed PMID: 12435851.
120. Rangarajan A, Hong SJ, Gifford A, Weinberg RA. Species- and cell type-specific requirements for cellular transformation. Cancer Cell. 2004;6(2):171-83. doi: 10.1016/j.ccr.2004.07.009. PubMed PMID: 15324700.
121. Horikawa I, Chiang YJ, Patterson T, Feigenbaum L, Leem SH, Michishita E, et al. Differential cis-regulation of human versus mouse TERT gene expression in vivo: identification of a human-specific repressive element. Proc Natl Acad Sci U S A. 2005;102(51):18437-42. Epub 20051212. doi: 10.1073/pnas.0508964102. PubMed PMID: 16344462; PubMed Central PMCID: PMCPMC1317953.
122. Zhang F, Cheng D, Wang S, Zhu J. Human Specific Regulation of the Telomerase Reverse Transcriptase Gene. Genes (Basel). 2016;7(7). Epub 20160628. doi: 10.3390/genes7070030. PubMed PMID: 27367732; PubMed Central PMCID: PMCPMC4962000.
123. Cheng, Wang S, Jia W, Zhao Y, Zhang F, Kang J, et al. Regulation of human and mouse telomerase genes by genomic contexts and transcription factors during embryonic stem cell differentiation. Sci Rep. 2017;7(1):16444. Epub 20171127. doi: 10.1038/s41598-017-16764-w. PubMed PMID: 29180668; PubMed Central PMCID: PMCPMC5703907.
124. Ludlow AT, Zimmerman JB, Witkowski S, Hearn JW, Hatfield BD, Roth SM. Relationship between physical activity level, telomere length, and telomerase activity. Med Sci Sports Exerc. 2008;40(10):1764-71. Epub 2008/09/19. doi: 10.1249/MSS.0b013e31817c92aa. PubMed PMID: 18799986; PubMed Central PMCID: PMC2581416.
125. Cherkas LF, Hunkin JL, Kato BS, Richards JB, Gardner JP, Surdulescu GL, et al. The association between physical activity in leisure time and leukocyte telomere length. Arch Intern Med. 2008;168(2):154-8. doi: 10.1001/archinternmed.2007.39. PubMed PMID: 18227361.
126. Savela S, Saijonmaa O, Strandberg TE, Koistinen P, Strandberg AY, Tilvis RS, et al. Physical activity in midlife and telomere length measured in old age. Exp Gerontol. 2013;48(1):81-4. Epub 20120222. doi: 10.1016/j.exger.2012.02.003. PubMed PMID: 22386580.
127. Puterman E, Lin J, Blackburn E, O'Donovan A, Adler N, Epel E. The power of exercise: buffering the effect of chronic stress on telomere length. PLoS One. 2010;5(5):e10837. Epub 20100526. doi: 10.1371/journal.pone.0010837. PubMed PMID: 20520771; PubMed Central PMCID: PMCPMC2877102.
128. Puterman E, Weiss J, Lin J, Schilf S, Slusher AL, Johansen KL, et al. Aerobic exercise lengthens telomeres and reduces stress in family caregivers: A randomized

controlled trial - Curt Richter Award Paper 2018. Psychoneuroendocrinology. 2018;98:245-52. Epub 20180802. doi: 10.1016/j.psyneuen.2018.08.002. PubMed PMID: 30266522.
129. Song S, Lee E, Kim H. Does Exercise Affect Telomere Length? A Systematic Review and Meta-Analysis of Randomized Controlled Trials. Medicina (Kaunas). 2022;58(2). Epub 20220205. doi: 10.3390/medicina58020242. PubMed PMID: 35208566; PubMed Central PMCID: PMCPMC8879766.
130. Valente C, Andrade R, Alvarez L, Rebelo-Marques A, Stamatakis E, Espregueira-Mendes J. Effect of physical activity and exercise on telomere length: Systematic review with meta-analysis. J Am Geriatr Soc. 2021;69(11):3285-300. Epub 20210623. doi: 10.1111/jgs.17334. PubMed PMID: 34161613.
131. Lin J, Epel E. Stress and telomere shortening: Insights from cellular mechanisms. Ageing Res Rev. 2022;73:101507. Epub 20211101. doi: 10.1016/j.arr.2021.101507. PubMed PMID: 34736994; PubMed Central PMCID: PMCPMC8920518.
132. Osthus IB, Sgura A, Berardinelli F, Alsnes IV, Bronstad E, Rehn T, et al. Telomere length and long-term endurance exercise: does exercise training affect biological age? A pilot study. PLoS One. 2012;7(12):e52769. Epub 20121226. doi: 10.1371/journal.pone.0052769. PubMed PMID: 23300766; PubMed Central PMCID: PMCPMC3530492.
133. Muniesa CA, Verde Z, Diaz-Urena G, Santiago C, Gutierrez F, Diaz E, et al. Telomere Length in Elite Athletes. Int J Sports Physiol Perform. 2017;12(7):994-6. Epub 20161205. doi: 10.1123/ijspp.2016-0471. PubMed PMID: 27918657.
134. LaRocca TJ, Seals DR, Pierce GL. Leukocyte telomere length is preserved with aging in endurance exercise-trained adults and related to maximal aerobic capacity. Mech Ageing Dev. 2010;131(2):165-7. Epub 20100112. doi: 10.1016/j.mad.2009.12.009. PubMed PMID: 20064545; PubMed Central PMCID: PMCPMC2845985.
135. Brandao CFC, Nonino CB, de Carvalho FG, Nicoletti CF, Noronha NY, San Martin R, et al. The effects of short-term combined exercise training on telomere length in obese women: a prospective, interventional study. Sports Med Open. 2020;6(1):5. Epub 20200116. doi: 10.1186/s40798-020-0235-7. PubMed PMID: 31950310; PubMed Central PMCID: PMCPMC6965549.
136. Werner CM, Hecksteden A, Morsch A, Zundler J, Wegmann M, Kratzsch J, et al. Differential effects of endurance, interval, and resistance training on telomerase activity and telomere length in a randomized, controlled study. Eur Heart J. 2019;40(1):34-46. doi: 10.1093/eurheartj/ehy585. PubMed PMID: 30496493; PubMed Central PMCID: PMCPMC6312574.
137. Konopka AR, Laurin JL, Schoenberg HM, Reid JJ, Castor WM, Wolff CA, et al. Metformin inhibits mitochondrial adaptations to aerobic exercise training in older adults. Aging Cell. 2019;18(1):e12880. Epub 20181211. doi: 10.1111/acel.12880. PubMed PMID: 30548390; PubMed Central PMCID: PMCPMC6351883.
138. Mathur S, Ardestani A, Parker B, Cappizzi J, Polk D, Thompson PD. Telomere length and cardiorespiratory fitness in marathon runners. J Investig Med. 2013;61(3):613-5. doi: 10.2310/JIM.0b013e3182814cc2. PubMed PMID: 23360839.

139. Seki Y, Aczel D, Torma F, Jokai M, Boros A, Suzuki K, et al. No strong association among epigenetic modifications by DNA methylation, telomere length, and physical fitness in biological aging. Biogerontology. 2023;24(2):245-55. Epub 20230102. doi: 10.1007/s10522-022-10011-0. PubMed PMID: 36592269; PubMed Central PMCID: PMCPMC10006047.
140. Aguiar SS, Sousa CV, Santos PA, Barbosa LP, Maciel LA, Coelho-Junior HJ, et al. Master athletes have longer telomeres than age-matched non-athletes. A systematic review, meta-analysis and discussion of possible mechanisms. Exp Gerontol. 2021;146:111212. Epub 20201230. doi: 10.1016/j.exger.2020.111212. PubMed PMID: 33387607.
141. Schellnegger M, Lin AC, Hammer N, Kamolz LP. Physical Activity on Telomere Length as a Biomarker for Aging: A Systematic Review. Sports Med Open. 2022;8(1):111. Epub 20220904. doi: 10.1186/s40798-022-00503-1. PubMed PMID: 36057868; PubMed Central PMCID: PMCPMC9441412.
142. Bianchi A, Marchetti L, Hall Z, Lemos H, Vacca M, Paish H, et al. Moderate Exercise Inhibits Age-Related Inflammation, Liver Steatosis, Senescence, and Tumorigenesis. J Immunol. 2021;206(4):904-16. Epub 20210113. doi: 10.4049/jimmunol.2001022. PubMed PMID: 33441438; PubMed Central PMCID: PMCPMC7851741.
143. Ludlow AT, Witkowski S, Marshall MR, Wang J, Lima LC, Guth LM, et al. Chronic exercise modifies age-related telomere dynamics in a tissue-specific fashion. J Gerontol A Biol Sci Med Sci. 2012;67(9):911-26. Epub 20120301. doi: 10.1093/gerona/gls002. PubMed PMID: 22389464; PubMed Central PMCID: PMCPMC3436090.
144. Collins M, Renault V, Grobler LA, St Clair Gibson A, Lambert MI, Wayne Derman E, et al. Athletes with exercise-associated fatigue have abnormally short muscle DNA telomeres. Med Sci Sports Exerc. 2003;35(9):1524-8. doi: 10.1249/01.MSS.0000084522.14168.49. PubMed PMID: 12972872.
145. Rae DE, Vignaud A, Butler-Browne GS, Thornell LE, Sinclair-Smith C, Derman EW, et al. Skeletal muscle telomere length in healthy, experienced, endurance runners. Eur J Appl Physiol. 2010;109(2):323-30. Epub 20100126. doi: 10.1007/s00421-010-1353-6. PubMed PMID: 20101406.
146. Kadi F, Ponsot E. The biology of satellite cells and telomeres in human skeletal muscle: effects of aging and physical activity. Scand J Med Sci Sports. 2010;20(1):39-48. Epub 20090901. doi: 10.1111/j.1600-0838.2009.00966.x. PubMed PMID: 19765243.
147. Brett JO, Arjona M, Ikeda M, Quarta M, de Morree A, Egner IM, et al. Exercise rejuvenates quiescent skeletal muscle stem cells in old mice through restoration of Cyclin D1. Nat Metab. 2020;2(4):307-17. Epub 20200413. doi: 10.1038/s42255-020-0190-0. PubMed PMID: 32601609; PubMed Central PMCID: PMCPMC7323974.
148. Gan W, Liu XL, Yu T, Zou YG, Li TT, Wang S, et al. Urinary 8-oxo-7,8-dihydroguanosine as a Potential Biomarker of Aging. Front Aging Neurosci. 2018;10:34. Epub 20180227. doi: 10.3389/fnagi.2018.00034. PubMed PMID: 29535624; PubMed Central PMCID: PMCPMC5835306.
149. Ludlow AT, Spangenburg EE, Chin ER, Cheng WH, Roth SM. Telomeres shorten in response to oxidative stress in mouse skeletal muscle fibers. J Gerontol A

Biol Sci Med Sci. 2014;69(7):821-30. Epub 20140113. doi: 10.1093/gerona/glt211. PubMed PMID: 24418792; PubMed Central PMCID: PMCPMC4111633.
150. Zhang X, Englund DA, Aversa Z, Jachim SK, White TA, LeBrasseur NK. Exercise Counters the Age-Related Accumulation of Senescent Cells. Exerc Sport Sci Rev. 2022;50(4):213-21. Epub 20220701. doi: 10.1249/JES.0000000000000302. PubMed PMID: 35776782; PubMed Central PMCID: PMCPMC9680689.
151. Sharifi-Sanjani M, Oyster NM, Tichy ED, Bedi KC, Jr., Harel O, Margulies KB, et al. Cardiomyocyte-Specific Telomere Shortening is a Distinct Signature of Heart Failure in Humans. J Am Heart Assoc. 2017;6(9). Epub 20170907. doi: 10.1161/JAHA.116.005086. PubMed PMID: 28882819; PubMed Central PMCID: PMCPMC5634248.
152. Tedone E, Huang E, O'Hara R, Batten K, Ludlow AT, Lai TP, et al. Telomere length and telomerase activity in T cells are biomarkers of high-performing centenarians. Aging Cell. 2019;18(1):e12859. Epub 20181128. doi: 10.1111/acel.12859. PubMed PMID: 30488553; PubMed Central PMCID: PMCPMC6351827.
153. da Silveira MP, da Silva Fagundes KK, Bizuti MR, Starck E, Rossi RC, de Resende ESDT. Physical exercise as a tool to help the immune system against COVID-19: an integrative review of the current literature. Clin Exp Med. 2021;21(1):15-28. Epub 20200729. doi: 10.1007/s10238-020-00650-3. PubMed PMID: 32728975; PubMed Central PMCID: PMCPMC7387807.
154. Werner C, Furster T, Widmann T, Poss J, Roggia C, Hanhoun M, et al. Physical exercise prevents cellular senescence in circulating leukocytes and in the vessel wall. Circulation. 2009;120(24):2438-47. doi: 10.1161/CIRCULATIONAHA.109.861005. PubMed PMID: 19948976.
155. Hagman M, Werner C, Kamp K, Fristrup B, Hornstrup T, Meyer T, et al. Reduced telomere shortening in lifelong trained male football players compared to age-matched inactive controls. Prog Cardiovasc Dis. 2020;63(6):738-49. Epub 20200601. doi: 10.1016/j.pcad.2020.05.009. PubMed PMID: 32497584.
156. Denham J, Sellami M. Exercise training increases telomerase reverse transcriptase gene expression and telomerase activity: A systematic review and meta-analysis. Ageing Res Rev. 2021;70:101411. Epub 20210717. doi: 10.1016/j.arr.2021.101411. PubMed PMID: 34284150.
157. Ludlow AT, Gratidao L, Ludlow LW, Spangenburg EE, Roth SM. Acute exercise activates p38 MAPK and increases the expression of telomere-protective genes in cardiac muscle. Exp Physiol. 2017;102(4):397-410. Epub 20170314. doi: 10.1113/EP086189. PubMed PMID: 28166612; PubMed Central PMCID: PMCPMC5378631.
158. Werner C, Hanhoun M, Widmann T, Kazakov A, Semenov A, Poss J, et al. Effects of physical exercise on myocardial telomere-regulating proteins, survival pathways, and apoptosis. J Am Coll Cardiol. 2008;52(6):470-82. doi: 10.1016/j.jacc.2008.04.034. PubMed PMID: 18672169.
159. Chilton WL, Marques FZ, West J, Kannourakis G, Berzins SP, O'Brien BJ, et al. Acute exercise leads to regulation of telomere-associated genes and microRNA expression in immune cells. PLoS One. 2014;9(4):e92088. Epub 20140421. doi: 10.1371/journal.pone.0092088. PubMed PMID: 24752326; PubMed Central PMCID: PMCPMC3994003.

160. Cluckey TG, Nieto NC, Rodoni BM, Traustadottir T. Preliminary evidence that age and sex affect exercise-induced hTERT expression. Exp Gerontol. 2017;96:7-11. Epub 20170603. doi: 10.1016/j.exger.2017.06.003. PubMed PMID: 28587932.
161. Chen JL, Greider CW. Determinants in mammalian telomerase RNA that mediate enzyme processivity and cross-species incompatibility. EMBO J. 2003;22(2):304-14. doi: 10.1093/emboj/cdg024. PubMed PMID: 12514136; PubMed Central PMCID: PMCPMC140099.
162. Smogorzewska A, van Steensel B, Bianchi A, Oelmann S, Schaefer MR, Schnapp G, et al. Control of human telomere length by TRF1 and TRF2. Mol Cell Biol. 2000;20(5):1659-68. doi: 10.1128/MCB.20.5.1659-1668.2000. PubMed PMID: 10669743; PubMed Central PMCID: PMCPMC85349.
163. Harley CB, Futcher AB, Greider CW. Telomeres shorten during ageing of human fibroblasts. Nature. 1990;345(6274):458-60. Epub 1990/05/31. doi: 10.1038/345458a0. PubMed PMID: 2342578.
164. Lormand JD, Buncher N, Murphy CT, Kaur P, Lee MY, Burgers P, et al. DNA polymerase delta stalls on telomeric lagging strand templates independently from G-quadruplex formation. Nucleic Acids Res. 2013;41(22):10323-33. Epub 2013/09/17. doi: 10.1093/nar/gkt813. PubMed PMID: 24038470; PubMed Central PMCID: PMCPMC3905856.
165. Morin GB. The human telomere terminal transferase enzyme is a ribonucleoprotein that synthesizes TTAGGG repeats. Cell. 1989;59(3):521-9. doi: 10.1016/0092-8674(89)90035-4. PubMed PMID: 2805070.
166. Wright WE, Piatyszek MA, Rainey WE, Byrd W, Shay JW. Telomerase activity in human germline and embryonic tissues and cells. Dev Genet. 1996;18(2):173-9. doi: 10.1002/(SICI)1520-6408(1996)18:2<173::AID-DVG10>3.0.CO;2-3. PubMed PMID: 8934879.
167. Zou Y, Sfeir A, Gryaznov SM, Shay JW, Wright WE. Does a sentinel or a subset of short telomeres determine replicative senescence? Mol Biol Cell. 2004;15(8):3709-18. Epub 2004/06/08. doi: 10.1091/mbc.e04-03-0207. PubMed PMID: 15181152; PubMed Central PMCID: PMCPMC491830.
168. Seluanov A, Chen Z, Hine C, Sasahara TH, Ribeiro AA, Catania KC, et al. Telomerase activity coevolves with body mass not lifespan. Aging Cell. 2007;6(1):45-52. Epub 2006/12/19. doi: 10.1111/j.1474-9726.2006.00262.x. PubMed PMID: 17173545; PubMed Central PMCID: PMCPMC2693359.
169. Gomes NM, Ryder OA, Houck ML, Charter SJ, Walker W, Forsyth NR, et al. Comparative biology of mammalian telomeres: hypotheses on ancestral states and the roles of telomeres in longevity determination. Aging Cell. 2011;10(5):761-8. Epub 2011/04/27. doi: 10.1111/j.1474-9726.2011.00718.x. PubMed PMID: 21518243; PubMed Central PMCID: PMCPMC3387546.
170. Shay JW, Bacchetti S. A survey of telomerase activity in human cancer. Eur J Cancer. 1997;33(5):787-91. Epub 1997/04/01. doi: 10.1016/S0959-8049(97)00062-2. PubMed PMID: 9282118.
171. Hahn WC, Stewart SA, Brooks MW, York SG, Eaton E, Kurachi A, et al. Inhibition of telomerase limits the growth of human cancer cells. Nat Med. 1999;5(10):1164-70. Epub 1999/09/30. doi: 10.1038/13495. PubMed PMID: 10502820.

172. Nguyen THD, Tam J, Wu RA, Greber BJ, Toso D, Nogales E, et al. Cryo-EM structure of substrate-bound human telomerase holoenzyme. Nature. 2018;557(7704):190-5. Epub 2018/04/27. doi: 10.1038/s41586-018-0062-x. PubMed PMID: 29695869; PubMed Central PMCID: PMCPMC6223129.
173. Wang Y, Susac L, Feigon J. Structural Biology of Telomerase. Cold Spring Harb Perspect Biol. 2019;11(12). Epub 2019/08/28. doi: 10.1101/cshperspect.a032383. PubMed PMID: 31451513; PubMed Central PMCID: PMCPMC6886448.
174. Yi X, Shay JW, Wright WE. Quantitation of telomerase components and hTERT mRNA splicing patterns in immortal human cells. Nucleic Acids Res. 2001;29(23):4818-25. doi: 10.1093/nar/29.23.4818. PubMed PMID: 11726691; PubMed Central PMCID: PMCPMC96692.
175. Withers JB, Ashvetiya T, Beemon KL. Exclusion of exon 2 is a common mRNA splice variant of primate telomerase reverse transcriptases. PLoS One. 2012;7(10):e48016. Epub 20121024. doi: 10.1371/journal.pone.0048016. PubMed PMID: 23110161; PubMed Central PMCID: PMCPMC3480478.
176. Weinrich SL, Pruzan R, Ma L, Ouellette M, Tesmer VM, Holt SE, et al. Reconstitution of human telomerase with the template RNA component hTR and the catalytic protein subunit hTRT. Nat Genet. 1997;17(4):498-502. Epub 1997/12/17. doi: 10.1038/ng1297-498. PubMed PMID: 9398860.
177. Horn S, Figl A, Rachakonda PS, Fischer C, Sucker A, Gast A, et al. TERT promoter mutations in familial and sporadic melanoma. Science. 2013;339(6122):959-61. Epub 2013/01/26. doi: 10.1126/science.1230062. PubMed PMID: 23348503.
178. Huang FW, Hodis E, Xu MJ, Kryukov GV, Chin L, Garraway LA. Highly recurrent TERT promoter mutations in human melanoma. Science. 2013;339(6122):957-9. Epub 2013/01/26. doi: 10.1126/science.1229259. PubMed PMID: 23348506; PubMed Central PMCID: PMCPMC4423787.
179. Kilian A, Bowtell DD, Abud HE, Hime GR, Venter DJ, Keese PK, et al. Isolation of a candidate human telomerase catalytic subunit gene, which reveals complex splicing patterns in different cell types. Hum Mol Genet. 1997;6(12):2011-9. doi: 10.1093/hmg/6.12.2011. PubMed PMID: 9328464.
180. Escobar-Hoyos L, Knorr K, Abdel-Wahab O. Aberrant RNA Splicing in Cancer. Annu Rev Cancer Biol. 2019;3(1):167-85. Epub 2019/03/01. doi: 10.1146/annurev-cancerbio-030617-050407. PubMed PMID: 32864546; PubMed Central PMCID: PMCPMC7453310.
181. Wong MS, Chen L, Foster C, Kainthla R, Shay JW, Wright WE. Regulation of telomerase alternative splicing: a target for chemotherapy. Cell Rep. 2013;3(4):1028-35. Epub 20130404. doi: 10.1016/j.celrep.2013.03.011. PubMed PMID: 23562158; PubMed Central PMCID: PMCPMC3640656.
182. Ran FA, Hsu PD, Wright J, Agarwala V, Scott DA, Zhang F. Genome engineering using the CRISPR-Cas9 system. Nat Protoc. 2013;8(11):2281-308. Epub 2013/10/26. doi: 10.1038/nprot.2013.143. PubMed PMID: 24157548; PubMed Central PMCID: PMCPMC3969860.
183. Ludlow AT, Robin JD, Sayed M, Litterst CM, Shelton DN, Shay JW, et al. Quantitative telomerase enzyme activity determination using droplet digital PCR with single cell resolution. Nucleic Acids Res. 2014;42(13):e104. Epub 2014/05/28. doi:

10.1093/nar/gku439. PubMed PMID: 24861623; PubMed Central PMCID: PMCPMC4117742.
184. Sayed ME, Slusher AL, Ludlow AT. Droplet Digital TRAP (ddTRAP): Adaptation of the Telomere Repeat Amplification Protocol to Droplet Digital Polymerase Chain Reaction. J Vis Exp. 2019;(147). Epub 2019/05/21. doi: 10.3791/59550. PubMed PMID: 31107456.
185. Mender I, Shay JW. Telomere Restriction Fragment (TRF) Analysis. Bio Protoc. 2015;5(22). doi: 10.21769/bioprotoc.1658. PubMed PMID: 27500189; PubMed Central PMCID: PMCPMC4972328.
186. Maurya DK. ColonyCountJ: A User-Friendly Image J Add-on Program for Quantification of Different Colony Parameters in Clonogenic Assay. Journal of Clinical Toxicology. 2017;7(358):2161-0495.1000358. doi: 10.4172/2161-0495.1000358.
187. GDAC. Firehose stddata_2016_01_28 run. In: Center bitgda, editor. 2017.
188. Patro R, Duggal G, Love MI, Irizarry RA, Kingsford C. Salmon provides fast and bias-aware quantification of transcript expression. Nat Methods. 2017;14(4):417-9. Epub 2017/03/07. doi: 10.1038/nmeth.4197. PubMed PMID: 28263959; PubMed Central PMCID: PMCPMC5600148.
189. Karolchik D, Hinrichs AS, Furey TS, Roskin KM, Sugnet CW, Haussler D, et al. The UCSC Table Browser data retrieval tool. Nucleic Acids Res. 2004;32(Database issue):D493-6. Epub 2003/12/19. doi: 10.1093/nar/gkh103. PubMed PMID: 14681465; PubMed Central PMCID: PMCPMC308837.
190. R Core Team. R: A Language and Environment for Statistical Computing. Vienna, Austria. R Foundation for Statistical Computing; 2018.
191. Therneau TM. A Package for Survival Analysis in S. 2.38 ed2015.
192. Sun W, Duan T, Ye P, Chen K, Zhang G, Lai M, et al. TSVdb: a web-tool for TCGA splicing variants analysis. BMC Genomics. 2018;19(1):405. Epub 20180529. doi: 10.1186/s12864-018-4775-x. PubMed PMID: 29843604; PubMed Central PMCID: PMCPMC5975414.
193. Wang L, Soria JC, Kemp BL, Liu DD, Mao L, Khuri FR. hTERT expression is a prognostic factor of survival in patients with stage I non-small cell lung cancer. Clin Cancer Res. 2002;8(9):2883-9. Epub 2002/09/17. PubMed PMID: 12231532.
194. Golas MM, Sander B, Will CL, Luhrmann R, Stark H. Molecular architecture of the multiprotein splicing factor SF3b. Science. 2003;300(5621):980-4. Epub 2003/05/10. doi: 10.1126/science.1084155. PubMed PMID: 12738865.
195. Tanaka Y, Ohta A, Terashima K, Sakamoto H. Polycistronic expression and RNA-binding specificity of the C. elegans homologue of the spliceosome-associated protein SAP49. J Biochem. 1997;121(4):739-45. Epub 1997/04/01. doi: 10.1093/oxfordjournals.jbchem.a021648. PubMed PMID: 9163526.
196. Calabretta S, Bielli P, Passacantilli I, Pilozzi E, Fendrich V, Capurso G, et al. Modulation of PKM alternative splicing by PTBP1 promotes gemcitabine resistance in pancreatic cancer cells. Oncogene. 2016;35(16):2031-9. Epub 20150803. doi: 10.1038/onc.2015.270. PubMed PMID: 26234680; PubMed Central PMCID: PMCPMC4650269.
197. Ray D, Yun YC, Idris M, Cheng S, Boot A, Iain TBH, et al. A tumor-associated splice-isoform of MAP2K7 drives dedifferentiation in MBNL1-low cancers via JNK activation. Proc Natl Acad Sci U S A. 2020;117(28):16391-400. Epub 20200629. doi:

10.1073/pnas.2002499117. PubMed PMID: 32601196; PubMed Central PMCID: PMCPMC7368273.
198. Rajendran D, Zhang Y, Berry DM, McGlade CJ. Regulation of Numb isoform expression by activated ERK signaling. Oncogene. 2016;35(39):5202-13. Epub 20160404. doi: 10.1038/onc.2016.69. PubMed PMID: 27041567.
199. Li CY, Chu JY, Yu JK, Huang XQ, Liu XJ, Shi L, et al. Regulation of alternative splicing of Bcl-x by IL-6, GM-CSF and TPA. Cell Res. 2004;14(6):473-9. doi: 10.1038/sj.cr.7290250. PubMed PMID: 15625014.
200. Harvey SE, Cheng C. Methods for Characterization of Alternative RNA Splicing. Methods Mol Biol. 2016;1402:229-41. doi: 10.1007/978-1-4939-3378-5_18. PubMed PMID: 26721495; PubMed Central PMCID: PMCPMC4770877.
201. McEachern MJ, Blackburn EH. Runaway telomere elongation caused by telomerase RNA gene mutations. Nature. 1995;376(6539):403-9. Epub 1995/08/03. doi: 10.1038/376403a0. PubMed PMID: 7630414.
202. Sun C. The SF3b complex: splicing and beyond. Cell Mol Life Sci. 2020;77(18):3583-95. Epub 2020/03/07. doi: 10.1007/s00018-020-03493-z. PubMed PMID: 32140746; PubMed Central PMCID: PMCPMC7452928.
203. Shen Q, Nam SW. SF3B4 as an early-stage diagnostic marker and driver of hepatocellular carcinoma. BMB Rep. 2018;51(2):57-8. Epub 2018/02/06. doi: 10.5483/bmbrep.2018.51.2.021. PubMed PMID: 29397868; PubMed Central PMCID: PMCPMC5836557.
204. Yamada T, Takechi M, Yokoyama N, Hiraoka Y, Ishikubo H, Usami T, et al. Heterozygous mutation of the splicing factor Sf3b4 affects development of the axial skeleton and forebrain in mouse. Dev Dyn. 2020;249(5):622-35. Epub 2020/01/05. doi: 10.1002/dvdy.148. PubMed PMID: 31900962.
205. Shay JW, Wright WE. Senescence and immortalization: role of telomeres and telomerase. Carcinogenesis. 2005;26(5):867-74. Epub 20041007. doi: 10.1093/carcin/bgh296. PubMed PMID: 15471900.
206. Holohan B, Wright WE, Shay JW. Cell biology of disease: Telomeropathies: an emerging spectrum disorder. J Cell Biol. 2014;205(3):289-99. doi: 10.1083/jcb.201401012. PubMed PMID: 24821837; PubMed Central PMCID: PMCPMC4018777.
207. Batista LF, Pech MF, Zhong FL, Nguyen HN, Xie KT, Zaug AJ, et al. Telomere shortening and loss of self-renewal in dyskeratosis congenita induced pluripotent stem cells. Nature. 2011;474(7351):399-402. Epub 20110522. doi: 10.1038/nature10084. PubMed PMID: 21602826; PubMed Central PMCID: PMCPMC3155806.
208. Guterres AN, Villanueva J. Targeting telomerase for cancer therapy. Oncogene. 2020;39(36):5811-24. Epub 20200730. doi: 10.1038/s41388-020-01405-w. PubMed PMID: 32733068; PubMed Central PMCID: PMCPMC7678952.
209. Wang ET, Sandberg R, Luo S, Khrebtukova I, Zhang L, Mayr C, et al. Alternative isoform regulation in human tissue transcriptomes. Nature. 2008;456(7221):470-6. doi: 10.1038/nature07509. PubMed PMID: 18978772; PubMed Central PMCID: PMCPMC2593745.
210. Fleisig HB, Hukezalie KR, Thompson CA, Au-Yeung TT, Ludlow AT, Zhao CR, et al. Telomerase reverse transcriptase expression protects transformed human cells against DNA-damaging agents, and increases tolerance to chromosomal instability.

Oncogene. 2016;35(2):218-27. Epub 20150420. doi: 10.1038/onc.2015.75. PubMed PMID: 25893297.
211. Zhu S, Rousseau P, Lauzon C, Gandin V, Topisirovic I, Autexier C. Inactive C-terminal telomerase reverse transcriptase insertion splicing variants are dominant-negative inhibitors of telomerase. Biochimie. 2014;101:93-103. Epub 20140109. doi: 10.1016/j.biochi.2013.12.023. PubMed PMID: 24412622.
212. Ludlow AT, Shelton D, Wright WE, Shay JW. ddTRAP: A Method for Sensitive and Precise Quantification of Telomerase Activity. Methods Mol Biol. 2018;1768:513-29. doi: 10.1007/978-1-4939-7778-9_29. PubMed PMID: 29717462; PubMed Central PMCID: PMCPMC6046637.
213. Lai TP, Wright WE, Shay JW. Generation of digoxigenin-incorporated probes to enhance DNA detection sensitivity. Biotechniques. 2016;60(6):306-9. Epub 20160601. doi: 10.2144/000114427. PubMed PMID: 27286808.
214. Lennox AL, Mao H, Silver DL. RNA on the brain: emerging layers of post-transcriptional regulation in cerebral cortex development. Wiley Interdiscip Rev Dev Biol. 2018;7(1). Epub 20170824. doi: 10.1002/wdev.290. PubMed PMID: 28837264; PubMed Central PMCID: PMCPMC5746464.
215. Buckanovich RJ, Posner JB, Darnell RB. Nova, the paraneoplastic Ri antigen, is homologous to an RNA-binding protein and is specifically expressed in the developing motor system. Neuron. 1993;11(4):657-72. doi: 10.1016/0896-6273(93)90077-5. PubMed PMID: 8398153.
216. Li Q, Zheng S, Han A, Lin CH, Stoilov P, Fu XD, et al. The splicing regulator PTBP2 controls a program of embryonic splicing required for neuronal maturation. Elife. 2014;3:e01201. Epub 20140121. doi: 10.7554/eLife.01201. PubMed PMID: 24448406; PubMed Central PMCID: PMCPMC3896118.
217. Boutz PL, Stoilov P, Li Q, Lin CH, Chawla G, Ostrow K, et al. A post-transcriptional regulatory switch in polypyrimidine tract-binding proteins reprograms alternative splicing in developing neurons. Genes Dev. 2007;21(13):1636-52. doi: 10.1101/gad.1558107. PubMed PMID: 17606642; PubMed Central PMCID: PMCPMC1899473.
218. Qu XH, Liu JL, Zhong XW, Li XI, Zhang QG. Insights into the roles of hnRNP A2/B1 and AXL in non-small cell lung cancer. Oncol Lett. 2015;10(3):1677-85. Epub 20150703. doi: 10.3892/ol.2015.3457. PubMed PMID: 26622731; PubMed Central PMCID: PMCPMC4533760.
219. Xu C, Xie N, Su Y, Sun Z, Liang Y, Zhang N, et al. HnRNP F/H associate with hTERC and telomerase holoenzyme to modulate telomerase function and promote cell proliferation. Cell Death Differ. 2020;27(6):1998-2013. Epub 20191220. doi: 10.1038/s41418-019-0483-6. PubMed PMID: 31863069; PubMed Central PMCID: PMCPMC7244589.
220. Gao Y, Zhang X, Wang T, Zhang Y, Wang Q, Hu Y. HNRNPCL1, PRAMEF1, CFAP74, and DFFB: Common Potential Biomarkers for Sporadic and Suspected Lynch Syndrome Endometrial Cancer. Cancer Manag Res. 2020;12:11231-41. Epub 20201104. doi: 10.2147/CMAR.S262421. PubMed PMID: 33177874; PubMed Central PMCID: PMCPMC7649238.
221. Avin BA, Umbricht CB, Zeiger MA. Human telomerase reverse transcriptase regulation by DNA methylation, transcription factor binding and alternative splicing

(Review). Int J Oncol. 2016;49(6):2199-205. Epub 20161020. doi: 10.3892/ijo.2016.3743. PubMed PMID: 27779655; PubMed Central PMCID: PMCPMC6903903.
222. Vuong JK, Lin CH, Zhang M, Chen L, Black DL, Zheng S. PTBP1 and PTBP2 Serve Both Specific and Redundant Functions in Neuronal Pre-mRNA Splicing. Cell Rep. 2016;17(10):2766-75. doi: 10.1016/j.celrep.2016.11.034. PubMed PMID: 27926877; PubMed Central PMCID: PMCPMC5179036.
223. Polydorides AD, Okano HJ, Yang YY, Stefani G, Darnell RB. A brain-enriched polypyrimidine tract-binding protein antagonizes the ability of Nova to regulate neuron-specific alternative splicing. Proc Natl Acad Sci U S A. 2000;97(12):6350-5. doi: 10.1073/pnas.110128397. PubMed PMID: 10829067; PubMed Central PMCID: PMCPMC18606.
224. Wang F, Cheng Y, Zhang C, Chang G, Geng X. A novel antisense oligonucleotide anchored on the intronic splicing enhancer of hTERT pre-mRNA inhibits telomerase activity and induces apoptosis in glioma cells. J Neurooncol. 2019;143(1):57-68. Epub 20190318. doi: 10.1007/s11060-019-03150-x. PubMed PMID: 30887243.
225. Zhou J, Li T, Geng X, Sui L, Wang F. Antisense oligonucleotide repress telomerase activity via manipulating alternative splicing or translation. Biochem Biophys Res Commun. 2021;582:118-24. Epub 20211021. doi: 10.1016/j.bbrc.2021.10.034. PubMed PMID: 34710826.
226. Victorelli S, Passos JF. Telomeres and Cell Senescence - Size Matters Not. EBioMedicine. 2017;21:14-20. Epub 20170321. doi: 10.1016/j.ebiom.2017.03.027. PubMed PMID: 28347656; PubMed Central PMCID: PMCPMC5514392.
227. Shay JW, Wright WE. Telomeres are double-strand DNA breaks hidden from DNA damage responses. Mol Cell. 2004;14(4):420-1. doi: 10.1016/s1097-2765(04)00269-2. PubMed PMID: 15149591.
228. Greider CW, Blackburn EH. Identification of a specific telomere terminal transferase activity in Tetrahymena extracts. Cell. 1985;43(2 Pt 1):405-13. doi: 10.1016/0092-8674(85)90170-9. PubMed PMID: 3907856.
229. Plyasova AA, Zhdanov DD. Alternative Splicing of Human Telomerase Reverse Transcriptase (hTERT) and Its Implications in Physiological and Pathological Processes. Biomedicines. 2021;9(5). Epub 20210509. doi: 10.3390/biomedicines9050526. PubMed PMID: 34065134; PubMed Central PMCID: PMCPMC8150890.
230. Liu K, Schoonmaker MM, Levine BL, June CH, Hodes RJ, Weng NP. Constitutive and regulated expression of telomerase reverse transcriptase (hTERT) in human lymphocytes. Proc Natl Acad Sci U S A. 1999;96(9):5147-52. doi: 10.1073/pnas.96.9.5147. PubMed PMID: 10220433; PubMed Central PMCID: PMCPMC21831.
231. Brousset P, al Saati T, Zenou RC, Delsol G. Telomerase activity might persist in the human thymus throughout life. Mol Pathol. 1998;51(3):170-3. doi: 10.1136/mp.51.3.170. PubMed PMID: 9850343; PubMed Central PMCID: PMCPMC395632.
232. Patrick M, Weng NP. Expression and regulation of telomerase in human T cell differentiation, activation, aging and diseases. Cell Immunol. 2019;345:103989. Epub

20190919. doi: 10.1016/j.cellimm.2019.103989. PubMed PMID: 31558266; PubMed Central PMCID: PMCPMC6873926.
233. Iwama H, Ohyashiki K, Ohyashiki JH, Hayashi S, Yahata N, Ando K, et al. Telomeric length and telomerase activity vary with age in peripheral blood cells obtained from normal individuals. Hum Genet. 1998;102(4):397-402. doi: 10.1007/s004390050711. PubMed PMID: 9600234.
234. Ramlee MK, Wang J, Toh WX, Li S. Transcription Regulation of the Human Telomerase Reverse Transcriptase (hTERT) Gene. Genes (Basel). 2016;7(8). Epub 20160818. doi: 10.3390/genes7080050. PubMed PMID: 27548225; PubMed Central PMCID: PMCPMC4999838.
235. Bhadra M, Howell P, Dutta S, Heintz C, Mair WB. Alternative splicing in aging and longevity. Hum Genet. 2020;139(3):357-69. Epub 20191213. doi: 10.1007/s00439-019-02094-6. PubMed PMID: 31834493; PubMed Central PMCID: PMCPMC8176884.
236. Spielmann G, McFarlin BK, O'Connor DP, Smith PJ, Pircher H, Simpson RJ. Aerobic fitness is associated with lower proportions of senescent blood T-cells in man. Brain Behav Immun. 2011;25(8):1521-9. Epub 20110719. doi: 10.1016/j.bbi.2011.07.226. PubMed PMID: 21784146.
237. de Araujo AL, Silva LC, Fernandes JR, Matias Mde S, Boas LS, Machado CM, et al. Elderly men with moderate and intense training lifestyle present sustained higher antibody responses to influenza vaccine. Age (Dordr). 2015;37(6):105. Epub 20151019. doi: 10.1007/s11357-015-9843-4. PubMed PMID: 26480853; PubMed Central PMCID: PMCPMC5005841.
238. Ubaida-Mohien C, Gonzalez-Freire M, Lyashkov A, Moaddel R, Chia CW, Simonsick EM, et al. Physical Activity Associated Proteomics of Skeletal Muscle: Being Physically Active in Daily Life May Protect Skeletal Muscle From Aging. Front Physiol. 2019;10:312. Epub 20190326. doi: 10.3389/fphys.2019.00312. PubMed PMID: 30971946; PubMed Central PMCID: PMCPMC6443906.
239. Fahy GM, Brooke RT, Watson JP, Good Z, Vasanawala SS, Maecker H, et al. Reversal of epigenetic aging and immunosenescent trends in humans. Aging Cell. 2019;18(6):e13028. Epub 20190908. doi: 10.1111/acel.13028. PubMed PMID: 31496122; PubMed Central PMCID: PMCPMC6826138.
240. Gomez-Garcia L, Sanchez FM, Vallejo-Cremades MT, de Segura IA, del Campo Ede M. Direct activation of telomerase by GH via phosphatidylinositol 3'-kinase. J Endocrinol. 2005;185(3):421-8. doi: 10.1677/joe.1.05766. PubMed PMID: 15930168.
241. Wideman L, Weltman JY, Hartman ML, Veldhuis JD, Weltman A. Growth hormone release during acute and chronic aerobic and resistance exercise: recent findings. Sports Med. 2002;32(15):987-1004. doi: 10.2165/00007256-200232150-00003. PubMed PMID: 12457419.
242. Schmidt JC, Dalby AB, Cech TR. Identification of human TERT elements necessary for telomerase recruitment to telomeres. Elife. 2014;3. Epub 20141001. doi: 10.7554/eLife.03563. PubMed PMID: 25271372; PubMed Central PMCID: PMCPMC4359370.
243. Santos JH, Meyer JN, Skorvaga M, Annab LA, Van Houten B. Mitochondrial hTERT exacerbates free-radical-mediated mtDNA damage. Aging Cell. 2004;3(6):399-411. doi: 10.1111/j.1474-9728.2004.00124.x. PubMed PMID: 15569357.

244. Jeong SA, Kim K, Lee JH, Cha JS, Khadka P, Cho HS, et al. Akt-mediated phosphorylation increases the binding affinity of hTERT for importin alpha to promote nuclear translocation. J Cell Sci. 2015;128(12):2287-301. Epub 20150521. doi: 10.1242/jcs.166132. PubMed PMID: 25999477.
245. Seimiya H, Sawada H, Muramatsu Y, Shimizu M, Ohko K, Yamane K, et al. Involvement of 14-3-3 proteins in nuclear localization of telomerase. EMBO J. 2000;19(11):2652-61. doi: 10.1093/emboj/19.11.2652. PubMed PMID: 10835362; PubMed Central PMCID: PMCPMC212742.
246. Li H. New strategies to improve minimap2 alignment accuracy. Bioinformatics. 2021;37(23):4572-4. doi: 10.1093/bioinformatics/btab705.
247. Li H. Minimap2: pairwise alignment for nucleotide sequences. Bioinformatics. 2018;34(18):3094-100. doi: 10.1093/bioinformatics/bty191.
248. Danecek P, Bonfield JK, Liddle J, Marshall J, Ohan V, Pollard MO, et al. Twelve years of SAMtools and BCFtools. GigaScience. 2021;10(2). doi: 10.1093/gigascience/giab008.
249. Wyman D, Mortazavi A. TranscriptClean: variant-aware correction of indels, mismatches and splice junctions in long-read transcripts. Bioinformatics. 2018;35(2):340-2. doi: 10.1093/bioinformatics/bty483.
250. Wyman D, Balderrama-Gutierrez G, Reese F, Jiang S, Rahmanian S, Forner S, et al. A technology-agnostic long-read analysis pipeline for transcriptome discovery and quantification. bioRxiv. 2020:672931. doi: 10.1101/672931.
251. Reese F, Mortazavi A. Swan: a library for the analysis and visualization of long-read transcriptomes. Bioinformatics. 2021;37(9):1322-3. doi: 10.1093/bioinformatics/btaa836. PubMed PMID: 32991665; PubMed Central PMCID: PMCPMC8189675.
252. RStudio Team. RStudio: Integrated Development Environment for R. RStudio, PBC; 2020.
253. Wickham H. Reshaping Data with the reshape Package. Journal of Statistical Software. 2007;21(12):1--20.
254. Wickham H, François R, Henry L, Müller K, Vaughan D. dplyr: A Grammar of Data Manipulation. 2023.
255. Wickham H. ggplot2: Elegant Graphics for Data Analysis: Springer-Verlag New York; 2016.
256. Taipale M, Tucker G, Peng J, Krykbaeva I, Lin ZY, Larsen B, et al. A quantitative chaperone interaction network reveals the architecture of cellular protein homeostasis pathways. Cell. 2014;158(2):434-48. doi: 10.1016/j.cell.2014.05.039. PubMed PMID: 25036637; PubMed Central PMCID: PMCPMC4104544.
257. Kano S, Nishida K, Kurebe H, Nishiyama C, Kita K, Akaike Y, et al. Oxidative stress-inducible truncated serine/arginine-rich splicing factor 3 regulates interleukin-8 production in human colon cancer cells. Am J Physiol Cell Physiol. 2014;306(3):C250-62. Epub 20131127. doi: 10.1152/ajpcell.00091.2013. PubMed PMID: 24284797.
258. Ovcharenko D, Jarvis R, Hunicke-Smith S, Kelnar K, Brown D. High-throughput RNAi screening in vitro: from cell lines to primary cells. RNA. 2005;11(6):985-93. doi: 10.1261/rna.7288405. PubMed PMID: 15923380; PubMed Central PMCID: PMCPMC1370783.

259. Counter CM, Hahn WC, Wei W, Caddle SD, Beijersbergen RL, Lansdorp PM, et al. Dissociation among in vitro telomerase activity, telomere maintenance, and cellular immortalization. Proc Natl Acad Sci U S A. 1998;95(25):14723-8. doi: 10.1073/pnas.95.25.14723. PubMed PMID: 9843956; PubMed Central PMCID: PMCPMC24516.
260. Armbruster BN, Banik SS, Guo C, Smith AC, Counter CM. N-terminal domains of the human telomerase catalytic subunit required for enzyme activity in vivo. Mol Cell Biol. 2001;21(22):7775-86. doi: 10.1128/MCB.21.22.7775-7786.2001. PubMed PMID: 11604512; PubMed Central PMCID: PMCPMC99947.
261. Armbruster BN, Linardic CM, Veldman T, Bansal NP, Downie DL, Counter CM. Rescue of an hTERT mutant defective in telomere elongation by fusion with hPot1. Mol Cell Biol. 2004;24(8):3552-61. doi: 10.1128/MCB.24.8.3552-3561.2004. PubMed PMID: 15060173; PubMed Central PMCID: PMCPMC381596.
262. Banik SS, Guo C, Smith AC, Margolis SS, Richardson DA, Tirado CA, et al. C-terminal regions of the human telomerase catalytic subunit essential for in vivo enzyme activity. Mol Cell Biol. 2002;22(17):6234-46. doi: 10.1128/MCB.22.17.6234-6246.2002. PubMed PMID: 12167716; PubMed Central PMCID: PMCPMC134020.
263. Gordon DM, Santos JH. The emerging role of telomerase reverse transcriptase in mitochondrial DNA metabolism. J Nucleic Acids. 2010;2010. Epub 20100921. doi: 10.4061/2010/390791. PubMed PMID: 20936168; PubMed Central PMCID: PMCPMC2945669.
264. Sharma NK, Reyes A, Green P, Caron MJ, Bonini MG, Gordon DM, et al. Human telomerase acts as a hTR-independent reverse transcriptase in mitochondria. Nucleic Acids Research. 2011;40(2):712-25. doi: 10.1093/nar/gkr758.
265. Kleih M, Bopple K, Dong M, Gaissler A, Heine S, Olayioye MA, et al. Direct impact of cisplatin on mitochondria induces ROS production that dictates cell fate of ovarian cancer cells. Cell Death Dis. 2019;10(11):851. Epub 20191107. doi: 10.1038/s41419-019-2081-4. PubMed PMID: 31699970; PubMed Central PMCID: PMCPMC6838053.
266. Subasri M, Shooshtari P, Watson AJ, Betts DH. Analysis of TERT Isoforms across TCGA, GTEx and CCLE Datasets. Cancers (Basel). 2021;13(8). Epub 20210413. doi: 10.3390/cancers13081853. PubMed PMID: 33924498; PubMed Central PMCID: PMCPMC8070023.
267. Rowland TJ, Dumbovic G, Hass EP, Rinn JL, Cech TR. Single-cell imaging reveals unexpected heterogeneity of telomerase reverse transcriptase expression across human cancer cell lines. Proc Natl Acad Sci U S A. 2019;116(37):18488-97. Epub 20190826. doi: 10.1073/pnas.1908275116. PubMed PMID: 31451652; PubMed Central PMCID: PMCPMC6744858.
268. Haendeler J, Hoffmann J, Brandes RP, Zeiher AM, Dimmeler S. Hydrogen peroxide triggers nuclear export of telomerase reverse transcriptase via Src kinase family-dependent phosphorylation of tyrosine 707. Mol Cell Biol. 2003;23(13):4598-610. doi: 10.1128/MCB.23.13.4598-4610.2003. PubMed PMID: 12808100; PubMed Central PMCID: PMCPMC164856.
269. Del Bufalo D, Rizzo A, Trisciuoglio D, Cardinali G, Torrisi MR, Zangemeister-Wittke U, et al. Involvement of hTERT in apoptosis induced by interference with Bcl-2

expression and function. Cell Death Differ. 2005;12(11):1429-38. doi: 10.1038/sj.cdd.4401670. PubMed PMID: 15920535.
270. Santos JH, Meyer JN, Van Houten B. Mitochondrial localization of telomerase as a determinant for hydrogen peroxide-induced mitochondrial DNA damage and apoptosis. Hum Mol Genet. 2006;15(11):1757-68. Epub 20060413. doi: 10.1093/hmg/ddl098. PubMed PMID: 16613901.
271. Ahmed S, Passos JF, Birket MJ, Beckmann T, Brings S, Peters H, et al. Telomerase does not counteract telomere shortening but protects mitochondrial function under oxidative stress. J Cell Sci. 2008;121(Pt 7):1046-53. Epub 20080311. doi: 10.1242/jcs.019372. PubMed PMID: 18334557.
272. Haendeler J, Drose S, Buchner N, Jakob S, Altschmied J, Goy C, et al. Mitochondrial telomerase reverse transcriptase binds to and protects mitochondrial DNA and function from damage. Arterioscler Thromb Vasc Biol. 2009;29(6):929-35. Epub 20090305. doi: 10.1161/ATVBAHA.109.185546. PubMed PMID: 19265030.
273. Green PD, Sharma NK, Santos JH. Telomerase Impinges on the Cellular Response to Oxidative Stress Through Mitochondrial ROS-Mediated Regulation of Autophagy. Int J Mol Sci. 2019;20(6). Epub 20190326. doi: 10.3390/ijms20061509. PubMed PMID: 30917518; PubMed Central PMCID: PMCPMC6470917.
274. Palchaudhuri R, Lambrecht MJ, Botham RC, Partlow KC, van Ham TJ, Putt KS, et al. A Small Molecule that Induces Intrinsic Pathway Apoptosis with Unparalleled Speed. Cell Rep. 2015;13(9):2027-36. Epub 20151119. doi: 10.1016/j.celrep.2015.10.042. PubMed PMID: 26655912; PubMed Central PMCID: PMCPMC4683402.
275. Ale-Agha N, Jakobs P, Goy C, Zurek M, Rosen J, Dyballa-Rukes N, et al. Mitochondrial Telomerase Reverse Transcriptase Protects From Myocardial Ischemia/Reperfusion Injury by Improving Complex I Composition and Function. Circulation. 2021;144(23):1876-90. Epub 20211021. doi: 10.1161/CIRCULATIONAHA.120.051923. PubMed PMID: 34672678.
276. Bashari A, Siegfried Z, Karni R. Targeting splicing factors for cancer therapy. RNA. 2023;29(4):506-15. Epub 20230125. doi: 10.1261/rna.079585.123. PubMed PMID: 36697261; PubMed Central PMCID: PMCPMC10019363.
277. Araki S, Ohori M, Yugami M. Targeting pre-mRNA splicing in cancers: roles, inhibitors, and therapeutic opportunities. Front Oncol. 2023;13:1152087. Epub 20230605. doi: 10.3389/fonc.2023.1152087. PubMed PMID: 37342192; PubMed Central PMCID: PMCPMC10277747.
278. Talior I, Yarkoni M, Bashan N, Eldar-Finkelman H. Increased glucose uptake promotes oxidative stress and PKC-delta activation in adipocytes of obese, insulin-resistant mice. Am J Physiol Endocrinol Metab. 2003;285(2):E295-302. doi: 10.1152/ajpendo.00044.2003. PubMed PMID: 12857675.
279. Zhou J, Deo BK, Hosoya K, Terasaki T, Obrosova IG, Brosius FC, 3rd, et al. Increased JNK phosphorylation and oxidative stress in response to increased glucose flux through increased GLUT1 expression in rat retinal endothelial cells. Invest Ophthalmol Vis Sci. 2005;46(9):3403-10. doi: 10.1167/iovs.04-1064. PubMed PMID: 16123445.
280. Liemburg-Apers DC, Willems PH, Koopman WJ, Grefte S. Interactions between mitochondrial reactive oxygen species and cellular glucose metabolism. Arch Toxicol.

2015;89(8):1209-26. Epub 20150606. doi: 10.1007/s00204-015-1520-y. PubMed PMID: 26047665; PubMed Central PMCID: PMCPMC4508370.